Towards an understanding of multiple paralogues for metal-handling genes in a coastal cyanobacterium

By

Jie Chu

A Thesis Submitted in Partial Fulfilment of the requirement for the Degree of Doctor of Philosophy

University of Warwick

Molecular Organisation and Assembly in Cells (MOAC)

Doctoral Training Centre

August 2012

Table of Contents

List of Figures

List of Tables

Acknowledgements

First and foremost I would like to extend my sincerest thanks to Dr. Claudia Blindauer for providing me with an opportunity to undertake this project, and her continued, strong support, guidance and friendship over the past years. Special thanks to Professor David Scanlan for his guidance and support during the project.

A big thanks to all members, of the Blindauer and Scanlan groups; especially Dr. Oksana Leszczyszyn, Dr. Jin Lu, Dr. Martin Ostrowski, Dr. Andrew Millard and Dr. Sophie Mazard.

I would like to say thank you to all the members of MOAC, both past and present, especially Professor Alison Rodger, Dorothea Mangels, Mónica de Lucena and Sarah Shute.

I would like to take this opportunity to thank my husband Xin, who has given me so much love and support, and taking care of all my worries. Finally I wish to thank my parents who were encouraged me to take an interest in the natural world.

Declaration

I hereby declare that the work presented in this thesis is original and has not been submitted for any other degree. Experimental work was conducted by the author, unless stated below, under the supervision of Dr Claudia A. Blindauer and Prof. David J. Scanlan, University of Warwick. All sources of information have been specifically acknowledged by means of reference.

The 2D ^{1}H NMR assignment was performed with the kind assistance of Dr. Claudia A. Blindauer. Molecular modelling work in Chapter 4 was performed by Dr. Claudia Blindauer. The recombinant plasmids containing *sync_0853* and *sync_1081* were cloned by Liam Jones.

Jie Chu

Abstract

Marine picocyanobacteria are the most abundant photosynthetic bacterioplankton occupying a wide range of habitats across the world's oceans. In order to survive in such diverse habitats, these organisms have developed various mechanisms to respond to specific environmental challenges they might encounter. One such challenge for cyanobacteria is the acquisition and homeostasis of micronutrients such as Zn and Cu, especially for those organisms occupying a variable ecosystem with an erratic nutrient supply. Metallothioneins are metal-binding proteins that potentially participate in such metal homeostasis mechanisms in these marine picocyanobacteria.

Metallothioneins are small, cysteine-rich proteins capable of binding multiple metal ions, and have attracted intense scientific interest since their discovery in the 1950s. Over the last decade, they have been reported in every kingdom, from prokaryotic to eukaryotic, from bacteria to plants, from worms to mammals. Eukaryotic metallothioneins have been extensively studied. However, characterisation of bacterial metallothioneins is still rare.

This research focused on the coastal cyanobacterium *Synechococcus* sp. CC9311, which is unusual in possessing four metallothionein genes (*sync_0853*, *sync_1081*, *sync_2379* and *sync_2426*) while most marine picocyanobacteria contain only one, or none. Three metallothioneins were comprehensively characterised using a range of analytical and biophysical techniques. Mass spectrometry and nuclear magnetic resonance studies combined with homology modelling led to an unambiguous Zn_3Cys_8His cluster for BmtA0853, a highly likely $Zn_4Cys_9His_2$ cluster for BmtA2426, and three possible configurations for BmtA1081. Analysis of gene expression profiles revealed that the four metallothioneins selectively participated in zinc scavenging, zinc homeostasis, cadmium detoxification, or protection from oxidising conditions. Growth of *Synechococcus* sp. CC9311 under various metal treatments also revealed that this coastal strain has developed a metal intensive physiology compared to the open ocean strain *Synechococcus* sp. WH8102.

Abbreviations

5F-BAPTA	1,2-bis(2-amino-5-fluorophenoxy)ethane N,N,N',N'-tetraacetic acid
ASW	Artificial SeaWater
cDNA	complementary DNA
CIAP	Calf intestinal alkaline phosphatase
DNA	Deoxyribonucleic Acid
dNTP	Deoxyribonucleotide triphosphate
dNTP	Deoxyribonucleotide triphosphate
DTNB	5,5-dithiobis (2-nitrobenzoic acid) or Ellman's reagent
EDTA	Ethylenediaminetetraacetic Acid
ESI-MS	Electrospray ionization mass spectrometry
FPLC	Fast protein liquid chromatography
HL	High light
HLIP	High light-inducible protein
HSQC	Heteronuclear Single Quantum Coherence
ICP-OES	Inductively coupled Plasma/Optical Emission Spectroscopy
IPTG	isopropyl-β-D-thiogalactopyranoside
LB	Luria-Bertani
MES	2-(N-morpholino)ethanesulfonic acid
MOPS	3-(N-morpholino)propanesulfonic acid
MT(s)	Metallothionein(s)

NMR	Nuclear Magnetic Resonance
NOESY	Nuclear Overhauser effect spectroscopy
PCR	Polymerase Chain Reaction
qPCR	quantitative PCR
RNA	RiboNucleic Acid
SDS	Sodium Dodecyl Sulfate
SDS-PAGE	Sodium Dodecyl Sulfate Polyacrylamide Gel Electrophoresis
SEC	Size exclusion chromatography
SOW	Synthetic Ocean Water
TAC	Tri-Chloro Acetic Acid
TOCSY	Total Correlation Spectroscopy
UV	Ultraviolet
X-gal	5-bromo-4-chloro-indolyl-β-D-galactopyranoside

1

Introduction

1.1 Cyanobacteria

Cyanobacteria are abundant and globally distributed photosynthetic organisms occupying a wide range of habitats including freshwater, oceans, hot springs, deserts *etc* (Thomas, 2005; Heywood *et al.*, 2006). Cyanobacteria are known as the first and the most important oxygenic photosynthetic prokaryotes converting the early reducing atmosphere into an oxidizing one and dramatically changing the composition of life forms on Earth (Gupta *et al.*, 1992; Shi *et al.*, 1992a; Cavet *et al.*, 2003; Williams and Silva, 2003). Also, cyanobacteria became the first organisms that had to face the oxidised metal forms in the new aerobic environment (Cavet *et al.*, 2003).

Today, cyanobacteria are still crucially important in global biogeochemical cycles including carbon cycling; especially two marine genera, *Prochlorococcus* and *Synechococcus*, which are responsible for approximately 20–40 % of global carbon fixation although they are only accounting for 1% of photosynthetic biomass (Partensky *et al.*, 1999; Ono and Cuello, 2007; Jardillier *et al.*, 2010). Cyanobacteria are also the only phototrophic organisms that are able to fix nitrogen (Karl *et al.*, 2002).

1.2 Marine *Synechococcus* molecular ecology

Marine *Synechococcus*, comprising marine sub-cluster 5.1 (Herdman *et al.*, 2001), are widely distributed in oceanic waters, occupying polar, temperate, tropical and sub-tropical waters, which encompass both mesotrophic and oligotrophic conditions (Partensky *et al.*, 1999; Heywood *et al.*, 2006; Zwirglmaier *et al.*, 2007; Zwirglmaier *et al.*, 2008; Scanlan *et al.*, 2009). The north and south Atlantic gyres are excellent examples of oligotrophic open ocean waters with nanomolar nutrient levels but a relatively constant ecosystem. In contrast, coastal environments encounter a more erratic nutrient supply, and are a generally more variable ecosystem because of wind-driven inputs from the deep ocean and riverine inputs from land (Palenik *et al.*, 2006a; Zwirglmaier *et al.*, 2007; Zwirglmaier *et al.*, 2008; Scanlan *et al.*, 2009; Stuart *et al.*, 2009).

Synechococcus 5.1 subcluster was subdivided into 10 lineages based on 16S rRNA gene analysis (Fuller *et al.*, 2003b). The ecological data for marine *Synechococcus* were summarised by Scanlan *et al.* (2009) including the four most abundant lineages, clades I to IV (Table 1.1). *Synechococcus* clade IV and I show high abundance at high latitudes i.e. above 30°N and below 30°S. In contrast, clade II proliferates in subtropical and tropical latitudes between 30°S and 30°N; clade III demonstrated no particular latitude preference but appears to be confined to a fairly narrow range of macronutrient concentrations e.g. nitrate and phosphate in the nanomolar range, and hence can be considered an oligotrophic lineage (Zwirglmaier *et al.*, 2008; Scanlan *et al.*, 2009).

Table 1.1 Overview of the broad ecological conditions of marine Synechococcus clades in subcluster 5.1 (from Scanlan et al., 2009).

Clade	Ecological conditions of largest relative abundance
I	Coastal and/or temperate mesotrophic open ocean waters largely above 30°N and below 30°S
II	Offshore, continent shelf, oligotrophic tropical or subtropical waters between 30°N and 30°S
III	Ultra-oligotrophic open-ocean waters
IV	Coastal and/or temperate mesotrophic open ocean waters largely above 30°N and below 30°S
V/VI/VII	Relatively wide distribution but in low abundance in various oceanic waters; have been seen to dominate mesotrophic upwelling regions, e.g., Arabian Sea, while clade VII genotypes specifically have been shown to dominate in the Costa Rica upwelling dome

Correspondence of molecular ecology and special distribution patterns of specific marine *Synechococcus* lineages demonstrate the existence of connection between physiological properties and environmental factors.

1.3 Metal utilisation by marine Cyanobacteria

As phototrophic prokaryotes, cyanobacteria require specific trace metals ions to implement the oxygenic photosynthetic process including iron for iron-sulfur clusters, cytochromes and non-heme iron, manganese for the water-splitting complex, copper for Plastocyanin (Pc) and magnesium for chlorophylls (Morel *et al.*, 1979; Raven *et al.*, 1999; Cavet *et al.*, 2003). (Morel *et al.*, 1979; Raven *et al.*, 1999; Cavet *et al.*, 2003). It is generally agreed that cyanobacteria are responsible for changing the early reducing atmosphere into an oxidising one. As a consequence, these organism were amongst the first that had to cope with the changes in the chemical composition that the oxygenation brought (Gupta *et al.*, 1992; Shi *et al.*, 1992a; Cavet *et al.*, 2003; Saito *et al.*, 2003; Williams and Silva, 2003). For metal ions, the oxidising condition meant a significant increase of the availability of zinc, cadmium and copper, and a dramatic decrease of ion, cobalt, nickel and manganese (Da Silva and Williams, 2001; Williams, 2011).

It has been suggested that cyanobacteria are capable of releasing trace metal-binding molecules into their environment to modulate their bioavailability and influence the biogeochemical cycling of these metals (Leão *et al.*, 2007). For example, Rue and Bruland (1995) reported two classes of Fe(III) ligands L1 and L2 in seawater, which are siderophores released by cyanobacteria (Wells and Trick, 2004; Leão *et al.*, 2007).

Cyanobacteria play a crucial role in metal utilisation, not only scavenging trace metals essential for their growth, but also to keep toxic trace metals from

reaching intolerable levels (Leão *et al.*, 2007; Blindauer, 2008a; Pokrovsky *et al.*, 2008). Trace metal concentrations vary due to several processes including external sources (hydrothermal inputs, rivers, aerosol deposition) and removal processes (biological uptake, burial in marine sediments) (Bruland and Lohan, 2006). The GEOTRACES project, an International program focusing on marine geochemistry, has been established to monitor trace metal concentrations in seawater across the world (see http://www.geotrace.org/). For example, dissolved zinc and cadmium concentrations in oceanic waters range between 0.19 and 7.12 nM, 0.23 to 0.88 nM respectively (see Figure 1.1 and Table 1.2; Aparicio-González *et al.*, 2012). Both metal excess and limited metal availability can generate a metal stress response in cyanobacteria. Therefore, intracellular metal homeostasis mechanisms play a vital role in cyanobacterial growth.

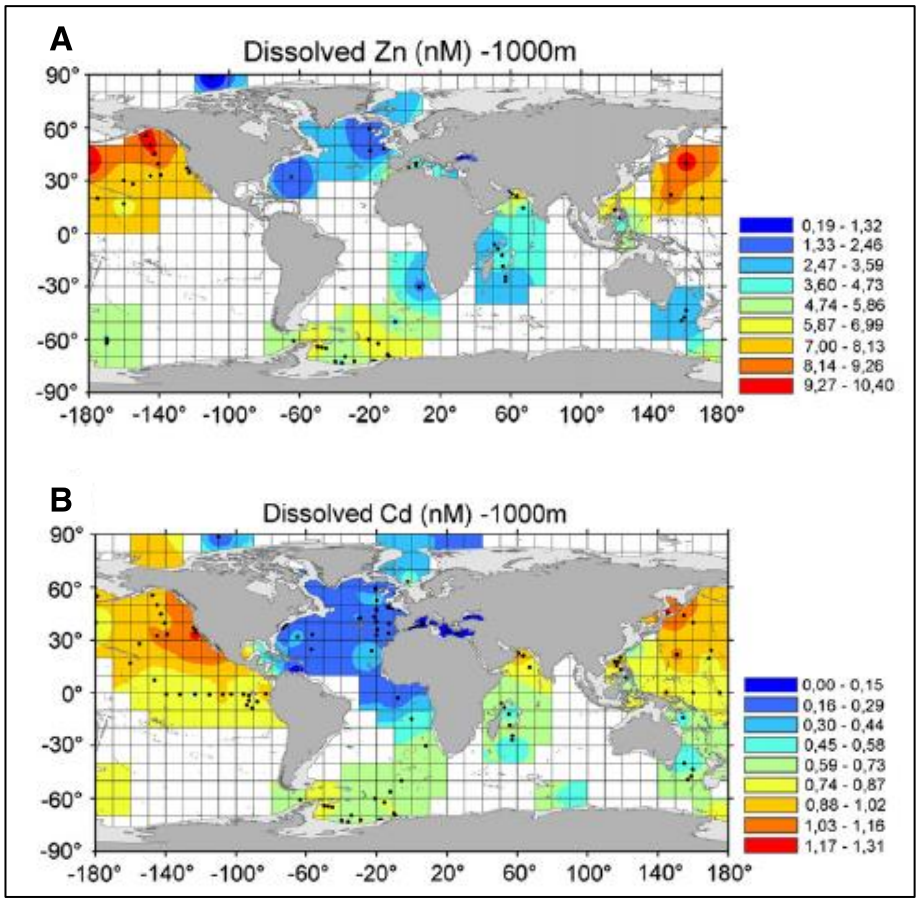

Figure 1.1. Concentration of dissolved Zn (A) and Cd (B) in marine ecosystems. (Adapted from Aparicio-González et al., 2012).

Table 1.2. The average oceanic concentration of dissolved trace metals reported at 1000 m depth (measurements taken between 1976-2009). SDV: Standard deviation; n: number of samples. (Adapted from Aparicio-González *et al.*, 2012).

		Arctic	Atlantic	Indian	Pacific	Southern
Cd (nM)	Average	0.43	0.23	0.70	0.88	0.69
	SDV	0.3	0.1	0.2	0.2	0.1
	n	2	55	9	56	23
Co (pM)	Average	nd	80.80	nd	27.39	28.82
	SDV		83.5		13.3	11.2
	n		12		21	14
Cu (nM)	Average	2.40	1.53	1.43	2.24	2.55
	SDV		0.5	0.3	0.8	0.4
	n	1	60	11	34	23
Mo (nM)	Average	nd	151	nd	102.12	nd
	SDV				6.7	
	n		1		12	
Ni (nM)	Average	nd	4.31	6.24	8.40	6.52
	SDV		1.3	1.3	1.6	0.4
	n		47	11	19	20
Pb (pM)	Average	nd	97.32	58.75	19.70	12.94
	SDV		55.9	69.1	6.6	6.7
	n		11	4	23	17
Zn (nM)	Average	0.19	3.35	4.21	7.12	5.60
	SDV		2.0	1.8	2.3	1.3
	n	1	12	10	24	26

Cyanobacteria have developed various mechanisms to respond to these challenges, which have been studied by several authors e.g. Cerda *et al.* (2008) and Los *et al.* (2008). Copper is an essential element for the synthesis of plastocyanin and cytochrome *c*. These two proteins can replace each other to fulfil the same biological function: when the copper concentration falls below a certain level, many cyanobacteria, such as *Synechocystis* PCC 6803 synthesise the soluble electron carrier cytochrome c (encoded by *petJ*) instead of plastocyanin (encoded by *petE*) (Sandmann *et al.*, 1983; Zhang *et al.*, 1992; Cavet *et al.*, 2003; Cerda *et al.*, 2008). Synthesis of one protein or another, in

response to the copper concentrations in the medium, has added a further dimension to copper homeostasis in cyanobacteria.

Iron is an essential metal for all photosynthetic organisms (Cerda *et al.*, 2008), most studies in iron handling by cyanobacteria have focused on iron deficiency (Sen *et al.*, 2000; Katoh *et al.*, 2001; Singh *et al.*, 2003), and less is known about iron excess. In *Synechocystes*, iron deficiency will increase the expression levels of *isiA* (a gene coding for an additional antenna system around photosystem I PSI), *isiB* (coding for flavodoxin) and *isiA* (coding for an integral subunit of PSII) (Kunert *et al.*, 2003; Lax *et al.*, 2007). The *fut* genes (*futA1*, *futA2*, *futB* and *futC*), codifying for an ABC-type ferric iron transporter in *Synechocystes*, have been identified to play major role in iron acquision (Katoh *et al.*, 2001). Although there is no experimental evidence, a potential iron repressor, *fur*, can be tentatively assigned in a noticeable number of picocyanobacterial genomes, indicating that there is a means of regulating iron homeostasis in these organisms (Scanlan *et al.*, 2009).

Zn is recognised as an essential element for the majority of living organisms (Sousa *et al.*, 2007). In aquatic photoautotrophs including cyanobacteria, zinc is believed to be required for carbonic anhydrase and alkaline phosphatase. There is evidence for zinc and carbon co-limitation in marine phytoplankton (Morel *et al.*, 1994). Several putative systems involved in zinc homeostasis have been identified in cyanobacteria, including the putative high-affinity ABC transporter (*znuABC*) and regulator (*zur*) which are participating in zinc uptake systems were

found in most stains of marine cyanobacteria (Cavet *et al.*, 2003; Blindauer, 2008b; Scanlan *et al.*, 2009). The zinc-specific efflux pump ZiaA and its regulator ZiaR (a zinc-specific repressor protein) has been identified in the freshwater cyanobacterium *Synehcocystis* sp. PCC 6803 (Thelwell *et al.*, 1998). However, most marine cyanobacterial strains show lack of zinc-specific efflux pumps (Blindauer, 2008b; Scanlan *et al.*, 2009), which could be an adaption to their low zinc concentration environment. Instead, some marine cyanobacteria developed a zinc storage mechanism, the bacterial metallothioneins (BmtAs; Blindauer, 2008b), to cope with occasionally zinc excess. It is reported that when exposed to several divalent metal cations, the transcription of metallothionein in *Synechococcus* sp. PCC7942 is enhanced for example with 1 μM of cadmium; the same effect is observed for copper and zinc (Huckle *et al.*, 1993; Ybarra and Webb, 1999). In *Synechococcus* sp. PCC7942, the zinc sensor SmtB regulates *smtA* (encoding metallothionein), which in turn triggers internal zinc sequestration (Thelwell *et al.*, 1998; Cavet *et al.*, 2003).

1.4 Metallothioneins and their biological function

Metallothioneins (MTs) are cysteine-rich proteins of low molecular weight, usually 5-10 kDa, and are usually occupied with multiple ions, such as zinc and copper or even the toxic cadmium ion (Nies, 2003; Silver and Phung, 2005; Robinson, 2008).

The first metallothionein was reported in 1957 (Vallee, 1957) and since this time research on metallothioneins has been on-going. Genes encoding metallothioneins are found in all kingdoms, from prokaryotic to eukaryotic, from bacteria to plants, from worms to mammals (Nordberg *et al.*, 1972; Kägi, 1993; Vasak and Kägi, 1994; Thelwell *et al.*, 1998). So far, over 1600 metallothionein-encoding genes can be retrieved form the Protein Information Resources (PIR) (Wu *et al.*, 2003): animal and plant MTs dominate the collection, with of 44% and 39%, respectively. Prokaryotic and fungal MTs only contribute a small portion, 8% of each (Figure1.2A). The ubiquity of MTs in all kingdoms strongly demonstrate their significant importance in life processes.

A

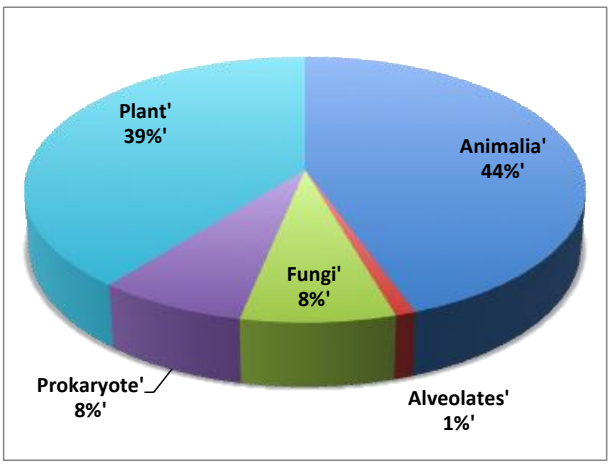

B

I	Vertebrate
II	Mollusc
III	Crustacean
IV	Echinodermata
V	Diptera
VI	Nematoda
VII	Ciliata
VIII	Fungi I
IX	Fungi II
X	Fungi III
XI	Fungi IV
XII	Fungi V
XIII	Fungi VI
XIV	Prokaryote
XV	Plant

Figure 1.2. The Distribution of MTs. (A) An analysis of the MTs retrieved form the PIR database (Wu et al., 2003). (B) The 15 subfamilies of the MT family.

A nomenclature system for MTs was adopted in 1978 (Nordberg and Kojima, 1979) and this was extended in 1985 by introducing a subdivision of all MTs into three classes (Fowler *et al.*, 1987) based on their sequence similarities and phylogenetic relationships. Class I MTs are defined to contain polypeptides related in primary structure to mammalian MTs, while class II includes those MTs with very distant evolutionary relationships to mammalian forms. Class III MTs contain enzymatically synthesised polypeptides (phytochelatins and cadcystins) comprising atypical γ–glutamylcysteinyl units (Rauser, 1990). As more and more MT sequences have been found, MTs have become subdivided into families, subfamilies, subgroups, isoforms and allelles. The MT family has now grown into 15 subfamilies described by Binz and Kägi in 2001 (see http://www.bioc.unizh.ch/mtpage/MT.html), as shown in Figure 2.2B.

MTs differ from other metal-containing proteins by their much larger metal content, their unusual bioinorganic structure and their kinetic lability which enable them to participate in rapid metal transfer, metal regulatory processes and protection from metal toxicity (Vasak and Kägi, 1994; Nordberg and Nordberg, 2009). In the past decades, numerous researches projects have been accomplished to study the biophysical properties (Blindauer and Leszczyszyn, 2010) and biological functions (Davis and Cousins, 2000; Cobbett and Goldsbrough, 2002; Klaassen *et al.*, 2009) of MTs. It has been accepted that MTs can function in heavy metal detoxification: two MT genes have been identified to be differentially unregulated in the presence of cadmium and copper in *Drosophila melanogaster* (Egli *et al.*, 2006a), and the respective knockout mutants of MT show increasing sensitivity in the presence of cadmium and

copper (Egli *et al.*, 2006b). Those observations demonstrate these MT are capable of protection against cadmium and copper excess.

Metallothioneins are not only associated with heavy metal ions, but also may respond to various other stresses, such as ionising radiation, which can also trigger the expression of mammalian MTs (Karin *et al.*, 1985). In plants, drought, osmotic and even temperature could also regulate the expression of MTs, as demonstrated for example in the embryos of Douglas-fir (Chatthai *et al.*, 1997). Recent studies of two MTs in *Caenorhabditis elegans* demonstrate that MTs are able to function as free radical scavengers themselves, and therefore potentially protect against oxidative stress (Zeitoun-Ghandour *et al.*, 2011).

MT associated zinc homeostasis is a popular hypothesis. Evidence for studied mammalian MTs has shown that, at least for vertebrates, MTs may play a role as zinc ion transporters to carbonic anhydrase (Jacob *et al.*, 1998) and zinc finger peptides (Hathout *et al.*, 2001), consistent with function in essential Zn homeostasis (Maret, 2009; Colvin *et al.*, 2010).

To summarise, MTs are capable of functioning as heavy metal scavengers, defenders against oxidative stress, and intracellular metal distributers and detoxifiers (Palmiter, 1998; Gold *et al.*, 2008). They may also serve a storage function storing copper and zinc when there are at elevated levels (Kelly *et al.*, 1996).

1.5 Bacterial metallothioneins

1.5.1 Discovery and Regulation

The first prokaryotic metallothionein was detected by Olafson *et al.* from a marine cyanobacterium *Synechococcus* sp. RRIMP N1 (Olafson *et al.*, 1979a; Olafson *et al.*, 1980; Cavet *et al.*, 2003). Since then, more bacterial metallothioneins (Bmts) have been isolated, and the mt gene, *smtA* from *Synechococcus* sp. PCC7942 was identified in 1990 (Robinson *et al.*, 1990), as a prototype of prokaryotic metallothionein, is the first extensively characterised prokaryotic metallothionein (Blindauer *et al.*, 2001). The production of SmtA was shown to be regulated by the zinc sensing repressor SmtB (Huckle *et al.*, 1993). The apo form SmtB is able to bind to the *smtA* operator promoter to inhibit its expression; and when the zinc concentration exceeds a critical level, zinc ions will bind to SmtB and lead to a conformational change that allow *smtA* expression. Once the zinc concentration returns to the acceptable level, the apo form of SmtB again represses SmtA expression.

1.5.2 Structure and function

Bacterial MTs, BmtAs, have a number of special features that distinguish them from other metallothioneins. The most important characteristic of BmtAs is a zinc finger-like protein fold. Also, they contain conserved aromatic residues including histidine while other MTs do not. Metallothioneins and zinc fingers were thought to be restricted to eukaryotes, but now it is known that, besides Pseudomonads and some proteobacteria, a significant number of both freshwater

and marine cyanobacterial strains also contain MT genes (Blindauer, 2008a; Blindauer, 2009). Besides, it is essentially true that the BmtAs show very little sequence similarity to all of previously characterized MTs except for the high cysteine content (Olafson *et al.*, 1988; Blindauer and Leszczyszyn, 2010).

The three-dimensional structure of SmtA was determined using zinc and cadmium loaded SmtA (Blindauer *et al.*, 2001), nine cysteine and two histidine residues formed a $Cys_9His_2Zn_4$ metal binding cluster (Figure 1.3). The metal binding site A (formed by Cys 9, Cys 14, Cys 32 and Cys 36) is the zinc finger site that is insert towards metal exchange and displays shower zinc release kinetics; the four ligands in this site are the only completely conserved ligands among all available BmtAs (Blindauer, 2011) (Figure 1.4). The site C (composed by Cys 16, Cys 32, Cys 47 and His 49) is the most accessible in SmtA, and plays a crucial role in the zinc transfer reaction from SmtA (Blindauer *et al.*, 2007a; Leszczyszyn *et al.*, 2007a). The histidine residue (His49) especially, provides a strong but solvent accessible zinc ligand in the protein. Also, a multiple sequence alignment of all available bacterial metallothioneins reveals that sequence variations occur predominantly around this residue (Figure 1.3), and this region is termed the variable loop (Blindauer *et al.*, 2007a).

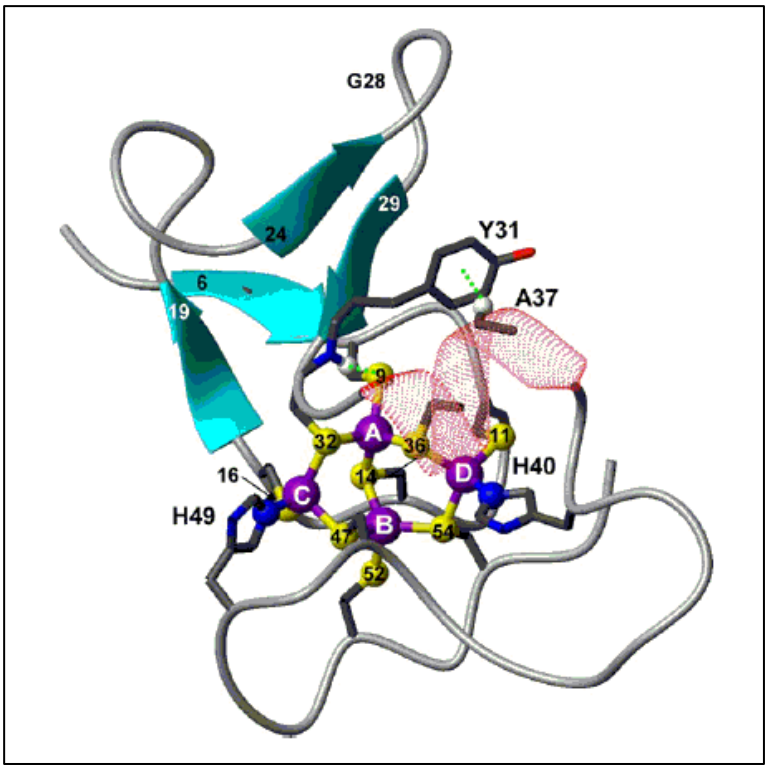

Figure 1.3. Solution structure of SmtA from Synechococcus sp. PCC7942. A, B, C, and D are the metal ion binding-sites, alpha-helical and beta-strand regions are designated in red and cyan respectively (Blindauer et al., 2001).

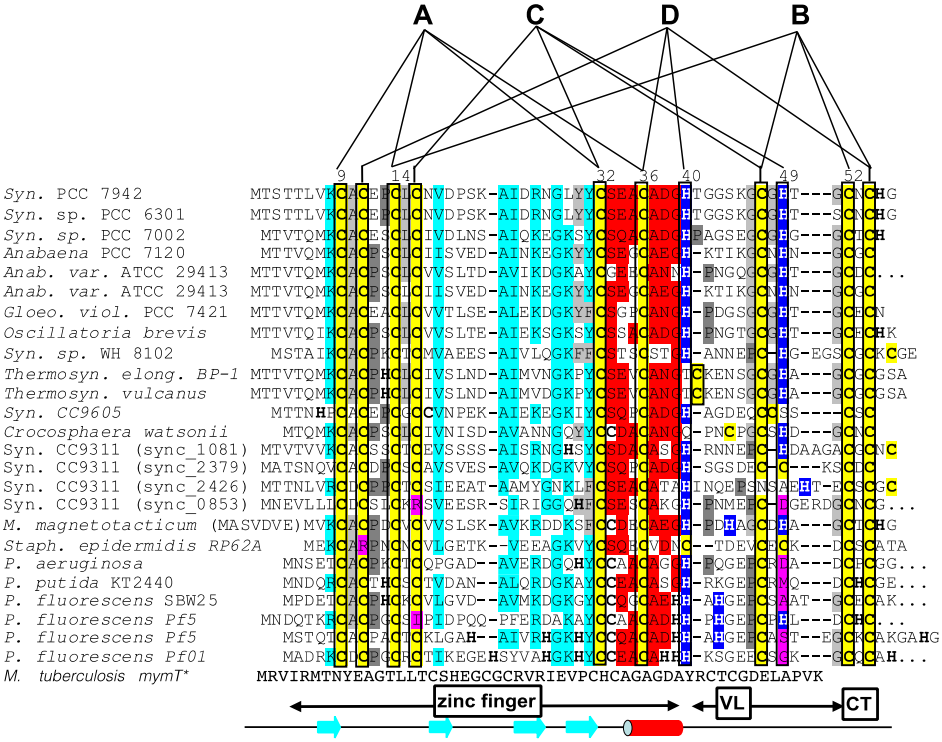

Figure 1.4. Multiple sequence alignment of available bacterial metallothioneins. A, B, C and D are the metal ion binding sites, Cys and His residues are highlighted in Gold and Blue; zinc finger fold residues (α-helices and β-strand) are highlighted in Red and Cyan respectively; grey indicates semi-conserved residues, Pro residues in vicinity to metal-binding residues are highlighted in dark grey; magenta highlights residues in positions of metal-binding residues (redrawn from Blindauer et al., 2007). *Metallothionein discovered during a screen for resistance against a potential drug, but show no revolution relation with BmtA.

However, the site C is more conserved in sequences from freshwater cyanobacterial species (CxH motif), while the majority of marine species demonstrate a CH or CC motif or have even lost these residues (Blindauer *et al.*, 2007a; Leszczyszyn *et al.*, 2007a). Besides, not all cyanobacteria contain a bacterial metallothionein gene. Of 45 species analysed 22 had the gene for

metallothionein (Blindauer, 2008a). Therefore, metal binding properties of marine and freshwater cyanobacterial metallothioneins are expected to be quite distinct due to the differing environments they inhabit (Blindauer, 2008a). With this in mind, we hypothesise that specific marine cyanobacterial MTs, with potentially different metal binding properties, are expressed under particular environmental conditions.

Apart form their abilities associated with intracelluar metal ions, BmtAs have also been reported to be able to scavenge free radicals (e.g. oxygen and nitrogen species ROS, RNS) therefore protect cells from their toxic effects (Cai *et al.*, 2000; Zhou *et al.*, 2002). Transcription of the freshwater cyanobacteria MT SmtA is elevated when cells are exposed to excess of zinc, cadmium, copper and etc., which provided evidence of its role of heavy metal detoxification; and a recent study, by transinfecting *E.coli*, SmtA provided protection to *E.coli* form certain forms of oxidative stress, which could be a hint towards further functions of BmtAs (Davis, 2011).

1.6 *Synechococcus* sp. CC9311 and its metallothionein genes

The marine cyanobacterial strain *Synechococcus* sp. CC9311, isolated from the California Current in the Pacific Ocean, had its complete genome sequence characterised in 2006 (Palenik *et al.*, 2006b). As a member of clade I *Synechococcus* sp. CC9311 is thought to be a ‘coastal/opportunist’ strain,

occupying coastal areas containing relatively high nutrient levels, but having to cope with a fairly variable environment (Zwirglmaier *et al.*, 2008). Moreover, this *Synechococcus* strain has been postulated to have a greater need for metals in its coastal habitat, or a greater need to respond to excess metal ions, or that cells experience episodic metal concentrations (Palenik *et al.*, 2006b).

Genome analysis demonstrates that this coastal strain is significantly different from open ocean strains occupying more stable environments. Thus, *Synechococcus* sp. CC9311 contains a higher number of two-component systems compared to open ocean strains e.g. 11 histidine sensor kinases and 17 response-regulators, while there are only about half (five sensor kinases and nine response regulators) in the open ocean strain *Synechococcus* sp. WH8102 (Palenik *et al.*, 2006b; Dufresne *et al.*, 2008). The functions of those extra sensors are not known yet, but it is possible that they are involved in more complex metal regulation (Palenik *et al.*, 2006b), which could include metal homeostasis.

It has also been reported that *Synechococcus* sp. CC9311 has a number of metal enzymes or cofactors not present in open ocean strains, including a FeoA/B ferrous iron transporter and five bacterial ferritins compared to one in most cyanobacterial genomes (Palenik *et al.*, 2006b). Surprisingly, genome analysis also demonstrates that *Synechococcus* sp. CC9311 has a great capacity for metal storage/homeostasis by containing four metallothionein genes (*sync_0853, sync_1081, sync_2379 and sync_2426*), while other marine *Synechococcus* strains contain only one, or none (Palenik *et al.*, 2006b; Scanlan *et al.*, 2009).

1.7 Aims and objectives

As described before, I hypothesise that specific cyanobacterial MTs, with potentially different metal binding properties, are expressed under particular environmental conditions.

I believe the marine cyanobacterium *Synechococcus* sp. CC9311 is a potentially excellent model system to test this hypothesis given it contains four metallothionein genes, *sync_1081, sync_0853, sync_2426, sync_2379,* while the majority of cyanobacteria appear to contain only one, while also possessing a metal-intensive physiology (see section 1.7). Interestingly, the four MT proteins of *Synechococcus* sp. CC9311 display sequence variations (Figure 1.3) around one particular metal binding residue (His49 in the prototype SmtA from *Synechococcus* sp. PCC7942) (Figure 1.3) in the variable loop. Compared with SmtA (C47-x-H49 motif), *sync_0853* has lost the H49 whilst *sync_1081* and *sync_2379* contain a C-H and C-C linkage respectively and *sync_2426* has lost these residues. These variations are expected to influence not only metal content and affinity, but also metal ion transfer kinetics.

The ultimate aim of this project is to establish the relationship between environmental factors, expression patterns and biophysical properties, including metal thermodynamics and kinetics, and the structure of expressed proteins.

To test the hypothesis stated above, it is highly desirable to investigate the relationship between the biophysical properties of the four MT homologues and their expression pattern under different conditions, including:

1. Comprehensively characterize the metallothionein proteins in *Synechococcus* sp. CC9311, including their metal-binding affinity and specificity, protein folding and structure, and metal uptake and release kinetics;
2. Culture *Synechococcus* sp. CC9311 in defined media with different trace metal composition, and assess the effects of metal toxicity and deficiency on bacterial growth, in comparison to other *Synechococcus* strains;
3. Investigate differential expression of metal-handling genes, with a focus on metallothioneins.

2

Materials and Methods

2.1 Bacterial Strains and Culture Conditions

2.1.1 *Escherichia coli* strains and maintenance

The *Escherichia coli* strains used to reconstruct plasmids and produce recombinant proteins are described in Table 2.1. The *Escherichia coli* stock strains were streaked onto solid Luria-Bertani (LB) agar (section 2.1.2) with antibiotics (section 2.1.2) and grown at 37°C. Agar plates were kept at 4°C for up to four weeks. For longer storage, overnight cultures were prepared at 37°C, and then mixed with 1 volume of sterile 70% v/v glycerol, and snap frozen with liquid nitrogen before storing at -80°C. The -80°C stocks were thawed on ice and streaked on plates followed by growth in LB medium overnight to recover strains when necessary.

Table 2.1 Escherichia coli strains used in this study, including genotypes, resistance and supplier.

Strain	Genotype	Resistance	Supplier
Cloning strains			
TOP10	F– *mcr*A Δ(*mrr-hsd*RMS-*mcr*BC) Φ80*lac*ZΔM15 Δ*lac*X74 *rec*A1 *ara*D139 Δ(*ara leu*) 7697 *gal*U *gal*K *rps*L (StrR) *end*A1 *nup*G	-	Invitrogen
DH5α	F– Φ80*lac*ZΔM15 Δ(*lac*ZYA-*arg*F) U169 *rec*A1 *end*A1 *hsd*R17 (rK–, mK+) *pho*A *sup*E44 λ– *thi*-1 *gyr*A96 *rel*A1	-	Invitrogen
Expression strain			
Rosetta (DE3) α	F – *ompT hsd*SB(rB– mB–) *gal dcm* (DE3) pRARE6 (Cm^r)	Cm^r	Invitrogen

2.1.2 *Escherichia coli* culture media and growth conditions

All *Escherichia coli* strains were cultured in Luria-Bertani (LB) broth (Gibco^{R}), containing 10 g peptone 140, 5 g yeast extract and 5 g sodium chloride per liter. When cultures were used for protein expression 10% (w/v) glucose was added. Then pH was adjusted to about 7.0 with NaOH before sterilising at 121°C for 30 minutes. LB agar plates contained 15 g bactoagar per litre.

2.1.3 Cyanobacterial strains and maintenance

The non-axenic marine cyanobacterial strain *Synechococcus* sp. CC9311, and two axenic *Synechococcus* strains, WH8012 and WH7805, were used in this study, provided by D. Scanlan, School of Life Sciences, University of Warwick. *Synechococcus* CC9311 is a coastal strain; WH7805 is more a generalist, while *Synechococcus* WH8012 is an open-ocean strain. All cyanobacterial stocks were maintained at 23°C with a continuous 5 μE m^{-2} s^{-1} white light and sub-cultured every month by 10 fold dilution into fresh medium.

2.1.4 Cyanobacteria growth media

All cyanobacterial strains *Synechococcus* sp. CC9311, WH8102 and WH7805 were cultured in artificial seawater Aquil medium pH8.0-8.1 unless otherwise stated. Aquil medium is originally developed by Morel *et al.* (1979) and Price *et*

al. (1989), and modified by Sunda *et al.* (2005). This medium is used in trace metal studies and rich with macro- and micronutrients.

To prepare the Aquil medium, three solutions were prepared separately: synthetic ocean water (SOW), major nutrients and trace metals (Table 2.2). SOW is autoclaved at 120°C for 15 minutes, and the major nutrients and trace metal solutions were filter sterilised. To remove trace metals, the SOW solution went through a chromatography column fitted with Chelex 100, which comprised a styrene-dicinyl benzene matrix derivatized with an iminodiacetate functional group that chelated trace metals (e.g. iron, copper, zinc, cadmium, nickel, cobalt), and collected in acid-treated polycarbonate vessels (Sunda *et al.*, 2005). The MilliQ 185 Plus water system (Millipore UK Ltd) was used to obtain water for all media and buffers. All chemicals used in this growth media were purchased from Fisher Chemicals unless stated otherwise.

Table 2.2: Composition of Aquil medium

SOW[C]	**Final concentration**
NaCl	400 mM
$MgCl_2.6H_2O$	41 mM
Na_2SO_4	21.6 mM
$CaCl_2.2H_2O$	7.9 mM
KCl	7 mM
KBr	0.63 mM
H_3BO_3	0.372 mM
$SrCl_2.6H_2O$	0.0488 mM
NaF	0.0476 mM

Table 2.2: Continued

Major nutrients	Final concentration
$Na_2EDTA\text{-}2H_2O$ [TS]	0.113 mM
$NaNO_3$ [C]	9.0 mM
K_2HPO_4 [C]	0.0875 mM
Na_2CO_3	0.0968 mM
$NaHCO_3$	1.97 mM
HEPES pH8.0 TS	1.5 mM

Trace Metals	Final concentration
$CoCl_2$	0.086 µM
$MnCl_2.4H_2O$	7.1 µM
$Na_2MoO_4.2H_2O$	1.61 µM
Citric acid hydrate	29.7 µM
$NiCl_2.6H_2O$	0.01 µM
$ZnSO_4.7H_2O$*	0.772 µM
$FeCl_3$*	8 µM

[C]: Chelex-treated
[T]: Trace metal grade
[S]: pH with trace metal grade NaOH
* Stored separately

2.1.5 Cyanobacterial growth conditions

All cyanobacterial cultures were grow in Aquil medium, shaking at 23°C, with continuous white light at 5 µE $m^{-2}s^{-1}$. For the purpose of characterising cyanobacterial growth, cells were cultured in 100 mL chelex-treated Aquil medium. However, in order to extract sufficient RNA during time courses, cultures were grown in 400 mL volumes.

2.1.6 Routine check for contamination

In order to verify that *Synechococcus* sp. WH8102 and WH7805 strains remained axenic, cultures were streaked on ASW contamination plates, containing 0.05% (w/v) yeast extract, and 1.5% (w/v) agar. The plates were incubated at 30°C for 72 hours in the dark. If there was no heterotrophic bacterial growth, the culture was assumed to be axenic.

2.1.7 Monitoring of bacterial growth

Optical density (OD) is a convenient direct measurement for monitoring of bacterial growth. Since cyanobacterial cells contain pigments whose concentration varies due to culture age and growth condition (TANG and VINCENT, 1998; Griffiths *et al.*, 2011), a wavelength outside the range of absorbance by pigments, 750 nm, was chosen to measure the optical density of cyanobacterial culture samples. For heterotrophic bacterial growth i.e. *Escherichia coli*, 600 nm was the wavelength used. Optical density was measured using either an UV/visible spectrophotometer Ultrospec 3000 (PHARMACIA) or an Inst UV-VIS spectrometer 335908P (Thermo Electron Sci) for cyanobacteria and *E. coli* cultures respectively.

2.1.8 Growth rate calculation

Cyanobacterial growth rates were calculated under the different growth conditions by the growth rate constant equation as shown in Equation (1).

$$\mu = \text{Log } 2 \times 1/t \times (\text{Log}A_t/\text{Log}A_0) \qquad (1)$$

μ = growth rate constant

A_t = Final population

A_0 = Initial population

t = Time (Hours)

2.2 Common Molecular Biology Techniques

2.2.1 Genomic DNA extraction from cyanobacteria

The method used to extract total genomic DNA from small-scale cyanobacterial cultures, especially *Synechococcus* was a modified method developed from Murray and Thompson (1980).

Reagents:

TE Buffer	10mM Tris/Cl, 1mM EDTA (pH8.0)
SDS solution	10% (w/v)
Phenol: chloroform	(v/v) 1:1
Phenol:chloroform:isoamylalcohol	(v/v) 25:24:1
Sodium acetate	3.5 M
Ethanol	100%, 70 %
Water	Nuclease free

Cyanobacterial culture (15 mL) was harvested by centrifugation at 5000 × g for 5 minutes at 4°C. The supernatant was removed and the pellet resuspended in 500 µl TE buffer, 0.5% (w/v) SDS, and the mixture incubated at 65°C for 1 hour. Following incubation, the mixture was transferred to a 1.5 ml Eppendorf tube, an equal volume of phenol added, mixed and left for 5 minutes on the bench. The mixture was then centrifuged for 5 minutes at 13,000 × g.

The aqueous layer was transferred into a fresh Eppendorf tube, an equal volume of phenol:chloroform (24:1) was added, mixed and left for 5 minutes on the bench, and then centrifuged for 5 minutes at 13,000 ×g. The aqueous layer was then extracted and mixed with an equal volume of phenol:chloroform:isoamylalcohol (25:24:1), mixed and left for 5 min on the bench, followed by further centrifugation for 5 minutes as above. The aqueous layer was transferred to a new Eppendorf tube before a 10% volume of 3.5 M sodium acetate and an excess of 100% (v/v) ethanol were added. The mixture then was incubated at -20°C for >2 hours, followed by centrifugation at 13,000× g for 30 minutes at 4°C to pellet the DNA before washing by adding 100 µl of 70 % (v/v) ethanol and centrifugation for 20 minutes at 13000 ×g at 4°C. The DNA pellet was then air-dried, resuspended in 100 µl sterile water, and frozen at -20°C until further use.

2.2.2 Polymerase Chain Reaction (PCR) general conditions

PCR reactions to amplify target genes were carried out in a total reaction volume of 50 µl unless otherwise stated. Each PCR reaction contained 1-10 ng template DNA, 2 µM of each forward and reverse primer, 800 µM dNTPs (from a 100 mM stock, Invitrogen), 500 µM $MgCl_2$ (from a 50 mM stock, Invitrogen), 5 µl Pfx50 10× PCR Reaction buffer, 5U Pfx50 DNA polymerase (Invitrogen) (see Table 2.4), and made up to 50 µl with sterilized MilliQ water. Primers used in PCR reaction were designed by the author as shown in Table 2.3. Primers for the two genes (*sync_2379* and *sync_2426*) were designed to be very specific 27- to 30-base single-stranded and with a single deoxythymidine (T) overhang in the pCR™ 2.1-TOPO® vector. The forward and reverse primer carried restriction site *Bam*H I and *Nde* I respectively. The template was *Synechococcus* sp. CC9311 genomic DNA in TE buffer (10mM Tris/HCl, 1mM EDTA, pH8.0)

Table 2. 3 Primers of sync_2426 and sync_2379. Restriction site of Nde I and BamH I are shown as underline.

sync_2379F	CACTCAACATATGGCTACTAGCAATCAAGT
sync_2379R	CGACGGATCCTCAGCAGCAATCGCAGC
sync_2426F	GTACCATATGACAACAAATCTTGTTCGG
sync_2426R	GATGGATCCTTAACAGCCGCAACTACA

Table 2.4 General PCR reaction reagents

Template DNA	1-10 ng
Forward and Reverse Primer	2 µM
dNTPs (dATP, dCTP, dGTP, dTTP)	800 µM
$MgSO_4$	500 µM
Pfx50 10× PCR Reaction buffer	5 µl
Pfx50 DNA polymerase	1 µl
Sterilised MilliQ water	x µl
Total volume	50 µl

PCR reactions were performed on a Biometra Tgradient T3000 Thermocycler. The general reaction cycle consisted of an initial denaturation step at 94°C for 2 minutes, followed by 35-40 cycles of denaturation at 94°C for 15 seconds and annealing at 55-60°C as required by the primers set for 30 seconds and extension at 72°C for 90 seconds. Then the reaction was finished with a 10 minutes final extension step at 72°C and kept at 4°C until use (Table 2.5).

Table 2.5. PCR Cycling Parameters

Steps	Temperature	Time	Cycles
Initial Denaturation	94°C	2 min	1X
Denaturation	94°C	15 sec	35-40 X
Annealing	55-60°C	30 sec	
Extension	72°C	90 sec	
Final Extension	72°C	10min	1X

2.2.3 Purification of PCR products

DNA fragments amplified from PCR reactions were purified using QIAquick Spin Columns (Qiagen, Germany). 5 volumes of PB buffer were added to the PCR products and applied to the PCR purification column and centrifuged at 13000 ×g for 1 minute. Subsequently, a further 500 µl PE buffer was added and the sample centrifuged for 1 minute at room temperature. The flow-through was discarded and the column was centrifuged for a further 3 minutes to remove any buffer residue. A fresh Eppendorf tube was then used and 50 µl PE buffer added and the column left at room temperature and followed by centrifugation for 1 minute. Then the PCR products were ready for sequencing or stored at -4°C until further use.

2.2.4 Agarose Gel Electrophoresis

Agarose gel electrophoresis was used to analyse the size of DNA fragments. Gels were prepared with Agarose HighMelt/Wide Range (Dustcher Scientific) in 1× TAE buffer (1.0 mM EDTA, 40 mM Tris/Acetate, pH 8.2-8.4) as shown in Table 2.6. A final concentration of 0.5 µg/ml ethidium bromide was added to the gel. Samples and appropriate DNA size markers (1kb DNA ladder, 100bp DNA ladder, Invitrogen) were gently mixed with 5× GelPilot Loading Dye (QIAGEN) before loaded onto the gel. Agarose gels were run in 1× TAE buffer using an electrophoresis PowerPac™ Basic (BIO-RAD) at a constant voltage of 90V.

Table 2.6 Percentage of agarose in the gel.

% (w/v) agarose used in the gel	DNA fragment size
0.8	> 3 kb
1	600 bp – 3 kb
2	< 600 bp

2.2.5 DNA extraction and purification from agarose gel

DNA fragments from agarose gels were purified using the QIAQuick Gel Extraction kit (Qiagen, Hilden, Germany). This kit could clean up DNA fragments between 70 bp to 10 kb in size. The mass weight of the excised gel was determined and the slice was placed in a 1.5 ml Eppendorf tube with 3 volumes of QG buffer. The mix was then incubated at 50°C for 10 minutes or until the gel slice completely melted. Then 1 gel volume of isopropanol was added and the mixture was applied to a QIAquick spin column and centrifuged for 1 minute. The flow-through was discarded and 0.75 ml PE buffer was applied to wash the column. To remove any residual wash buffer the column was centrifuged at 13000 x g for two 1 minute periods and new Eppendorf tubes were changed in between. To elute the DNA fragments, 30-100 µl EB buffer or water was added to the centre of the QIAquick column membrane and left at room temperature for 1 minute followed by one-minute centrifugation. The purified DNA fragments could be used for sequencing or ligation directly.

2.3 Gene Cloning Techniques

2.3.1 TOPO Cloning

TOPO cloning was used to clone the target genes *sync_2426* and *sync_2379* as insert using TOPO cloning kit purchased from Invitrogen. TOPO® TA Cloning® is a highly efficient cloning strategy designed for the direct insertion of *Taq* polymerase amplified PCR products. The key of TOPO cloning is the enzyme DNA topoisomerase I, which plays a role as both restriction enzyme and as a ligase. This enzyme specifically recognises the sequences 5'-(C/T)CCTT-3' and forms a covalent bond with the phosphate group attached to the 3' thymidine. The TOPO vectors are engineered with topoisomerase I covalent bond to each 3' phosphate, which enables the vector to readily ligate DNA sequences with compatible ends. The *Taq* DNA polymerase has a non-template activity, which will add a single deoxyadenosine (A) to the 3' end of PCR products called 3'-A overhangs. Therefore, the TOPO cloning can be complete in 5 minutes and neither ligase nor primers of specific sequence are required (Figure 2.1).

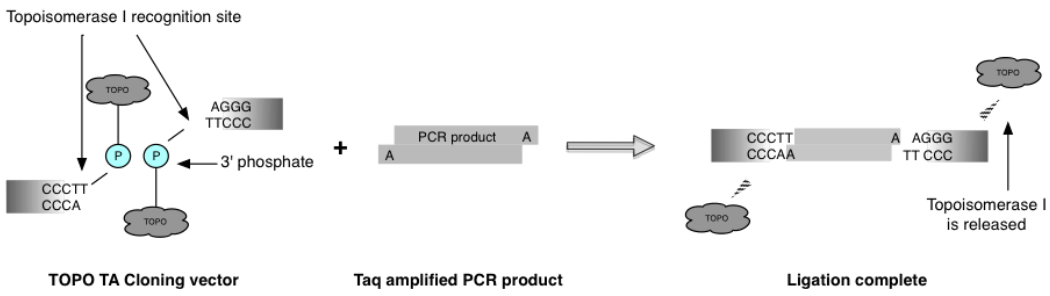

Figure 2.1: TOPO cloning with Taq amplified PCR product
(http://www.invitrogen.com/site/us/en/home/brands/Product-Brand/topo/The-Technology-Behind-TOPO-Cloning.html).

PCR products (Section 2.2.2) were extracted using QIAquick Gel Extraxtion kit purchased from Qiagen (Section 2.2.5) prior to TOPO cloning. TOPO cloning reaction was set up as shown in Table 2.7. The reaction was mixed gently and incubated at room temperature for 15 minutes.

Table 2.7 TOPO Cloning Reaction Setup

Fresh PCR product	4 µl
Salt solution	1 µl
TOPO vector	1 µl
Total volume	6 µl

3 µl of the annealing reaction were added directly to 50 µl of TOP10 *E. coli* cells and the mixture incubated on ice for 5 minutes, followed by heat shocking at 42°C for 1 minute, and then incubated on ice for 2 minutes. Finally, 250 µl of room temperature LB medium was added to the mixture and incubated at 37°C for 1 hour with shaking before plating on selective plates (50 µg/ml kanamycin, 20 µg/ml 5-bromo-4-chloro-indolyl-β-D-galactopyranoside (X-gal) dissolved in dimethyl formamide. The plates were incubated at 37°C overnight, and positive colonies were identified by Blue/White screening.

2.3.2 Blue/White screening

The Blue /White Screening is a widely used screening technique that allows for identification of successful recombinants in cloning. The β–galactosidase, a protein encoded by the *lacZ* gene, is able to react with 5-bromo-4-chloro-indolyl-

β-D-galactopyranoside (X-gal) and result in a characteristic blue colour. The vectors (such as the TOPO vector) carry the β–galactosidase gene, within the sequence there are multiple cloning sites, which can be cut by restriction enzymes, therefore foreign DNA can be inserted. Consequently, in cells containing the vector with an insert, no functional β–galactosidase can be produced, therefore colonies will appear white.

2.3.3 Restriction enzyme digestion of DNA

Restriction digestion was performed to cut the target gene from plasmids (TOPO vector and plasmid pET-26b(+) in this project). Restriction enzymes used in this project are the BamH I and Nde I (Invitrogen), digests of DNA fragments were carried out following manufacturer's guidelines. The digestion reactions were typically carried out in a volume of 20 µl consisting of 10U enzyme with the appropriate restriction buffer recommended for the enzyme. For the double digests, two restriction enzymes were mixed and all reactions were incubated at 37°C in a water bath for a period of 3 – 4 hours. Then the restriction fragments were analysed by agarose gel electrophoresis (see section 2.2.4).

2.3.4 Dephosphorylation of linearised vector DNA

Calf intestinal alkaline phosphatase CIAP (Invitrogen) was used to dephosphorylate the 5'-phosphorylated terminal of linearised vector DNA to prevent self-ligation. The dephosphorylation reaction consisted of 20 µl digested vector, 10 µl 10× CIAP buffer, 1U CIAP and sterile MilliQ water to a final volume of 100 µl. The reaction was carried out at 37°C in a water bath for 30

minutes and an extra 1U of CIAP was added and the incubation was prolonged for another 30 minutes at 37°C. The enzyme was then deactivated by incubating at 65°C for 15 minutes.

2.3.5 DNA Ligation Reaction

The digested DNA fragments and the linear vector pET-26b(+) were extracted from an agarose gel (section 2.2.5) and processed with a ligation reaction using T4 DNA ligase (Invitrogen).

The molar ratio of insert:vector was approximately 3:1. The insert DNA and the linearised vector were mixed gently with 1 µl 10× ligase buffer and 1U T4 ligase in a total volume of 10 µl. The mixture was then incubated at 25°C for 2.5 hours to overnight.

2.3.6 Preparation of *E. coli* chemically competent cells

LB medium (100 ml) was inoculated with 10 ml of an overnight culture of *E. coli* TOP10 and incubated at 37°C under agitation at 140 rpm until the optical density at 600 nm reached 0.4. The cells were then centrifuged at 3500 rpm and 4°C for 10 minutes, and the supernatant discarded. Cells were resuspended gently with 50 ml of ice cold 10 mM NaCl, and incubated on ice for 10 minutes followed by centrifuging again at 3500 rpm at 4°C for 10 minutes.

The cells were resuspended in 50 ml of ice cold 75 mM $CaCl_2$, and incubated on ice for 35 minutes and centrifuged at 3500 rpm at 4°C for 10 minutes. Ice cold 75

mM $CaCl_2$ (3 ml) was used to resuspend the cells, 0.488 ml ice cold 100% (v/v) sterile glycerol was added, and the cells incubated on ice for 1 hour. Aliquots of 50–100 µl cells were transferred into sterile 1.5 ml Eppendorf tubes that had been placed on dry ice. The chemically competent cells could be used directly after treatment or kept at -80°C until use.

2.3.7 Transformation of competent *E. coli* cells

The chemically competent *E. coli* cells (-80°C) were placed on ice to de-frost for 5 minutes. 0.5 – 1 µl DNA (plasmids or DNA fragments) was added to 50 µl competent cells and mixed gently, and then incubated on ice for 15 minutes. The suspension was then heat shocked at 42°C for 45 seconds in a water bath, followed by cooling on ice and supplemented with 250 µl pre-warmed LB medium, incubated at 37°C under agitation at 140 rpm for 60 minutes. The cells were then plated onto selective LB agar using the desired antibiotics, and incubated at 37°C overnight. The plates with recombinant colonies were sealed with parafilm and kept at 4°C.

2.3.8 Plasmid DNA extraction from *E. coli* cells

E. coli strains containing plasmid from frozen stock at -80°C or from colonies on an agar plate were used to inoculate 5 ml fresh LB medium containing appropriate antibiotics. The culture was then incubated at 37°C overnight under agitation at140 rpm. The cells were then centrifuged and plasmid DNA extracted using a QIAprep Spin Miniprep kit following the manufacturer's guidelines. The

plasmid purified on the column was eluted by 50 or 100 µl of EB buffer or sterile deionised water, and stored at -20°C until use.

2.3.9 DNA Sequencing

DNA sequencing was performed at the Molecular Biology service in the School of Life Sciences, University of Warwick. The template DNA was mixed with 5 pmol of primers in a total volume of 10 µl. The sequencing was carried out using the Applied Biosystems BigDye Terminator v3.1 cycle sequencing kit (Applied Biosystems, UK), and run on a 3130xl Genetic Analyzer. The consensus sequences were obtained using BioEdit software (http://www.mbio.ncsu.edu/bioedit/bioedit.html) and were analysed through BLAST (http://blast.ncbi.nlm.nih.gov/Blast.cgi).

2.4 RNA Techniques

2.4.1 Total RNA extraction from cyanobacteria

Total RNA extraction was carried out using a hot-phenol method (Gierga *et al.*, 2009) and modified by Dr. Millard (School of Life Science, University of Warwick)

Briefly, cells (50 mL) were harvested by centrifugation in 50 mL Falcon tubes at 4,754 ×g for 10 minutes at 4°C. The supernatant was discarded and the pellet re-suspended in 0.5 mL RNA suspension buffer (10mM NaAc, 200mM sucrose, 5mM EDTA, pH4.5), and then snap frozen in liquid nitrogen and stored at -80°C

until use. 1.5 mL Z6 extraction buffer (8M guanidinium hydrochloride; 50 mM beta-mercaptoethanol; 20 mM EDTA 20 mM MES; pH 7.0 with NaOH) was then added and the mixture left on the bench for 60 minutes to thaw. 0.75 mL ice-cold phenol pH 4.5 (Ambion®) was subsequently added, before incubation in a hot water bath at 65°C for 20 minutes. 0.75 mL$CHCl_3$:isoamyl alcohol (24:1) was added and the mixture left in the 65°C water bath for a further 10 minutes prior to centrifugation at 6,000 ×g for 10 minutes at 4°C. The top aqueous layer was then extracted and 1 volume of $CHCl_3$:isoamyl alcohol (24:1) added before centrifugation at 13,000 ×g for 10 minutes at 4°C. The top aqueous layer was then extracted and mixed with 1 volume ice-cold propan-2-ol and stored at -20°C overnight to precipitate the RNA. The sample was then spun at 13000 ×g at 4°C for 30 minutes to pellet the RNA, followed by washing with 70% (v/v) ethanol prior to centrifugation at 13,000 ×g for 20 minutes at 4°C. The ethanol was removed and the RNA air-dried and resuspended in 100 µL RNase-free water. Subsequently, DNase treatment was carried out to remove any DNA (89µL RNA, 10µL of turbo DNase buffer, 1µL of turbo DNase I, 37°C for 2 hours). Due to the size of the target RNA fragments (<250 bp), the sample was then precipitated with 3 volumes of EtOH/NaAc (30:1, 3M NaAc pH4.5) overnight at -20°C, prior to washing in 70% (v/v) ethanol and air drying. The sample was then stored at -20°C until further use.

2.4.2 Reverse Transcription of RNA

Reverse transcription was carried out in order to synthesise cDNA using Superscript III reverse transcriptase (Invitrogen). The method for reverse transcription followed the manufacturer's guidelines.

The concentration of samples were analysed on a NanoDrop 2000 Spectrophotometer (Thermo Scientific), which is able to measure absorbance spectra between 230–600 nm of both nucleic acid and proteins from 0.5 µl – 2.0 µl samples without cuvettes or capillaries. The lowest concentration was multiplied by 11 (Table 2.8), which would be the amount of total RNA (750-1000 ng per reaction, up to 5 µg) used in the reaction.

Reverse transcription reactions were performed in a total volume of 20 µl (Table 2.8) consisting of 1 µl of random hexamers (Fermentas 200 µg/µl), 1 µl dNTP mix (Invitrogen, 100 mM), RNA up to 11 µl max. The mixture was then heated at 65°C for 5 minutes before cooling on ice for 2 minutes. Then 4 µl 5× FS buffer, 10mM DTT, 40 U RNase inhibitor (Fermentas, 40 U/µl) and 200 U Superscript III RT were added and mixed gently followed by incubation at 25°C for 5 minutes, 60 minutes at 50°C and 12 minutes at 70°C before freezing at -80°C.

Table 2.8 Reverse transcription reaction components.

Random hexamers	1 µl
dNTPs	1 µl
RNA	x (≤11 µl)
RNase-free water	y µl
5× FS buffer	4 µl
10mM DTT	1 µl
RNase inhibitor	1 µl
Superscript III RT	1 µl
Total volume	20 µl

2.4.3 Primer and probe design for real time quantitative PCR (qPCR)

Primer oligonucleotides used for qPCR reactions were designed using the ABI PRISM Primer Express v2.0 software (Applied Biosystems, UK). The length of primers for qPCR should be 18–30 base-pairs and the G + C content of the primers may vary between 20 – 70% but the melting temperatures (T_m) of the primer pair should be less than 4°C different, and no more than two G/C bases should be present in the last five bases at the 3' end of the primer. When designing fluorescence labelled probes for qPCR, the T_m of the probe should be approximately 6-8 °C higher than the T_m of the primers, usually 68 - 70°C, and the length of the probe should be no more than 30 bases long to maximise the quenching of the fluorophore.

2.4.4 Real time quantitative PCR assays

Real time PCR assays were carried out to quantify the expression of specific genes during a time course experiment using a PrimTime qPCR assay (Integrated DNA Technologies, USA). Each real time PCR reaction was performed in a 25 µl volume in a MicroAmp optical 96-well Reaction Plate sealed with optical adhesive films (Applied Biosystems). The real time PCR assay was carried out using the TaqMan Universal PCR Master Mix (Applied Biosystems), PrimTime qPCR primers and probe, and 10 ng cDNA. Reactions were heated at 95°C for 10 minutes, then underwent 40 cycles of 95°C for 15 seconds and 60°C for 1 minute, performed on a 7500 Fast Real-Time PCR System (Applied Biosystems, UK).

2.5 Protein Purification Techniques

2.5.1 Production of recombinant proteins from *Synechococcus* sp. CC9311

A single *E. coli* colony containing the desired plasmid construct (see section 2.3.8) was picked and cultured in LB medium with appropriate antibiotics (typically 50 µg/ml kanamycin, 34 µg/ml chloramphenicol) at 37°C overnight. The next day, the overnight culture was inoculated into large-scale cultures (800 ml) and grown at 37°C with shaking (250 rpm) until the OD_{600} was between 0.6-0.8. 1 mM IPTG (isopropyl-β-D-thiogalactopyranoside), 0.5 mM $ZnSO_4$ was then added to induce protein over-expression. In order to optimise expression, a series of conditions were tested. In every condition, a time course experiment

was performed to monitor protein expression levels. Time points were taken at 0 hour, 1 hour, 3 hours, 4 hours, 5 hours, 6 hours and overnight after inducing. Cells were harvested by centrifugation (8,000 ×g for 15 min at 4°C), and the cell pellets frozen at -80°C until use. Protein expression levels were determined by SDS-PAGE Gel (Invitrogen) and silver staining (see sections 2.5.2 and 2.5.3).

2.5.2 Sodium Dodecyl Sulfate Polyacrylamide Gel Electrohoresis (SDS-PAGE)

SDS-PAGE was used to analyse recombinant proteins using Novex® NuPAGE SDS-PAGE Bis-Tris Gel (4%-12%) purchased from Invitrogen. *E. coli* cell pellet samples were resuspended in complete solubility protein buffer (1% (w/v) SDS, 2M Urea, 1.25% (v/v) 2-mercaptoethanol, 2.5% (v/v) glycerol, 15 mM Tris, pH 6.8) followed by heating at 95°C for 5 minutes. NuPAGE® LDS sample buffer was then added and mixed with pipetting (protein samples were mixed with sample buffer directly without heating). A protein ladder SeeBlue® Plus2 Prestained standard (Invitrogen) and 20 µl samples were gently loaded onto each polyacrylamide gel. The gel was placed in an electrophoresis tank, Mini-PROTEAN® Tetra System (BIO-RAD), with NuPAGE MOPS running buffer (Invitrogen), and run under constant voltage at 200 V.

2.5.3 Silver Staining of SDS polyacrylamide gels

The highly sensitive silver staining protocol (which detects protein in the low nano-gram range) was used to detect proteins in polyacrylamide gels (Goldberg and Warner, 1997). Freshly run polyacrylamide gels were placed in fixer solution (60 ml of 50% (v/v) acetone, 1.5 ml of 50% TCA, 25 µl 37% (v/v) formaldehyde) and gently shaken for 15 minutes to fix the proteins. The gels were then washed in MilliQ water with three quick washes, then five minutes shaking in MilliQ water followed by a further three quick washes. Gels were incubated in 50% (v/v) acetone for 5 minutes with shaking, then the solvent was poured off and 60 ml 1 mM Na_2SO_3 solution was added for 1 minute before three quick washes with MilliQ water. The gels were then placed in stain solution (160 mg silver nitrate, 600 µl 37% (v/v) formaldehyde, in 60 ml MilliQ water) for 8 minutes and rinsed with MilliQ water twice before being placed into developer solution (1.2g Na_2CO_3, 25 µl of 37% (v/v) formaldehyde, 2.5 mg Na_2SO_3, in 60 ml MilliQ water. When the desired colour was reached, the reaction was stopped with 1% (v/v) acetic acid. The gels were then rinsed with MilliQ water and stored at room temperature in water.

2.5.4 Protein precipitation using an organic solvent

Cell pellets from 800 ml LB medium were resuspended in 5 ml sonication buffer (50 mM Tris/Cl, 0.1 M KCl, 1 mM $ZnSO_4$ and 3 mM DTT, pH8.5) and sonicated for 5 minutes at amplitude 60 and pulse 4 (Ultrasonic Processor SONICS VC70T, Unibra Cell™). 10% (w/v) streptomycin (0.375 ml / g of wet cell weight) was

added to the suspension and the mixture was centrifuged at 18,000 ×g for 10 minutes at 4°C. A 1:1 volume of ice-cold ethanol/chloroform (100:8) was added to the supernatant and the mixture centrifuged at 8,000 ×g for 10 minutes at 4°C. Then a further 3 volumes of ice-cold ethanol/chloroform (100:8) mix was added to the supernatant over 1 hour with gentle stirring, followed by centrifugation at 8,000 ×g for 10 minutes at 4°C. The protein pellets containing the recombinant proteins were then dissolved in MilliQ water or 20 mM NH_4HCO_3 and stored at 4°C until further use.

2.5.5 Size Exclusion chromatography/FPLC

Purification of recombinant proteins was carried out by size exclusion chromatography using a FPLC AKTApurifier system (Amersham Biosciences) including a UPC-900 monitor, P-900 sample pump, and Frac-950 fraction collector. The solution containing the protein of interest was passed onto a HiLoad 16/60 Superdex 75 column (120 ml, Amersham Pharmacia) equilibrated with NH_4HCO_3 (20 mM, pH 8.6), and proteins eluted by their size. Protein elution was monitored by absorbance at 220 nm and 280nm. Absorbance at 220 nm is primarily contributed by peptide bonds (Dunn *et al.*, 2000); and absorbance at 280 nm is mainly caused by the aromatic amino acids, including tryptophan, Ttyrosine and phenylalanine (Scopes, 2001a; Scopes, 2001b; Kreusch *et al.*, 2003), which are less abundant in metallothionein proteins. Therefore, fractions with high absorbance at 220 nm and comparably low absorbance at 280 nm would be a hint of the presence of metallothionein proteins.

SDS-PAGE gel electrophoresis (section 2.5.2) and mass spectrometry (section 2.6.1) were taken to confirm the fractions really contained the desired proteins. Proteins were subsequently freeze-dried (lyophilisation) using a bench top K Manifold Freeze dryer (Vir Tis) and stored at -80°C until further use.

2.5.6 Estimation of metallothionein concentration

The concentration of recombinant metallothioneins was estimated using a modified method for quantitation of free thiols (ELLMAN, 1958). In the assay, metallothionein samples (10–200 µl) were diluted with 2.6 ml Tris/HCl buffer (0.1 M Tris, 1 mM EDTA, pH7.0) and 200 µl 5,5'-Dithio-bis (2-nitrobenzonic acid) DTNB solution (2.5 mM DTNB, 50 mM ammonium acetate, 1 mM EDTA, pH5.0). The reaction was allowed to react for 15-30 minutes at 37°C before measuring the absorbance at 412 nm using a spectrophotometer. Quantitation of thiols was acquired by the standard calibration of solutions with known cysteine concentrations (ELLMAN, 1958).

2.6 Protein Biophysical Techniques

2.6.1 Electrospray ionization mass spectrometry (ESI-MS)

ESI-MS was employed to identify the target protein, and study metal uptake and release kinetics. Protein samples, with a concentration between 12.5-25 µM, were dissolved in 10 mM ammonium acetate buffer, and the pH adjusted using

either acetic acid or ammonia to 7.4. After adding 10% (v/v) methanol, samples were injected directly into a Micromass Platform ESI-MS spectrometer MicroTOF (Bruker) at a rate of 4 µl/min. The source temperature for sample ionisation was 473 K. The spectrometer was operated in the positive mode with the following parameters: 100 V capillary exit, 450 V hexapole RF, 50 V skimmer, 24.2 V hexapole. Bruker Daltonics DataAnalysis 3.3 software was used for analysing the data (http://www.bdal.com/).

2.6.2 Inductively coupled Plasma/Optical Emission Spectroscopy (ICP-OES)

Metal specificity and stoichiometry of the target protein was analysed by Inductively Coupled Plasma-Optical Emission Spectroscopy (ICP-OES). Protein samples were diluted with 0.01 M HNO_3. The PerkinElmer optima 5300 DV ICP-OES spectrometer was calibrated with sulphur, zinc, copper and cadmium standard solutions in the same medium, prepared from 1,000 ppm standards (Fisher Scientific) (Table 2.9). Metal ions and the sulphur content were analysed simultaneously.

Table 2.9 Standards for ICP-OES spectroscopy.

Standards		Concentrations (ppm)
1	S	0
	Zn/Cu/Cd	
2	S	0.2
	Zn/Cu/Cd	
3	S	0.4
	Zn/Cu/Cd	
4	S	0.6
	Zn/Cu/Cd	
5	S	1
	Zn/Cu/Cd	
6	S	2
	Zn/Cu/Cd	1.8
7	S	5
	Zn/Cu/Cd	2.5

2.6.3 Nuclear Magnetic Resonance (NMR)

2.6.3.1 Two dimensional homonuclear NMR spectroscopy

Two dimensional homonuclear spectra were acquired on a Bruker DRX700 spectrometer operating at 700.13 MHz for ^{1}H at 298 K or 308 K. Both nuclear overhauser enhancement (NOESY) and total correlation (TOCSY) spectra were acquired with 32 scans with 4k data points in the F2 dimension, and 512 increments in F1 and spectral widths of 15.95 ppm. The mixing time was 100 ms. Raw data were apodised using squared sine-bell functions and Fourier-

transformed with 2k × 2k points. All two-dimensional data were processed with TOPSPIN v2.1 (Bruker).

2.6.3.2 ^{111}Cd NMR spectroscopy

^{111}Cd samples were prepared following a procedure developed by Vašák (1991). This involves stripping the native metal ions from the protein at pH 1-2 by gel filtration using PD-10 columns in 0.01M HCl, adding an appropriate amount of $^{111}CdCl_2$, and adjusting the pH to above 7 with 1 M Tris base. The protein solution was then buffer-exchanged into a 50 mM Tris buffer containing 50 mM NaCl, 10% v/v D_2O pH7.4 and transferred into a 5 mm Shigemi tube. The proton-decoupled 1D ^{111}Cd and 2D [1H, 111Cd] HSQC spectra were acquired on a Bruker DRX500 spectrometer (Bruker) fitted with a 5 mm broad hand observe (BBO) BB-1H probe at 308 K. All data were processed in TOPSPIN v2.0 (Bruker).

1D ^{111}Cd data were acquired using an inverse gated decoupling during acquisition (GARP) pulse with 8k complex data points, 299.2 ppm spectra width and 32k scans.

2D [^{1}H, ^{111}Cd] HSQC spectra were recorded after 1D ^{111}Cd spectra with different coupling constants: 30 and 60 Hz. In each experiment 272 scans were recorded with 2k complex data points in F2 and 80 in F1. Raw data were apodised using an exponential function and transformed with 2k × 256 in F2 and F1 respectively.

2.6.3.3 ^{19}F NMR spectroscopy

^{19}F NMR spectroscopy was performed on a DRX400 spectrometer (Bruker) with a QNP probe operating at 375.48 MHz. Protein samples (120 μM, 10 mM Tris/HCl, pH7.4) were incubated with 4 mM 5F-BAPTA (1,2-bis(2-amino-5-fluorophenoxy)ethane N,N,N',N'-tetraacetic acid) overnight at room temperature. Spectra were acquired at 298 K with a 24k scan number, an acquisition time of 0.87 s and a relaxation delay of 1.0 s. Data was subject to the squared-sine bell function and Fourier transformed with 65k complex data points for the apodisation. Spectral data were processed with TOPSPIN v2.1 (Bruker).

3

Generation of Expression Constructs for *sync_2426* and *sync_2379* from *Synechococcus* sp. CC9311, and Expression and Purification of Target Proteins in *Escherichia coli*

3.1 Introduction

As mentioned previously (see section 1.7) there are no less than four metallothionein genes in the coastal marine cyanobacterium *Synechococcus* sp. CC9311 genome: *sync_0853, sync_1081, sync_2379* and *sync_2426,* whereas most cyanobacteria contain only one gene copy (Palenik et al., 2006; Scanlan et al., 2009). In order to investigate the function of these genes, comprehensively characterising these paralogous proteins *in vitro* is essential, including discerning both their structure and biophysical properties. Consequently, over-expression of the four metallothionein genes in *E. coli* was attempted.

The expression constructs for the *sync_2426* and *sync_2379* genes were achieved by TOPO cloning (section 3.2.2) while the recombinant plasmids containing *sync_0853* and *sync_1081* were cloned previously by Liam Jones (University of Warwick, U.K.). Although 'tags' have been frequently used to over-express metallothioneins in order to make the purification step more straight forward e.g. the first full structure of a prokaryotic SmtA in *Synechococcus* PCC7942 was produced as a fusion protein with glutathione S-transferase (Daniels *et al.*, 1998), the fusion partner could have effects on the metal-binding ability of metallothioneins and result in impaired metal association or loss (Shi *et al.*, 1992b; Blindauer *et al.*, 2002), due to the small size of metallothioneins. However, the TOPO cloning approach used here avoided the use of 'tags' in cloning, and hence should produce a recombinant protein with a similar size to the original protein.

In this chapter, the cloning of expression constructs for *sync_2426* and *sync_2379*, the over-expression of all four *Synechococcus* sp. CC9311 metallothioneins and purification and identification of the recombinant metallothionein proteins are presented (see an overview in Figure 3.1).

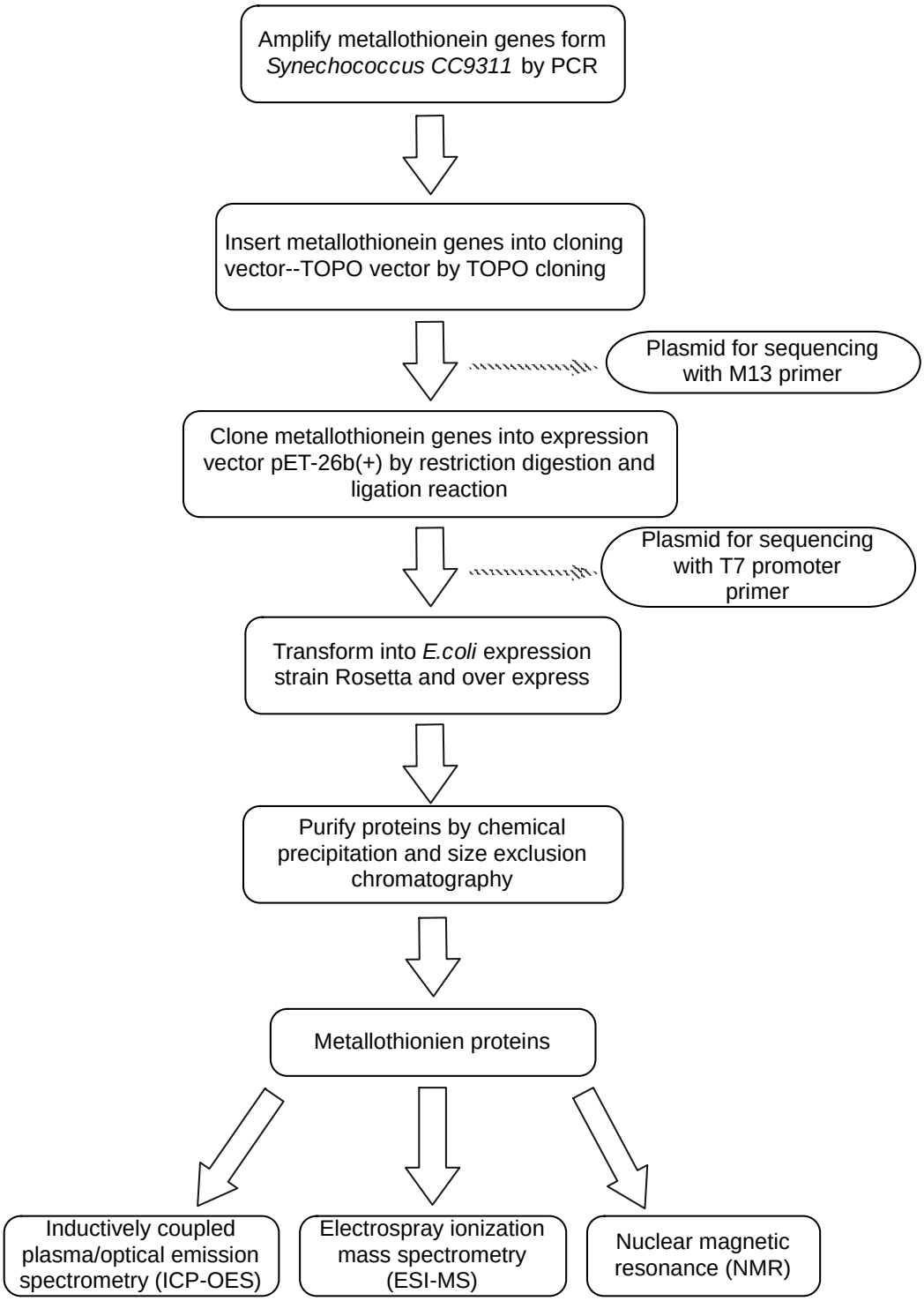

Figure 3.1: General steps of cloning and expression of the metallothionein genes in *Synechococcus* sp. CC9311, and analysis of the proteins

3.2 Cloning of *sync_2426* and *sync_2379* genes from *Synechococcus* sp. CC9311

3.2.1 Amplification of target genes in *Synechococcus* sp. CC9311 by PCR

PCR was carried out to amplify the target genes from *Synechococcus* CC9311 (see section 2.3.1). The specific primers designed included *Bam*H I and *Nde* I restriction sites (Table 2.3) and genomic DNA extracted from *Synechococcus* sp. CC9311 (section 2.2.1) was used as template in the PCR reaction. PCR products were subject to agarose gel electrophoresis (section 2.2.4) to ensure that target gene products of the correct size were present. As shown in Figure 3.2, PCR products corresponded with the expected size of BmtA2379 and BmtA2426 and were subsequently extracted from the gel (see section 2.2.5) and used in TOPO cloning (see section 2.3.1).

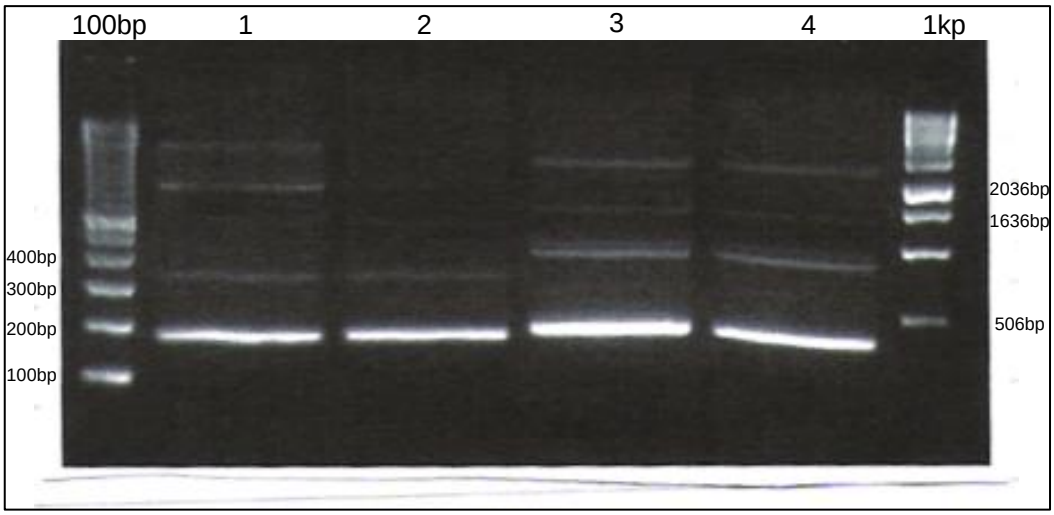

Figure 3.2. Analysis of Synechococcus sp. CC9311 metallothionein gene PCR products by agarose gel electrophoresis. 100bp DNA ladder and 1kb DNA ladder are used as markers (Invitrogen). Lanes 1 and 2: *sync_2379* (which gives a 159 bp product); lane 3 and 4: *sync_ 2426* (which gives a 174 bp product).

3.2.2 Cloning of target genes using the TOPO Cloning System

The PCR products carrying target metallothionein genes were inserted into the TOPO TA cloning vector (Invitrogen). TOPO® TA Cloning® is a highly efficient cloning strategy designed for the direct insertion of *Taq* polymerase amplified PCR products. The key of TOPO cloning is the enzyme DNA topoisomerase I, which plays a role as both restriction enzyme and as a ligase. This enzyme specifically recognises the sequences 5'-(C/T)CCTT-3' and forms a covalent bond with the phosphate group attached to the 3' thymidine. The TOPO vectors are engineered with topoisomerase I covalent bond to each 3' phosphate, which enables the vector to readily ligate DNA sequences with compatible ends. The *Taq* DNA polymerase has a non-template activity, which will add a single deoxyadenosine (A) to the 3' end of PCR products called 3'-A overhangs.

Therefore, the TOPO cloning can be complete in 5 minutes and neither ligase nor primers of specific sequence are required.

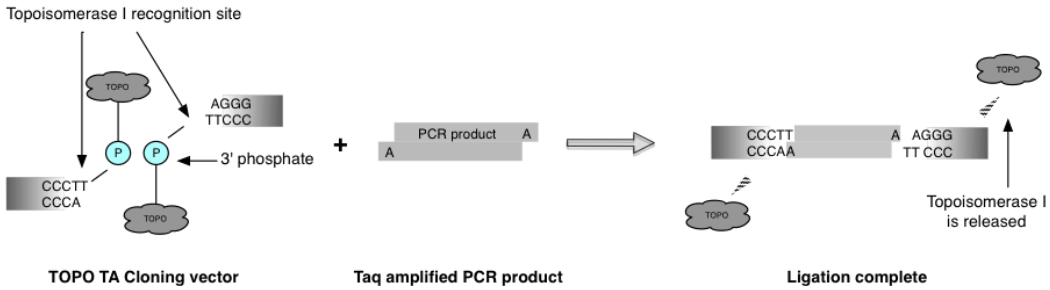

Figure 3.3: TOPO cloning with Taq amplified PCR product
(http://www.invitrogen.com/site/us/en/home/brands/Product-Brand/topo/The-Technology-Behind-TOPO-Cloning.html).

The TOPO vectors containing target genes were then transformed into competent *E.coli* TOP10 cells (see section 2.3.1).

3.2.3 Identifying positive cloning by Blue/white screening and DNA sequencing

Kanamycin-resistant 'white' *E.coli* TOP10 colonies appearing on LB agar plates were inoculated both onto a fresh agar plate and into LB medium containing kanamycin, and then incubated at 37°C with shaking (250 rpm) overnight. The next day, plasmid DNA was extracted (section 2.3.8) and subsequently submitted for DNA sequencing (section 2.3.9) using the M13 forward primer as the sequencing primer: 5'-GTAAAACGACGGCCAG-3'. The sequences returned were analysed using BioEdit software (biological sequence alignment editor) and aligned correctly with the gene sequence obtained from the NCBI database.

3.2.4 Sub-cloning of target genes into expression vector pET-26b(+)

The TOPO vector constructs containing the *sync_2426* and *sync_2379* genes, and plasmid pET-26b(+) DNA was extracted as described previously (section 2.3.7). Plasmids were subject to restriction digestion using *Bam*H I and *Nde* I (Invitrogen), and visually confirmed by agarose gel electrophoresis. The linear pET-26b(+) and *sync_2426*, *sync_2379* fragments were excised and extracted from the gel (section 2.2.5), the pET-26b(+) vector was dephosphorylated (see sections 2.2.4 and 2.3.3), and inserts ligated (see section 2.3.5) to sub clone the genes into pET-26b(+) before transformation into competent *E. coli* strain TOP10. Kanamycin resistant *E. coli* colonies were then grown in LB media plus kanamycin overnight at 37°C, plasmid DNA was extracted and the constructs confirmed by DNA sequencing as described before.

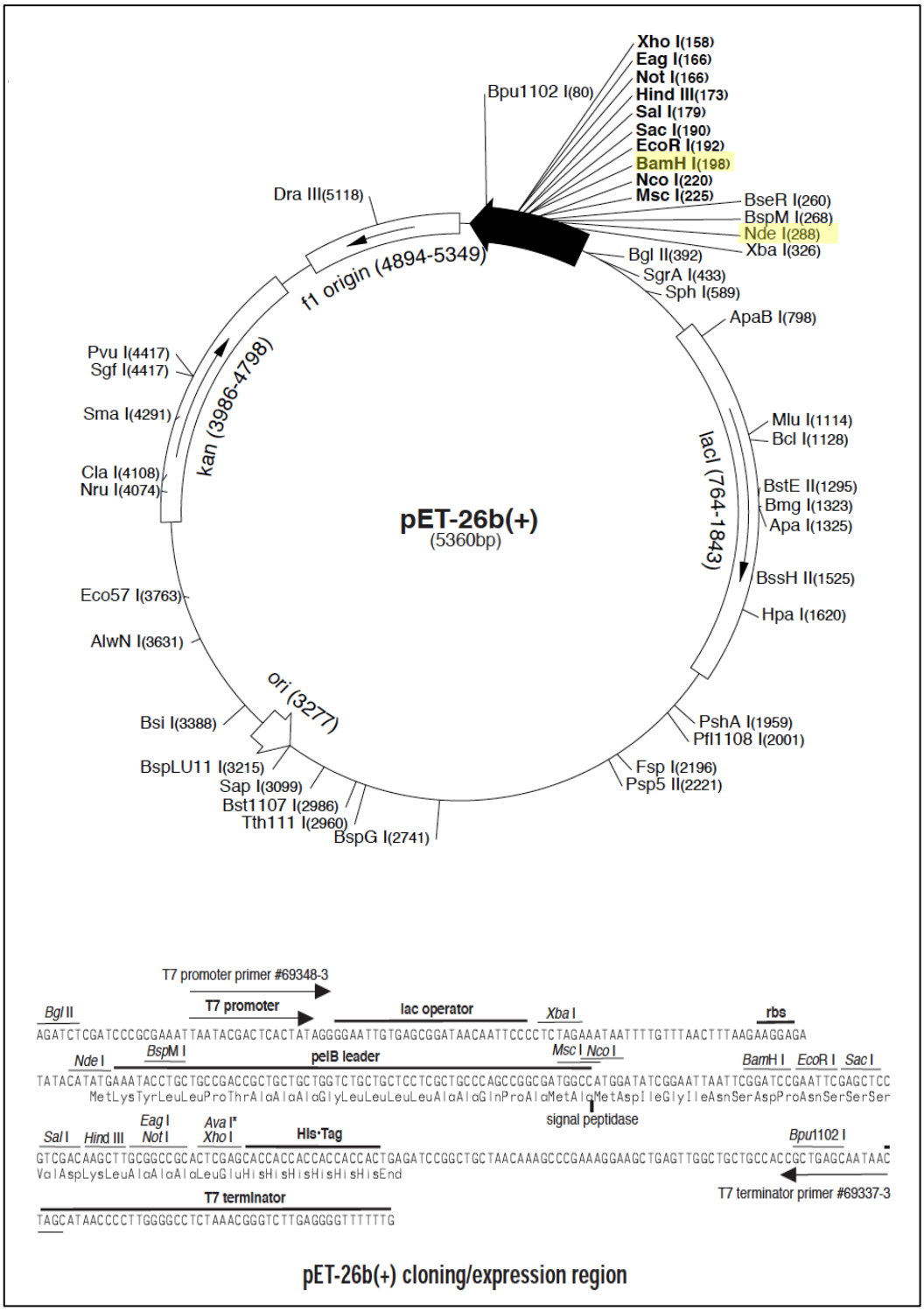

Figure 3. 4. pET-26b(+) restriction map and cloning/expression region (Novagen). Target gene was inserted between BamH I and Nde I (Highlighted in Gold).

3.3 Metallothionein over-expression and purification

3.3.1 Optimising expression conditions

When each pET-26b(+) construct was confirmed to carry the correct metallothionein gene following DNA sequencing, the four constructs were transformed into competent *E. coli* Rosetta (DE3) α cells. Small-scale expression of the four constructs was then performed to assess protein expression levels and determine the most suitable conditions to produce a good yield of soluble recombinant metallothionein protein. Different growth and induction conditions were assessed including: cells were cultured with and without 1% glucose, induction at OD_{600} of 0.4 and expression at 20ºC for 16 hours, and induction at OD_{600} of 0.6 and expression at 30ºC for 6 hours.

Expression levels under different conditions were monitored by SDS-PAGE (Figure 3.5). Aliquots of cell extracts were taken at various time intervals following induction with IPTG. Protein expression levels and conditions were optimised using the NuPage gel system (Invitrogen), and visualised by silver staining.

As Figure 3.5 shows, it is very difficult to deduce anything meaningful from these gels due the small size of each metallothionein protein, although silver staining enhanced bands. However, by combining the SDS-PAGE approach with various purification approaches (see following sections), the possible recombinant protein bands were identified. For three expression constructs the

following optimal conditions were found: for BmtA2426 and BmtA0853, LB medium containing 1% (w/v) extra glucose and induction at 30ºC for 6 hours, for BmtA2426 optimal conditions were LB medium only and 4 hours induction. However, for metallothionein BmtA2379, no obvious over-expression could be discerned by SDS-PAGE.

The apparent molecular weights of metallothionein protein on gels (Figure 3.5) are higher than calculated ones (Table 3.1) as has been previously observed in our lab.

Table 3.1 Theoretical molecular weight of four apo- form metallothionein in Synechococcus sp. CC9311. Calculated by Compute pI/Mw tool (http://web.expasy.org/compute_pi/).

Metallothionein MW (Da)	BmtA0853	BmtA1081	BmtA2379	BmtA2426
Met-MT	7360.4	5791.3	5314.9	6048.7
MT lost the initial Met	7229.2	5660.1	5183.7	5917.5

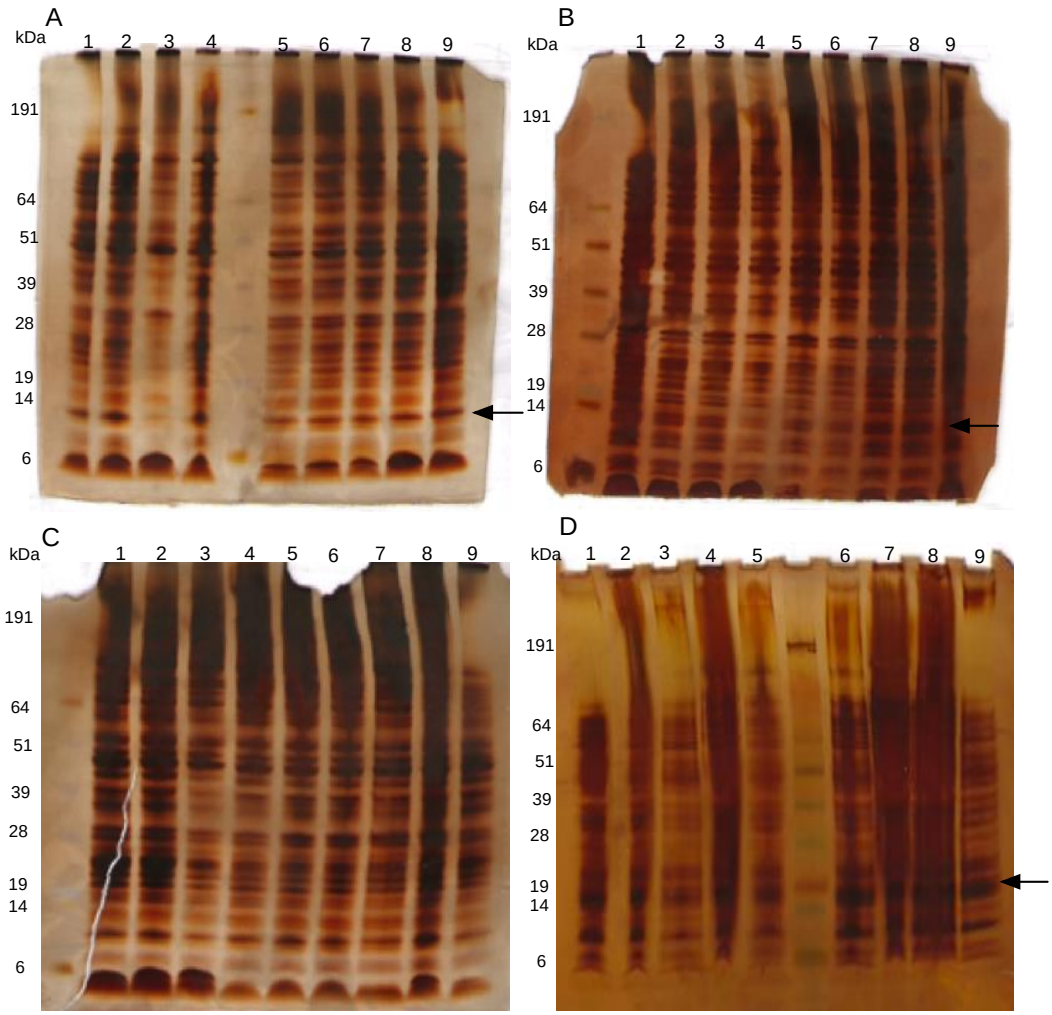

Figure 3.5 SDS-PAGE of over-expressed Synechococcus sp. CC9311 metallothionein genes in E. coli under different experimental conditions. A) BmtA0853; B) BmtA1081; C) BmtA2379; D) BmtA2426. Lanes 1-4: cultured in LB medium, and samples were collected at 4, 5, 6 and 16h after induction with IPTG, respectively. Lanes 5-9: cultured in LB + 1% (w/v) glucose. Samples were collected at 3, 4, 5, 6, and 16h after induction.

3.3.2 Protein purification: chemical precipitation

Proteins were extracted by chemical precipitation (see section 2.5.3), which will remove most of the large molecules including DNA. The cell pellets were resuspended in sonication buffer (50 mM Tris_HCl, 0.1 M KCl, 1 mM $ZnSO_4$, 3 mM DTT, pH 8.5) and sonicated (at 60 Hz for three minutes) to lyse cells before chemical precipitation. SDS-PAGE analysis of protein containing fractions following treatment with different volumes of $CHCl_3/C_2H_5OH$ is shown in Figure 3.6. As shown in Figure 3.6A, BmtA0853 precipitates completely after adding 2 volumes of $CHCl_3/C_2H_5OH$; while BmtA1081 and BmtA2426 (Figure 3.6 B and D, respectively) precipitate completely after 3.5 volumes.

However, chemical precipitation didn't separate BmtA2379 from other proteins (Figure 3.6 C); therefore, BmtA2379 was expressed and purified via size exclusion chromatography directly after sonication.

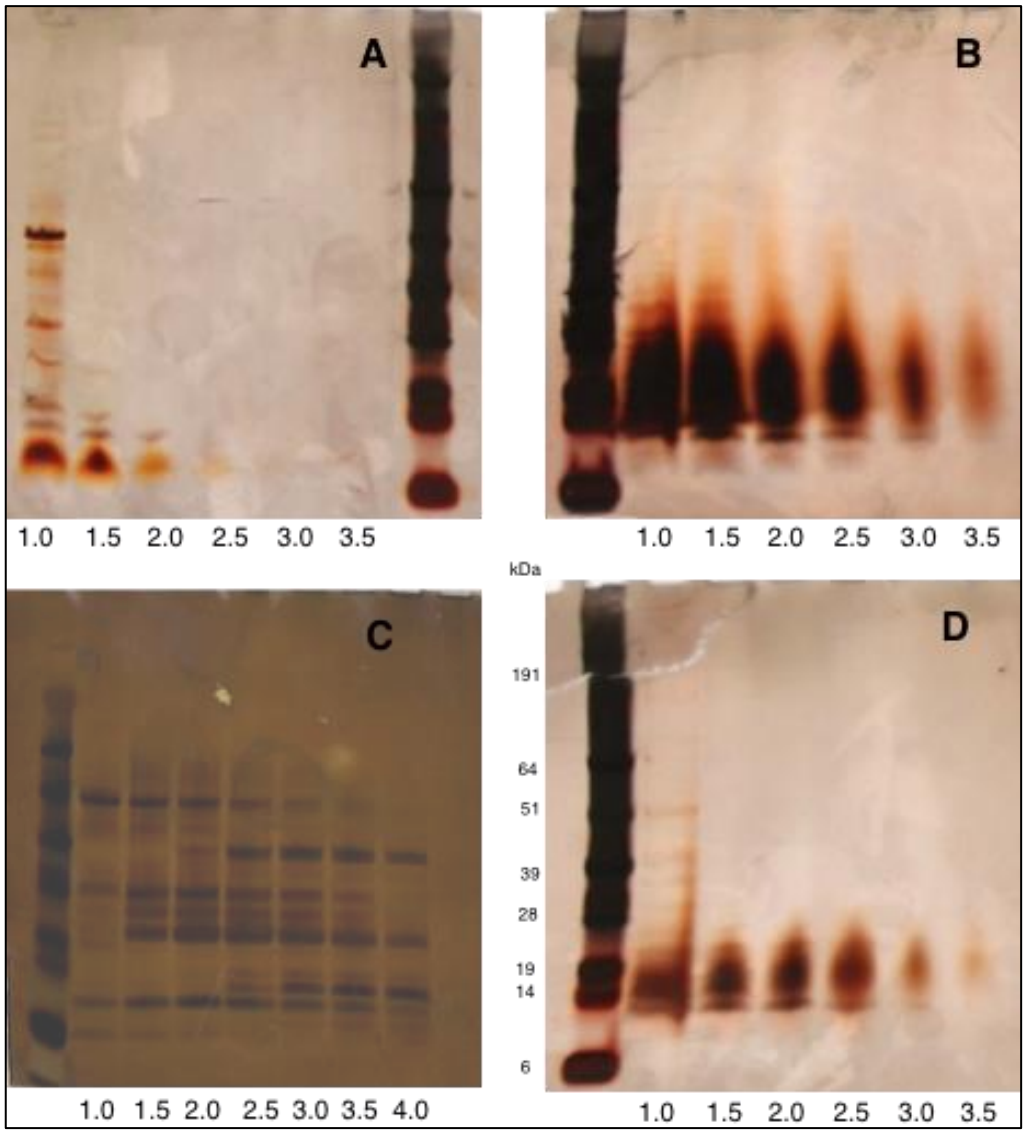

Figure 3.6. SDS-PAGE analysis of recombinant metallothionein proteins following chemical precipitation. A) BmtA0853, B) BmtA1081, C) BmtA2379, D) BmtA2426. Samples were collected after adding 1 volume and every 0.5 volumes of $CHCl_3/C_2H_5OH$.

3.3.3 Metallothionein purification by size exclusion chromatography

SDS-PAGE analysis indicated the presence of other large molecules after chemical precipitation (Figure 3.6); thus, an additional purification procedure

was required. The further purification of the chemically precipitated metallothionein proteins was achieved using size exclusion chromatography (SEC). The protein mixture was separated using the high absorbance of peptide bonds at 220 nm and the low absorbance of aromatic residues (which are low in number in these metallothioneins) at 280 nm as an indication of the presence of metallothioneins.

Figure 3.7 shows the typical size exclusion chromatography profile of the metallothionein proteins. Proteins were separated by their size. Samples were subsequently collected from the corresponding fractions and analysed by SDS-PAGE (Figure 3.8). Silver staining indicated the presence of the desired proteins. For BmtA1081 and BmtA2426, strong protein bands appeared on the gel (Figure 3.8 B and D picked out by arrows) corresponding to the sharp peaks in the 79 ml and 74 ml fractions, respectively (Figure 3.7), which suggested a good level of purity. For BmtA 0853 (Figure 3.8A), several bands appeared alongside the expected products in the 69 ml fraction, indicating the presence of other proteins; as a result this fraction was further processed with another run down the size exclusion chromatography column. As seen in Figure 3.9 a single polypeptide band suggests successful purification. For the BmtA1081, two groups of strong bands were observed (Figure 3.8B), one group of them shown significantly large molecular weight on the gel, which could be a formation of dimer. However, there were no strong bands in Figure 3.8 C, which could suggest a low level of yield for BmtA2379. The purity of the three isolated BmtAs were not known at this point, but will be explained later (Section 3.4.1).

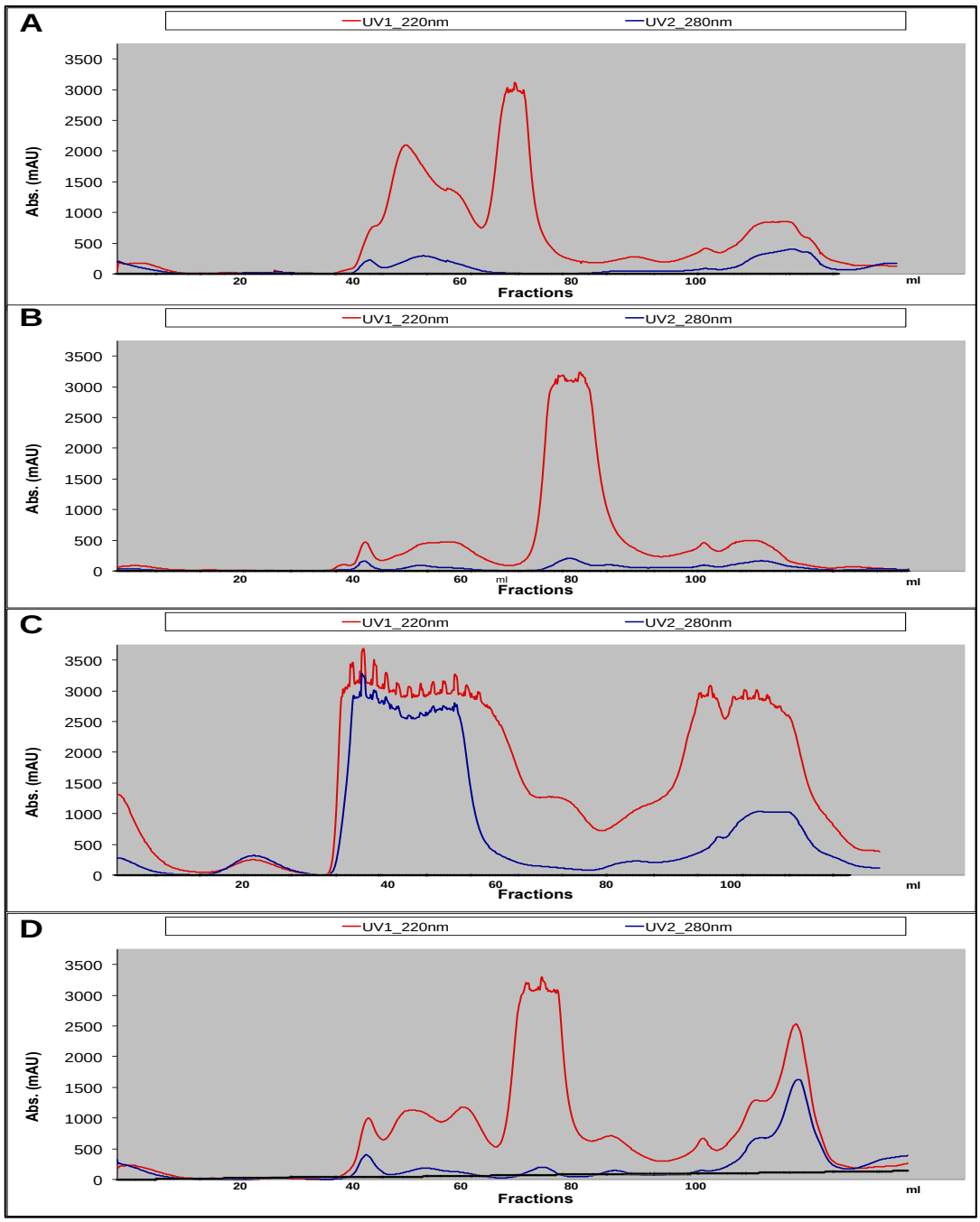

Figure 3.7 Size exclusion chromatograms of proteins eluted. A) BmtA0853, B) BmtA1081, C) BmtA2379, D) BmtA2426. Typically, 3 ml of the resuspended protein from the chemical precipitation step was injected onto a Superdex-75 column (16/60, Hiload) and protein was separated with 20 mM NH_4HCO_3 (~pH 8.0) at a flow rate of 1 ml/min.

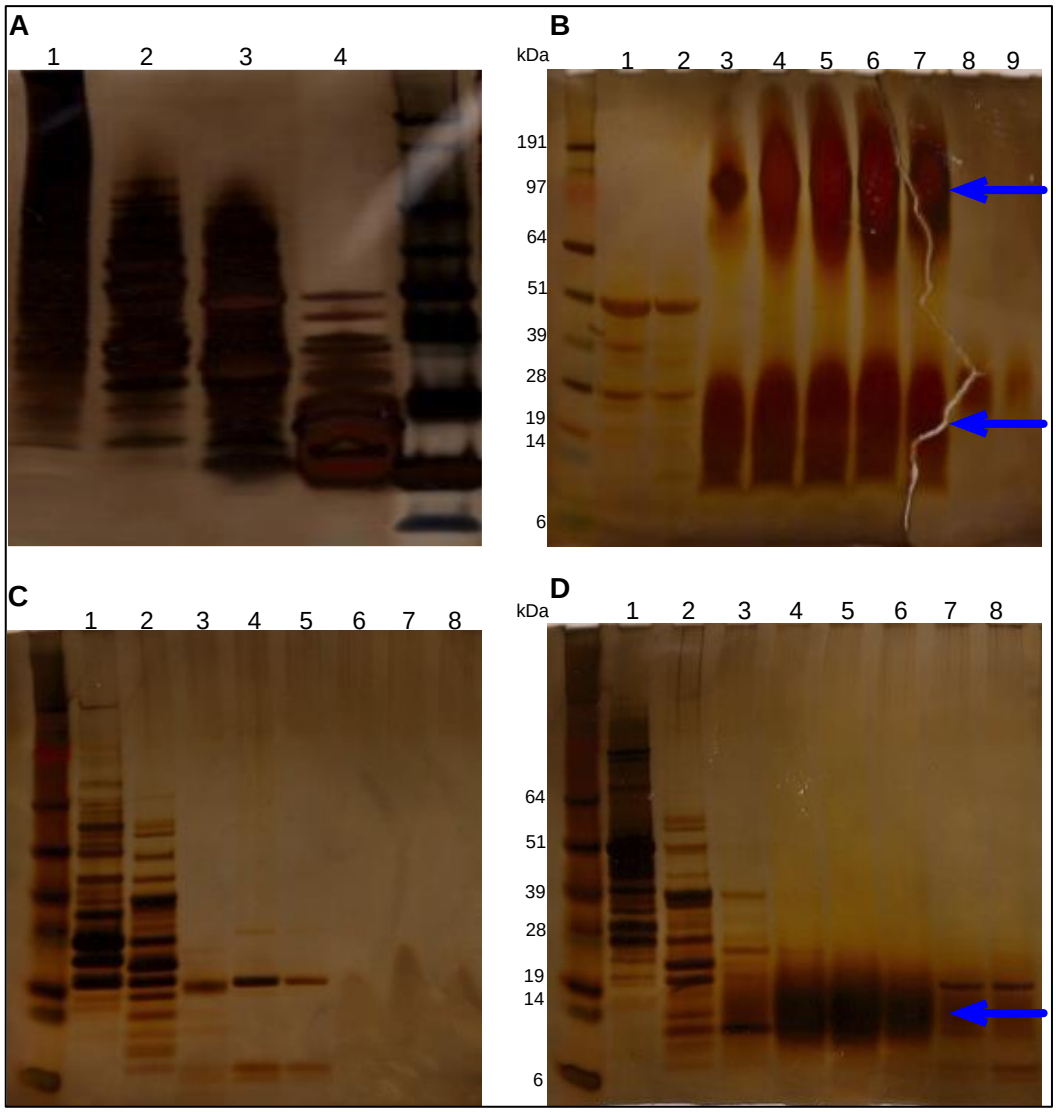

Figure 3.8. SDS-PAGE of protein fractions eluted from the size exclusion chromatography column and possible fractions analysed on NuPAGE gels (4-12%, Invitrogen). The protein bands were revealed by silver staining. A) BmtA0853, lanes 1-4 were collected from fractions 44, 50, 59 and 69 ml, respectively; B) BmtA1081, lanes 1-2 were collected form fractions 43 and 56 ml, lanes 3-7 were collected from fractions around 79 ml, lanes 8 and 9 were collected from 103 and 111 ml respectively; C) BmtA2379, lanes1-8 were collected from fractions 43, 60, 78, 90 and 102 ml, respectively; D) BmtA2426, lanes 1-3 were collected from fractions 44, 51 and 60 ml, lanes 4-6 were collected from fragments around 74 ml, and lanes 7 and 8 were collected form fractions 86 and 103 ml, respectively. Arrows picked out the possible bands for BmtAs.

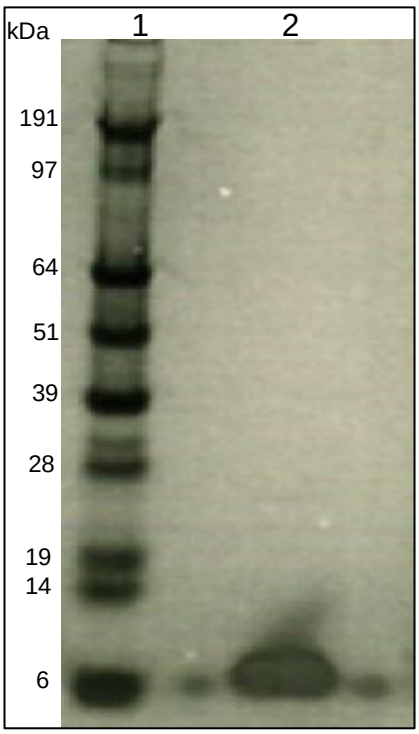

Figure 3.9. SDS-PAGE of over-expressed BmtA0853 protein collected following a second round of size exclusion chromatography. Lane 1, protein ladder. Lane 2 BmtA0853.

3.4 Identification of metallothionein proteins

3.4.1 ESI-Mass spectrometry: apo protein mass

Electrospray mass spectrometry (ESI-MS) was used to identify the recombinant protein products (Wehofsky *et al.*, 2001; Blindauer *et al.*, 2003). The samples were desalted and buffer exchanged into 10 mM ammonium acetate pH 7.4 using Sephadex 6-25 size exclusion columns (PD10, Invitrogen). To obtain the apo-protein, 1% (v/v) acetic acid was added to samples (~pH 2.0), and then the mixture was infused directly into the mass spectrometer. Mass spectra (Figure 3.10) were deconvoluted using Data Analysis software (Bruker Daltonics).

As shown in Figure 3.10A, the signal with a mass of 7358.9 Da corresponds to the expected product, Met-BmtA0853 (theoretical mass 7360.4 Da). Similarly, in Figure 3.10B, the most abundant signal with a mass of 5660.0 Da is in good agreement with the expected size of the BmtA1081 gene product that has lost its N-terminal methionine residue (theoretical mass 5660.1 Da).

As shown in Figure 3.10C, there are two abundant signals with masses of 6043.3 and 5911.3 Da. These two signals represent two forms of the apo-protein: retained with and without the initial methionine residue. Although there is a mass shift of 5.4 and 6.2 Da between the observed and the theoretical mass respectively, this might be due to oxidation or formation of a disulphide-bridge because of the electrospray in the positive mode (Prudent and Girault, 2009). The product with a mass of 6043.3 Da corresponds to the expected product Met-

BmtA2426 (theoretical mass 6048.7 Da); the second signal with a mass of 5911.3 Da corresponds to the product that has lost its N-terminal methionine (theoretical mass 5917.5 Da).

The N-terminal methionine is generally cleaved during recombinant expression in *E.coli*. But may also be retained depending on the efficiency of the bacterial exopeptidases, which is influenced significantly by the adjacent three amino residues following the initial methionine as well as the tertiary structure of the substrate (Münger *et al.*, 1985; Sherman *et al.*, 1985; Ben-Bassat *et al.*, 1987; Pedersen *et al.*, 1994; Brouwer *et al.*, 1995; Blindauer *et al.*, 2001; Polevoda *et al.*, 2009).

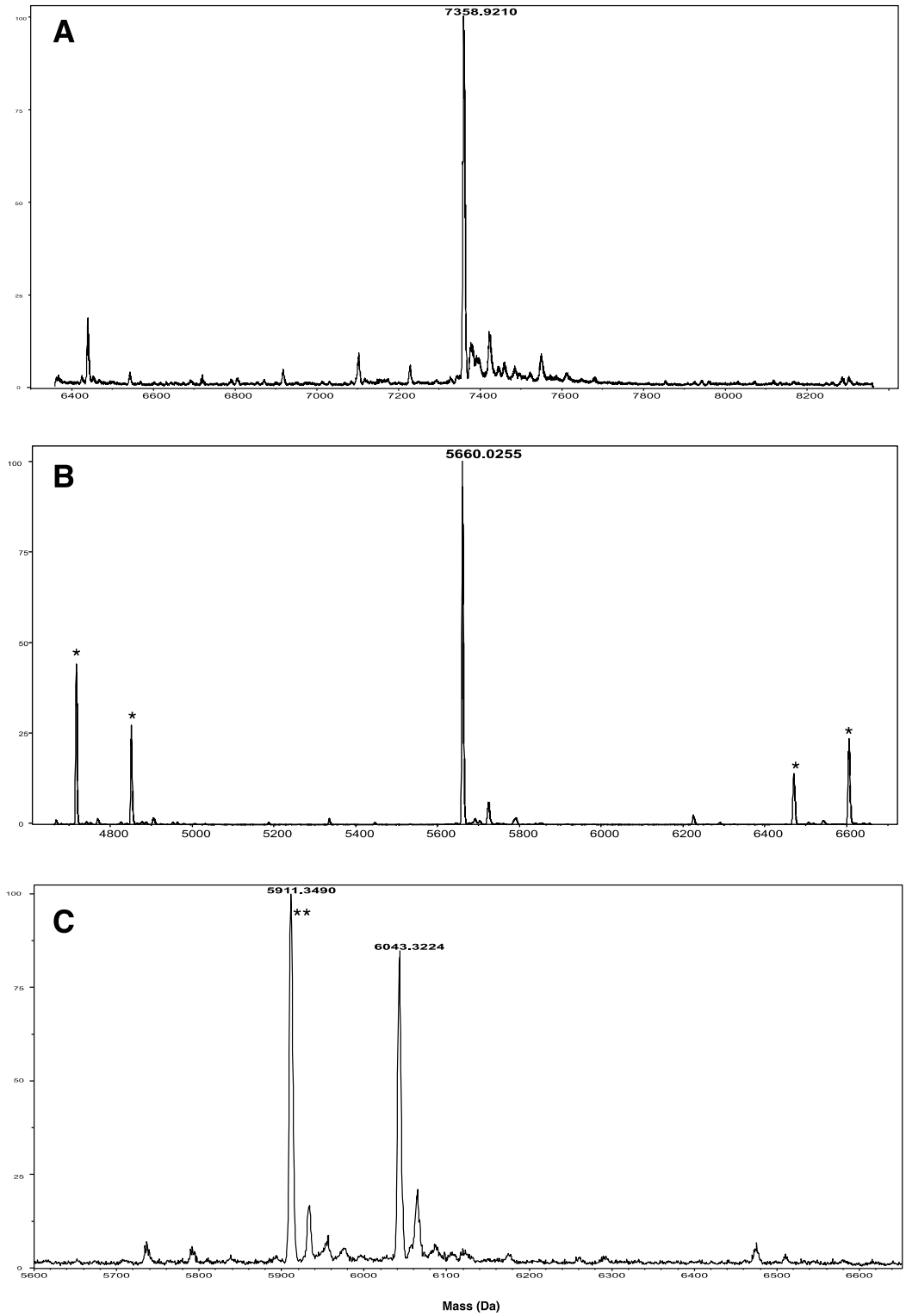

Figure 3.10. Identification of recombinant metallothionein proteins by ESI-MS. A) BmtA0853; B) BmtA1081; C) BmtA2426, all mass spectra were deconvoluted by +1 H. * artificial effects during deconvolution; ** donates the metallothionein which has lost the N-terminal methionine residue.

3.4.2 Native ESI-Mass spectrometry: Zn to protein stoichiometry

The recombinant proteins were analysed by ESI-mass spectrometry at a neutral pH (Bettmer *et al.*, 2009) shown in Figure 3.11. The deconvoluted spectra indicate the presence of different Zn species. In Figure 3.11A, three different signals with masses of 7551.9, 7424.3 and 7361.5 Da were obtained which represent three forms of BmtA0853 respectively: Zn_3, Zn_1 and the apo forms (theoretical masses 7551.5, 7424.7 and 7360.4 Da). The signal in Figure 3.11B with a mass of 5914.6 Da corresponds to the Zn_4 species of BmtA1081 that has lost the N-terminal methionine residue (theoretical mass 5914.7 Da).

Both of the two major signals in Figure 3.11C with masses of 6301.6 and 6171.1 Da correspond to the Zn_4 species of BmtA2426, one form with the N-terminal methionine and another form that has lost it (theoretical mass 6303.3 Da and 6172.2 Da, respectively). The presence of Zn prevents the existence of disulphide bonds in the three recombinant metallothionein proteins (Prudent and Girault, 2009). The theoretical masses of Zn-loaded species were calculated as follow:

$$MW_{Zn-MT} = MW_{apo-MT} + n * (MW_{Zn} - 2) \qquad (2)$$

Where MW = the molecular weight, and Zn-MT and apo-MT for the zinc species and apo form of metallothionein, respectively.

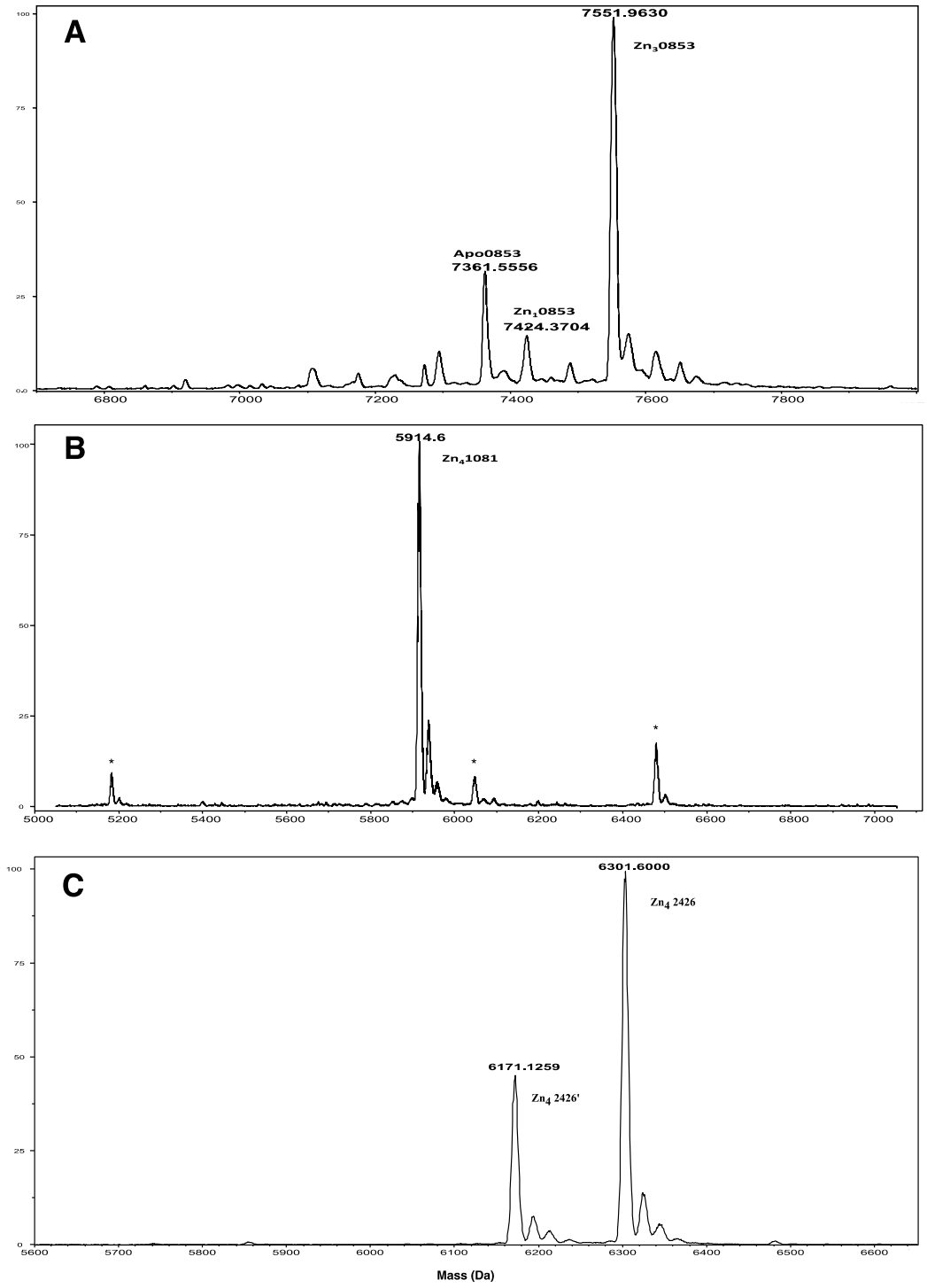

Figure 3.11 Mass spectrometry of recombinant metallothionein proteins at pH 7.4. A) BmtA0853, three signals represent three different Zn species Zn_3, Zn_2 and apo- forms ; B) BmtA1081, the signal corresponds to the Zn_4 species that has lost its N-terminal methionine residue; C) BmtA2426, the two signals represent two forms of the protein with and without the N-terminal methionine residue,

both of them are Zn_4 species. All mass spectra were deconvoluted by +1 H. * Artificial effects during deconvolution.

3.4.3 Metal to protein stoichiometry: elemental Analysis

Inductively coupled plasma – optical emission spectrometry (ICP-OES) was used for the determination of protein concentration and for analysing metal binding stoichiometries (Blindauer, 2008a). Standards used in this experiment were sulphur, zinc, copper and cadmium; the sulphur standard set ranged between 0.2-5 ppm, while metal standards ranged between 0.2-2.5 ppm (see section 2.6.2). Samples and standards were prepared in 0.1 M HNO_3. The data correspond with ESI-MS data, BmtA2426 and BmtA1081 bound 4 zinc ions and BmtA0853 bound 3 zinc ions (Table 3.2), and no presence of copper or cadmium was detected. However, there was a large abundance of sulphur found in the potential BmtA2379 sample but no presence of any metal at all, which suggests disulphide bond formation without any metal occupation for protein BmtA2379.

Table 3.2 Composition of the four metallothioneins as determined from electrospray ionisation mass spectrometry (ESI-MS) and inductively coupled plasma (ICP-OES).

MT	ICP-OES	ESI-MS				
	Zinc content per protein molecule[a]	Apo mass (obs) (Da)	Apo mass (calc) (Da)	Native		
				Holo mass (Da)	Mass Diff.[b]	Metal stoichiometry
BmtA0853	2.5 ± 0.4	7358.9	7360.4	7551.9	193.0	Zn_3
BmtA1081	3.9 ± 0.3	5660.0	5660.1	5914.6	254.6	Zn_4
BmtA2379	0	-	5314.9	-	-	0
BmtA2426	4.0 ± 0.3	5911.3	5917.5	6169.7	258.4	Zn_4
		6043.3[c]	6048.7[c]	6304.6	261.3	Zn_4

[a] Calculated from the concentrations of Zn and S, based on the number of S atoms per protein molecule.

[b] Calculated mass differences between apo and metal-loaded species.

[c] Mass refers to the full length protein containing the N-terminal methionine.

3.5 Summary

In this chapter, metallothionein genes *sync_2426* and *sync_2379* from the cyanobacterium *Synechococcus* sp. CC9311 were cloned into plasmid pET-26b(+) using TOPO cloning (metallothionein *sync_1081* and *sync_0853* were cloned by a previous researcher, Liam Jones). By modifying culture conditions, three of the recombinant metallothioneins (metallothionein BmtA2426, BmtA1081 and BmtA0853*)* were produced in *E. coli* strain Rosetta at a good

protein yield, and chemical precipitation and size exclusion chromatography was used to purify the respective proteins.

Mass spectrometry confirmed that these three recombinant metallothionein proteins were produced with good agreement between experimental and theoretical masses for both of the apo and metal loaded forms. The three metallothioneins demonstrate different zinc binding capacity. BmtA0853 is able to bind with three zinc ions maximally at a neutral pH (~pH 7.4), and the Zn_1 and apo species were observed simultaneously but with lower abundance. On the other hand, BmtA1081 and BmtA2426 are capable of binding four zinc ions and only Zn_4 species were observed at neutral pH. The metal binding capacities of the three recombinant proteins were subsequently confirmed by ICP-OES.

The mass spectrometry data also revealed the retaining of the initial methionine residue for BmtA0853, but the complete cleavage for BmtA1081, and the incomplete cleavage for BmtA2426. As shown in Table 3.3, BmtA0853 has a methionine following the initial methionine, which disables the exopeptidases; while the initial methionine is followed by threonine, valine and threonine in BmtA1081, these three neighbouring residues are able to encourage the cleavage of exopeptidases. Interestingly, for BmtA2426 the first methionine is followed by threonine, threonine and asparagine that also make the first methionine cleavable; even so, incomplete cleavage suggests that the tertiary structure of the protein affects the cleavage ability of exopeptidases.

Table 3.3 Amino acid sequences of the four metallothioneins in *Synechococcus sp. CC9311*.

Bmt A0853	MMNEVLLLCDCSLCKRSVEESRSIRIGGQHFCSESCAKGHPNMEPCDGERDGCNCGIAELELLLAAAD
Bmt A1081	MTVTVVKCACSSCTCEVSSSSAISRNGHSYCSDACASGHRNNEPCHDAAGACGCNCGS
Bmt A2379	MATSNQVCACDPCSCAVSVESAVQKDGKVYCSQPCADGHSGSDECCKSCDCC
Bmt A2426	MTTNLVRCDCPPCTCSIEEATAAMYGNKLFCSEACATAHINQEPSNSAEHTECSCGC

However, the recombinant BmtA2379 exhibited a significantly lower expression level, which made it difficult to obtain a mass spectrum. ICP-OES results suggest the presence of high sulphur level but with no metal ions, which is a clue to the existence of disulphide bonds in the potential recombinant BmtA2379.

Over expression of the four BmtAs in *E.coli* was performed in the presence of Cd as well. However, the expression levels were decreased compared with expression in the presence of Zn, and the final yields after one purification step were too low to perform any analysis (Data no shown). Therefore, it was suspected that these BmtAs might be better suited to bind Zn rather than Cd.

4

Biophysical Characterisation: Protein folding, metal-ligand connectivities, 3D structure and metal release kinetics and thermodynamics of BmtAs in *Synechococcus* sp. CC9311

4.1 Introduction

This chapter presents the results from studies regarding metal-binding affinity and metal uptake and release kinetics for the three recombinant metallothioneins BmtA0853, BmtA1081 and BmtA2426. Protein folding as studied by NMR spectroscopy will also be discussed.

4.2 Protein Folding: Towards Solution Structures

In order to gain more understanding of the structure and protein folding of the three metallothioneins, 2D [^{1}H, ^{1}H] NMR spectroscopy was carried out (Wagner *et al.*, 1988; Howard, 1998).

4.2.1 2D [^{1}H, ^{1}H] TOCSY / 2D [^{1}H, ^{1}H] NOESY Spectroscopy

Two dimensional [^{1}H, ^{1}H] NMR spectroscopy was performed on zinc species and cadmium species to study protein folding and structure. The zinc species spectra are spread well with well-resolved chemical shifts, which directly demonstrate that the proteins were well-folded and single species (Figure 4.1 and 4.2). Several spectral features characteristic of the prototype cyanobacterial metallothionein SmtA are present in the spectra, indicating that the respective structural features, namely the zinc finger fold, are also present in these proteins

(Blindauer *et al.*, 2001; Blindauer *et al.*, 2002). Residues displaying the most diagnostic chemical shifts are highlighted. The low-field chemical shift for the backbone NH proton of Cys 32 (10.05 ppm in SmtA) that binds to the zinc ion of the zinc finger is one of these key features. This low-field shift is brought about by the NH proton forming a hydrogen bond to the sulfur of Cys 9 in SmtA. Similar low-field chemical shifts were observed for the NH of the corresponding cysteine residues in the three metallothioneins under study here: BmtA0853 (Cys 32, 10.21 ppm), BmtA1081 (Cys 31, 9.88 ppm) and BmtA2426 (Cys 31, 10.05 ppm). Another characteristic structural feature in SmtA is that the aromatic ring of Tyr 31 interacts with the CH(α) proton of Ala 37, which leads to a unusual high-field chemical shift for the CH(α) proton of Ala 37 (1.71 ppm). These tyrosine and alanine residues are also present in the three BmtAs, and the CH(α) of the Ala residues show similar high-field shifts: BmtA0853 (Ala 37, 1.49 ppm), BmtA1081 (Ala 36, 1.61 ppm) and BmtA2426 (Ala 36, 1.31 ppm). For BmtA0853 and BmtA2426, another aromatic amino acid, phenylalanine (Phe), takes the place of tyrosine. These residues display a low-field shifted CH(α) resonance (Table 4.1).

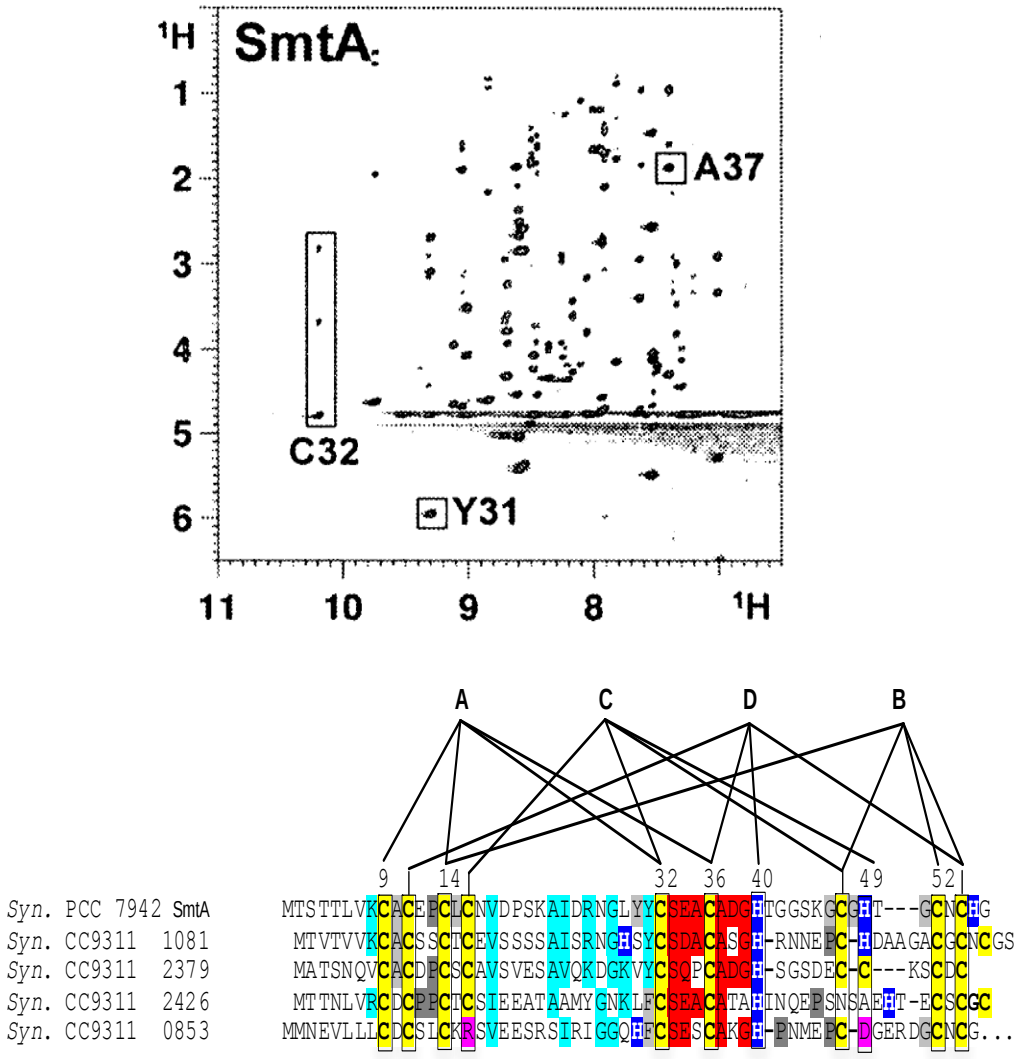

Figure 4.1. Fingerprint region of two-dimensional [^{1}H,^{1}H] TOCSY spectrum of SmtA (Blindauer) and multiple sequence alignment (Blindauer *et al.*, 2007b). A, B, C and D represent four metal binding sites; Cys and His are highlighted in Gold and Blue respectively; α-helices and β-strands are highlighted in Red and Cyan, respectively.

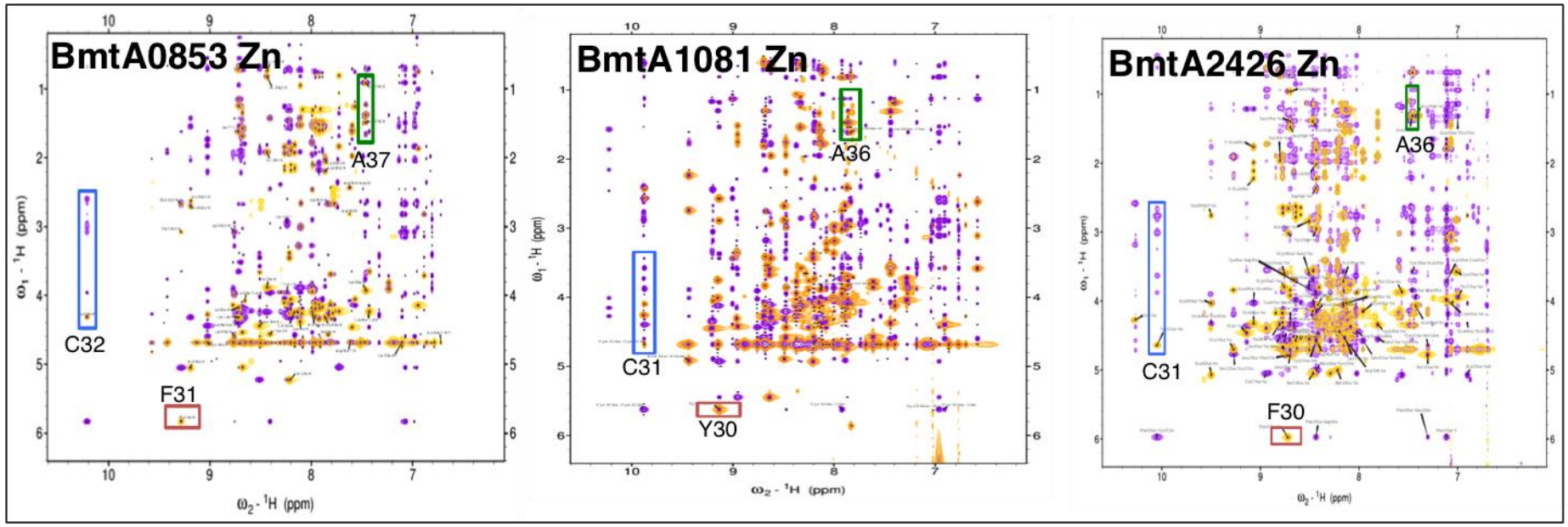

Figure 4.2. Fingerprint region of the three metallothioneins loaded with zinc ions in 2D [^{1}H, ^{1}H] NMR spectra. TOCSY and NOESY represented in gold and purple respectively. Spectra were recorded on a 700 MHz NMR spectrometer (AV II-700, Bruker) in 50 mM[D_{11}]Tris/Cl, 50 mM NaCl and 10% D_2O, pH 7.0, at 298 K. The structural features of SmtA are present in these three metallothioneins. Residues with the most diagnostic chemical shifts are highlighted.

4.2.2 Resonance Assignments

Sequential resonance assignment was carried out based on the homonuclear [^{1}H,^{1}H] NMR data, using standard literature protocols (Wagner *et al.*, 1988; Wishart *et al.*, 1992; Wu *et al.*, 2003) and with assistance from Dr. Claudia Blindauer. Previous NMR spectral data of the cyanobacterial metallothionein SmtA from the Biological Magnetic Resonance Data Bank (BMRB), entry BMRB 4306 (Blindauer *et al.*, 2001), were used to help with assignment of spectra. NOESY spectra for BmtA0853 and BmtA1081 were partially assigned with some missing residues, see Appendix A and B for details (Figure 4.3 and Figure 4.4, respectively); the spectrum of BmtA2426 was fully assigned (Figure 4.5).

The CH(α) proton chemical shifts are influenced by protein secondary structure, which provides a hit for prediction of α-helices and β-strands (Wishart *et al.*, 1992). Briefly, the NH and CH(α) chemical shifts in β-strands are higher than random-coil shifts, and those in α-helices are lower than random-coil shifts. Although there are some differences between the respective chemical shifts, a comparison of the chemical shifts of CH(α) proton and backbone NH proton of the three metallothioneins from *Synechococcus* sp. CC9311 with the chemical shifts of SmtA from *Synechococcus* PCC 7942 indicates that overall the three metallothionein proteins are folded and are likely to display secondary structure properties similar to those found in SmtA (Table 4.1). Notably, the secondary structure associated with a GATA-like zinc finger fold of the three

metallothioneins is relatively well conserved in the *Synechococcus* sp. CC9311 MTs.

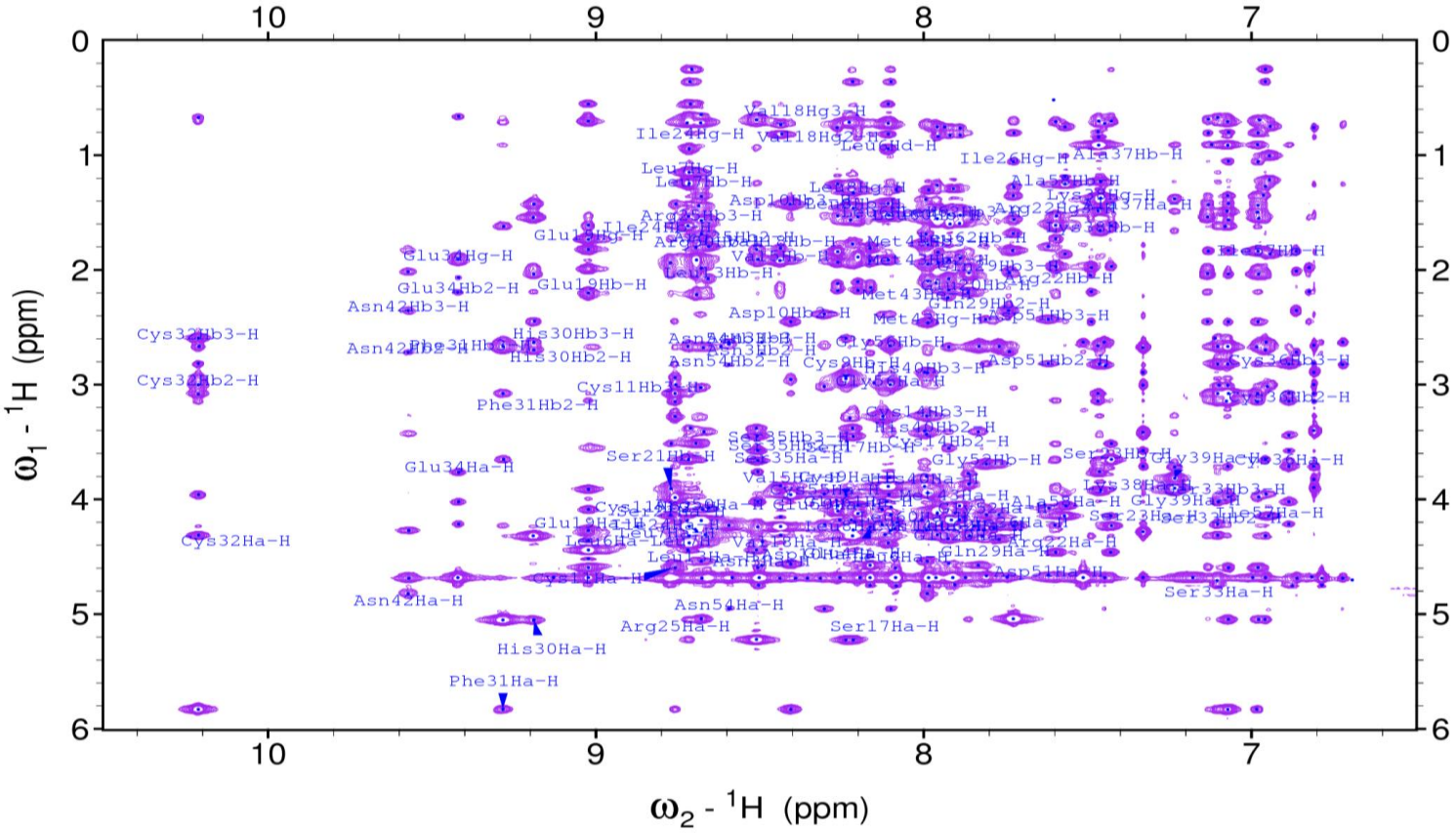

Figure 4.3. Sequential assignment of 2D NOESY NMR spectrum for BmtA0853 in the presence of zinc. Spectra were recorded at a 700 MHz spectrometer (AV II-700, Bruker) in 50 mM[D_{11}]Tris/Cl, 50 mM NaCl and 10% D_2O, pH 7.0, at 298 K.

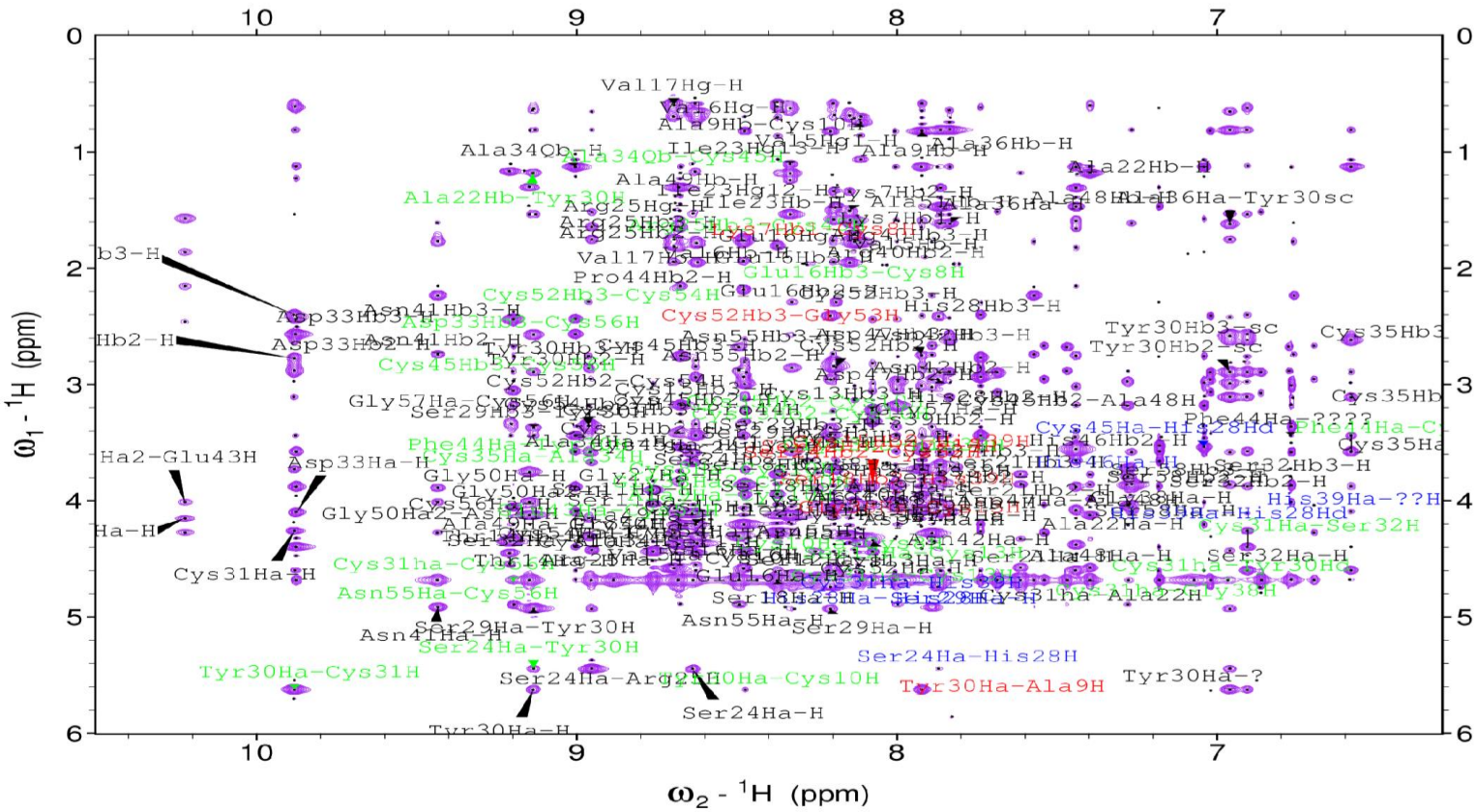

Figure 4.4. Sequential assignment of 2D NOESY NMR spectrum for BmtA1081 in the presence of zinc ions. Spectra were recorded at a 700 MHz spectrometer (AV II-700, Bruker) in 50 mM[D_{11}]Tris/Cl, 50 mM NaCl and 10% D_2O, pH 7.0, at 298 K.

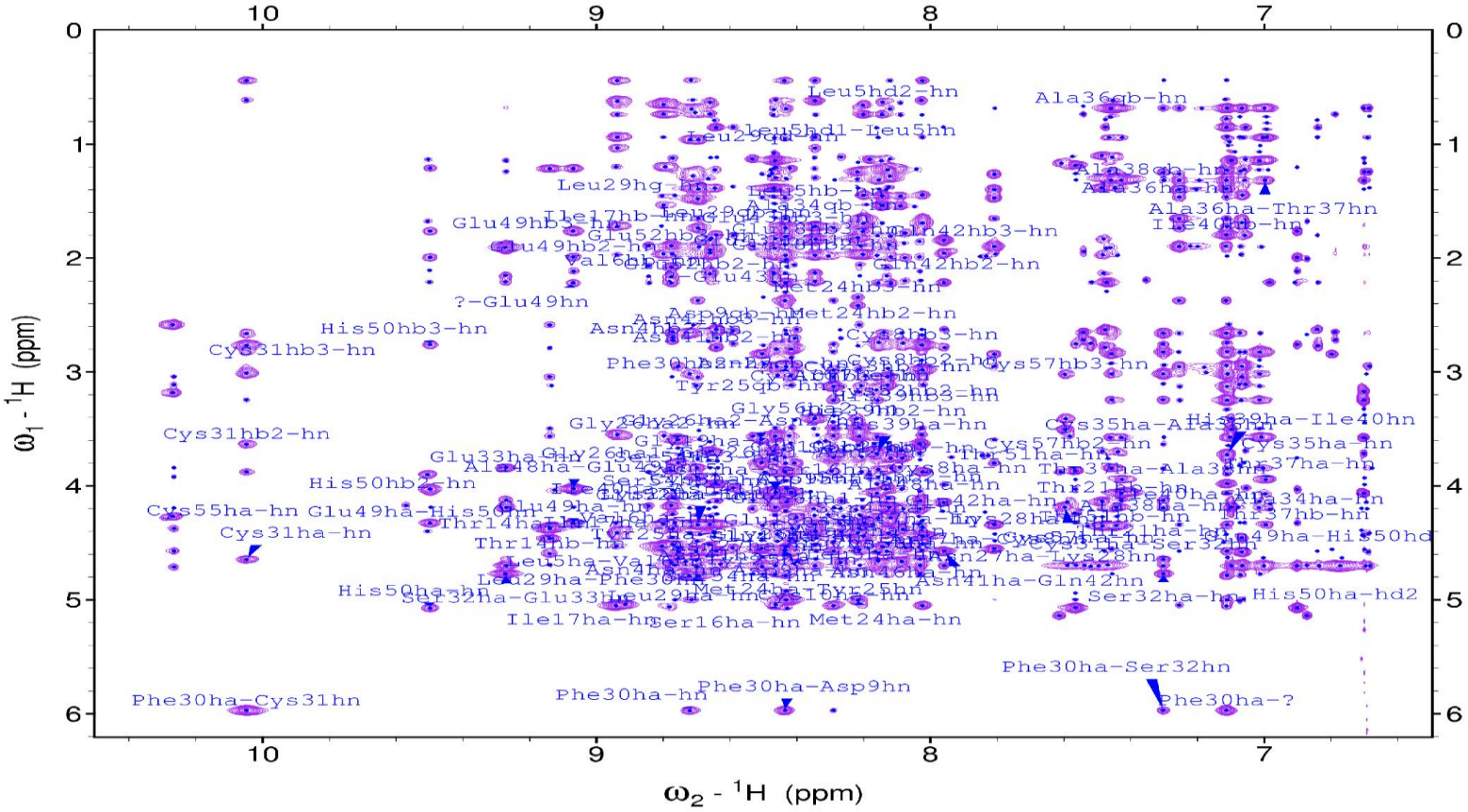

Figure 4. 5. Sequential assignment of 2D NOESY NMR spectrum for BmtA2426 in the presence of zinc. Spectra were recorded at a 700 MHz spectrometer (AV II-700, Bruker) in 50 mM[D11]Tris/Cl, 50 mM NaCl and 10% D2O, pH 7.0, at 298 K.

Table 4.1. Comparison of 1H chemical shifts (ppm) for selected backbone protons of residues of Zn-loaded metallothioneins BmtA0853 (0), BmtA1081 (1), BmtA2426 (2) from Synechococcus sp. CC9311 and SmtA (S) from Synechococcus sp. PCC7942 (BMRB entry BMRB 4306; Blindauer *et al.*, 2001). Abbreviations: Residues involved in the secondary structure elements of the zinc finger of SmtA are highlighted: α-helices, Red; β-strands, Cyan; turns, italic.

Residue	NH (p.p.m)	CH(α) (p.p.m)	Residue	NH (p.p.m)	CH(α) (p.p.m)
V7 (S)	8.74	4.50	C16 (S)	8.16	3.81
L7 (0)	8.79	4.40	R16 (0)	-[a]	4.61
V6 (1)	8.71	4.38	C15 (1)	8.71	4.29
V6 (2)	8.87	4.41	C15 (2)	8.48	4.12
K8 (S)	8.35	4.43	N17 (S)	8.49	5.32
L8 (0)	8.30	4.35	S17 (0)	8.30	5.31
L7 (1)	8.23	4.15	E16 (1)	8.56	4.66
R7 (2)	8.27	4.51	S16 (2)	8.53	5.12
C9 (S)	8.93	3.96	V18 (S)	9.64	4.52
C9 (0)	8.31	4.04	V18 (0)	8.59	4.53
C8 (1)	8.28	3.82	V17 (1)	8.78	4.35
C8 (2)	8.09	3.94	I17 (2)	9.01	4.47
A10 (S)	8.01	4.07	A23 (S)	7.44	4.56
D10 (0)	8.49	4.65	S23 (0)	7.51	4.31
A9 (1)	8.01	4.03	A22 (1)	7.48	4.21
D9 (2)	8.50	4.64	A22 (2)	7.51	4.25
C11 (S)	7.95	4.63	I24 (S)	7.72	4.03
C11(0)	8.84	4.68	I24 (0)	8.80	4.26
C10 (1)	8.56	4.52	I23 (1)	8.42	4.19
C10 (2)	8.36	5.12	A23 (2)	8.19	4.48
C14 (S)	8.07	4.16	D25 (S)	8.46	5.27
C14 (0)	8.07	4.35	R25 (0)	8.76	5.12
C13 (1)	8.16	4.43	S24 (1)	8.72	5.53
C13 (2)	8.28	4.44	M24 (2)	8.28	5.07

Table 4.1 Continuted.

Residue	NH (p.p.m)	CH(α) (p.p.m)	Residue	NH (p.p.m)	CH(α) (p.p.m)
L15 (S)	8.51	4.42	R26 (S)	8.94	4.57
K15 (0)	-[a]	-[a]	I26 (0)	7.81	4.31
T14 (1)	9.29	4.53	R25 (1)	9.04	4.51
T14 (2)	9.21	4.53	Y25 (2)	8.50	4.64
N27 (S)	9.22	4.32	E34 (S)	9.41	3.78
G27 (0)	-[a]	-[a]	E34 (0)	9.50	3.85
N26 (1)	-[a]	4.41	D33 (1)	9.96	4.18
G26 (2)	8.82	-[a]	E33 (2)	9.34	3.90
G28 (S)	8.91	3.95;3.41	A35 (S)	8.13	3.87
G28 (0)	-[a]	3.95	S35 (0)	8.59	3.74
G27 (1)	8.77	3.92	A34 (1)	9.09	3.52
N27 (2)	8.57	4.62	A34 (2)	8.53	4.25
L29 (S)	7.29	4.18	C36 (S)	7.24	3.71
Q29 (0)	7.94	4.40	C36 (0)	6.97	3.82
H28 (1)	7.96	4.83	C35 (1)	6.67	3.66
K28 (2)	7.88	4.41	C35 (2)	7.08	3.64
Y30 (S)	7.45	5.37	A37 (S)	7.52	1.73
H30 (0)	9.27	5.13	A37 (0)	7.55	1.57
S29 (1)	8.29	5.01	A36 (1)	7.92	1.70
L29 (2)	8.76	4.86	A36 (2)	7.53	1.38
Y31 (S)	9.20	5.84	H40 (S)	8.59	3.82
F31 (0)	9.36	5.91	H40 (0)	8.08	3.97
Y30 (1)	9.22	5.71	H39 (1)	8.09	4.10
F30 (2)	8.79	6.04	H39 (2)	8.22	3.78
C32 (S)	10.09	4.68	C47 (S)	8.61	4.91
C32 (0)	10.29	4.40	C47 (0)	-[a]	-[a]
C31 (1)	9.97	4.34	C45 (1)	8.76	3.62
C31 (2)	10.12	4.71	S45 (2)	8.19	4.35

Table 4.1 Continued.

Residue	NH (p.p.m)	CH(α) (p.p.m)	Residue	NH (p.p.m)	CH(α) (p.p.m)
S33 (S)	7.42	4.80	G47 (S)	8.36	3.82;3.63
S33 (0)	7.19	4.79	-[b]		
S32 (1)	6.99	4.48	-[b]		
S32 (2)	7.37	4.84	N46 (2)	8.22	4.73
H49 (S)	6.91	5.17	N53 (S)	8.62	5.17
D49 (0)	8.00	-[a]	N54 (0)	8.67	5.03
H46 (1)	7.53	3.74	N53 (1)	8.41	3.66
S47 (2)	8.15	4.45	S54 (2)	8.77	4.78
			N55 (1)*	8.49	4.89
C52 (S)	7.54	4.60	C54 (S)	8.14	3.98
C53 (0)	-[a]	4.30	C55 (0)	8.39	4.04
C52 (1)	8.27	4.71	C54 (1)	9.05	4.39
C53 (2)	8.20	4.64	C55 (2)	10.34	4.33
C54 (1)*	9.05	4.39	C56 (1)*	9.28	4.14

a. Unassigned residues. b. No corresponding residue. *. Second possible corresponding residue.

4.3 Metal-ligand connectivity: ^{111}Cd NMR Spectroscopy

Because of the spectroscopic silence of Zn (II), it is impossible to detect the zinc-binding site directly by most spectroscopies (Maret, 2004). However, replacement of Zn with the ^{111}Cd or ^{113}Cd isotope, combined with NMR spectroscopy, has been widely used for direct observation of metal-ligand connectivities in metallothioneins and zinc fingers (Vasak, 1998; Chen *et al.*, 2000; Blindauer *et al.*, 2001; Hemmingsen *et al.*, 2004; Blindauer *et al.*, 2007b; Blindauer, 2009). Besides, it has been reported that cadmium and zinc are able to

replace each other isostructurally (Wang *et al.*, 1995; Palumaa *et al.*, 2002). The chemical shifts of cadmium are especially sensitive to its coordination environment including the type of ligand, bond length, and geometry (Hemmingsen *et al.*, 2004), which makes $^{111/113}$Cd NMR spectroscopy an excellent technique for structure determination of Zn-containing proteins (Good *et al.*, 1988). 1D ^{111}Cd and 2D [^{1}H,^{111}Cd] HSQC (Heteronuclear Single Quantum Coherence) spectroscopy was carried out in this study (Henehan *et al.*, 1993), as well as 2D ^{1}H NMR spectroscopy in the presence of cadmium ions.

4.3.1 Homogeneity and Heterogeneity of NMR Samples Loaded with Cadmium Ions

Protein samples for all NMR experiments with cadmium ions were prepared by reconstitution of the demetallated apo-proteins (section 2.6.3 for details). Figure 4.6 shows the comparison of the fingerprint region of 1D ^{1}H spectra of BmtA 0853 in two different sample preparations: the original protein expressed in the presence of Zn ions, a sample reconstituted with ^{111}Cd ions used for recording 2D [^{1}H, ^{1}H] spectra, and a further reconstituted sample used for the acquisition of 1D ^{111}Cd and 2D [^{1}H, ^{111}Cd] HSQC spectra. The spectrum in the presence of zinc was recorded at 298 K, whereas all cadmium-related spectra were recorded at 308 K, since high temperature resulted in more resolved, high intensity signals for cadmium loaded samples. This has previously been observed for SmtA as well (Blindauer *et al.*, 2001). The three 1D ^{1}H spectra exhibited high intensity signals with good resolution and dispersion and the existence of key feature

residues (e. g. Cys32) directly demonstrated that all three batches of protein were well folded and samples were prepared successfully with only one single species observed in each case.

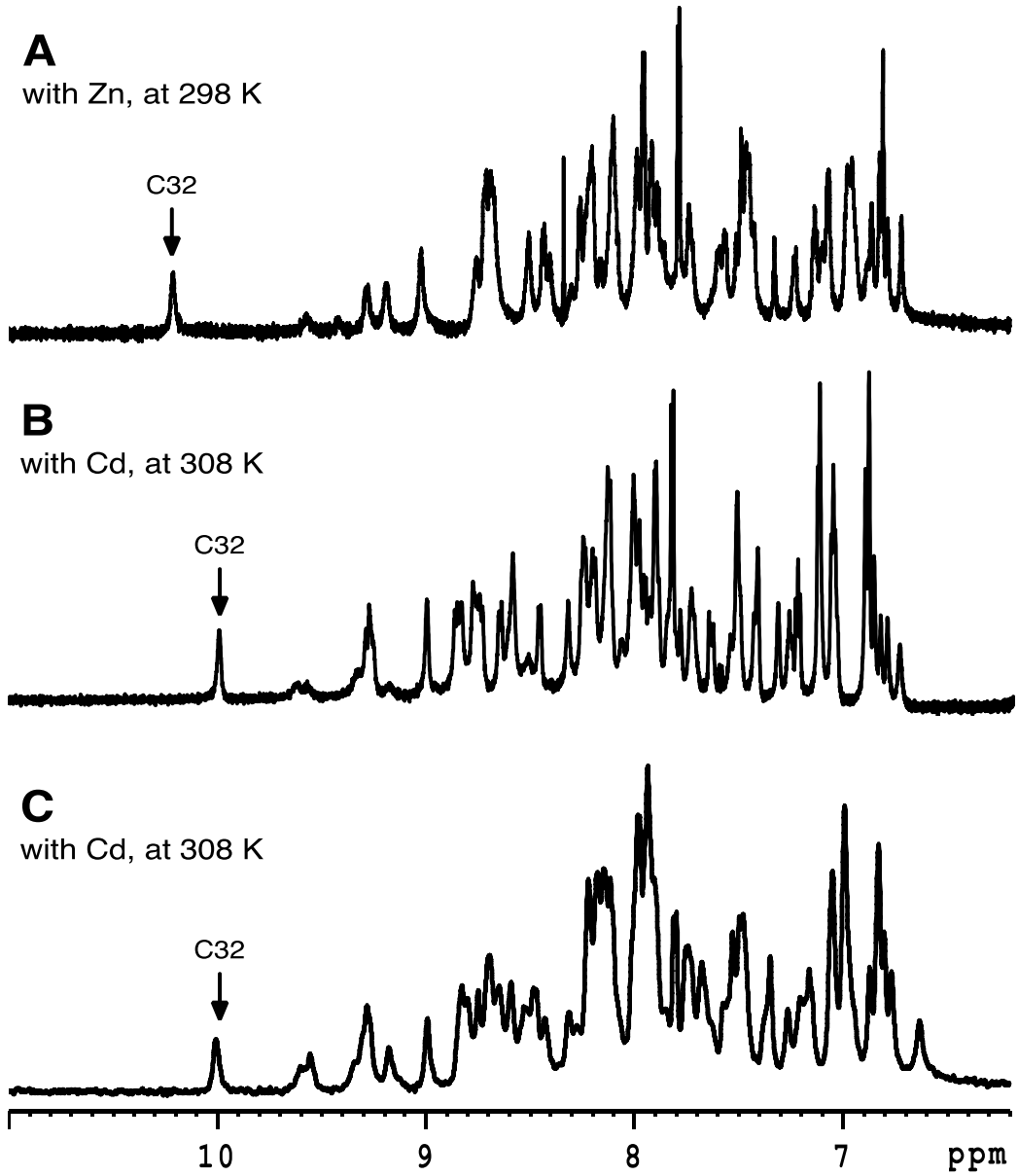

Figure 4.6. Stacked plots of 1H NMR spectra (fingerprint region) of the BmtA0853 protein in the presence of Zn(II) and Cd(II). Samples were prepared with 2-2.5 mM BmtA0853 protein in 50 mM[D_{11}]Tris/Cl, 50 mM NaCl and 10% D_2O, pH 7.0. (A) and (B) were recorded on a 700 MHz spectrometer (AV II-700, Bruker), for 2D [^{1}H, ^{1}H] spectra; (C) was recorded on a 500 MHz spectrometer (DRX500, Bruker), which was utilised for recording 1D ^{111}Cd spectra and 2D [^{1}H, ^{111}Cd] HSQC spectra. The arrows pick out the resonance of the NH of Cys 32.

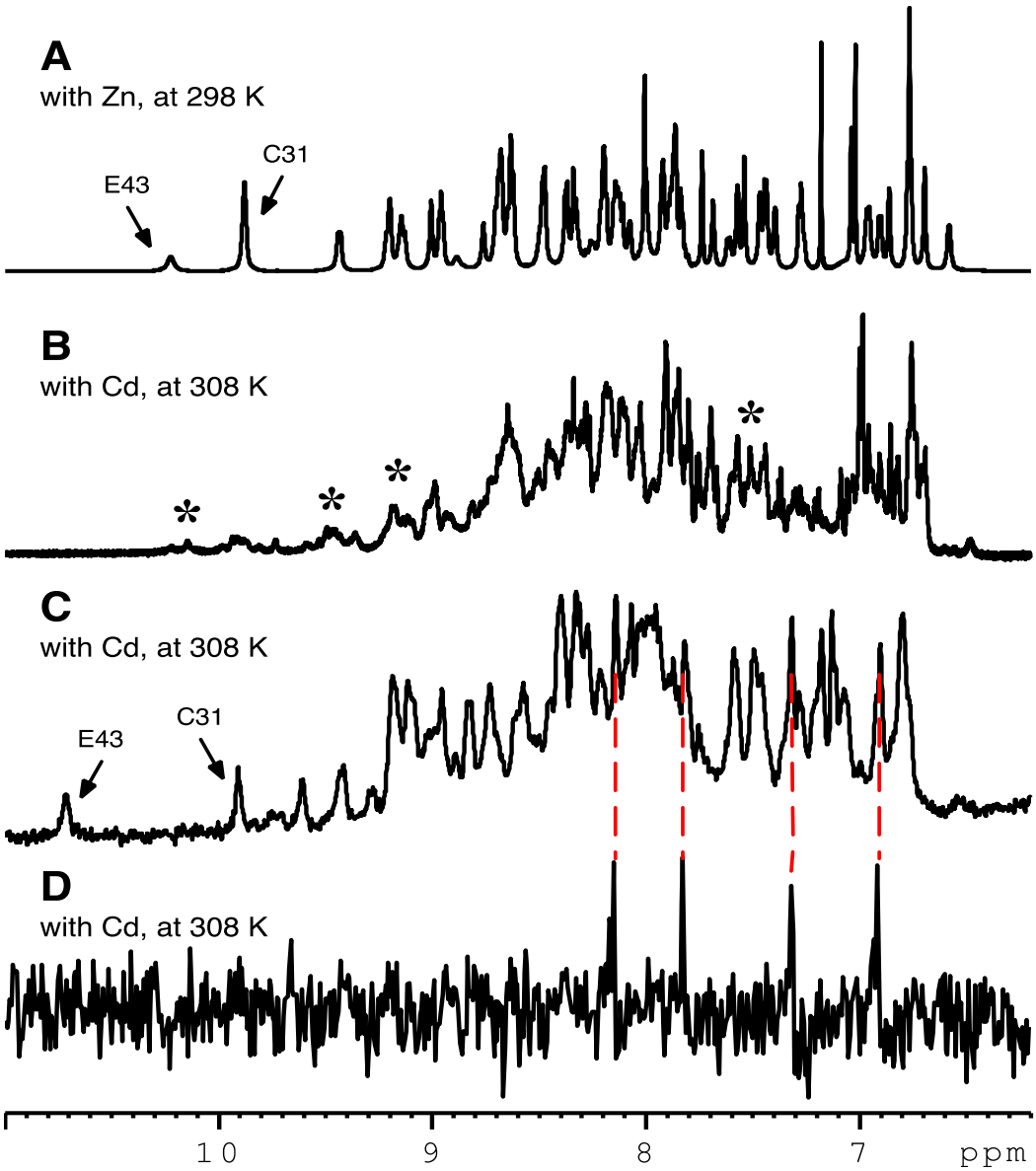

Figure 4.7. Stacked plots of 1D NMR spectra (fingerprint region) of the BmtA1081 protein in the presence of Zn(II) and Cd(II). Samples were prepared with 2-2.5 mM BmtA1081 protein in 50 mM[D_{11}]Tris/Cl, 50 mM NaCl and 10% D_2O, pH 7.0. (A) and (B) are 1D ^{1}H spectra recorded on a 700 MHz spectrometer (AV II-700, Bruker), utilised for recording 2D [^{1}H, ^{1}H] spectra; (C) is 1D ^{1}H spectra in the presence of Cd (D) 1D ^{1}H, ^{111}Cd HSQC spectra ^{3}J=10 Hz, (C) and (D) are recorded on a 500 MHz spectrometer (DRX500, Bruker), utilised for recording 1D ^{111}Cd spectra and 2D [^{1}H, ^{111}Cd] HSQC spectra. The arrows pick out the resonance of the NH of Cys31 and Glu43. The red lines indicate the resonances of His Hε1 and Hδ2 protons coupled to ^{111}Cd in (D); these align perfectly with the corresponding peaks in dataset (C), but not (B).

The same comparison of 1D ^{1}H spectra for BmtA1081 is presented in Figure 4.7. Samples used for the acquisition of 2D [^{1}H, ^{1}H] spectra of zinc species (A) and a cadmium-reconstituted preparation (B), a further cadmium-reconstituted preparation used for the acquisition of 1D ^{111}Cd and 2D [^{1}H, ^{111}Cd] HSQC spectra (C) are shown. Spectrum (D) is a 1D Cd-edited HSQC spectrum, showing His Hε1 and Hδ2 protons coupled to ^{111}Cd. The last two datasets match perfectly, and (C) indicates good homogeneity. However, this is not the case for the preparation used for the acquisition of 2D [^{1}H, ^{1}H] spectra of cadmium species (B): the remarkable high-field residue Cys31 and Glu43 are missing in this spectrum, and low intensity and broad signals, marked in Figure 4.7 B by asterisks, indicate the presence of multiple species or different dynamic properties. Clearly, this batch of sample was not prepared as successfully as the others; therefore any further interpretation of these datasets has to take this into account.

For BmtA2426, the comparison of 1D ^{1}H spectra is shown in Figure 4.8. The zinc loaded sample used the acquisition of 2D [^{1}H, ^{1}H] spectra demonstrated perfect sample preparation, with narrow and well-resolved signals. The low-field shifted NH protons of Cys 31 and Cys 55 are picked out by arrows (Figure 4.8 A). The samples in the presence of cadmium ions used for the recording of 2D [^{1}H, ^{1}H] spectra (B), and another preparation used for recording 1D ^{111}Cd spectra and 2D [^{1}H, ^{111}Cd] HSQC spectra (C) agreed with each other, as the signal groups aligned by broken lines match well, although they were form different batches. However, those signal groups also indicated clearly the heterogeneity in the presence of cadmium. The multiple species are also reflected in 1D ^{111}Cd

(Figure 4.18), 2D [^{1}H, ^{1}H] (Figure 4.17) and 2D [^{1}H, ^{111}Cd] HSQC spectra (Figure 4.19).

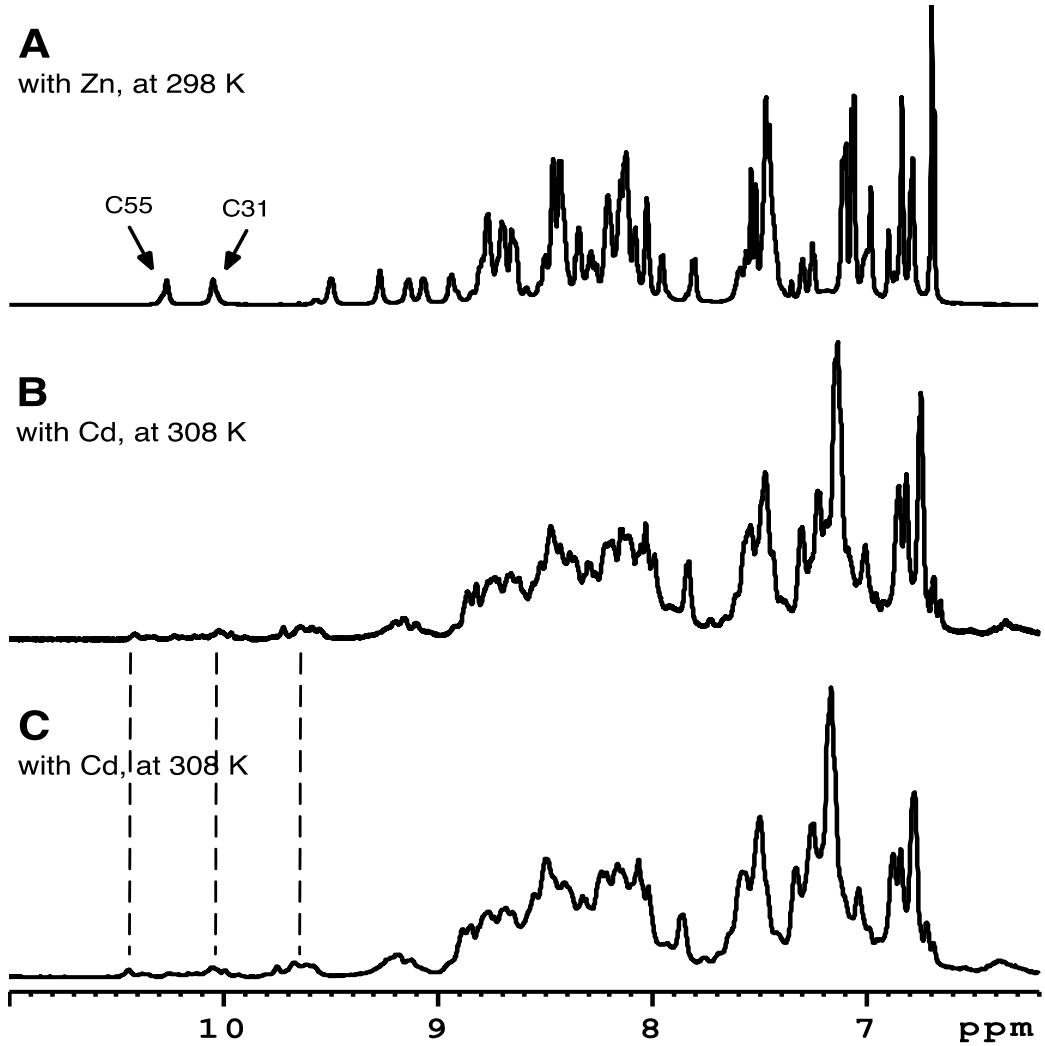

Figure 4. 8. Stacked plots of 1H NMR spectra (fingerprint region) of the BmtA2426 protein in the presence of Zn(II) and Cd(II) respectively. Samples were prepared with 2-2.5 mM BmtA2426 protein in 50 mM[D_{11}]Tris/Cl, 50 mM NaCl and 10% D_2O, pH 7.0. (A) and (B) were recorded on a 700 MHz spectrometer (AV II-700, Bruker), utilised for 2D [^{1}H, ^{1}H] spectra; (C) was recorded on a 500 MHz spectrometer (DRX500, Bruker), utilised for 1D ^{111}Cd and 2D [^{1}H, ^{111}Cd] HSQC spectra. The arrows pick out the resonance of the NH of Cys31 and Cys55.

Clearly, the three metallothioneins interact in different ways with Zn and Cd. All three proteins fold well in the presence of Zn, but not all fold equally well in the presence of Cd. Whilst BmtA0853 led to homogeneous preparation, folding of BmtA1081 in the presence of Cd was inconsistent, whilst loading BmtA2426 with Cd led consistently to multiple species.

4.3.2 2D [^{1}H, ^{1}H] TOCSY / 2D [^{1}H, ^{1}H] NOESY Spectroscopy with Cd

As described previously, for cadmium-loaded samples, metallothionein BmtA0853 was prepared with single species, which was reflected in the corresponding 2D [^{1}H, ^{1}H] spectra (Figure 4.9 A). The spectrum was relatively well dispersed, with single resonance peaks indicating a relatively well-folded protein. The key features mentioned earlier were also present (C32, F31 and A37). An equally well-folded protein irrespective of Zn or Cd binding is also reflected in an overlay of the TOCSY spectra in the presence of zinc and cadmium ions (Figure 4. 13).

For BmtA1081 and BmtA2426 (Figure 4.9 B and C, Figures 4.14 and 4.15), the signals were less well distributed and multiple species can be observed. Sequential resonance assignments were also performed, although there was a reduced number of observed resonances due to the presence of multiple species as well as a loss of signal dispersion, indicated by the increased intensity in the region around 8.5 ppm, where resonances for unfolded regions appear (Figure

4.10, 4.11 and 4.12). For BmtA1081, the chemical shifts for histidines were very similar to those observed for the Zn-loaded species, especially for His39, which was also nicely shaped; but for the other two histidines, multiple species were observed clearly, with at least 3 different conformations for His28 (Figure 4.10). The heterogeneity was also reflected in Cys31and Tyr30: there were eight backbone NH-Hα cross-peaks observed for Cys31 in the TOCSY spectrum (Figure 4.17 A), which indicated at least as many different species in this batch of cadmium loaded sample; and correspondingly, eight cross peaks between Cys 31 and Tyr 30 were observed in the respective NOESY spectrum, shown in Figure 4.17 B.

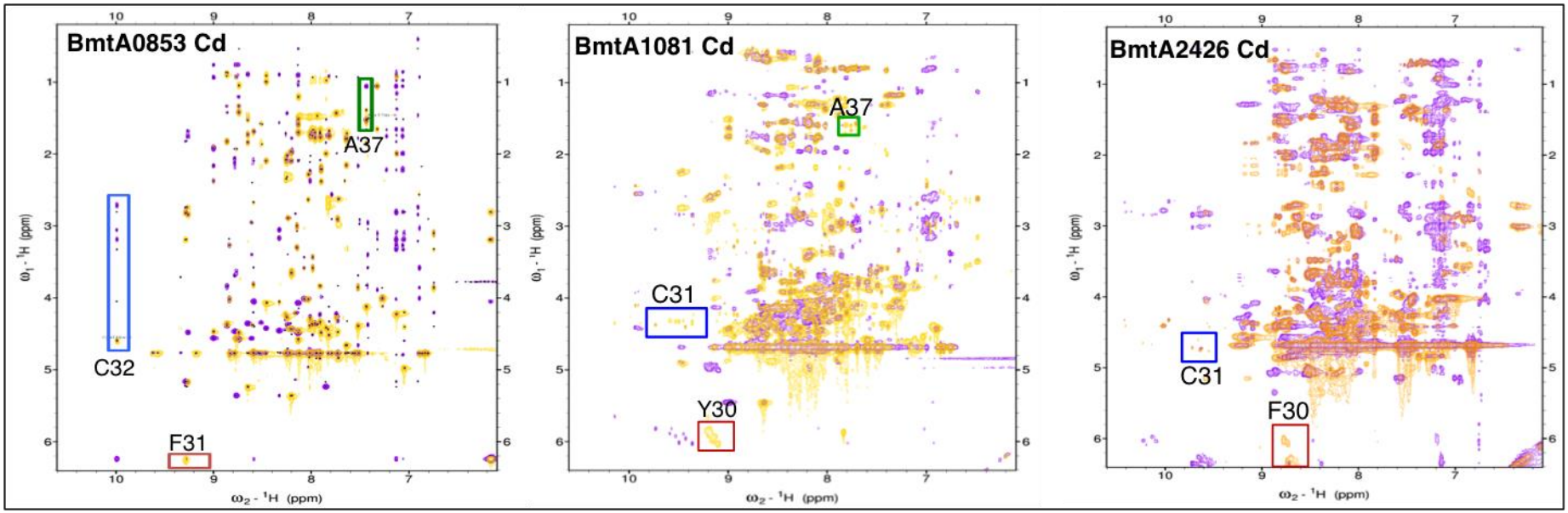

Figure 4.9. Fingerprint region of 2D [^{1}H, ^{1}H] NMR spectra for the three metallothioneins loaded with cadmium ions (TOCSY and NOESY represented in gold and purple, respectively). Spectra were recorded on a 700 MHz NMR spectrometer (AV II-700, Bruker) in 50 mM[D_{11}]Tris/Cl, 50 mM NaCl and 10% D_2O, pH 7.0, at 308 K. The structural features of SmtA are present in these three metallothioneins. Residues with the most diagnostic chemical shifts are highlighted.

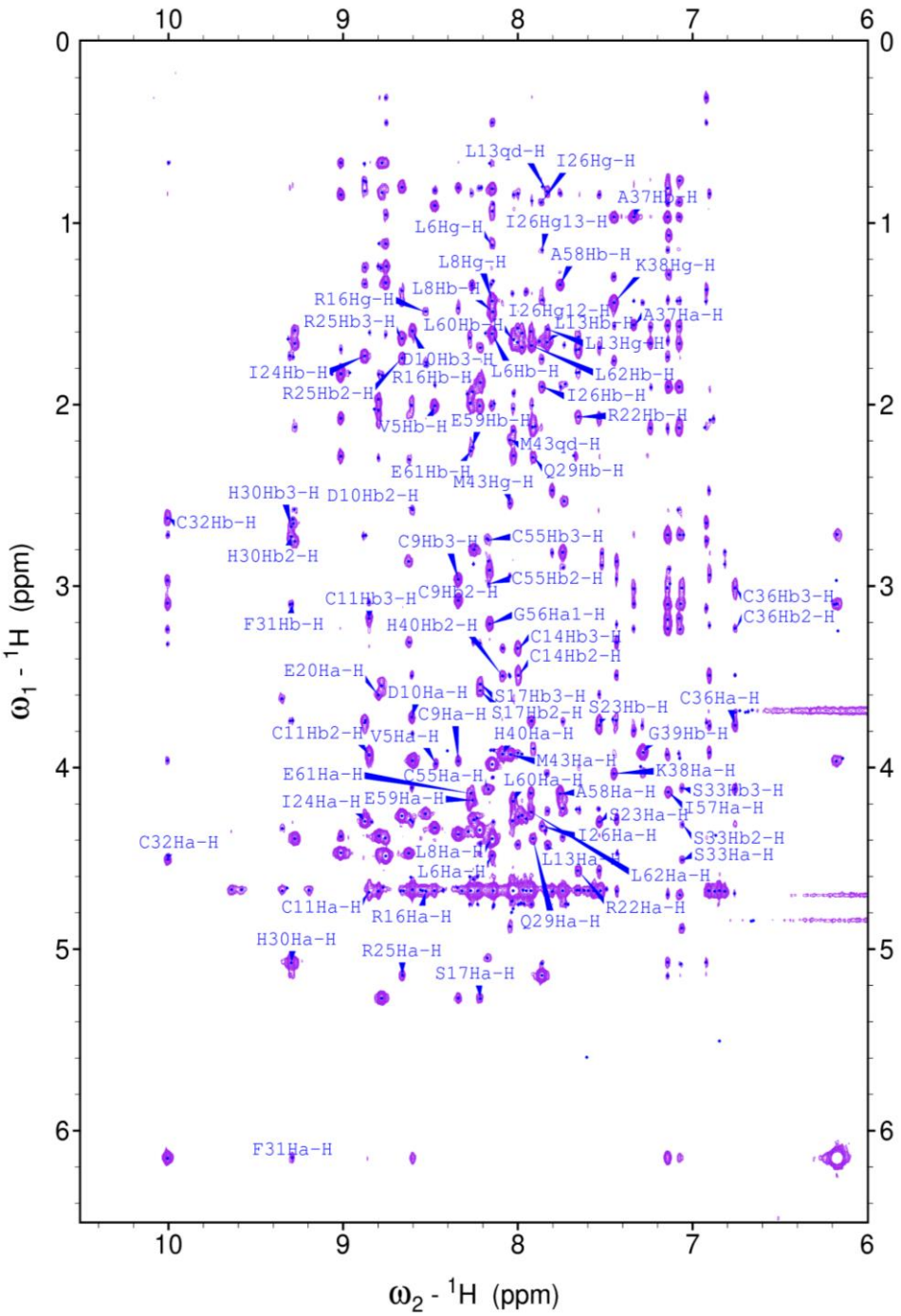

Figure 4. 10. Resonance sequential assignment of 2D NOESY NMR spectra for BmtA0853 in the presence of cadmium ions. Spectra were recorded at a 700 MHz spectrometer (AV II-700, Bruker) in 50 mM[D_{11}]Tris/Cl, 50 mM NaCl and 10% D_2O, pH 7.0, at 308 K

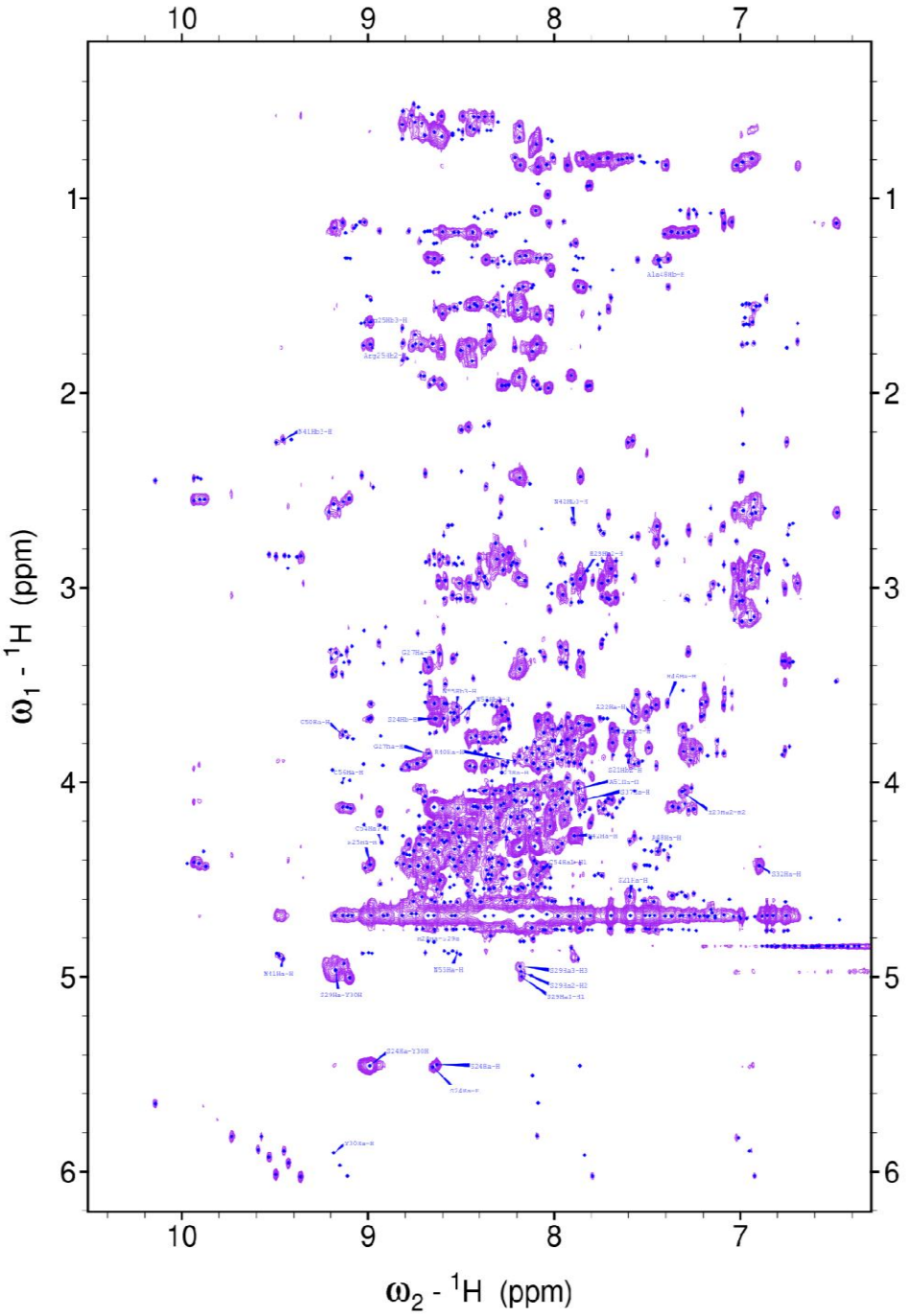

Figure 4. 11. Resonance sequential assignment of 2D NOESY NMR spectra for BmtA1081 in the presence of cadmium ions. Spectra were recorded at a 700 MHz spectrometer (AV II-700, Bruker) in 50 mM[D_{11}]Tris/Cl, 50 mM NaCl and 10% D_2O, pH 7.0, at 308 K.

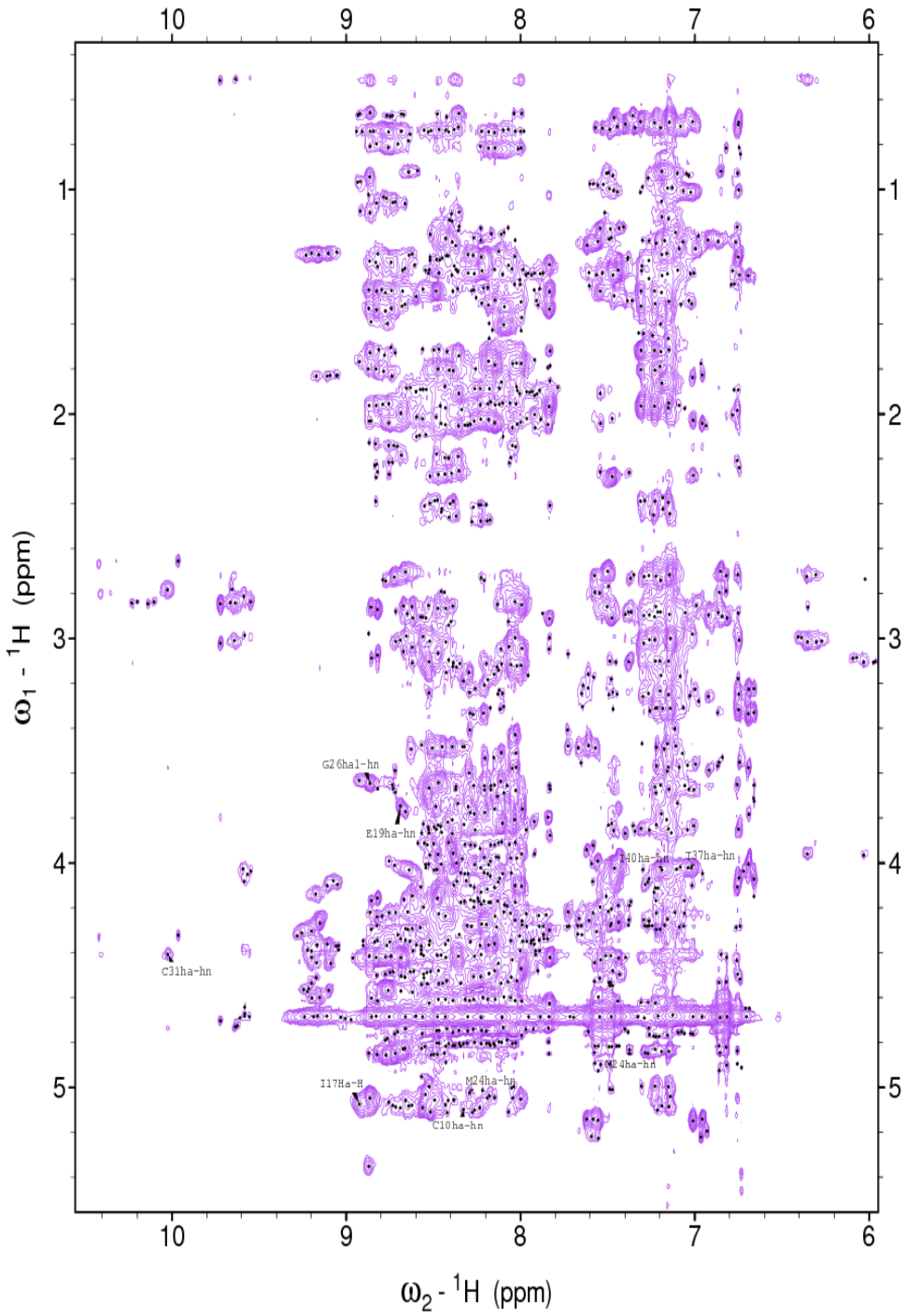

Figure 4. 12. Resonance sequential assignment of 2D NOESY NMR spectra for BmtA2426 in the presence of cadmium ions. Spectra were recorded at a 700 MHz spectrometer (AV II-700, Bruker) in 50 mM[D_{11}]Tris/Cl, 50 mM NaCl and 10% D_2O, pH 7.0, at 308 K.

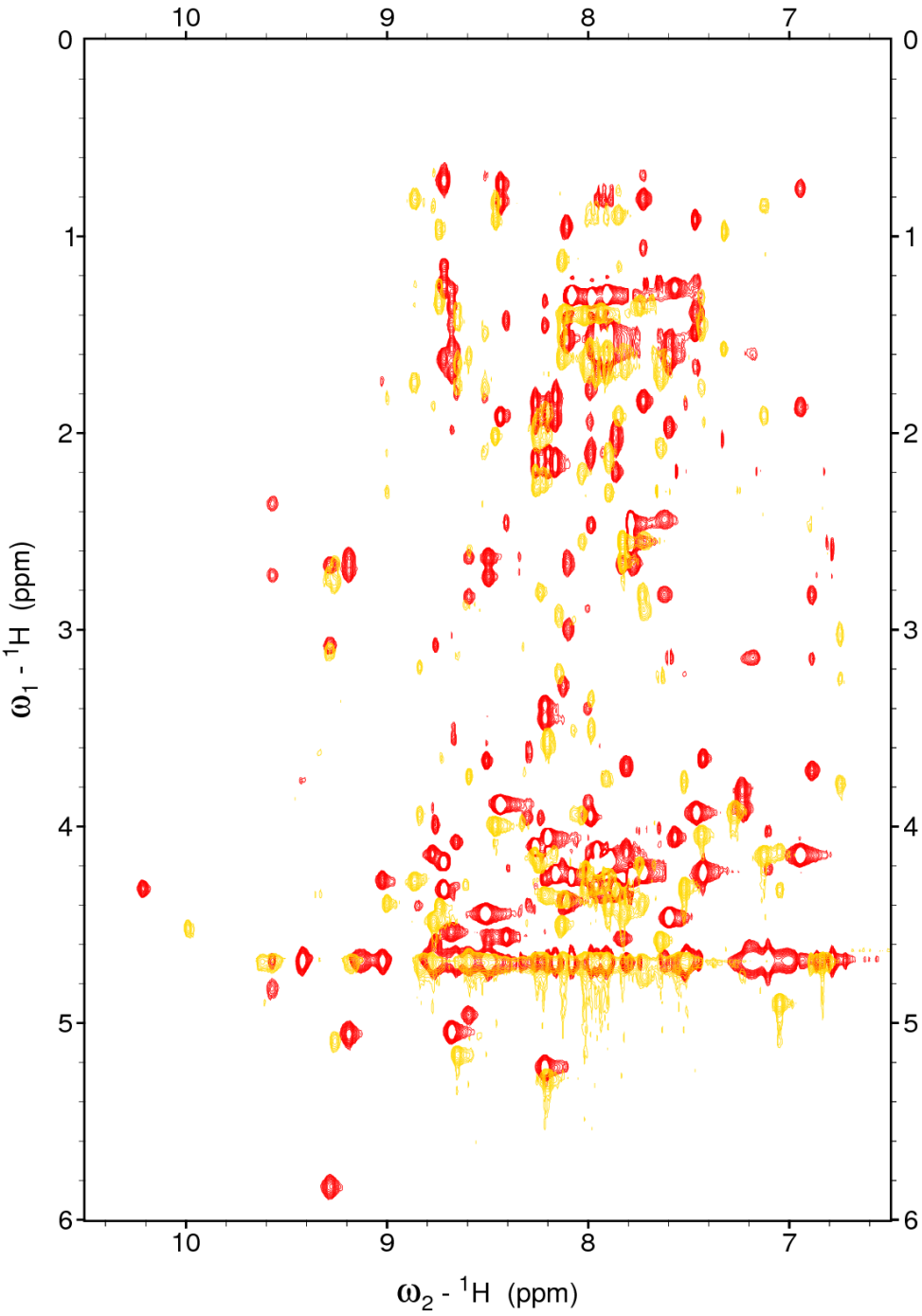

Figure 4.13. Overlay of fingerprint region of 2D TOCSY NMR spectra of BmtA0853. Red and Gold represent zinc and cadmium loaded BmtA0853, respectively.

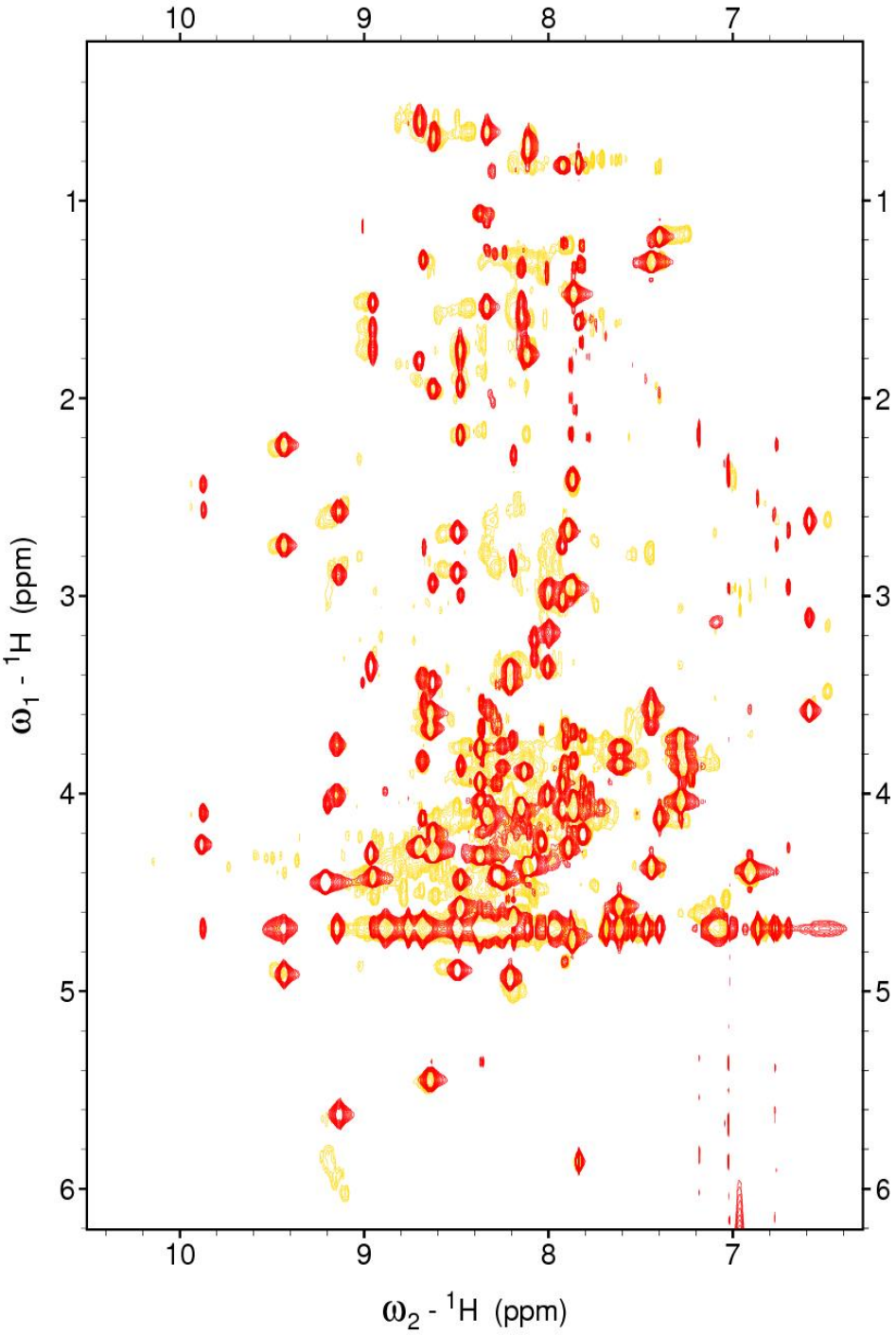

Figure 4.14. Overlay of fingerprint region of 2D TOCSY NMR Spectra of BmtA1081. Red and Gold spectra represent zinc and cadmium loaded BmtA1081, respectively.

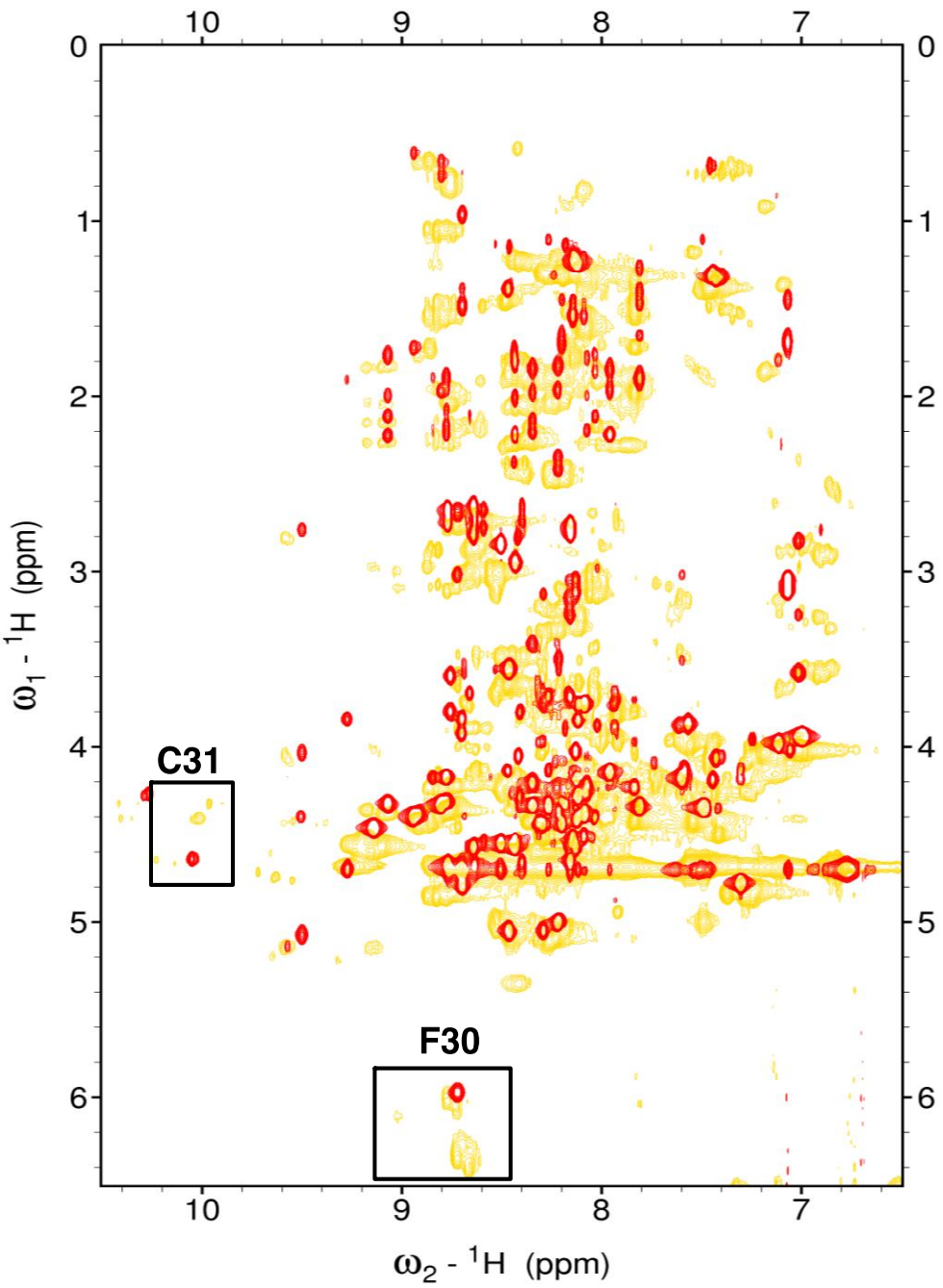

Figure 4.15. Overlay of fingerprint region of 2D TOCSY NMR Spectra of BmtA2426. Red and Gold spectra represent zinc and cadmium loaded BmtA2426 protein, respectively.

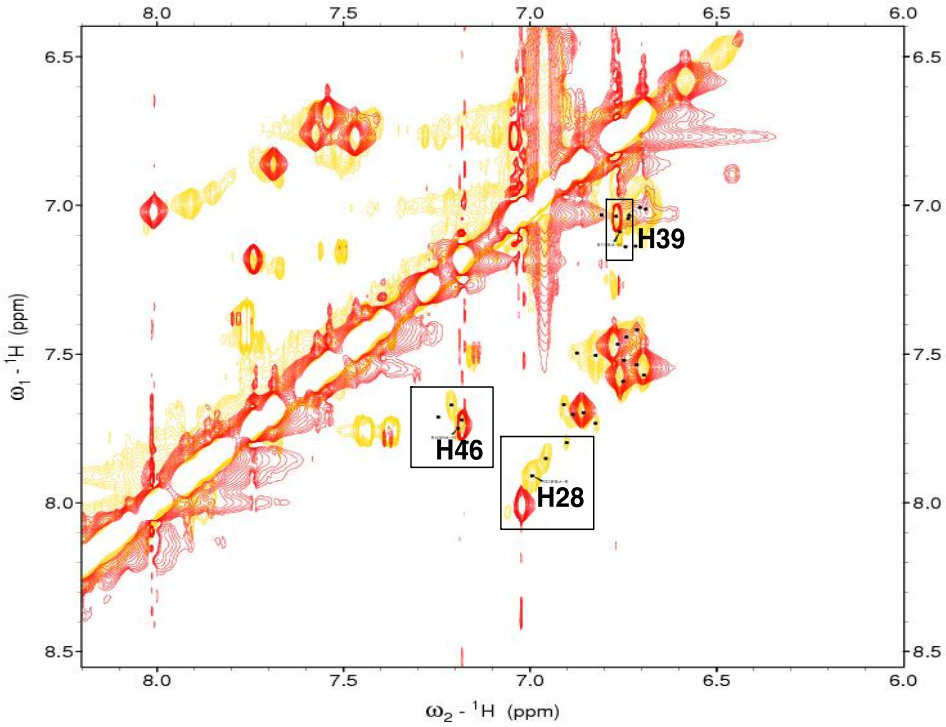

Figure 4.16. Overlay of TOCSY spectra of three histidines in BmtA1081 in the presence of zinc and cadmium. Red and Gold spectra represent zinc and cadmium loaded BmtA1081 protein, respectively. The chemical shifts of the three histidines are similar, especially for His39 (nicely shaped single peak); for His28 and His 46, there are clearly multiple species present (two and three peaks respectively).

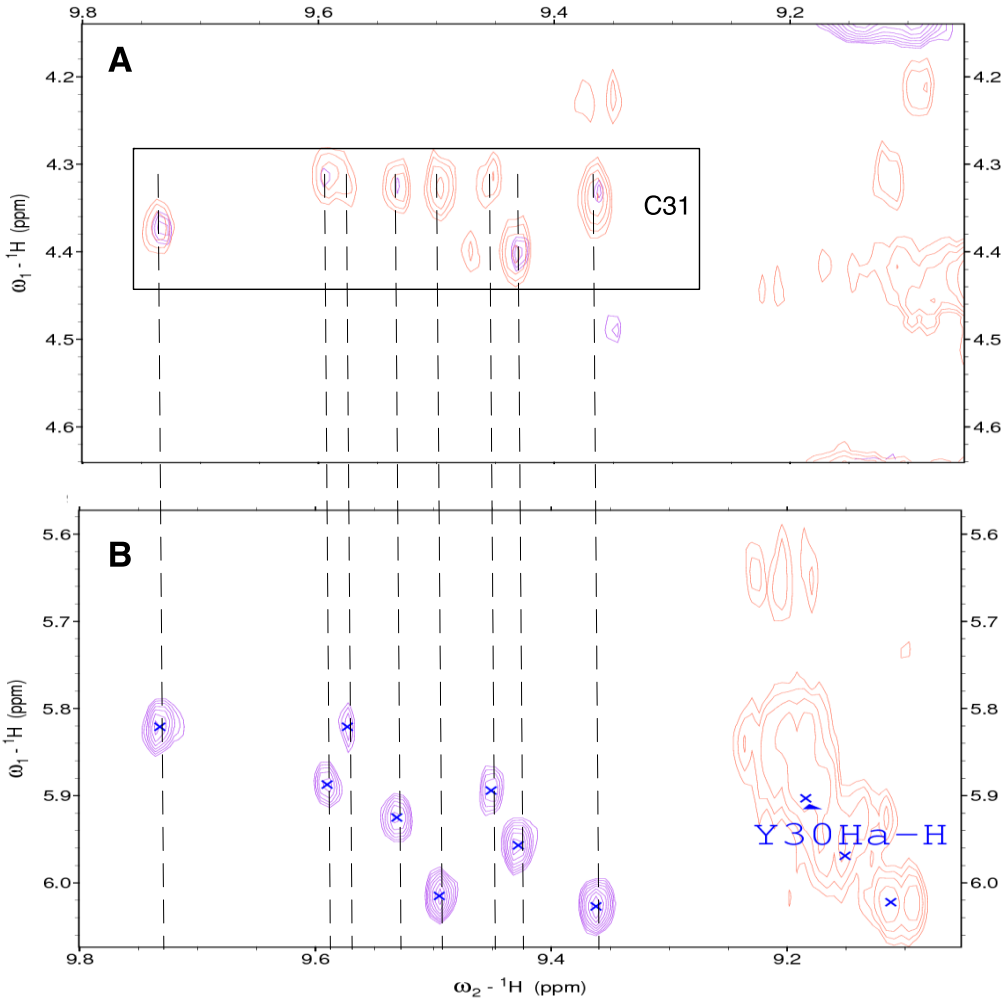

Figure 4. 17. 2D [1H, 1H] NMR spectra showing Cys 31 and Tyr 30 in cadmium loaded BmtA1081. Purple and Gold spectra represent NOESY and TOCSY spectrum, respectively. (A) For the H-Hα cross peaks of Cys31, at least eight species were observed; (B) The H-Hα cross peaks of Tyr30 (Gold peaks), multiple species were observed. Broken lines align cross-peaks between Tyr30 and Cys31.

4.3.3 1D ^{111}Cd NMR spectroscopy

When all zinc ions were replaced with cadmium ions in the three metallothioneins, three peaks were observed in the NMR spectrum of BmtA0853

while four peaks were observed for BmtA1081 as expected (Figure 4.18). The preparation for BmtA2426 showed at least three groups of peaks, but the heterogeneity of this sample is also reflected in the ^{111}Cd spectrum, and 2D 1H, ^{111}Cd HSQC spectroscopy was necessary to determine the number of observed peak groups. Compared with the four peaks in the 1D ^{111}Cd spectrum of Cd_4SmtA at 712 (A), 660 (B), 596 (C) and 567 (D) ppm (Blindauer *et al.*, 2001), there were similarities and differences. The peaks observed at 698 (BmtA 0853), 735 (BmtA1081), and 716 (BmtA2426) ppm were close to site A in SmtA (712 ppm). For BmtA 0853, the peaks at 670 and 568 ppm were very close to site B (660 ppm) and site D (567 ppm), the sites expected to be present in BmtA0853, based on the multiple sequence alignment (Figure 4.1). Both BmtA1081 and BmtA2426 are likely to contain, besides the Cys_4 site A, another Cys_4 site (651 and 682 ppm, respectively), with similar chemical shifts to SmtA site B. Comparison with the sequence alignment and connectivity pattern in Figure 4.1 indicates that not all site B residues are clearly conserved in either sync_1081 or BmtA2426, so the ligand composition of these sites is ambiguous.

The other peaks in BmtA1081 (532 and 489 ppm) and BmtA2426 (519 and 509 ppm) are in the range for Cys3His or Cys2His2 coordination, and they showed large differences compared with those observed in SmtA, so ligand connectivities might differ considerably.

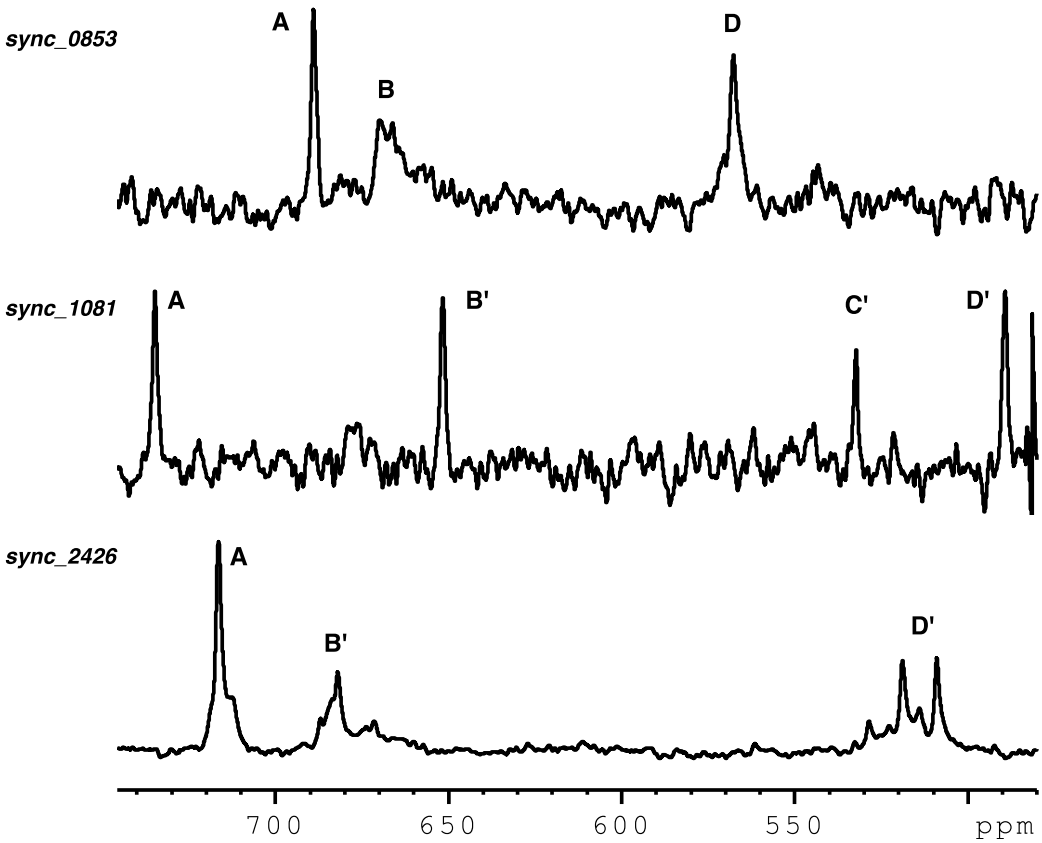

Figure 4.18. Proton-decoupled 1-dimensional 111Cd NMR spectra of 111Cd-reconstituted metallothioneins in Synechococcus sp. CC9311. Samples were prepared in 50 mM Tris-D_{11}/HCl, 50 mM NaCl, 10% D_2O pH 7.0. Spectra were recorded on a 500 MHz NMR spectrometer (DRX500, Bruker), at 308 K. Three peaks were observed in BmtA0853: 698 ppm, 670 ppm and 568 ppm; four peaks in BmtA1081: 735 ppm, 651 ppm, 532 ppm and 489 ppm; and at least four peaks in BmtA2426: 717 ppm, 682 ppm, 519 ppm and 509 ppm, although the latter two might correspond to the same site, as peaks A and B' also show signs of heterogeneity.

4.3.4 2D [^{1}H, ^{111}Cd] Heteronuclear Single Quantum Coherence Spectroscopy

The metal-ion-ligand connectivities were studied by 2D [^{1}H,^{111}Cd] Heteronuclear single quantum coherence (HSQC) NMR spectroscopy (Bonvin *et al.*, 2005;

Wang *et al.*, 2006; Digilio *et al.*, 2009). To observe the connectivities between cadmium ions and protons of ligating cysteine residues, the spectra were acquired with coupling constant $^{3}J_{1H,111Cd}$ = 25-55 Hz (Blindauer *et al.*, 2001; Blindauer *et al.*, 2002; Blindauer, 2008a).

In the [^{1}H, ^{111}Cd] HSQC spectra, the correlations of beta protons with cadmium resonances may be observed (Figure 4.19). The ligands in the Cd(II) binding sites were assigned by using chemical shifts observed in both of zinc and cadmium loaded 2D proton NMR spectra. The 2D [^{1}H,^{1}H] spectra of Cd-loaded species were due to the heterogeneity of samples, of limited utility. Therefore, the chemical shifts of CH2(β) protons from Zn-loaded species were also used. This is permissible because the chemical shifts of beta protons should be affected in a small way, as long as the replacement of Zn by Cd is isostructural.

There was only one cadmium-proton cross-peak observed for BmtA0853, the chemical shift of it indicated the connectivities between Cys 32 and a cadmium ion, likely in site A.

Various evidences showed that the cadmium-loaded BmtA1081 could in principle be prepared as folded protein: comparison of TOCSY spectra of the zinc and cadmium species (Figure 4.14), the 1D ^{111}Cd spectrum (Figure 4.18); but it was also evident that Cd-loaded BmtA1081 could fold in more than one way as judged from the observed heterogeneity (Figure 4.16, Figure 4.17), which made it more difficult to assign all ligands to each site for BmtA1081. There were four sets of cross peaks observed in the HSQC spectrum of BmtA1081 with

coupling constant $^{3}J_{1H,111Cd}$ = 40 Hz (Figure 4.19 BmtA1081 A). Cys 31 and 8 were assigned as ligands to site A unambiguously, not only because of the agreement of observed chemical shifts, but also because the pattern of the cross-peaks resembled that observed for site A of SmtA studied previously by Blindauer *et al.* (2001). Site B' also showed similarities with site B in SmtA: Cys 13 also may be coupling at this site. Cys 54, 56 and 45 could also be confidently assigned as ligands in site B', which hence would correspond closely to site B in SmtA, if the two last cysteine residues are aligned in each sequence (different to the alignment shown in Figure 4.1). The chemical shift of sites A and B' observed in HSQC spectra (735 and 651 ppm, Figure 4. 19 BmtA1081 A and B) also matched exactly with the chemical shifts observed in the 1D ^{111}Cd spectrum (735 and 651 ppm, Figure 4.18). However, this was surprisingly not the case for sites C' and D': two sets of chemical shifts were generated by two separate batches of samples, although the samples were prepared in the same way. In one instance, there were two peaks at 580 and 619 ppm, the one at 580 ppm was close to site D in SmtA. A further peak at 593 ppm was observed during cadmium titration (data not shown) of Zn_4BmtA1081. For a second preparation, only a peak at 532 ppm was observed, and this peak corresponds to peak D' in the 1D ^{111}Cd spectrum (Figure 4.18). In the 2D HSQC experiment (BmtA1081B), the spectral range was too limited to also allow observation of the peak at 489 ppm (which was present in the 1D ^{111}Cd spectrum). Besides these significant differences in the ^{111}Cd chemical shifts for the putative sites C and D resonances, the ligands assigned to cadmium sites in these two datasets were highly similar for the peaks at 580 and 532 ppm, and comprised Cys 10 and Cys 56 (analogous to two site D ligands in SmtA). The large difference in ^{111}Cd chemical shifts for

a site involving the same two Cys residues could suggest that more than one cluster structure is possible to be formed for BmtA1081, at least in the presence of Cd. Cys 15 was assigned to site C'. Furthermore, Cys 13 is likely to bridge site A and site B'. Histidine connectivities are discussed below.

In agreement with the conclusions drawn from the 1D ^{111}Cd spectrum, the HSQC spectrum of BmtA2426 indicated that site A (716 ppm) was very similar to site A in SmtA (712 ppm). Cys 31, 8 and 35 were also observed to couple with the cadmium ion in site A; but it was not possible to determine whether Cys 53 or 55 participate in this site. Cys 10, 13 and 55 were confidently assigned to site B'. The cross-peak patterns for the two ^{111}Cd resonances at 519 and 509 ppm strongly suggest that both peaks correspond to the same site. Cys 10 and 35 were confidently assigned to this site, which can therefore be designated as site D'. Importantly, Cys 10 is highly likely to bridge sites B' and D' - in contrast to Cys 11 in SmtA where it is a terminal ligand to site D. Unfortunately, only Cys 15 was assigned to site C'.

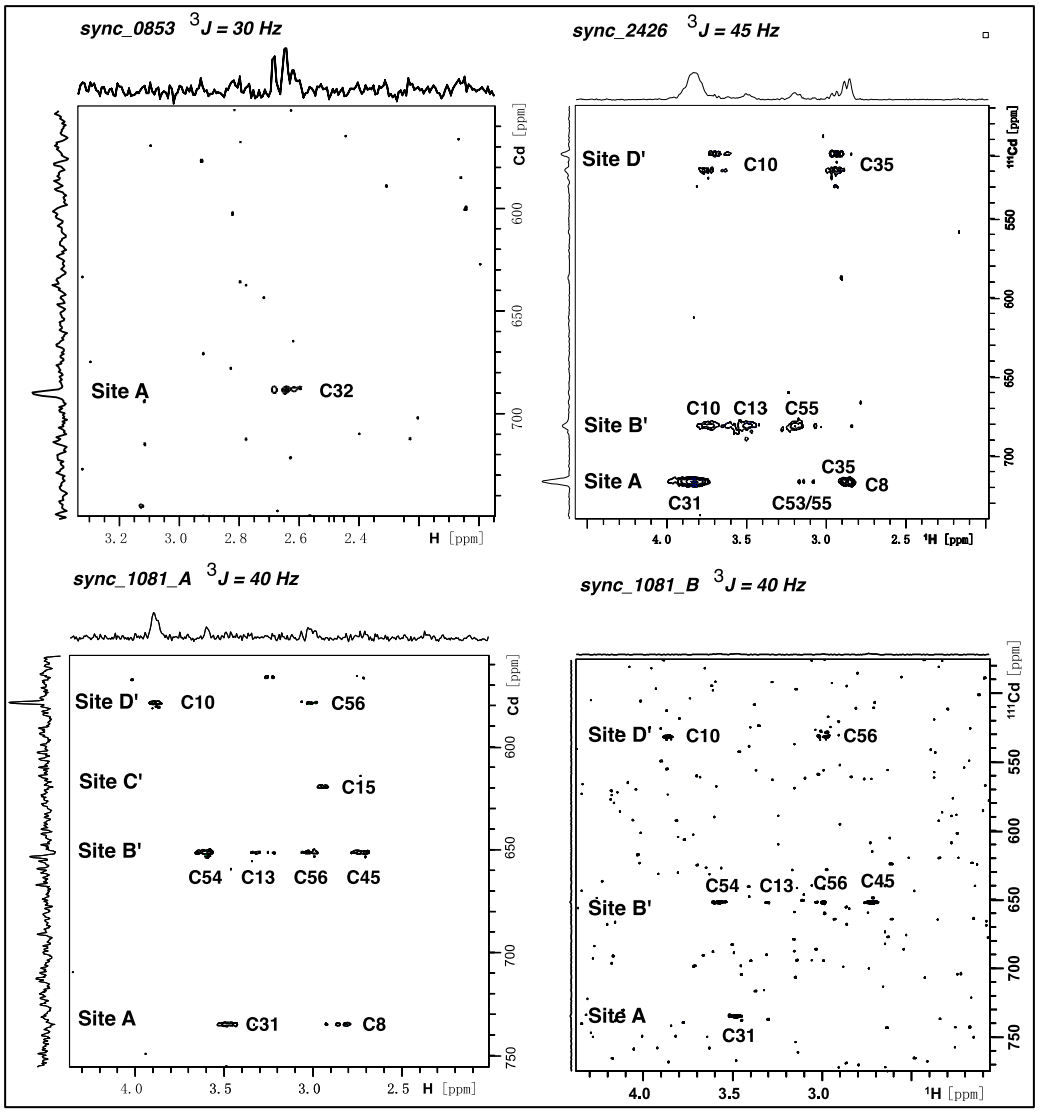

Figure 4.19. 2D [^{1}H, ^{111}Cd] HSQC NMR spectra for metallothioneins BmtA0853, BmtA1081 and BmtA2426 from Synechococcus sp. CC9311. Spectra were recorded on a 500MHz spectrometer (DRX500, Bruker) at 308 K, in 50 mM Tris-D_{11}/HCl, 50 mM NaCl, 10% D_2O pH 7.0. The chemical shift of Cd observed for BmtA0853 was at 689 ppm (site A). Four peaks were observed in the Cd dimension for BmtA1081A: 735 (site A), 651 (site B'), 580 (site D') and 619 ppm (site C'); three peaks for BmtA1081B: 735 (site A), 651 (site B'), 532 (site D'). BmtA1081A (555 – 755 ppm) and BmtA1081B (475 – 775 ppm) were recorded with a spectral width of 200 and 300 ppm respectively. Three peaks were observed for BmtA2426: 716 (site A), 682 (site B'), 519 and 509 ppm (site D').

4.3.5 Histidine connectivities in metal coordination

There are several histidines in the primary sequences of the metallothioneins from *Synechococcus* sp. CC9311, one of which immediately follows the conserved zinc finger region in all homologue sequences (Figure 4.20). The coordination of zinc-histidine has been reported in cyanobacterial metallothionein SmtA from *Synechococcus* PCC 7942 (Blindauer *et al.*, 2001) as well as other non-vetebrate MTs (Leszczyszyn *et al.*, 2007a; Bofill *et al.*, 2009; Peroza *et al.*, 2009; Zeitoun-Ghandour *et al.*, 2011). Therefore, whether histidines are also involved in metal coordination in metallothioneins in CC9311 becomes of significant interest. BmtA0853 has two histidine residues at position 30 and 40, and the latter one is in the conserved region and is predicted to be involved in metal coordination in site D'.

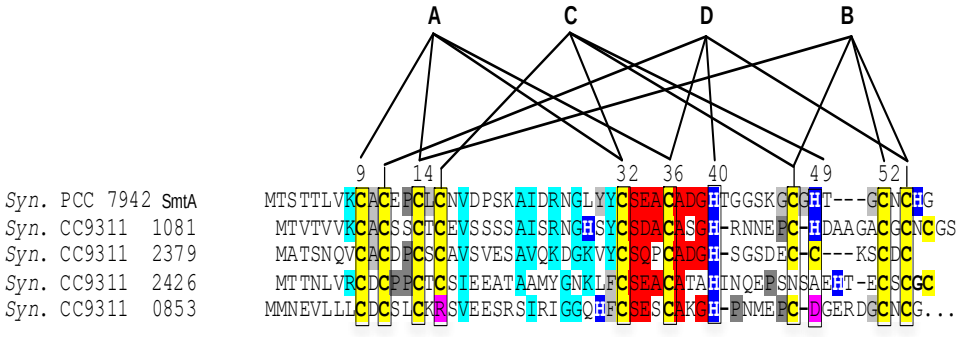

Figure 4.20. Multiple sequence alignment of SmtA in Synechococcus PCC7942 and metallothioneins in *Synechococcus* sp. CC9311 (Redrawn Blindauer et al., 2001; Blindauer et al., 2007).

There are two alternative ways that histidine can bind metals, these difference manifest themselves in the chemical shift of the $CH\varepsilon^1$ and $CH\delta^2$ protons changing, due to their sensing the coordinated metal nuclei (Figure 4.21 A and B).

His-Cd binding can also be captured by [^{1}H,^{111}Cd] HSQC spectroscopy; in this case, the $^3J_{1H,111Cd}$ coupling constants are very small (5-15 Hz). Figures 4.21 C and D show 1D ^{1}H,^{111}Cd HSQC experiments carried out with long mixing times (i.e. optimised for small couplings).

Three histidine residues are present in BmtA1081 at positions 28, 39 and 46. The chemical shifts of histidine resonances in the 1D HSQC NMR spectrum (this is the same sample as used for the 2D HSQC spectrum of BmtA 1081A, comprising ^{111}Cd resonances at 619 and 580 ppm, indicative of two possible Cys_3His sites) indicated that His 39 and 46 might coordinate (Figure 4.21 C). However, due to the heterogeneity of the corresponding 2D [^{1}H, ^{1}H] spectra in the presence of Cd (Figures 4.16 and 4.17), it was impossible to identify whether His 46 or His 39 corresponded to the peak at 7.309 ppm. Surprisingly His 28 seemed to participate as well, even though it is not in the predicted cluster region (Figure 4.20). This residue has the highest chemical shift in either Zn or Cd-loaded species in the 2D ^{1}H NMR spectra (8.10 ppm for Zn_4BmtA1081 and 7.91 ppm for one conformer of Cd_ BmtA1081, as observed from 2D ^{1}H NMR; see also Figure 4.16) among the three histidines; therefore His 28 is the only possible residue that might generate the resonance at 8.167 ppm. Overall, it appears that all three histidine residues are able to participate in metal binding for BmtA1081.

BmtA2426 contains two histidine residues at positions 39 and 50. In the spectra, at least two species were observed (Figure 4.18), as indicated by the doubling of peaks, but clearly His 39 is a coordinating residue (close chemical shifts to values form 2D ^{1}H data, 7.1 and 6.7 ppm) as shown in Figure 4.21D.

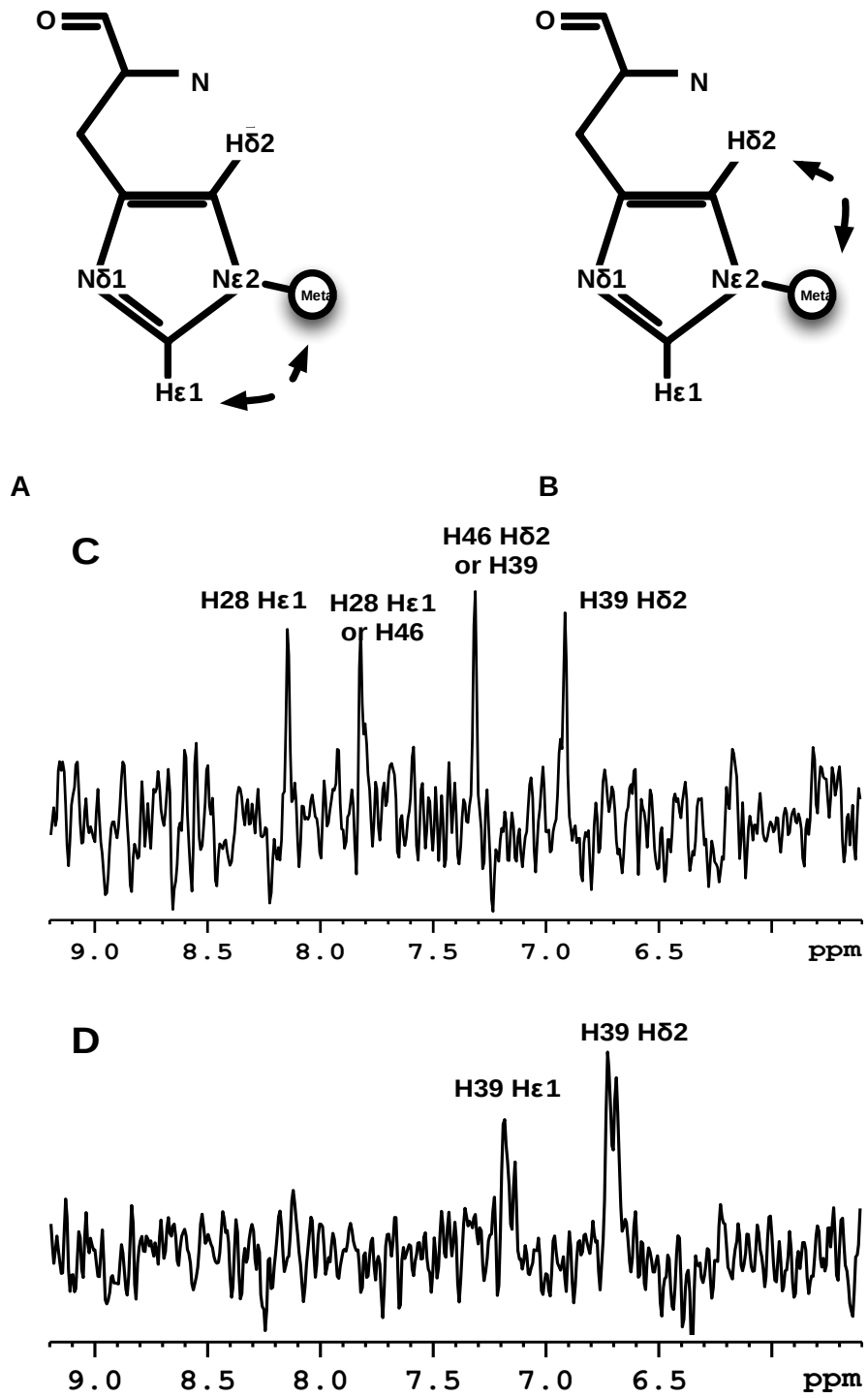

Figure 4.21. Identifying histidine resonance in ^{1}H NMR spectrum for BmtA 1081 and BmtA2426. Spectrum was recorded at a 500MHz spectrometer (DRX500, Bruker) at 308 K, ^{3}J= 10 or 15 Hz, in 50 mM Tris-D_{11}/HCl, 50 mM NaCl**.** (A) and (B) Annotated diagram showing the nomenclature of histidine resonances. (C) BmtA1081, Peaks at 8.167, 7.843, 7.309 and 6.908 ppm. (D) BmtA2426, Peaks at 7.185 and 6.726 ppm.

The participation of His 50 could not be confirmed in these experiments, but considering that site C' (which may contain this residue) was not observed in the 1D ^{111}Cd spectrum either, the absence of His 50 resonances coupled to Cd is not surprising.

To summarise, ^{111}Cd NMR spectroscopy on samples reconstituted with ^{111}Cd provided essential but incomplete information about the cluster structures of the three metallothioneins under study. When cadmium is bound, the binding sites of BmtA1081 and BmtA2426 display different dynamic properties, which made it impossible to observe all four metal binding sites in ^{111}Cd NMR spectra with sufficient signal intensity. Large differences in ^{111}Cd chemical shifts for site D' in BmtA1081 suggested that at least two alternative clusters may be formed. In particular, the experiments did not yield sufficient information on the variable site C'.

However, chemical shift analysis indicated that the backbone folds of the three metallothioneins are, at least in the zinc finger region, similar in the cadmium and zinc forms even when samples were heterogeneous, and ^{111}Cd NMR spectroscopy indicated that the zinc finger site A showed the least variations. Sites B', and D' in all three metallothioneins also showed some similarities with the corresponding sites in SmtA, whereas site C was absent in BmtA0853 as predicted, and was either not observed at all (BmtA2426) or only partially observable (BmtA1081). Therefore, only a limited identification of metal-cysteine connectives was possible to provide information for future structure calculations.

4.4 Towards three Dimensional Structures

With the results discussed so far, we are able to make some structure predictions for the metallothioneins in *Synechococcus* sp. CC9311. Preliminary homology models were generated using the 3D stucture of SmtA from the cyanobacterium *Synechococcus* PCC 7942 (pdb 1jjd) as a template (Figure 4.23).

Native ESI mass spectra (Chapter 3) revealed that only three metal ions were bound to BmtA0853, and the 1D ^{111}Cd and 2D ^{1}H NMR spectra also confirmed that site 'C' was missing. The homology model of BmtA0853 suggested that this site is replaced by salt bridges (Figure 4.22), formed by Arg 14 (replacing Cys16), as well as Asp45 and Asp49 (replacing His49). The remaining 8 Cys and His 40 can form unambiguously a Zn_3Cys_8His cluster, with sites A, B, and D formed by the equivalent residues in SmtA.

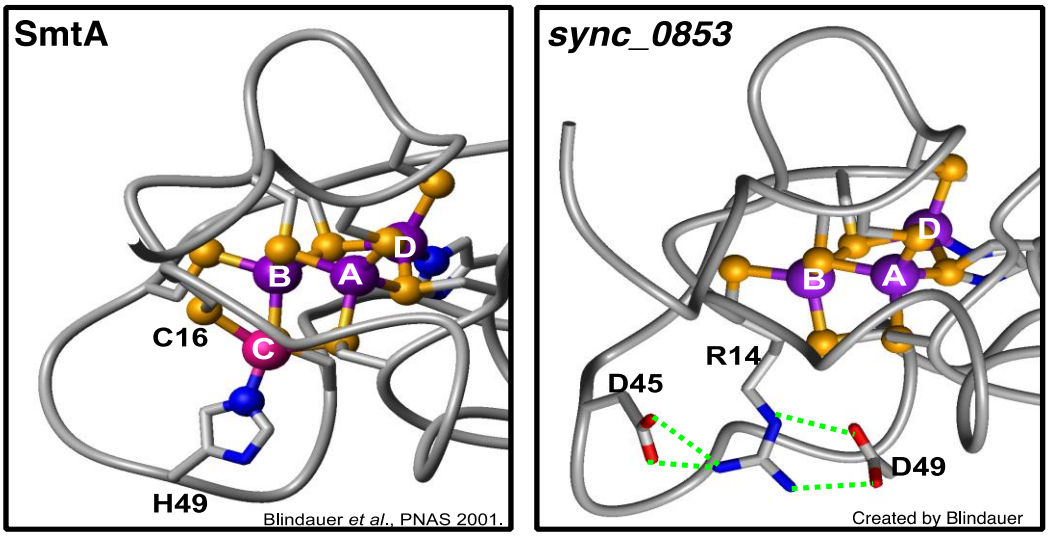

Figure 4.22. A part of the structure of SmtA from *Synechococcus* PCC 7942 and a homology model for BmtA0853 in *Synechococcus* sp. CC9311, showing the site C region. Structures and images were created by Dr. Claudia Blindauer.

For BmtA1081, site A was observed at 735 ppm, which was approximately 20 ppm different from that in SmtA; HSQC data indicated that Cys 8 and 31 were coordinating. The ^{111}Cd chemical shift for site B' was at 651 ppm, very close to the value for site B in SmtA, and the chemical shifts for Cys 13, 45, 54 and 56 were also comparable to shifts in SmtA, which indicate that site B' is probably also analogous to site B in SmtA. While for site C', the ^{111}Cd chemical shift were observed at 619 ppm, unfortunately only Cys 15 was identified to be the coordinating residue in site C'. Cys 10 and 56 were observed to coordinate to site D', but 2D ^{1}H data for zinc indicated that His 39, Cys 10, 35 and 56 are in close proximity, therefore likely coordinating to one zinc ion. The remaining Cys residue 52, His residues 28 and 46 are likely to coordinate in site C' in at least three possible ways (Figure 4.24). However, full structure determination will be required in order to identify the ligands more conclusively.

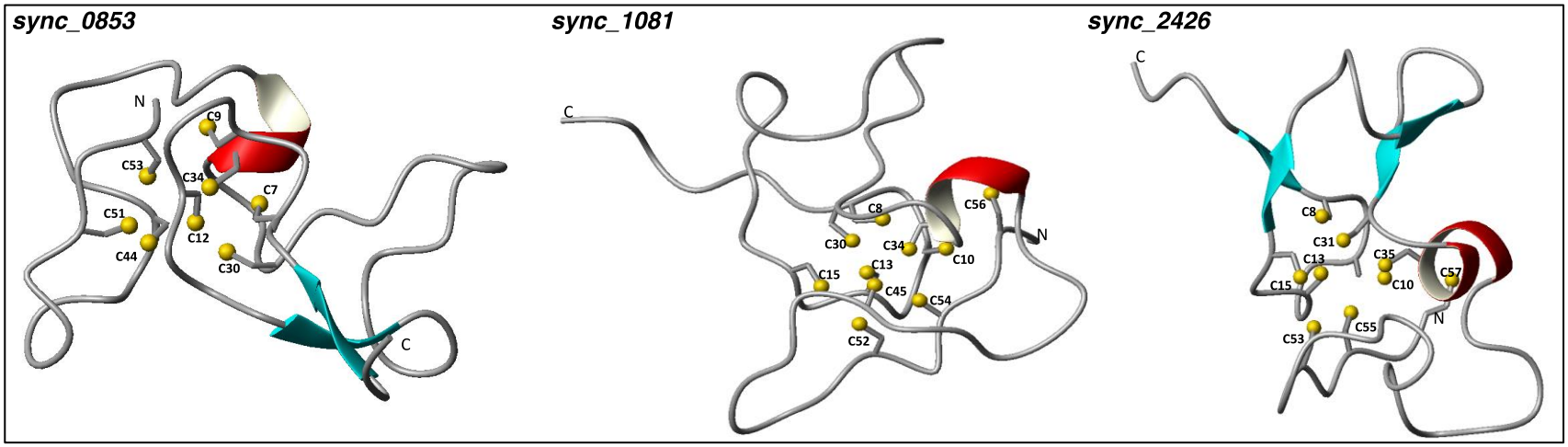

Figure 4.23. Preliminary homology model for BmtA0853, BmtA1081 and BmtA2426 in *Synechococcus* sp. CC9311. Generated by using the 3D stucture of SmtA from the cyanobacterium *Synechococcus* PCC 7942 (pdb 1jjd) as a template, showing the Cys residues. Structures and images were created by Dr. Claudia Blindauer.

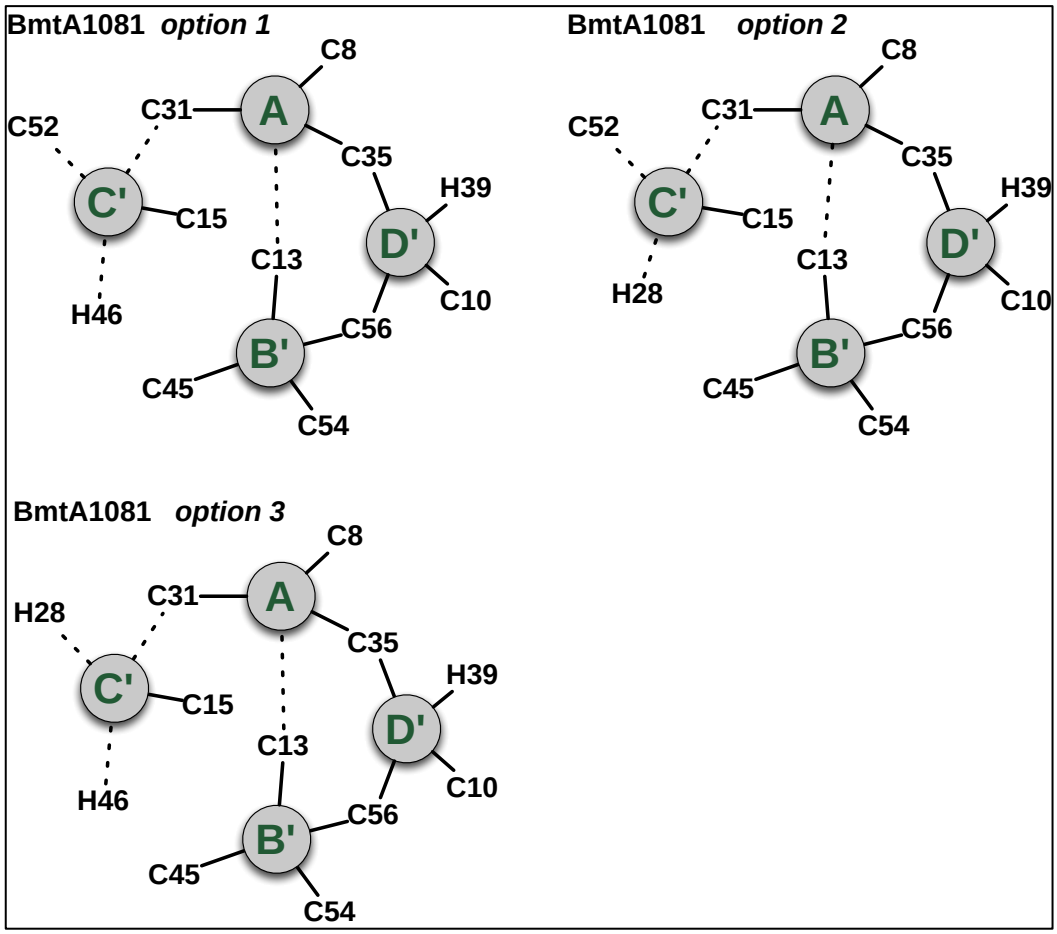

Figure 4.24. Schematic diagrams of possible cysteine- and histidine-zinc configurations for BmtA1081 in *Synechococcus* sp. CC9311. Dotted lines indicate ambiguous coordination bonds.

For BmtA2426, site A was observed at 716 ppm in both 1D ^{111}Cd and HSQC spectra, which is very close to the value for site A in SmtA. Also chemical shift data for Cys 8, 31 and 35 are comparable to the shifts in SmtA. The ^{111}Cd chemical shift of site B' was at 682 ppm, which is also close to the site B in SmtA, and Cys 10, 13 and 55 were highly likely to be part of site B'. For site D', the ^{111}Cd chemical shift was considerably different (more than 50 ppm) from that of site D in SmtA; but His 39, Cys 10 and 35 were shown to coordinate. In

addition, Zn 2D NOESY data showed proximity between Histidine 39, Cys 10, 35 and 57, which suggested tat these may be the coordinating residues in site D'. The difference in chemical shifts may be due to different surroundings and possibly geometry. However, site C' was not observed in 1D ^{111}Cd and HSQC, but 2D 1H data for zinc species show proximity of Histidine 50, Cys 15 and 31, suggesting these residues are likely coordinated to one zinc. The fourth ligand could not be identified, but it is possible that one of Cys 53 may coordinate. Therefore, a possible configuration is presented in Figure 4.25.

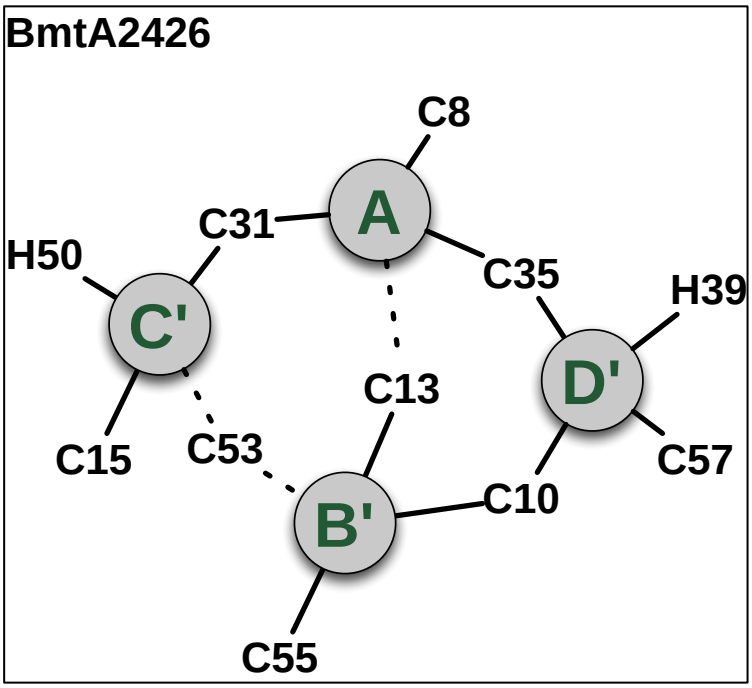

Figure 4.25. Schematic diagrams of possible cysteine- and histidine-zinc configurations for BmtA2426 in *Synechococcus* sp. CC9311.

It is hoped that the ambiguities may be resolved through complete NMR structure determinations, but it was not possible to tackle these in the available time.

4.5 Kinetics and Thermodynamics of zinc binding

In order to understand the relationship between the metal binding chemistry of metallothioneins and their biological functions in *Synechococcus sp.* CC9311, it is necessary to characterise their thermodynamic and kinetic properties.

4.5.1 Observation of Metal Release in Metallothioneins by Mass Spectrometry --Reactions with EDTA

Mass spectrometry was employed to study the metal release kinetics by monitoring the reaction of metallothioneins with EDTA at neutral pH (pH 7.4) (Li *et al.*, 1980; Leszczyszyn *et al.*, 2007a).

Before adding EDTA, the most abundant signals corresponding to the Zn-loaded species could be observed: for BmtA0853, Zn_3 species was the most abundant signal while Zn_1 and apo form were also present but with negligibly small signals (Figure 4.26); for BmtA1081, only one abundant signal was observed, the Zn_4 species (Figure 4.27); for BmtA2426, two abundant signals, both of them

corresponding to the Zn_4 species (-Met and +Met, respectively), were present in the mass spectra (Figure 4.28).

On the addition of EDTA (after ~ 3-6 minutes), the emergence of additional signals with lower masses than the original species could be observed in BmtA0853 and BmtA2426. As Figure 4.26 shows, the apo and Zn_1 species increased significantly when the Zn_3 BmtA0853 species was diminishing; while for BmtA2426, apo and Zn_3 species (both of –Met and +Met forms) emerged although the signals of those two species were less abundant (Figure 4.28). For BmtA1081, Zn_4 was still the most and only abundant signal (Figure 4.27).

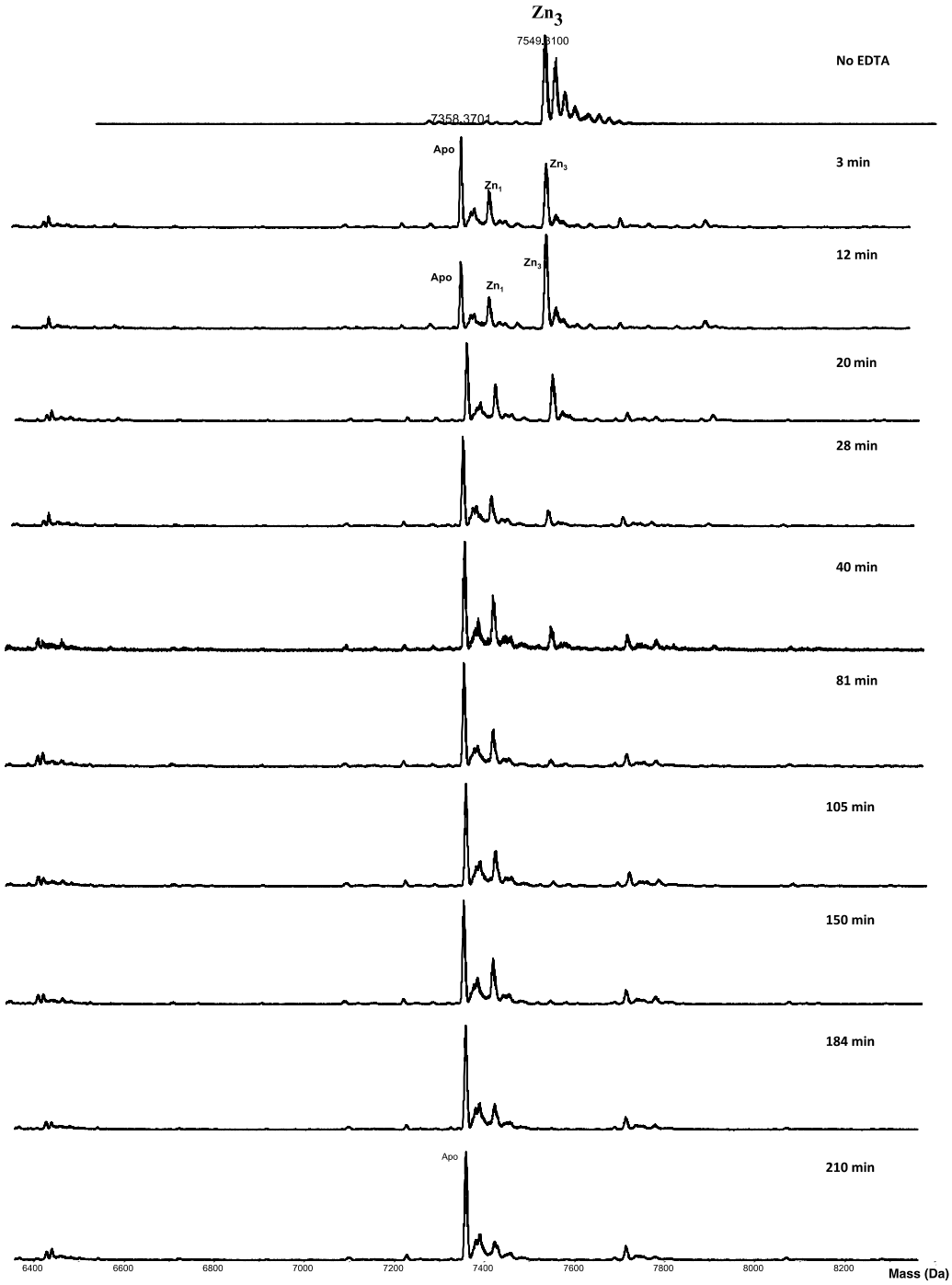

Figure 4.26. Mass spectrometric snapshots of the various species occurring during the reaction of BmtA0853 Zn_3species with EDTA (0.8 mM EDTA, 0.2 mM Zn(II), 10 mM ammonium acetate, pH 7.4). Three possible species were observed during the reaction: Zn_3, Zn_1 and apo-species. All spectra were deconvoluted by (+1) H.

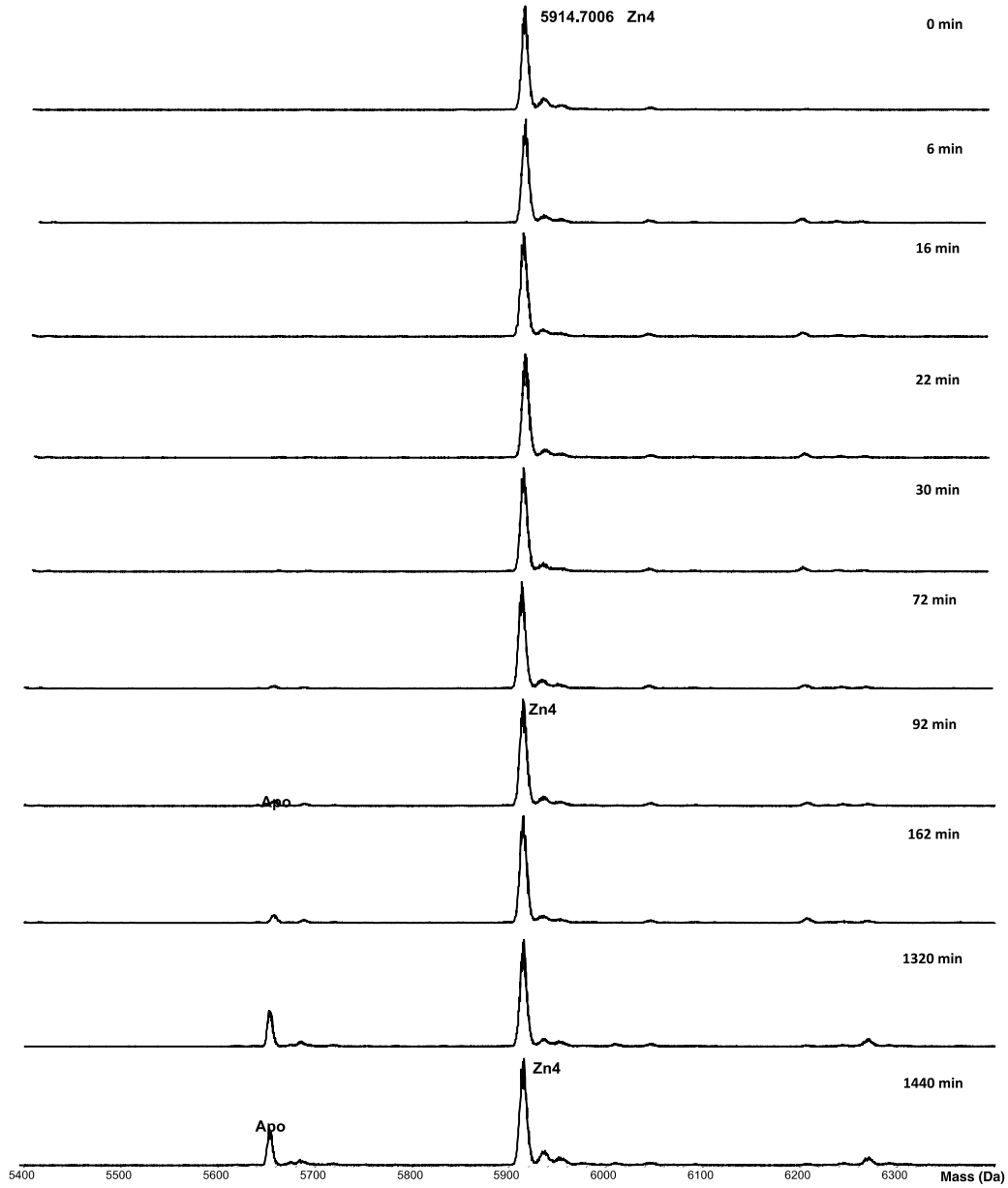

Figure 4.27. Mass spectrometric snapshot of the various species occurring during the reaction of BmtA1081 Zn_4 species with EDTA (0.8 mM EDTA, 0.2 mM Zn(II), 10 mM ammonium acetate, pH 7.4). Only two species, apo- and Zn_4, were observed. All spectra were deconvoluted by (+1) H.

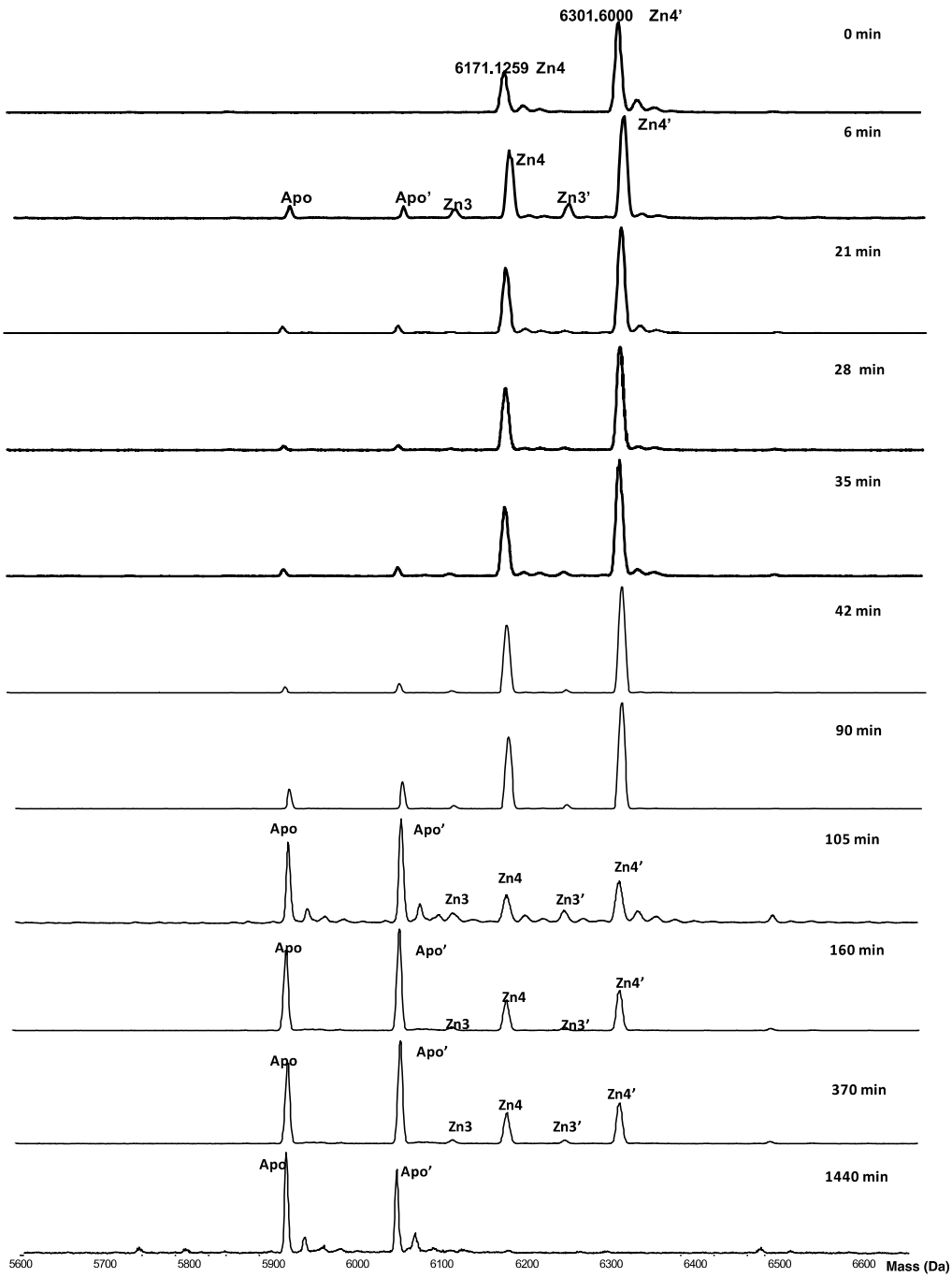

Figure 4.28. Mass spectrometric snapshot of the various species occurring during the reaction of BmtA2426 Zn_4 species with EDTA (0.8 mM EDTA, 0.2 mM Zn(II), 10 mM ammonium acetate, pH 7.4). The Zn_4 species is of BntA2426 that has lost the first methionine, the Zn_4' species is the full-length protein including the first methionine. Three species were observed during the time course, apo-, Zn_3 and Zn_4 species. All mass spectra were deconvoluted by +1 H.

The metallospecies observed and their relative abundance during the reaction with EDTA are plotted as semi quantitative plot against time in Figure 4.29 and Figure 4.30 for 1440 minutes and 200 minutes respectively.

For BmtA0853, the Zn_3 species is the overwhelming majority at the beginning; after addition of EDTA, the Zn_3 species diminishes rapidly and is present in only 2.2% after about 150 minutes. Concomitant with the loss of Zn_3 species, an increase of Zn_1 and Zn_0 metal species can be noticed, and the apo species becomes the most abundant species as the reaction progresses (Zn_1 25.4% and Zn_0 72.5% at about 150 minutes). After 1440 minutes, the apo species has become the only species. However, the Zn_2 species of BmtA0853 was never observed during the reaction. The observation of fully loaded species Zn_3 and the demetallated Zn_1 species, as well as the absence of demetallated Zn_2 species, suggest that when the first zinc ion is lost, BmtA0853 releases another zinc ion immediately and forms a relatively stable configuration with one zinc ion (Zn_1 metalloform) although the last zinc ion is also lost after a while. Obviously, the attack of EDTA on the first zinc ion of BmtA0853 is rapid, indicating that this particular zinc ion is labile and may be exposed in the structure. The remaining Zn ion in the Zn1 species is likely that bound to zinc finger site A, as previously observed for SmtA (Leszczyszyn *et al.*, 2007a). Clearly, the absence of the zinc ion in site C has led to the formation of an extremely labile cluster, which can be rapidly demetallated by EDTA. Whether access to sites B' and D' requires breaking of the salt bridge, or whether these sites are accessible otherwise, is not clear at this stage.

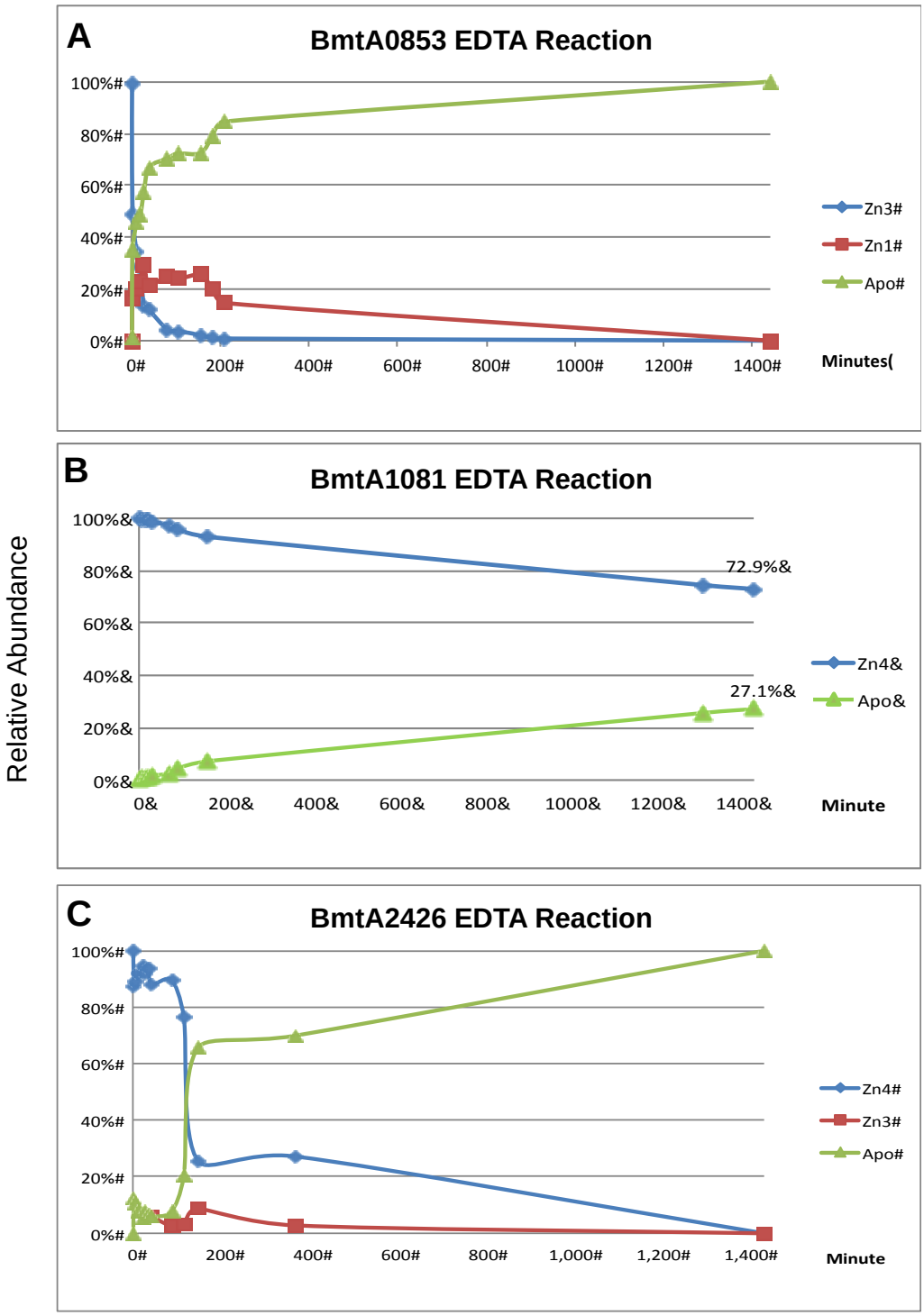

Figure 4.29. Semi-quantitative representation of speciation during the reaction of three metallothioneins with EDTA for 1440 minutes. Data are expressed as the relative abundance of the individual species in relation of the total observed species as the percentage.

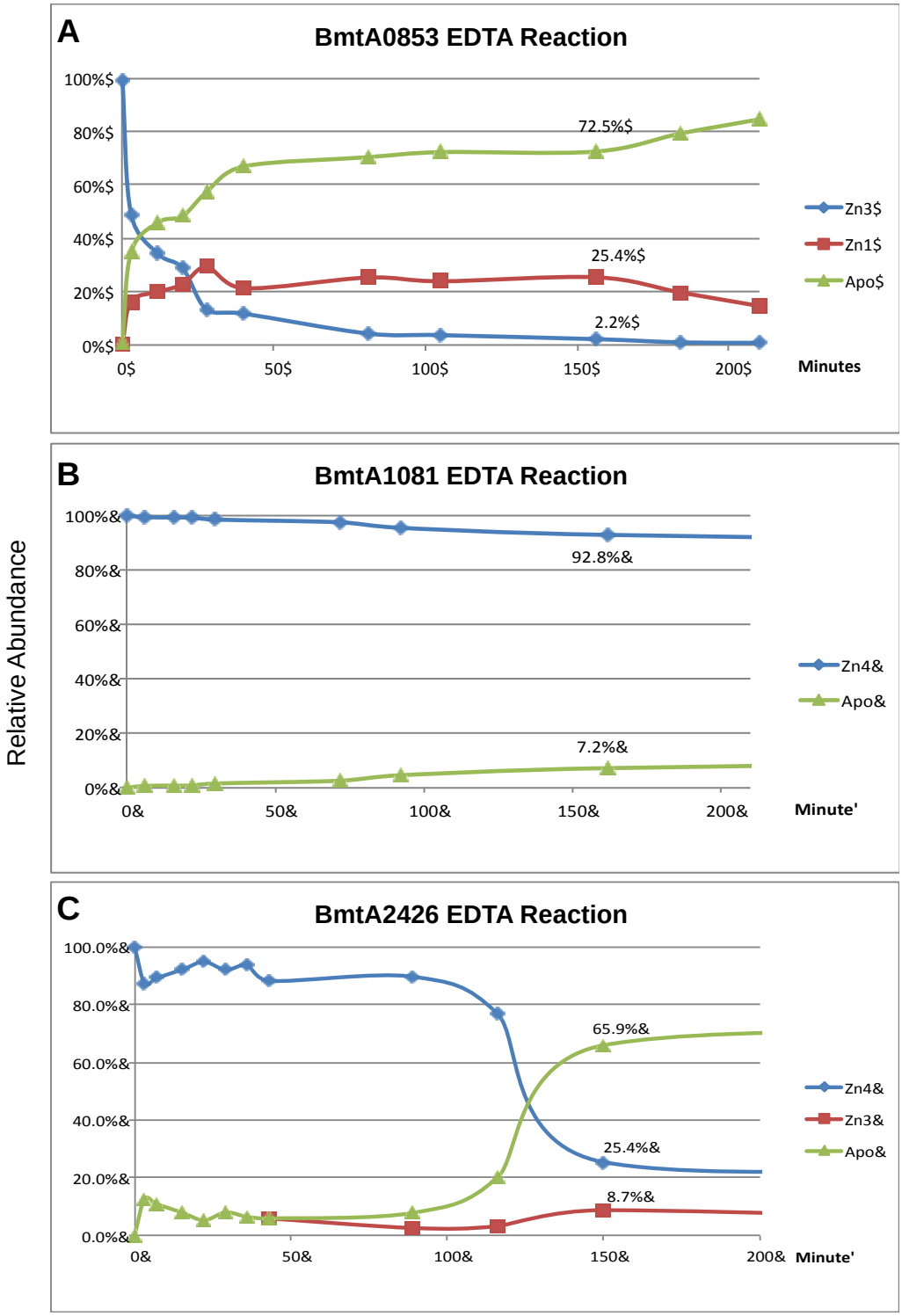

Figure 4.30. Semi-quantitative representation of speciation during the reaction of three metallothioneins with EDTA during the first 200 minutes. Data are expressed as the relative abundance of the individual species in relation of the total observed species as a percentage.

As for BmtA1081, the fully metal loaded Zn_4 species was the only species observed before adding of EDTA; with addition of EDTA, the apo form (Zn_0) BmtA1081 was noticed and after approximately 175 minutes, the Zn_0 species constituted 7.2% and Zn_4 species was at 92.8% of total observed species. As the reaction progresses, concomitant with the decreasing of Zn_4 species was the growth of Zn_0 species; after about 1440 minutes, Zn_4 and Zn_0 species correspond to 72.9% and 27.1% of total observed species, respectively, which suggests that BmtA1081 reacts extremely slowly and is relatively difficult to be attacked by EDTA. Unlike BmtA0853, none of the intermediate species was noted for BmtA1081: Zn_3, Zn_2 and Zn_1 species were not observed during the reaction with EDTA, which indicates that although the fully-formed Zn_4 BmtA1081 cluster is very resilient to metal removal, once it has lost its first zinc ion, it becomes very unstable and renders all three other zinc ions easily to be attacked by EDTA. This very particular zinc ion, predicted to be that bound to site C', is critical for metal occupation. It is possible that the altered geometry imposed by the "CH" motif (as opposed to the CxH motif in SmtA) generates a more inert site C. In addition, surface charges in the vicinity may also contribute - e.g Asp46 may hamper access of the negatively charged EDTA.

For BmtA2426, the Zn_4 metalloform (including both –Met and +Met forms) was the most and only abundant species before mixing with EDTA. After the introduction of EDTA the Zn_4 species diminished and the Zn_3 and apo species were noted. After about 150 minutes, the apo form BmtA2426 became the most abundant (65.9%), and the Zn_4 species was at 25.5% and the Zn_3 species at just 8.7%. As the reaction proceeded, the apo form became the single species that

was observed at the end (~1440 minutes). Similar to BmtA0853 and BmtA1081, not all possible demetallated species were observed for BmtA2426: the intermediate species Zn_2 and Zn_1 species were not observed during the reaction with EDTA. Apparently, the attack of EDTA on the first zinc ion of BmtA2426 is slower than for BmtA0853 but quicker than for BmtA1081. Taking into account the presence of Zn_3 and Zn_0 species and absence of Zn_2 and Zn_1 species, it is possible that the first zinc ion is relatively more difficult to attack compared with BmtA0853; but after the loss of the first zinc ion, the Zn_3 species still forms a moderately inert structure. Once another Zn ion is lost from this species, the remaining two zinc ions, including that in site A, are lost quickly. The reduced reactivity of the Zn_3 species (as compared to the same species of SmtA, for which no Zn_3 species could be observed) may be due to the different composition of the A-B-D cluster, and possibly, the switch from terminal to bridging nature of Cys 10 may play a role here. The latter hypothesis should be explored in the future.

4.5.2 Zinc Binding Constants via competition with 5F-BAPTA

In order to determine the zinc binding affinities of the three metallothioneins, BmtA0853, BmtA1081 and BmtA2426, a quantitative measurement procedure developed by Hasler *et al.* (2000) was employed to measure the zinc binding stability constant. This technique involves competition with the fluorinated metal chelator 5F-BAPTA (1,2-Bis(2-amino-5-fluorophenoxy)ethane-N, N, N', N'-tetraacetate), which is able to form a 1:1 complex with divalent metal ions

and can be detected in ^{19}F NMR spectroscopy (Long *et al.*, 1994; Benters *et al.*, 1997). The apparent binding constant of Zn-5F-BAPTA was reported as $8.13\times10^{9}M^{-1}$ in 50 mM Tris/Cl at pH7.4 (Hasler et al., 2000). Although the zinc binding constant calculated by this method is an average of all the individual zinc binding sites, it provides direct observation of the overall stability. Calculations were performed using the following equation:

$$K_{MT} = K_B\left(\frac{[ZnMT]_0\beta}{\alpha^2[B]_0}(\alpha+\beta)-\frac{\beta}{\alpha}\right)$$

K_{MT}: Zinc stability constant of metallothionein

K_B: binding constant of Zn to BAPTA, 8.13×10^{9} M^{-1} (50 mM Tris-Cl, pH7.4).

B: free 5F-BAPTA

ZnMT: Zn-MT complex

α: the integrals of the zinc-free 5F-BAPTA

β: the integrals of the zinc-bond 5F-BAPTA

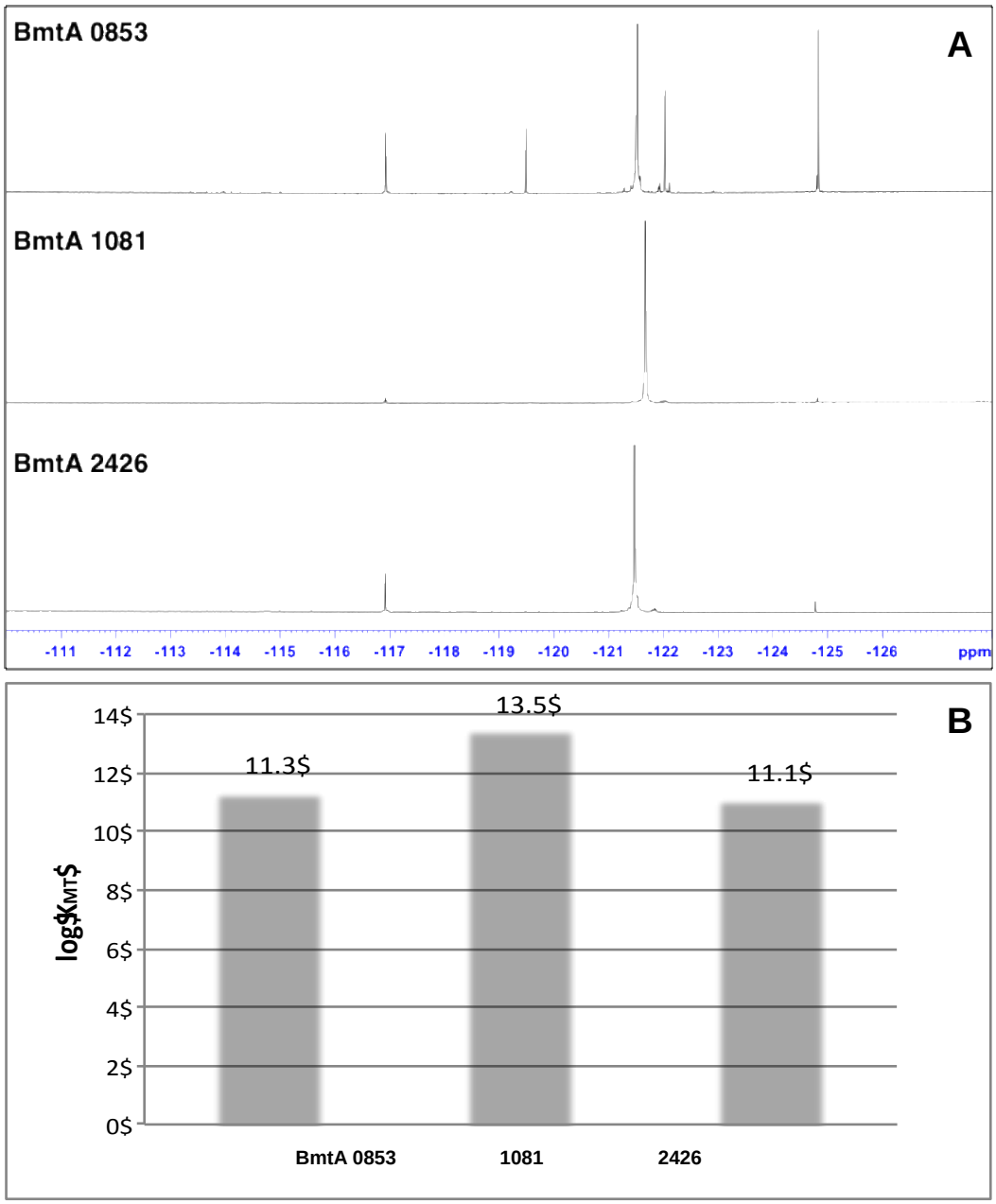

Figure 4. 31. 19F-NMR of bacterial BmtAs in the presence of Zn(II) ions. (A) NMR spectra; (B) Comparison of the log K binding constants of the three BmtAs. Experiments were carried out with 4mM 5F-BAPTA, 120 μM metallothionein (50 mM Tris-D11, 10% D2O, pH7.4).

The derived zinc-binding constant K_{app} for BmtA0853 is $2.1\times10^{11}M^{-1}$, followed by BmtA2426 (K_{app} = $1.2\times10^{11}M^{-1}$). However, the value of BmtA1081 (K_{app} = $3.0\times10^{13}M^{-1}$) is more than two orders of magnitude greater than the values for the BmtA0853 and BmtA2426, which indicate that BmtA1081 forms the most stable complex with zinc ions. The lower zinc binding affinity for BmtA0853 and BmtA2426, together with the kinetic data, also suggests that the zinc ion bound to those two metallothioneins may be transferable to other biomolecules.

4.6 Summary

In this chapter, the three isolated BmtA proteins (0853, 1081 and 2426) were characterized including protein folding and structure, metal release kinetics and metal binding thermodynamics.

The first BmtA 0853, in which His 49 is replaced by an Asp residue, but also lacks Cys 16, was observed to bind up to three zinc ions at neutral pH7.4. The 1D ^{111}Cd and 2D ^{1}H NMR results also confirmed the loss of site C. A homology model suggested that the remaining eight Cys and His 40 are able to form an unambiguous Zn_3Cys_8His cluster including site A, B and D by the equivalent residues in SmtA (section 4.4). The rapid metal release after introducing EDTA and the absence of demetallated Zn_2 species indicates that the loss of site C leads to an extremely labile cluster. In addition, the zinc-binding constant for BmtA 0853 (log K_{app} =11.3) also indicates the zinc ions bound may be more

transferable to other molecules compared to the SmtA in *Synechococcus* sp. PCC7942 (>13; Blindauer, 2008).

For the BmtA1081, four metal binding sites were observed in the 1D ^{111}Cd NMR spectra, which agreed with the ESI-MS spectra and ICP-OES analysis. With the information obtained form 2D homo- and heteronuclear NMR spectra, three metal binding sites A (Cys 8, 13, 31 and 35), B' (Cys 13,45, 54 and 56) and D' (Cys 10, 25, 56 and His 39) were unambiguously assigned; only one metal binding ligand was unambiguously identified for the site C' (Cys 15), which lead to three possible configurations (Figure 4.24). The EDTA reaction indicated that the fully metal-loaded BmtA1081 is highly resilient to metal release, although it becomes very unstable and releases all zinc ions once it has lost the first one. This special metal binding site is predicted as the site C', which is less exposed caused by the 'CH" motif compared to the 'CxH' motif in SmtA. The zinc-binding constant for BmtA1081 is much higher than BmtA0853 and 2426, suggesting the zinc ions bound to this protein are more difficult to transferable.

Another metallothionein protein, BmtA2426 is able to bind four zinc ions as observed by ESI-MS and ICP-OES. A possible $Zn_4Cys_9His_2$ metal binding cluster was generated with the information observed by ^{111}Cd and ^{1}H NMR spectra: site A shows high similarity to site A in SmtA (Cys 8, 31, 35 and possibly 13); Cys 10, 13 and 55 coordinate to one zinc in site B'; Cys 15, 31 and His 50 may be coordinated in site C'; Cys 10, 35, 57 and His 39 may coordinate in site D'; the remaining Cys 53 is possibly bridging between site B' and C' (Figure 4.25). In EDTA reaction, BmtA 2426 lost its first zinc ion more slowly than 0853 and formed a moderately stable Zn_3 cluster, which indicate that zinc

ion two is relatively more difficult to attack; but once the second zinc ion is attacked, it lose the remaining two zinc ions are lost rapidly. However, which of the site B’ or D’ is the second metal to be attacked is not clear yet, which requires more work in the future.

5

Growth Characteristics of *Synechococcus sp*. CC9311 with Different Metals

5.1 Introduction

Metallothioneins are capable of binding metal ions such as the essential metal Zn(II) as well as the toxic metal Cd(II) with high affinity. This is an indication that they serve a function in protecting cells against excess metal ions, especially zinc and cadmium (Olafson *et al.*, 1979b; Shi *et al.*, 1992b; Banci *et al.*, 2004). In chapter 4, the *in vitro* properties of three BmtAs 0853, 1081 and 2426 were investigated, including metal binding affinity, specificity, metal release kinetics and protein folding and structure. However, whilst *sync_2379* was successfully cloned into an expression plasmid (confirmed by DNA sequencing), due to low levels of expression in *E. coli*, *in vitro* studies were not possible. There are clear differences in protein sequence between these four metallothioneins. However, their biological function in *Synechococcus* sp. CC9311 is unknown. This begs the question does the possession of four distinct genome-encoded metallothionein genes provide an ecological advantage over other marine strains that encode only one or no copies of the metallothionein gene? In this chapter, the cell growth characteristics of *Synechococcus* sp. CC9311 in response to different environmental conditions were compared with two further *Synechococcus* sp. strains, WH8102 and WH7805, which contain one or no metallothionein gene(s), respectively (Scanlan *et al.*, 2009).

These three marine *Synechococcus* strains and the clades they represent inhabit contrasting environments, with *Synechococcus* sp. WH8102 (clade III) occupying oligotrophic open ocean waters low in nutrients but a relatively

constant ecosystem, whilst *Synechococcus* sp. CC9311 (clade I) inhabits the coastal aquatic environment which encounters a more erratic nutrient supply, and is a generally more variable ecosystem because of wind-driven inputs from the deep ocean and riverine inputs from land (Palenik *et al.*, 2006a; Zwirglmaier *et al.*, 2007; Zwirglmaier *et al.*, 2008; Scanlan *et al.*, 2009; Stuart *et al.*, 2009). For *Synechococcus* sp. WH7805 (clade VI) the precise ecological conditions under which this clade proliferates are less clear but it appears more of a generalist than the other two strains being broadly distributed in low numbers (Zwirglmaier *et al.*, 2008). In order to adapt to these differing habitats, these three strains are proposed to have developed different lifestyles, 'open-ocean specialist' (WH8102) 'coastal opportunist' (CC9311) or 'generalist' (WH7805) (Dufresne *et al.*, 2008; Scanlan *et al.*, 2009).

Genome analysis reveals that the costal strains CC9311 and WH7805 not only have larger genome size (2.61 and 2.62 Mbp respectively) compared to the open-ocean strain WH7805 (2.43 Mbp) but also contain more protein-encoded genes as shown in Table 5.1 (Palenik et al., 2003; Palenik et al., 2006; Dufresne et al., 2008), which may be the results of adaption to their special habitats. As predicted, CC9311 also contain 11 histidine kinase sensors and 17 response regulators which is almost double of the number in WH8102 (5 histidine kinase sensors and 9 response regulators); although the function of these additional sensors are not known at this point, these may participate in regulation of more complex metal metabolism (Palenik *et al.*, 2006b). This strain also contains three cation-dependent efflux transporters (*sync_0686*, *sync_1861* and *sync_1510*) compared

to two in WH8102, indicating it may have an increased capability to export metal jons at toxic levels (Palenik *et al*., 2006b).

Table 5.1. Summary of Synechococcus sp. CC9311, WH8102 and WH7805 genomes and Zn related gene orthologs (from Scanlan *et al*., 2009).

Genus and strain	Genome Size (Mb)	No. of genes	*zur*, cluster 1833	*smtA*(Zn), cluster 2886	*zmuA*, cluster 919	*znuA*-like, cluster 2462
CC9311	2.61	2,892	◆	4	◆	◆
WH8102	2.43	2,519	◆	◆	◆	◆
WH7805	2.62	2,934	◆	-	◆	-

Table 5.1 summarises the known and proposed genes involved in Zn homeostasis of the three strains, including the putative *zur*, *smtA*, *znu* and *znu*-like gene (Blindauer, 2008; Scanlan et al., 2009), which are present in all three strains. The Zur Proteins regulate Zn uptake and their Zn-loaded forms repress the expression of *znu*ABC (Patzer and Hantke, 2000).

5.2 Growth analysis with excess zinc

Since metallothioneins possibly play an important role in protecting cells from metal toxicity (Olafson *et al.*, 1979b), *Synechococcus* sp. CC9311 was grown under a range of zinc concentrations in Aquil medium (see section 2.1.4) and growth rates compared with two other *Synechococcus* strains, WH8102 and

WH7805. By monitoring the absorbance at 750 nm, growth curves were plotted for each strain under six different zinc concentrations ranging from the standard concentration of 772 nM (see section 2.1.4) up to 15 μM.

As shown in Figure 5.1, there was no significant difference in growth at zinc concentrations between 772 nM - 2.5 μM, for all three strains. However, when treated with 5 μM zinc growth of *Synechococcus* sp. CC9311 was inhibited. At concentrations of 10 and 15 μM zinc growth of *Synechococcus* sp. CC9311 was significantly impaired whilst cell death also occurred. For *Synechococcus* sp. WH8102, 5 μM zinc not only inhibited growth but also caused cell death as evidenced by a drop in optical density. Surprisingly, the growth of *Synechococcus* sp. WH7805 appeared unchanged when treated with up to 5 μM zinc, but similar to *Synechococcus* sp. CC9311, 10 μM zinc was toxic to *Synechococcus* sp. WH7805.

Analysis of the specific growth rate (for calculation details see section 2.1.8) for each strain also confirmed that at high zinc concentrations *Synechococcus*. sp. CC9311 was more tolerant to zinc excess compared to the oligotrophic strain WH8102. Thus, the growth rate was still measurable for *Synechococcus* sp. CC9311 at 15 μM zinc although it was significantly reduced compared to growth at 2.5 μM zinc. In contrast, *Synechococcus* sp. WH7805 and *Synechococcus* sp. WH8102 did not survive at concentrations of 10 μM and 5 μM zinc, respectively.

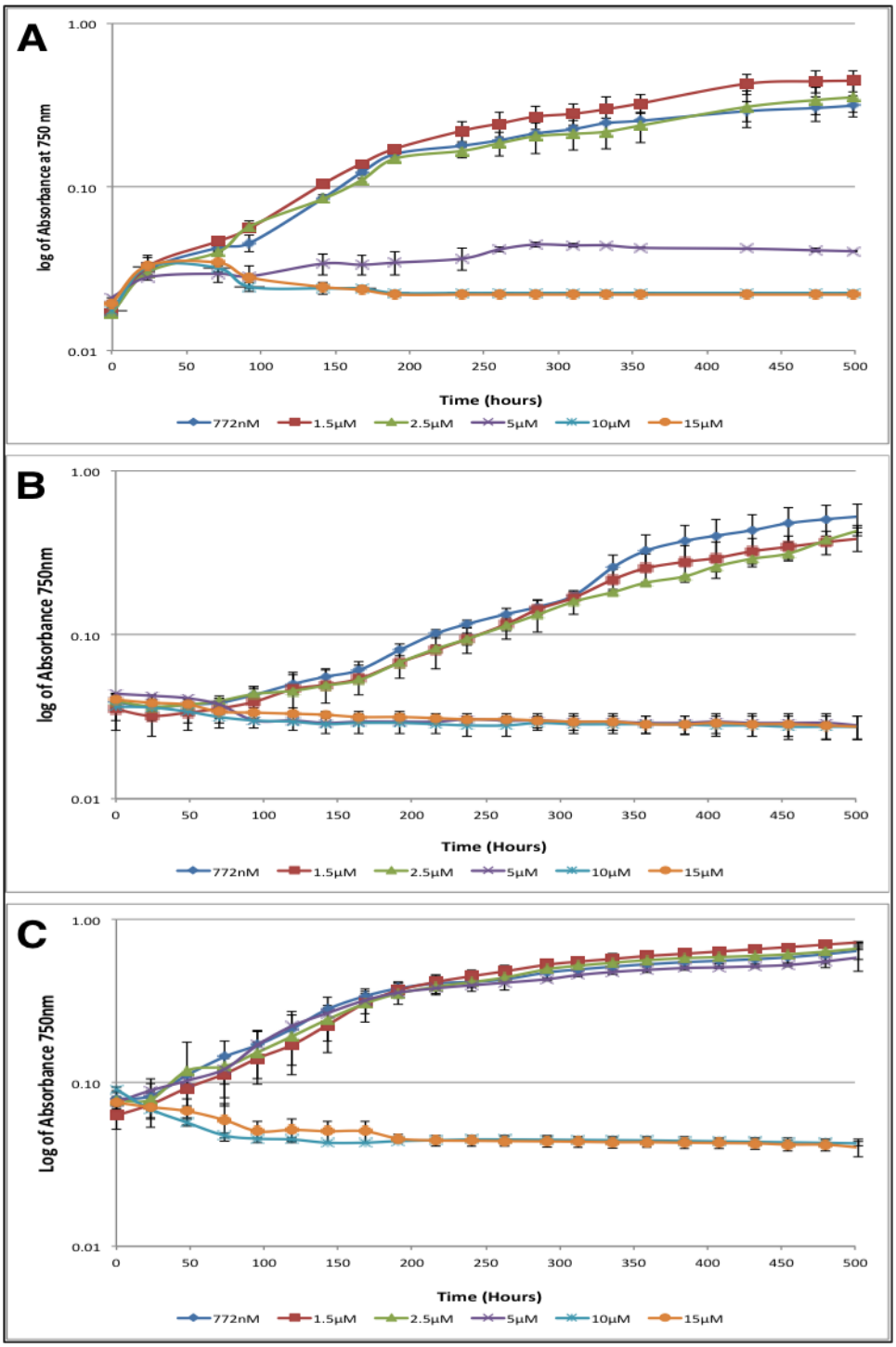

Figure 5.1 Growth of *Synechococcus* sp. CC9311 (A), *Synechococcus* sp. WH8102 (B) and *Synechococcus* sp. WH7805 (C) with various zinc concentrations. Error bars indicate error between two biological replicates.

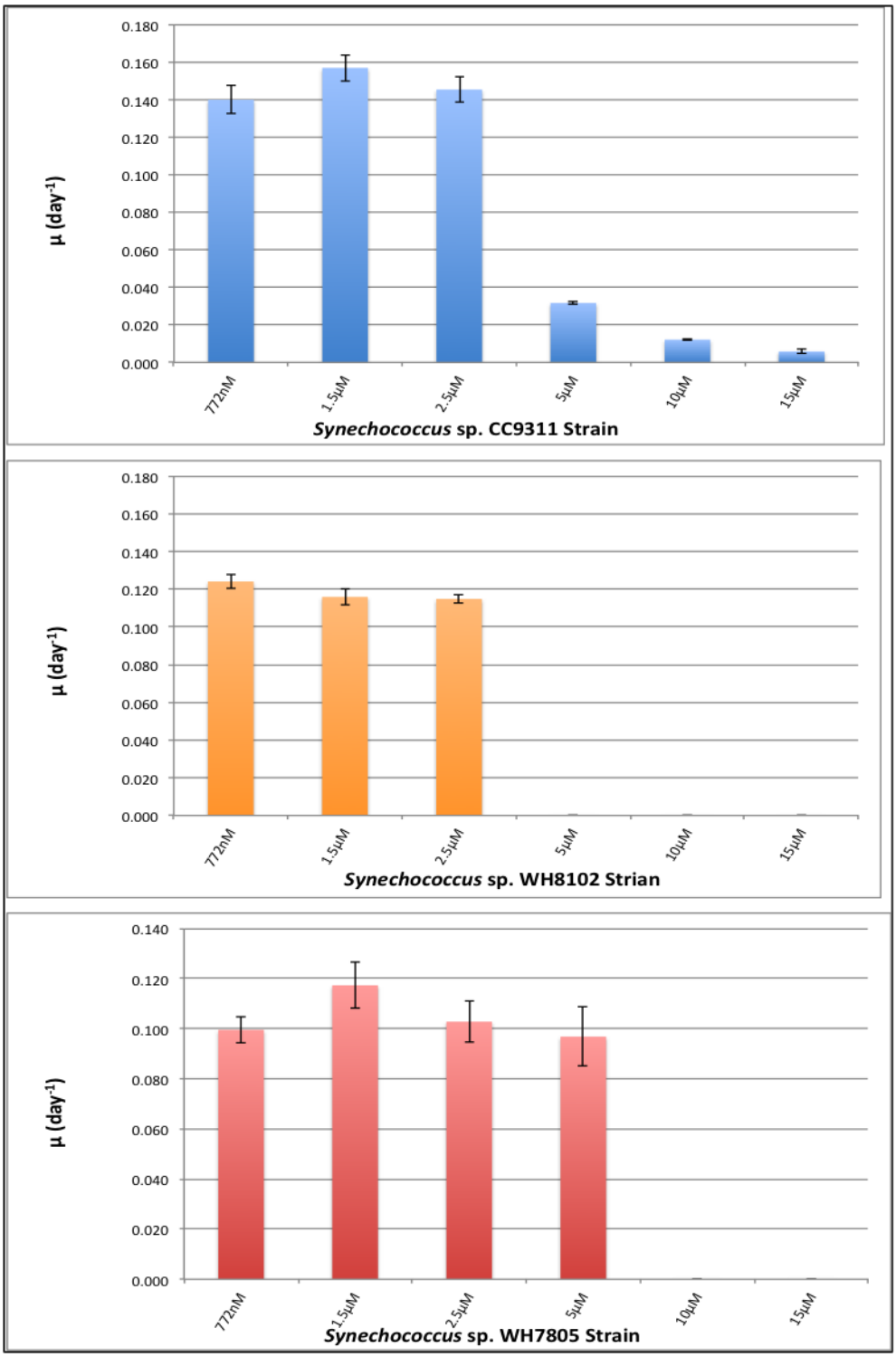

Figure 5.2. Specific growth rates for *Synechococcus* sp. CC9311, *Synechococcus* sp. WH8102 and *Synechococcus* sp. WH7805 with a range of zinc concentrations (772 nM, 1.5 μM, 2.5 μM, 5 μM, 10 μM and 15 μM).

Error bars indicate error between two biological replicates.

5.3 Growth analysis with excess cadmium

At least three of the metallothioneins from *Synechococcus* sp. CC9311, BmtA0853, 1081 and 2426, exhibited a capability to bind cadmium ions in a well-folded structure, especially for BmtA0853 (see section 4.3.2). Cadmium is also known to be present in ocean waters at concentrations up to 1 nM. This metal potentially possesses a nutrient-like profile with Cd concentrations lower in surface waters, and may play a crucial role in marine ecosystems but can be toxic at high concentrations (Cobbett and Goldsbrough, 2002; Pohl *et al.*, 2011; Aparicio-Gonzáleza *et al.*, 2012). In order to assess whether the presence of metallothionein gene(s) provide any ecological advantage for *Synechococcus* sp. CC9311 with respect to cadmium tolerance, cells were grown in Aquil medium (see section 2.1.4) in the presence of a range of cadmium concentrations.

As shown in Figure 5.3, *Synechococcus* sp. CC9311 showed remarkable cadmium tolerance (up to 10 μM cadmium) compared to the other two strains, for which cells began to lyse in the presence of 10 μM cadmium. Analysis of the specific growth rates (Figure 5.4) confirmed that *Synechococcus* sp. CC9311 was more tolerant towards cadmium, as the growth rate stayed in the same range when treated with up to 10 μM cadmium. Interestingly, the growth rate was mildly stimulated when treated with low cadmium concentrations (0.1 μM and 0.5 μM), observed as an increase in the growth rate compared to no addition. For the other two strains, *Synechococcus* sp. WH8102 and WH7805, cadmium

inhibited the growth of WH8102 moderately at 0.5 µM concentration, a concentration that didn't affect the growth of *Synechococcus* sp. WH7805, whilst at 10 µM concentration no growth was observed.

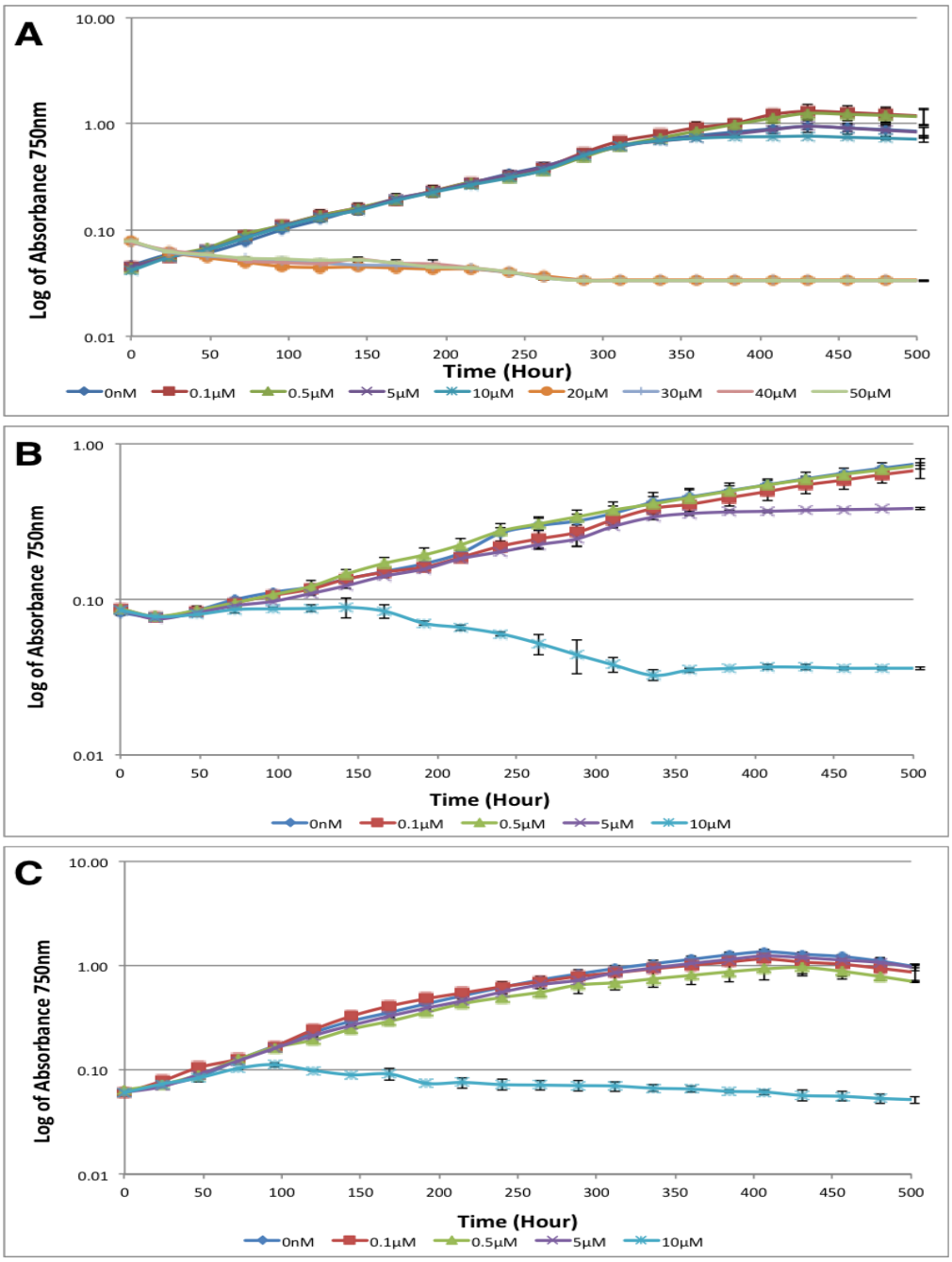

Figure 5.3. Growth of *Synechococcus* sp. CC9311 (A), *Synechococcus* sp. WH8102 (B) and *Synechococcus* sp. WH7805 (C) with a range of cadmium concentrations (0, 0.1 µM, 0.5 µM, 5 µM and 10 µM). Error bars indicate error between two biological replicates.

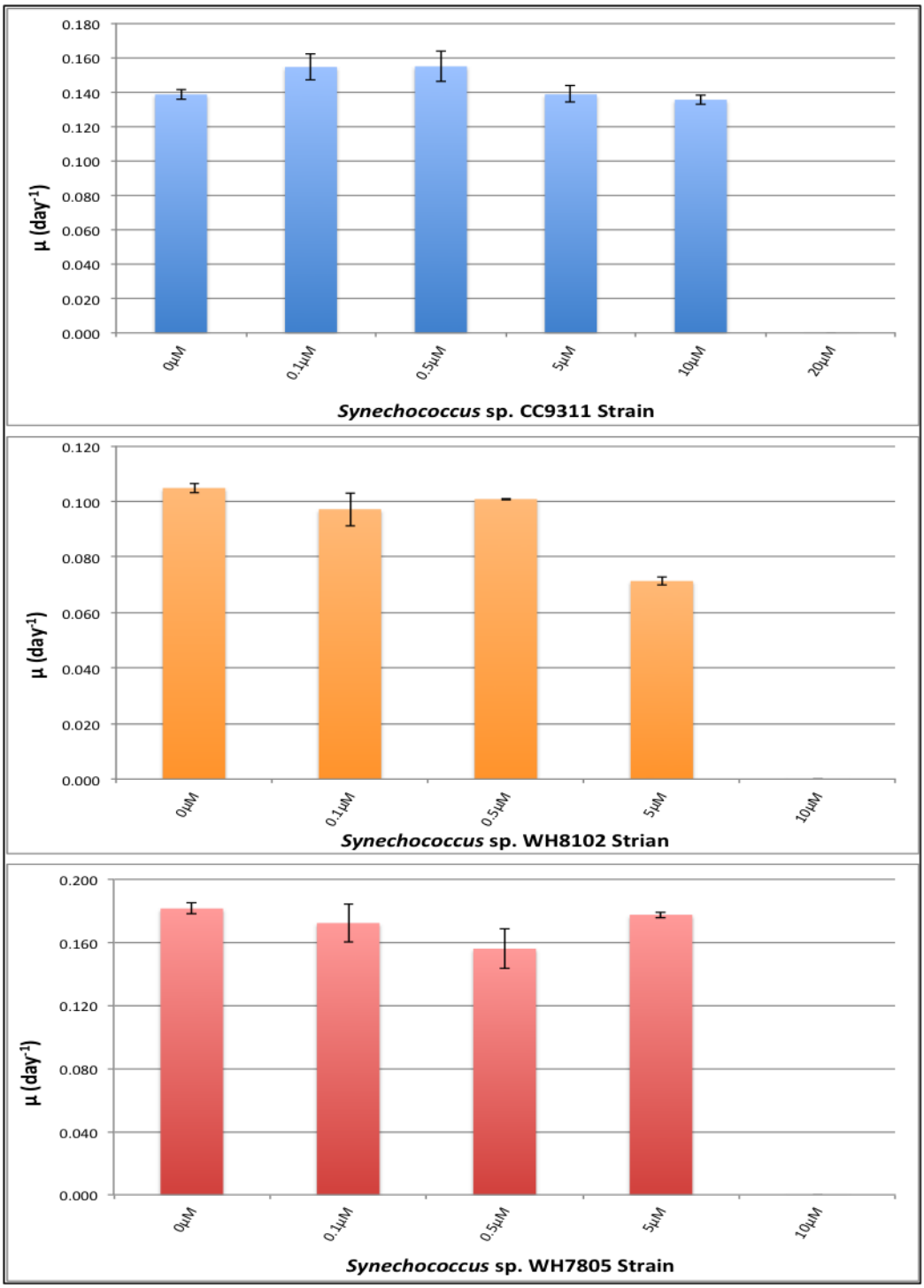

Figure 5.4. Specific growth rates for Synechococcus sp. CC9311, Synechococcus sp. WH8102 and Synechococcus sp. WH7805 across a range of cadmium concentrations (0, 0.1 µM, 0.5 µM, 5 µM and 10 µM). Error bars indicate error between two biological replicates.

5.4 Growth analysis during conditions of zinc depletion

It has been reported that metallothioneins in mammals function not only as protection against excess metal ions, but also play an important role in zinc homeostasis (Dalton *et al.*, 1996; Kelly *et al.*, 1996; Cobbett and Goldsbrough, 2002; Okumura *et al.*, 2011; Barnett *et al.*, 2012). With this in mind it is possible that cyanobacterial metallothioneins also help to scavenge scarce zinc. To test this hypothesis the growth of the three marine *Synechococcus* strains was studied under conditions of zinc depletion.

Growth of *Synechococcus* sp. CC9311, *Synechococcus* sp. WH8102 and *Synechococcus* sp. WH7805 was monitored in Aquil medium (see section 2.1.4) at four different zinc concentrations ranging from the standard concentration 772 nM down to 0.772 nM (Figure 5.5). Higher final optical densities were observed with *Synechococcus* sp. CC9311 grown at lower zinc concentrations (7.72 or 0.772 nM) and a similar situation was found for *Synechococcus* sp. WH8102. However, *Synechococcus* sp. WH7805 showed no obvious change in cell yield or growth response at the different zinc concentrations.

Specific growth rates revealed that there was no significant difference in growth rate for *Synechococcus* sp. CC9311 across the range of concentrations tested (Figure 5.6). In contrast, *Synechococcus* sp. WH8102 tended to grow slightly faster at lower zinc concentrations, whilst *Synechococcus* sp. WH7805 exhibited no significant difference in growth rate at 10- and 100-fold lower zinc

concentrations but growth was significantly reduced at 1000-fold (0.772 nM) less zinc in the medium.

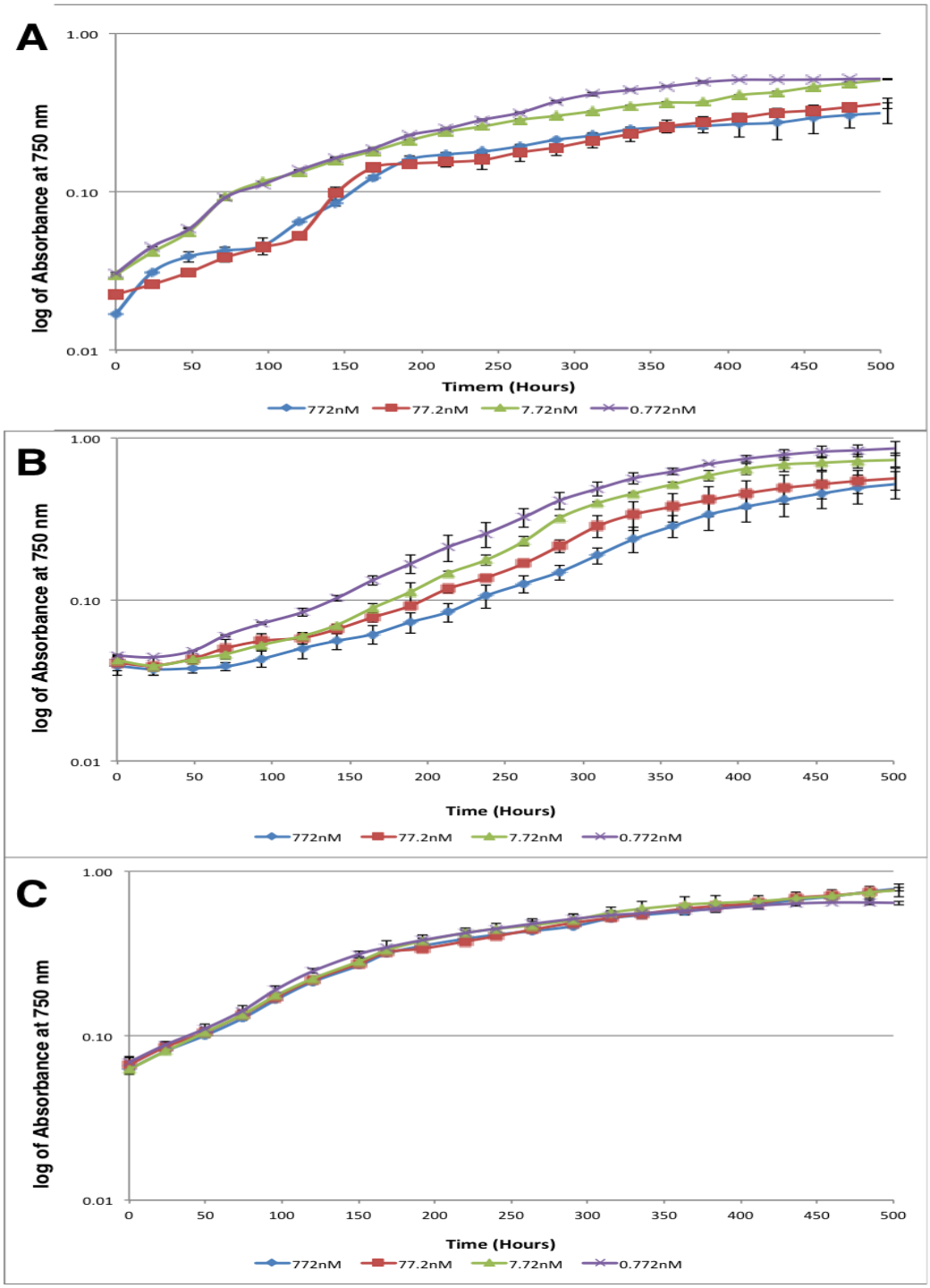

Figure 5.5. Growth of *Synechococcus* sp. CC9311 (A), *Synechococcus* sp. WH8102 (B) and *Synechococcus* sp. WH7805 (C) under conditions of zinc depletion. Error bars indicate error between two biological replicates.

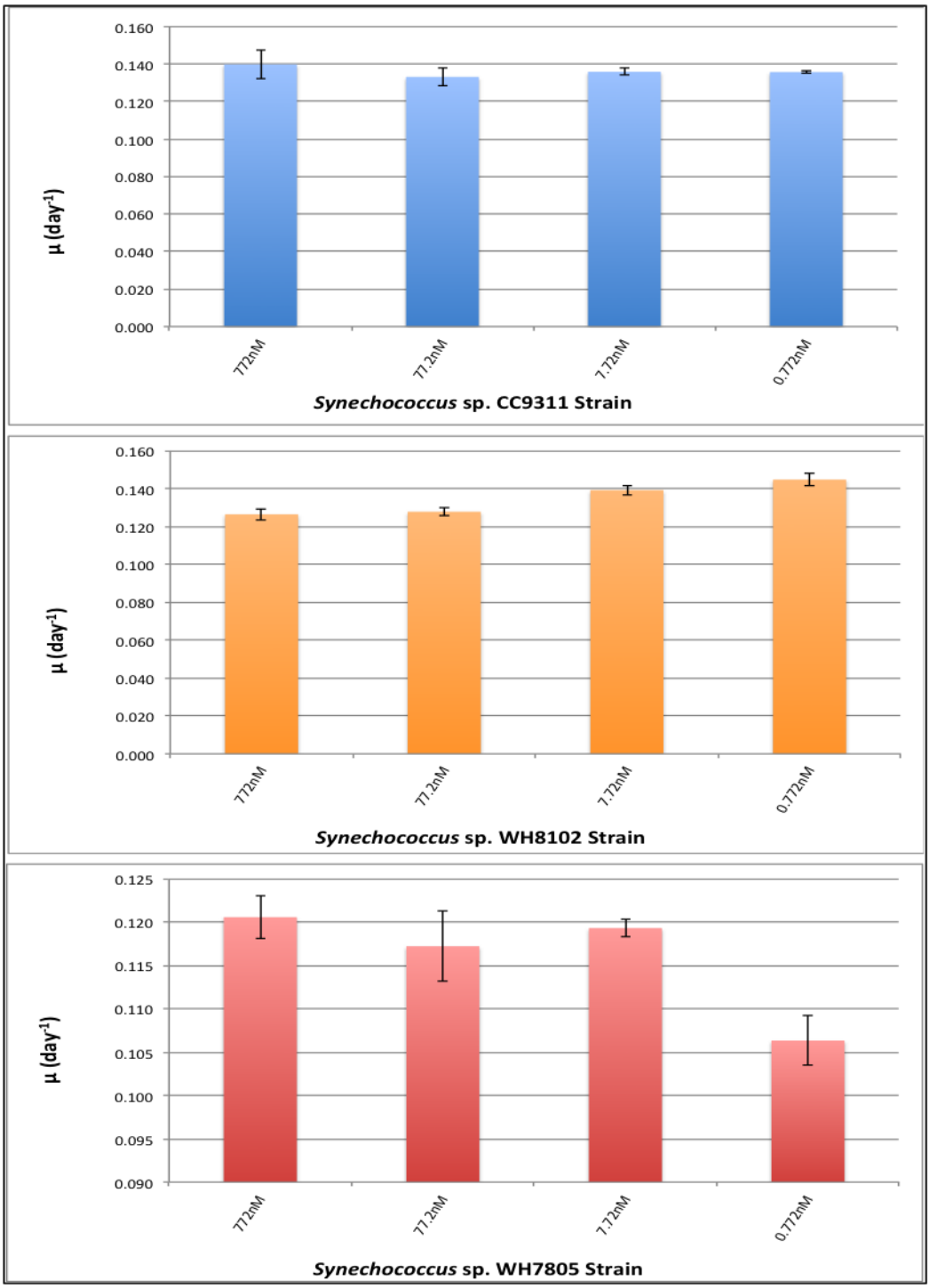

Figure 5.6. Specific growth rates for *Synechococcus* sp. CC9311, *Synechococcus* sp. WH8102 and *Synechococcus* sp. WH7805 across a range of zinc concentrations (772 nM, 77.2 µM, 7.72 µM and 0.77µM). Error bars indicate error between two biological replicates.

5.5 Growth yield of marine *Synechococcus* under conditions of Zn and Cd excess.

Analysis of cell yield (as determined by optical density at 750 nm) after 20 days (500 hours) growth of the three *Synechococcus* strains showed that *Synechococcus* sp. CC9311 produced similar cell yields across a wide range of zinc or cadmium concentrations (Figure 5.7) somewhat in contrast to the other strains.

Thus, *Synechococcus* sp. CC9311 was able to maintain relatively constant yields in the presence of a range of zinc concentrations, from 0.772-2500 nM zinc, while *Synechococcus* WH8102 gave higher cell yields at low zinc concentrations, and *Synechococcus* sp. WH7805 showed a slight increase in cell yield at intermediate-low zinc concentrations (7.72 nM to 772 nM) but decreased cell yield when treated with 1000-fold lower zinc (0.772 nM) or high zinc concentrations (≥1.5 μM) .

When treated with cadmium, *Synechococcus* sp. CC9311 showed a slight increase in cell yield at low cadmium concentrations (up to 0.5 μM). However, at 5 μM cadmium, the yield dropped to a value similar to that of growth with no added cadmium. Indeed, *Synechococcus* sp. CC9311 still maintained a relatively high cell yield even in the presence of 10 μM cadmium, a concentration at which neither *Synechococcus* sp. WH8102 or *Synechococcus* sp. WH7805 survived. Cell yields were generally lower in *Synechococcus* sp. WH8102 across a range of cadmium concentrations, and particularly so at 5 μM cadmium. In contrast, of

the three strains tested *Synechococcus* sp. WH7805 showed the highest cell yields during growth at 5 µM cadmium or in the absence of cadmium but with cell yield decreasing at 0.1 and 0.5 µM cadmium.

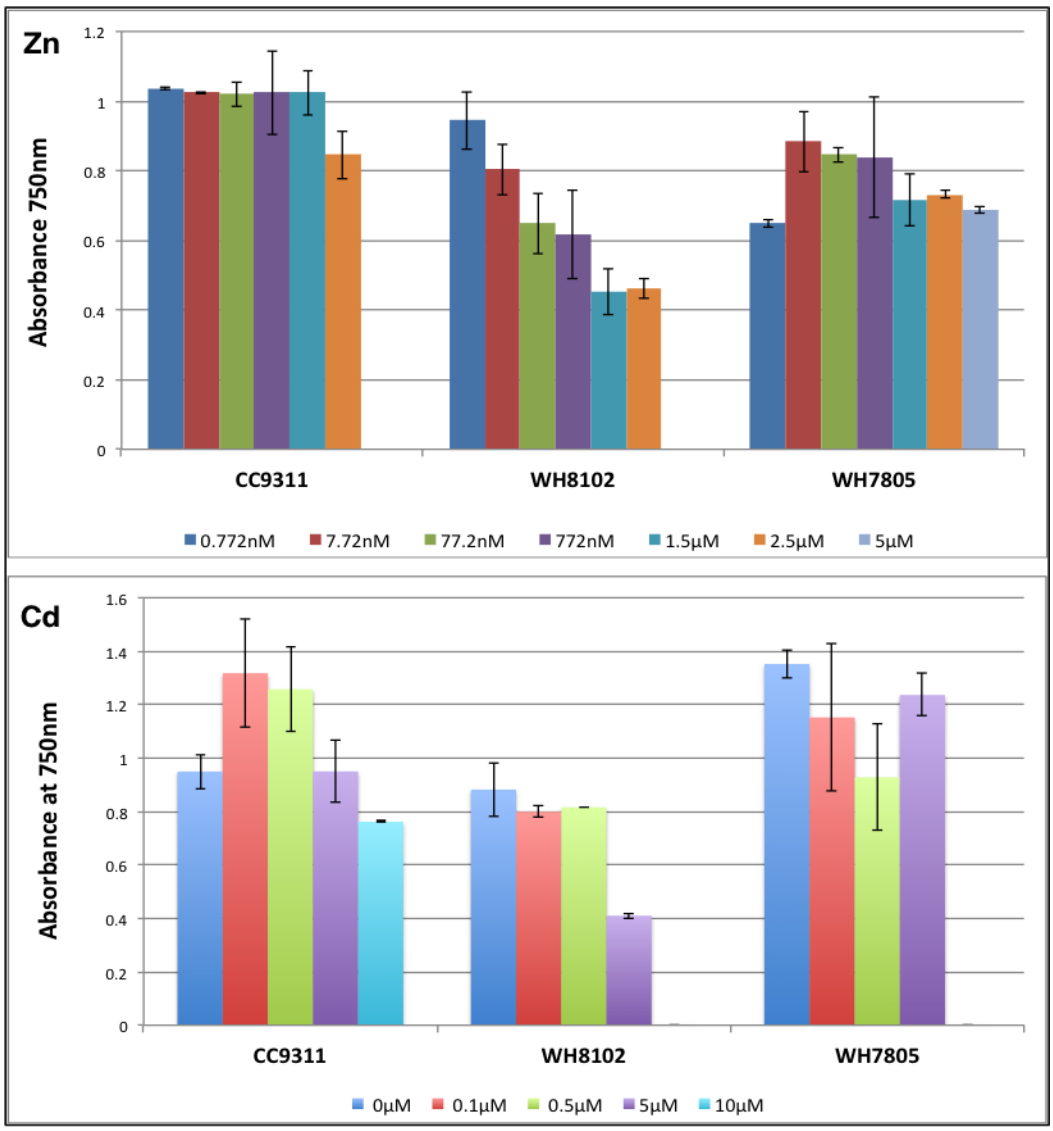

Figure 5.7. Cell yield of *Synechococcus* sp. CC9311, *Synechococcus* sp. WH8102 and *Synechococcus* sp. WH7805 across a range of zinc or cadmium concentrations, as monitored by optical density at 750 nm. Error bars indicate error between biological replicates. When the OD was out of the linear range of

the spectrophotometer, measurements were performed by diluting sample to the measurable range and multiplied by the dilution ratio.

5.6 Summary

In this chapter, the growth behaviour of *Synechococcus* sp. CC9311 was compared with two other *Synechococcus* strains, WH8102 and WH7805 across a range of zinc and cadmium concentrations. These three cyanobacterial strains contain four, one and no metallothionein genes, respectively. Each strain also belongs to phylogenetically discrete *Synechococcus* clades (Fuller *et al.*, 2003a) potentially inhabiting distinct environmental niches (Zwirglmaier *et al.*, 2007; Zwirglmaier *et al.*, 2008; Scanlan *et al.*, 2009).

In general agreement with the environmental niches predicted for each strain, the coastal opportunist *Synechococcus* sp. CC9311 showed growth across a broad range of both zinc (0.772-2500 nM) and cadmium (0.1-10 μM) concentrations and relatively constant cell yields, suggesting it is capable of coping with both excess and depletion of these micronutrients. In contrast, the open ocean strain *Synechococcus* sp. WH8102 could not tolerate excess zinc, but showed slightly faster growth rates at low zinc and cadmium concentrations, concomitant with inhabiting an oligotrophic environment. Finally, growth of *Synechococcus* sp. WH7805 was similar to *Synechococcus* sp. WH8102 but showed a slightly broader tolerance to elevated zinc and higher cell yields in the presence of cadmium compared to this latter strain. Previous studies on metal

toxicity in several freshwater *Synechococcus* strains have demonstrated the toxicity level for zinc in the range of 10^{-7} M (Miao *et al.*, 2005), and from 1-1.7 μM for cadmium (Gupta *et al.*, 1992; Payne and Price, 1999; Miao *et al.*, 2005).

Thus, compared to the growth behaviour of the other two *Synechococcus* strains, *Synechococcus* sp. CC9311 appears more adaptable to varying zinc and cadmium concentrations, both high and low, which agrees with the project hypothesis that the coastal strain *Synechococcus* sp. CC9311 has developed a metal intensive physiology compared to the open ocean strain *Synechococcus* sp. WH8102, consistent with adaptation to a coastal environment (Palenik *et al.*, 2006a).

Although it is known that *Synechococcus* sp. CC9311 contains four metallothionein genes whilst WH8102 and WH7805 contain only a single gene or no detectable gene copy, it is still unclear whether each of the four metallothionein genes in *Synechococcus* sp. CC9311 fulfills a distinct functional role. This question will be examined in the next chapter.

6

Expression Analysis of the Four Metallothionein Genes in *Synechococcus* sp. CC9311 under Metal and High Light Stress

6.1 Introduction

The three metallothioneins BmtA0853, 1081 and 2426 previously characterised *in vitro* via metal binding affinity, specificity, metal release kinetics and protein folding and structure showed obvious differences between them (see chapter 4). In addition, study of the growth behaviour of *Synechococcus* sp. CC9311 in the presence of a range of zinc and cadmium concentrations, demonstrated the adaptable nature of this strain concomitant with it occupying a coastal environment (see chapter 5).

However, it is still unclear whether each of the four metallothionein genes in *Synechococcus* sp. CC9311 fulfils a distinct functional role or indeed whether each of the genes is expressed, and if so, at what level? Moreover, it is also unknown whether these metallothionein genes are differentially expressed depending on environmental conditions. To begin to address this, in this chapter I am going to analyse the expression of each metallothionein gene under conditions of varying zinc and cadmium concentration as well as under high light stress using a real-time quantitative polymerase chain reaction (RT-qPCR) approach.

6.2 Real-Time Quantitative PCR

qPCR is used to detect and quantify specific PCR products in real-time during the amplification process. It is based on the quantitative relationship between the amount of target DNA present before the reaction and the amount of product formed during the reaction. Amplification is monitored by measuring the signal of fluorescent dyes interacting with double stranded DNA or fluorescently labelled oligonucleotides called probes whose fluorescence is correlated to the amount of PCR product, the change in concentration of the target DNA after each PCR cycle being detected (Higuchi *et al.*, 1992; Heid *et al.*, 1996; Kubista *et al.*, 2006). By monitoring the amount of PCR product after each round of amplification, the amount of template present at the beginning of the reaction can be calculated.

Figure 6.1 shows a typical real-time qPCR amplification curve as a function of cycle number. The cycle number at which fluorescence is detected as logarithmic is called the threshold cycle or Ct value, which is the most important parameter used for calculating the concentration of the initial DNA material in quantitative PCR.

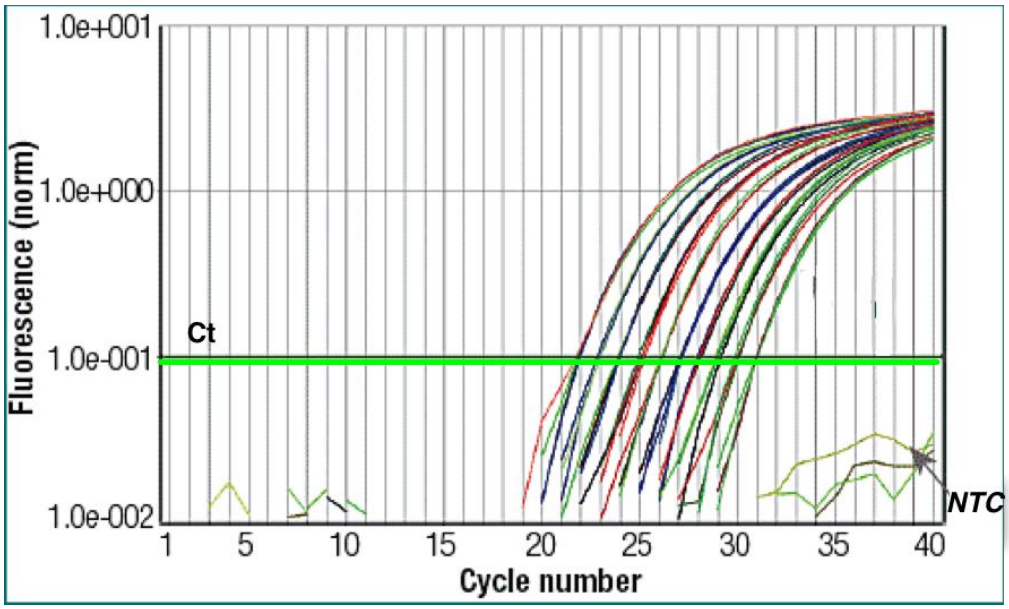

Figure 6.1: A typical qPCR amplification curve. Amplification of serial dilutions of template (plasmid) DNA, at concentrations ranging from 10 ng - 5 fg using TaqMan Universal PCR Master Mix (2X) in triplicate reactions. Reactions were performed using a ABI 7500 Fast Real-Time PCR instrument. NTC: negative control, i.e. without plasmid DNA added to the reaction.

6.2.1 Specific primers and probe design

In this study, the four metallothionein genes from *Synechococcus* sp. CC9311 were analysed at the same time. Multiple sequence alignment (Figure 6.2) shows the similarity among the four gene sequences with regions showing the binding of the specific primers and probes developed highlighted. In order to get the highest specificity, a fluorescently labelled Taqman probe was employed. There are two main detection methods used in qPCR: dye-based, referred to as non-specific detection, and probe-based, or sequence specific detection (qPCR Technical Guide, Sigma). In this latter TaqMan based approach, all three components (two primers and one probe) must hybridise to the target DNA to

generate detectable signal. Hence, this method provides greater specificity and higher accuracy (PrimeTime qPCR Guide, IDT) than the former.

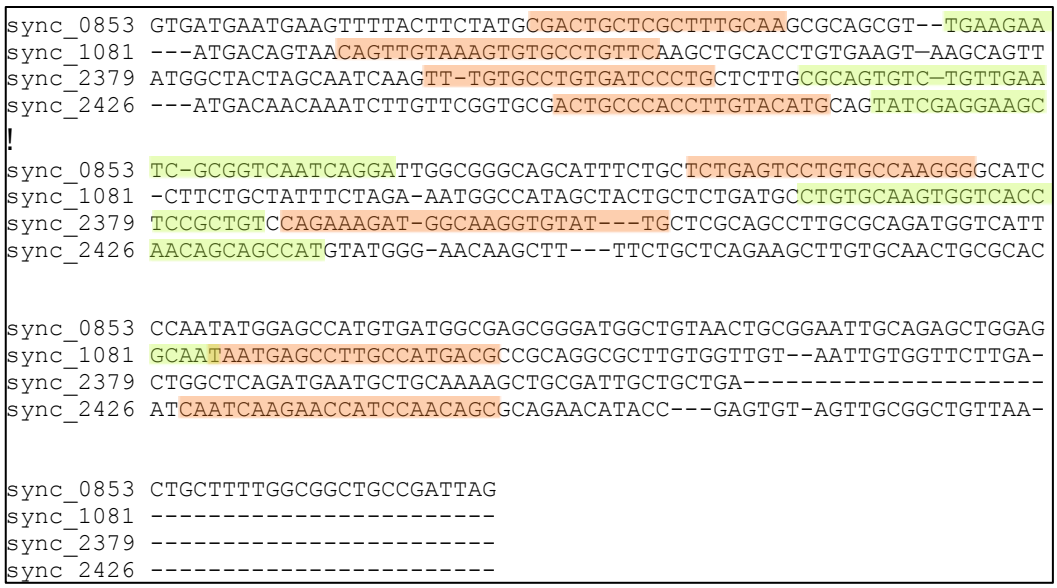

Figure 6.2. Multiple sequence alignment of the four metallothionein genes in *Synechococcus* sp. CC9311. Primers were highlighted in orange and probes were in green.

The primers and probes used in this study were designed using the IDT RealTime PCR Design Tool available in the SciTools section of the IDT website (http://idtdna.com). In order to gain the maximum efficiency during amplification, primers and probes adhere to Applied Biosystems guidelines (Applied Biosystems 2004). Different primer/probe combinations were tried in order to get the most specificity for each gene by using specific plasmid standard (cloned metallothioneins gene constructs). The qPCR reactions were set up as described previously (section 2.4.4).

Table 6.1 qPCR primers and TaqMan probes used for specific amplification of the four metallothionein genes from *Synechococcus* sp. CC9311. The *rnpB* primer set and control probe is also indicated.

Gene Name	Primer and Probe Name	Sequence 5' -3'
sync_0853	0853F	CGACTGCTCGCTTTGCAA
	0853R	CCCTTGGCACAGGACTCAGA
	0853P	FAM/TGAAGAATC/ZEN/GCGGTCAATCAGGA/3IABKFQ
sync_1081	1081F	CAGTTGTAAAGTGTGCCTGTTC
	1081R	CGTCATGGCAAGGCTCATTA
	1081P	FAM/CTGTGCAAG/ZEN/TGGTCACCGCAAT/3IABKFQ
sync_2379	2379F	TTTGTGCCTGTGATCCCTG
	2379R	CAATACACCTTGCCATCTTTCTG
	2379P	FAM/ACAGCGGAT/ZEN/TCAACAGACACTGCG/3IABKFQ
sync_2426	2426F	ACTGCCCACCTTGTACATG
	2426R	GCTGTTGGATGGTTCTTGATTG
	2426P	FAM/TGGCTGCTG/ZEN/TTGCTTCCTCGATA/3IABKFQ
rnpB	rnpB_F	TTCCCCGTTCCGTCTTTG
	rnpB_R	GGTTCTGTTCACCCTTCCAAG
	rnpB_P	FAM/ATCTGGGATCGCCGTTACCGAC/3IABKFQ

6.2.2 Relative and absolute quantification analysis

Two approaches are generally used to analyse qPCR data. Relative quantification is the most widely used method. This requires calculation of the expression of the target gene normalised to a reference gene in the same sample, and expressed as the fold difference in gene expression between the target and the reference gene (Livak and Schmittgen, 2001; Pfaffl, 2001). The expression level of the chosen reference gene has to be stable under various experimental conditions (Cook *et al.*, 2009). In this study, the *rnpB* gene encoding RNase P was chosen to be the reference gene (Herrmann *et al.*, 2000), since in cyanobacteria there is good evidence that this is a stable housekeeping gene not responding to light or other environmental conditions (Alfonso *et al.*, 2001; Holtzendorff *et al.*, 2001; Mary *et al.*, 2004; Li *et al.*, 2010).

A common analysing methodology for relative quantitation of gene expression is the relative standard curve method (Applied Biosystems 2004). In this method, a standard curve of the amount of DNA against the Ct value is required in each reaction plate, and this approach provides rigorous quantitation since the quantitative values of the unknown sample are interpolated from the standard curve. For a more detailed explanation see Appendix D.

Another popular method for analysing qPCR data is absolute quantitation analysis, requiring that absolute quantities of the standards used for the standard curves is known with great accuracy (Pfafflm and Hageleit, 2001). It is critical that the amplification efficiencies of the standard and the unknown sample are

identical and the standard is a single pure species, since the reliability of this method is dependent on this (Pfaffl, 2006). In this study, recombinant plasmids carrying each individual *Synechococcus* sp. CC9311 metallothionein gene (section 3.2) were used which allows transcript abundance to be compared between genes (Clokie *et al.*, 2006).

As described above, quantitation of an unknown sample is normalised to the reference gene (*rnpB*) using a standard curve generated using *Synechococcus* sp CC9311 genomic DNA. Then multiplied by 3.92×10^5 (the number of *Synechococcus* sp CC9311 genome equivalents per 1 ng genomic DNA) to convert the fold difference normalised to the reference gene into the number of copies of the gene per 1 ng cDNA starting material. These values can be along a time course for comparison between genes. For a more detailed explanation see Appendix E.

6.2.3 Standard curve and primer amplification efficiency determination

A standard curve, generated by performing qPCR with a series of diluted template (*Synechococcus* sp. CC9311 genomic DNA) that has been accurately quantified, is not only essential for valid analysis of qPCR data but also an excellent tool to test the assay efficiency, sensitivity and precision.

Figure 6.3 shows the standard curve linear regression plot of Ct value versus the log of DNA input concentration. The correlation coefficient of the line, R^2 is an

indication of how well the data fits the model. If the correlation coefficient R^2 is ≤ 0.985, the assay may not give reliable results (Applied Biosystems 2004).

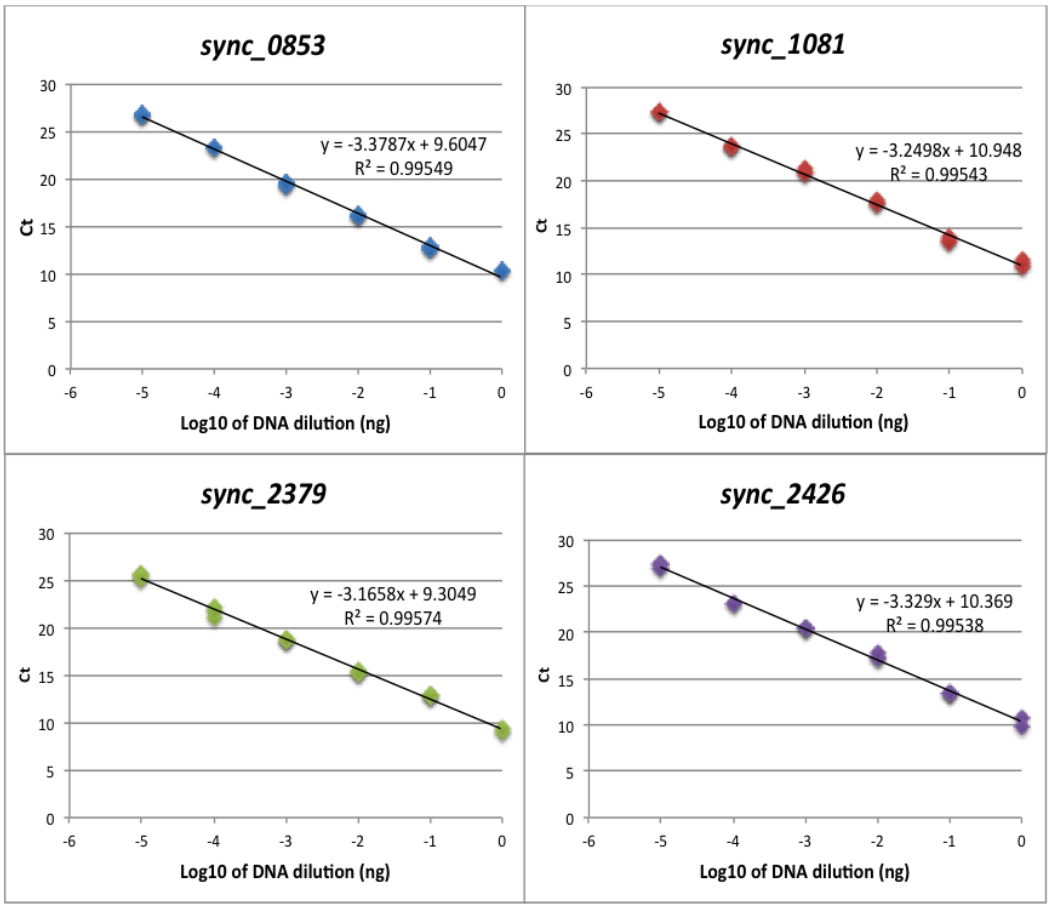

Figure 6.3. Graph of Ct value against log10 DNA input concentrations (ng) with a linear regression for the four metallothionein genes. The R^2 should be > 0.985 to give reliable results.

The efficiency of the qPCR reaction is calculated using the slope of the standard curve by the following equation:

$$\boldsymbol{Amplification\ Efficiency} = \mathbf{10}^{(-\mathbf{1}/\boldsymbol{slope})} - \mathbf{1}$$

Under ideal conditions, i.e. when the PCR reaction is 100% efficient, the amount of PCR product will double with each cycle, which means the slope of the standard curve will be -3.33. Generally, a slope between -3.9 and -3.0 (80-110% efficiency) is acceptable.

6.2.4 qPCR Assay Setup

Each qPCR assay (see section 2.4.4) was set up with multiple replicates and controls. Two types of replicates were used in this study:

i) Two biological replicates were used for each time course studied, plus an untreated control (i.e. standard growth conditions);

ii) Three technical replicates were performed for each experimental sample plus the no template control sample for each qPCR assay tested (see Figure 6. 4).

RNA extraction, the synthesis of cDNA and DNA contamination check were processed as described previously (section 2.4)

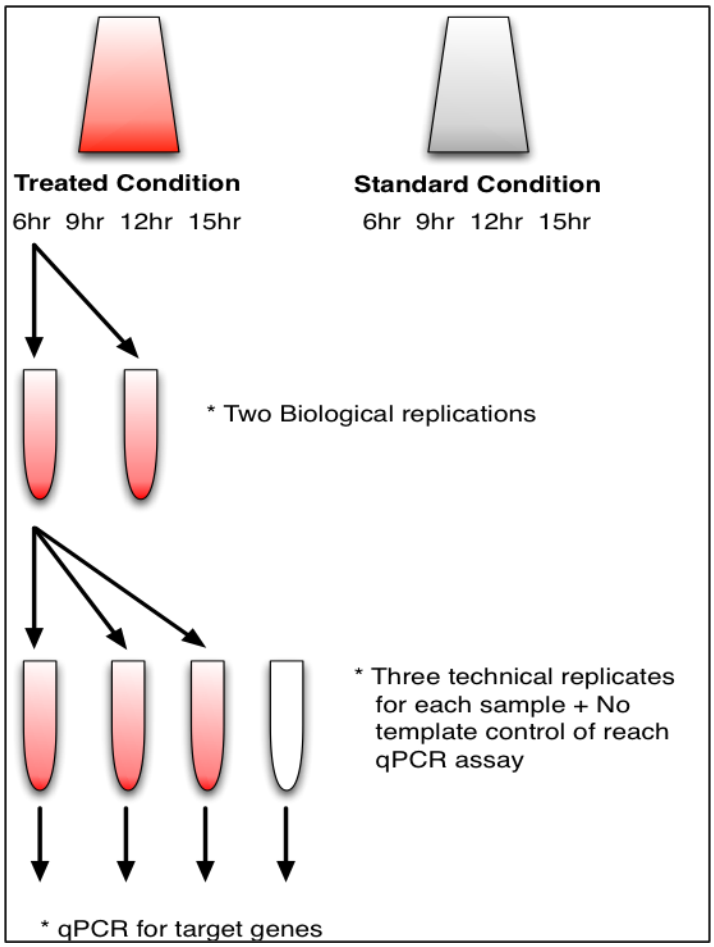

Figure 6.4. Graph to illustrate qPCR assay setup. All qPCR assays were performed with two biological replicates and three technical replicates.

6.3 Analysis of *Synechococcus* sp. CC9311 metallothionein gene expression as a function of zinc concentration

6.3.1. *Synechococcus* sp. CC9311 metallothionein gene expression profiles during conditions of zinc shock

For analysis of metallothionein gene expression under conditions of zinc shock, *Synechococcus* sp. CC9311 was grown in standard SOW medium (772 nM Zinc, see section 2.1.4 for detailed medium composition) at 23°C to an OD_{750} of 0.5 before exposure to excess zinc, 15 μM (a toxic level as observed by previous growth experiments, see section 5.2). The culture was then grown for a further 15 hours and cells were collected immediately after zinc addition and then at 6h, 9h and 15h after zinc shock for subsequent RNA isolation (see section 2.4.1), cDNA synthesis (section 2.4.2) and qPCR analysis (see sections 2.4.4 and 6.2).

To evaluate expression across the time course, fold change in gene expression is reported relative to gene expression at time zero (i.e. the 0 h time point).

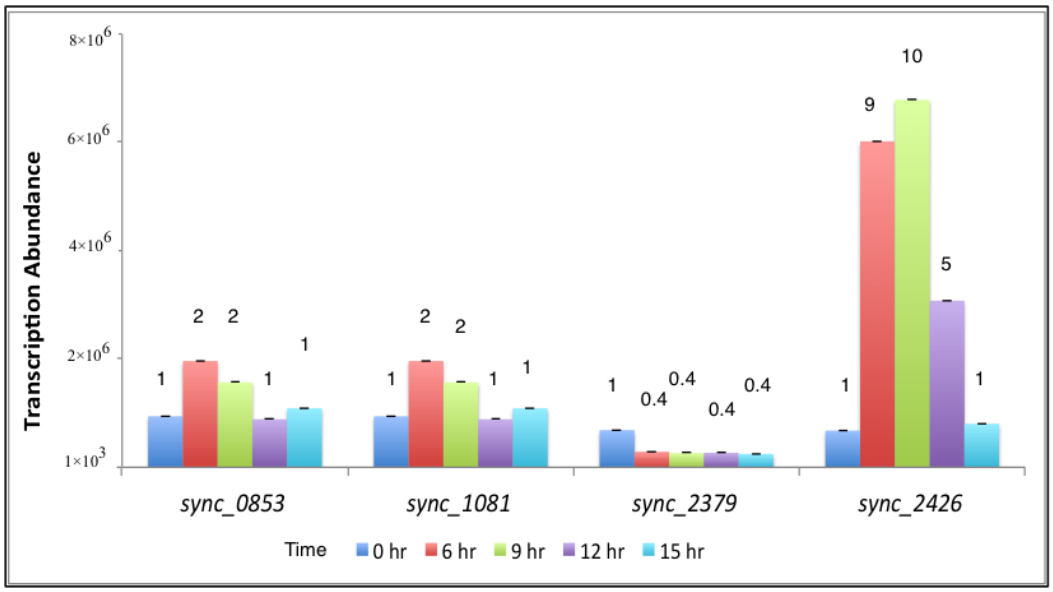

Figure 6. 5. Absolute transcription abundance of *Synechococcus* sp. CC9311 metallothionein genes *sync_0853, sync_1081, sync_2379* and *sync_2426* following exposure to 15 µM zinc over a 15 h time course. Bar height represents the absolute transcript abundance per ng cDNA present in each qPCR reaction. Numbers above each bar represent the fold change in gene expression of each metallothionein gene compared to transcript abundance at 0 h.

Exposure to 15 µM zinc caused a differing response in the four metallothionein genes. Thus, there was a ca. 2-fold increase in expression of *sync_0853* and *sync_1081* whilst expression of *sync_2379* reduced ca. 2.5 fold to 0.4 the level at time zero and remained at this level during the whole time course. In contrast, the expression of *sync_2426* increased markedly following exposure with a 9-fold increase at 6 h before reaching a maximum 10-fold increase 9 h after exposure to 15 µM zinc. However, this response was transient, expression decreasing at 12 h and returning to pre-shock levels by 15 h. Expression levels of *sync_0853* and *sync_1081* were similar: expression increasing 2-fold at 6 and 9 h before returning to pre-shock levels at 12 h.

6.3.2. *Synechococcus* sp. CC9311 metallothionein gene expression profiles during growth at differing zinc concentrations

As described in section 5.4, metallothioneins may not only participate in protection against excess metal ions, but also contribute to zinc homeostasis (Dalton *et al.*, 1996; Kelly *et al.*, 1996; Cobbett and Goldsbrough, 2002; Das *et al.*, 2006; Yang *et al.*, 2009; Okumura *et al.*, 2011). To test this hypothesis *in vivo*, growth across a range of zinc concentrations and a zinc starvation time course experiment were performed.

For the growth experiments, *Synechococcus* sp. CC9311 was grown in SOW (section 2.1.4) with four different zinc concentrations ranging from the standard concentration 772 nM to 0.77 nM. Samples were harvested at an OD_{750} of 0.5 for RNA isolation (see section 2.4.1), cDNA synthesis (section 2.4.2) and qPCR analysis (see sections 2.4.4 and 6.2).

Absolute transcript abundance of the four metallothionein genes in response to a range of low zinc concentrations showed that expression of *sync_0853* and *sync_1081* increased around 5-fold in response to 77.2 and 7.7 nM zinc concentrations. However, expression of these two genes markedly increased (23-fold and 38-fold, respectively) in the lowest zinc concentration (0.77 nM).

Growth of *Synechococcus* sp. CC9311 in 0.77 nM zinc induced a smaller increase in *sync_2379* gene expression (4-fold) whilst growth in 77 nM and 7.7 nM zinc showed no change in expression compared to growth in normal medium (see Figure 6.6). Surprisingly, 0.77 nM zinc induced a decrease in *sync_2426* gene expression (0.4 fold equivalent to 2.5-fold decreasing).

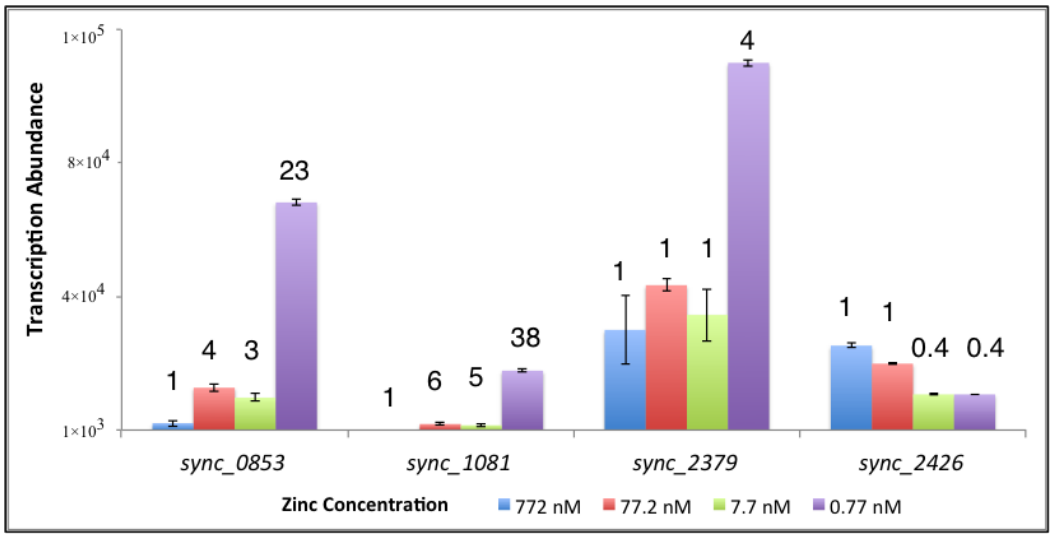

Figure 6. 6. Absolute transcript abundance of *Synechococcus* sp. CC9311 metallothionein genes, *sync_0853*, *sync_1081*, *sync_2379* and *sync_2426* following growth in a range of zinc concentrations (i.e. from the standard concentration in SOW medium of 772 nM down to 0.77 nM). Bar height represents the absolute transcript abundance per ng cDNA present in each qPCR reaction. Numbers above each bar represent the fold change in metallothionein gene expression compared to expression levels during growth in 772 nM zinc.

The expression pattern of these four metallothionein genes in response to varying zinc concentrations provides a hint to their function. It has been reported that the dissolved zinc concentration in natural oceanic waters is in the low nanomolar range e.g. in surface waters of the Pacific Ocean the zinc concentration is around 2 nM, whilst in the Atlantic Ocean it is around 3 nM (Morel and Price, 2003; Aparicio-Gonzáleza *et al.*, 2012). The standard zinc concentration of 772 nM used in SOW medium is hence more than sufficient to sustain growth. Thus, it is unsurprising that expression levels of each metallothionein gene remain similar during growth at 772 nM, 77 nM, and 7.7 nM zinc. However, at 0.77 nM zinc,

which is lower than natural levels, expression of metallothioneins is induced to scavenge scarce zinc. Interestingly, the fold change in expression of *sync_0853* and *sync_1081* is higher than the other two metallothionein genes, which potentially suggests a greater role in zinc scavenging for the former two genes.

6.3.3. *Synechococcus* sp. CC9311 metallothionein gene expression profiles during zinc starvation.

Zinc starvation was realised by pre-culturing *Synechococcus* sp. CC9311 in standard SOW medium (i.e. containing 772 nM zinc), and once an OD_{750} of 0.5 was reached the culture was pelleted by centrifugation and cell pellets resuspended in SOW medium lacking zinc (0 nM Zn, 100 μM EDTA). Cells were washed again in this medium, pelleted by centrifugation to remove all zinc ions and subsequently transferred to fresh SOW (0 nM Zn), before samples were collected immediately after ressuspension (0 hr) and at 2 hr and 4 hr post transfer.

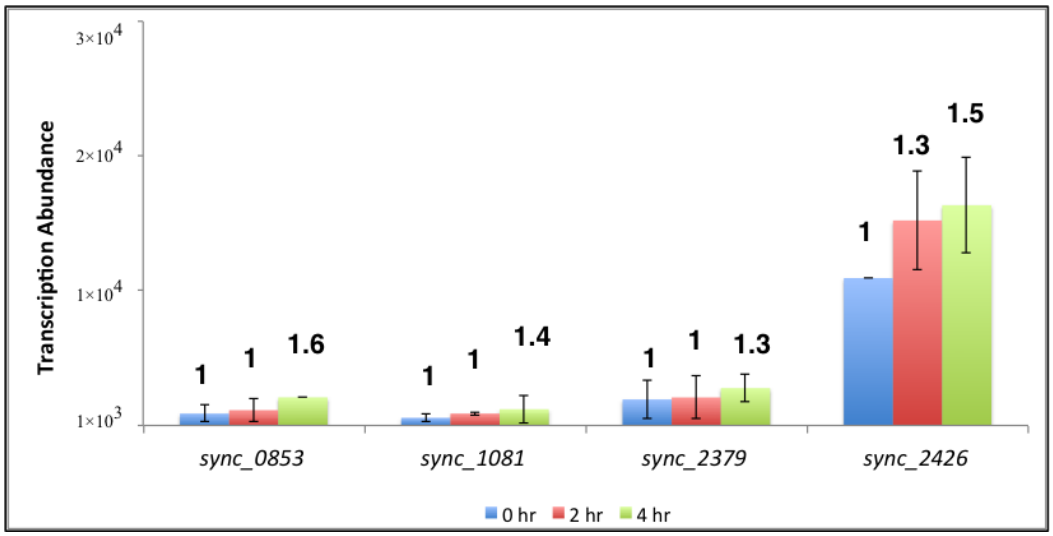

Figure 6. 7. Absolute transcription abundance of *Synechococcus* sp. CC9311 metallothionein genes *sync_0853, sync_1081, sync_2379* and *sync_2426* following zinc depletion over a 4 h time course. Bar height represents absolute transcript abundance per ng cDNA present in each qPCR reaction. Numbers above each bar represent the fold change in gene expression for each metallothionein gene compared to level at time zero.

After removal of all available zinc ions in the medium, three metallothionein genes, *sync_0853*, *sync_1081*, *sync_2379* and *sync_2426*, demonstrated a similar expression pattern: transcript abundance remaining at approximately the same level (<2-fold increase) (Figure 6.7).

6.4 Analysis of *Synechococcus* sp. CC9311 metallothionein gene expression as a function of cadmium concentration

In previous growth experiments in the presence of cadmium (see section 5.3), *Synechococcus* sp. CC9311 demonstrated a remarkable tolerance to this metal

(up to 10 µM cadmium). In order to assess the expression pattern of the four metallothionein genes in response to a range of non-toxic cadmium concentrations, *Synechococcus* sp. CC9311 was grown in the presence of a range of cadmium concentrations from 0.1-10 µM (see section 5.3). Samples were harvested at the end of the growth experiment at an OD_{750} of about 1 for RNA isolation (see section 2.4.1), cDNA synthesis (section 2.4.2) and qPCR analysis (see sections 2.4.4 and 6.2).

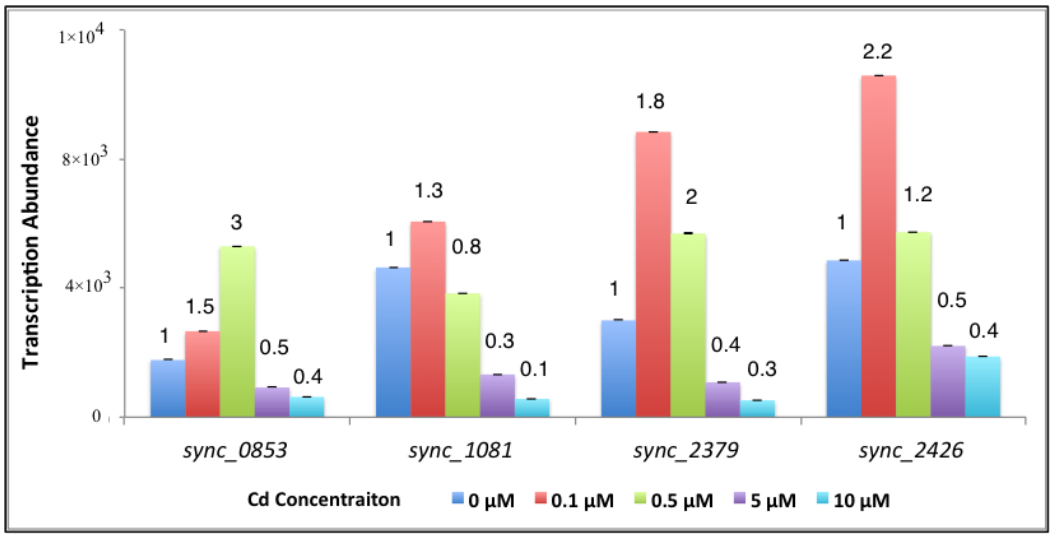

Figure 6. 8. Absolute transcription abundance of *Synechococcus* sp. CC9311 metallothionein genes *sync_0853, sync_1081, sync_2379* and *sync_2426* grown in the presence of a range of cadmium concentrations. Bar height represents absolute transcript abundance per ng cDNA present in each qPCR reaction. Numbers above each bar represent the fold change in gene expression of each metallothionein gene compared to transcript abundance in cultures grown with no added cadmium (i.e. 0 nM).

In the presence of a range of cadmium concentrations, all four metallothionein gene *sync_0853, sync_1081, sync_2379* and *sync_2426* showed a similar expression pattern (Figure 6. 8): a small increase in expression at low cadmium concentrations (0.1-0.5 μM) but a decrease in expression at concentration of 5 and 10 μM cadmium reaching minimum values of 0.4, 0.1, 0.3 and 0.4 equivalent 2.5-fold, 10-fold, 3-fold or 2.5-fold respectively, drop in expression at 10 μM cadmium.

The expression pattern of the four metallothioneins potentially indicates that they are participating in detoxification of low levels of cadmium, possibly by reducing their cellular availability (Zhou and Goldsbrough, 1994; Ybarra and Webb, 1999). This would agree with previous growth experiments in the presence of cadmium (section 5.3): with the growth rate of *Synechococcus* sp. CC9311 being mildly stimulated and the yield showing a slight increase when treated with low cadmium concentrations (0.1 μM and 0.5 μM).

This agreement may be an indication that the metallothioneins are participating in protection from cadmium ions within a certain level of range, possibly by reducing their cellar availability (Zhou and Goldsbrough, 1994; Ybarra and Webb, 1999). Another possible explanation is that cadmium may be utilized by *Synechococcus* sp. CC9311; in principle metallothioneins could participate in buffering cadmium, as long as concentrations are not too high.

For analysis of metallothionein gene expression under conditions of cadmium shock, *Synechococcus* sp. CC9311 was grown in standard SOW medium at 23°C

to an OD_{750} of 0.5 before exposure to 20 μM cadmium (a toxic level as defined previously see section 5. 3). The culture was then grown for a further 15 hours and cells were collected immediately after cadmium addition and then at 6 h, 9h and 15h after cadmium shock for RNA isolation. Exposure to 20 μM cadmium caused a dramatic decrease in expression of all four metallothionein genes; however, the first batch of samples were collected after 6 hours of cadmium treatment, at this point cells were already began to lyse (data not shown).

6.5 Analysis of *Synechococcus* sp. CC9311 metallothionein gene expression in response to high light.

It is well known that growth and photosynthesis of cyanobacteria is influenced by temperature and light intensity (Grossman *et al.*, 1993; Webb and Sherman, 1994; Salem and van Waasbergen, 2004a; Salem and van Waasbergen, 2004b). Several recent studies have revealed that metal availability and toxicity are also influenced by light intensity (Wang and Wang, 2008; Zeng and Wang, 2011). Genome analysis indicates that *Synechococcus* sp. CC9311 possesses a large number of high light-inducible protein (HLIP) gene family members (14) compared for example to the open ocean strain WH8102 (with 8). This increase in HLIP number has been associated with an ability to occupy high light environments or under changing light conditions found during water column mixing (Palenik *et al.*, 2006a). With this in mind, the expression of *Synechococcus* sp. CC9311 metallothionein genes in response to high light exposure was analysed.

Synechococcus sp. CC9311 was grown in SOW medium under standard conditions (i.e. 5 µmol photons m^{-2} s^{-1} continuous white light) to an OD_{750} of 0.5, followed by a period of high light (HL) exposure (200 µmol photons m^{-2} s^{-1} over three hours). The culture was then transferred back to standard light levels (5 µmol photons m^{-2} s^{-1}). Samples for RNA extraction were taken immediately before shifting the culture to high light and at 0.5 h, 1 h, 3 h after exposure and 0.5 h, 1 h, 3 h after moving back to standard light environment i.e. post high-light exposure (pHL).

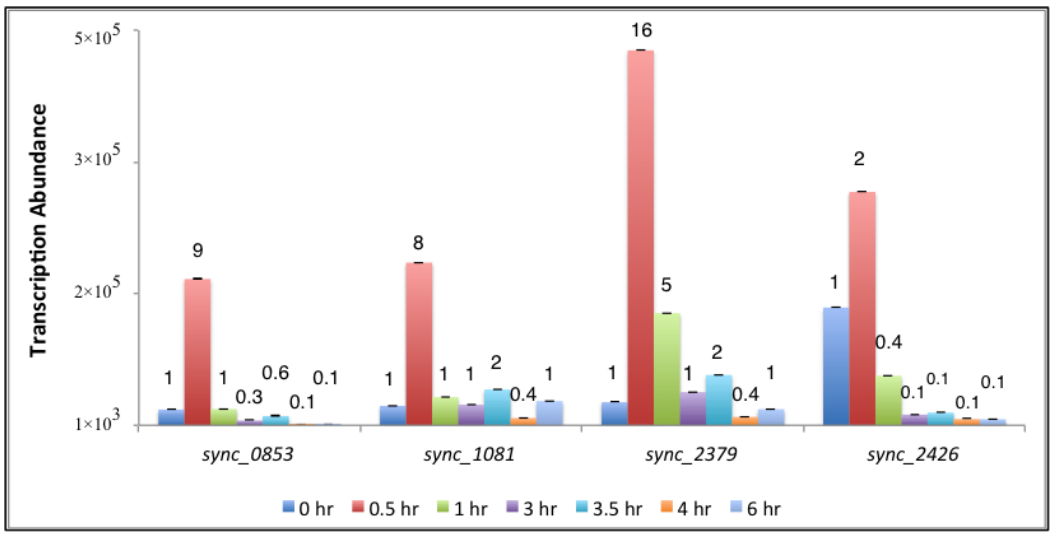

Figure 6.10. Absolute transcript abundance of *Synechococcus* sp. CC9311 metallothionein genes *sync_0853, sync_1081, sync_2379* and *sync_2426* following a high light shock and post high light shock recovery. Cultures were growing in high light (200 µmol photons $m^{-2}s^{-1}$) for 3 hours and subsequently during recovery in standard growth conditions (5 µmol photons m^{-2} s^{-1} white light) for another 3 hours. Bar height represents absolute transcript abundance per ng cDNA present in each qPCR reaction. Numbers above each bar represent the fold change in gene expression for each metallothionein gene compared to expression at 0 hr.

As shown in Figure 6.10, high light exposure triggered a rapid increase in expression of all four metallothionein genes i.e. within 0.5 h. Expression of *sync_0853*, *sync_1081*, *sync_2379* increased 9-, 8- and 16-fold, respectively. Subsequently, transcription of these genes decreased during the remainder of the high light shock period. Transcription of *sync_0853* returned to initial expression levels within 1 h, but then kept decreasing to 0.3 (i.e. a 3-fold decrease) by 3 h of exposure to high light. Transcription of *sync_1081* also returned to initial expression levels within 1 h but remained at this level until being shifted back to the standard light intensity. Similarly, *sync_2379* expression decreased by 1 h but decreased further to initial levels only after 3 h of high light exposure. The shift back to standard low light conditions elicited a slight increase in expression of these three metallothionein genes, but the response was transient, expression of *sync_0853* decreasing to a minimum 0.1 value (10-fold decrease) by 4 h before remaining at this level; expression of *sync_1081* and *sync_2379* decreased to 0.4 (2.5-fold decrease) before returning to initial expression levels. For *sync_2426*, expression showed a slight increase following high light exposure but then dropped significantly reducing 10-fold by 3 h exposure and remaining at this level during recovery in low light.

When exposed to a high light intensity, it is envisaged that the rate of photosynthetic oxygen evolution in cyanobacterium *Synechococcus* sp. CC9311 will increase. As a consequence, cells are exposed to a highly oxidizing environment. It has been reported that metal ions such as zinc, copper and cadmium has negative influence on the rate of photosynthetic oxygen evolution (Ybarra and Webb, 1999). Metallothioneins are been reported as free radical

generator scavengers themselves, and can potentially protect against oxidative stress (Zeitoun-Ghandour *et al.*, 2011). It is possible that by increasing expression of metallothionein genes cells have a mechanism to reduce the number of oxidized metal ions by decreasing their cellular concentration. However, it is unclear why this response is transient, with decreasing expression of metallothionein genes after longer high light exposure, and likewise why expression further decreases when cells are transferred back to a standard light intensity. Further study is required to resolve this.

6.6 Summary

In this chapter, expression analysis of all four metallothionein genes from *Synechococcus* sp. CC9311 was performed following growth under various zinc and cadmium concentrations or following exposure to high light intensity. Differential expression of each gene was observed dependent on environmental conditions (summarised in Table 6. 2).

Table 6.2. Summary of the expression of metallothionein genes with respect to metal ion treatment or highlight exposure. + indicates an increase in expression of the respective metallothionein gene; - indicates a decrease in expression of the respective metallothionein gene.

	sync_0853	***sync_1081***	***sync_2379***	***sync_2426***
Zn shock	0	0	0	++
Zn depletion	+++	+++	0	0
Zn starvation	0	0	0	+
Cd shock	---	---	---	---
Cd tolerant	+	0	+	+
High light shock	+	+	+	0

Sync_0853 exhibited highest expression levels in response to zinc depletion, but growth at low cadmium concentrations and high light intensity also increased expression, suggesting that *sync_0853* participates in zinc scavenging, protection against low levels of cadmium, as well as protecting against oxidised metal ions. *Sync_1081* also seems to play a role in zinc scavenging and protection against oxidising metal ions. In contrast, *sync_2379* appears to play a key role during high light stress, expression of *sync_2379* increasing the most of the four metallothioneins analysed during high light exposure, but also seems to protect against low cadmium levels. *Sync_2426* was the only metallothionein not to increase in expression following high light exposure, but was markedly induced following zinc shock, and markedly shut down following zinc starvation suggesting it plays a key role in zinc homeostasis in this organism.

7

Conclusions

7.1 Introduction

The marine cyanobacterium *Synechococcus* sp. CC9311 (clade I) inhabits a coastal environment that encounters a relatively rich but erratic nutrient supply due to wind-driven input from the deep ocean and riverine input from land (Palenik *et al.*, 2006b; Zwirglmaier *et al.*, 2007; Zwirglmaier *et al.*, 2008; Scanlan *et al.*, 2009; Stuart *et al.*, 2009).

Genomic analysis demonstrates that *Synechococcus* sp. CC9311 contains many genes involved in metal transport and storage including four metallothionein genes (Palenik *et al.*, 2006b). Metallothioneins are believed to participate in metal homeostasis, heavy metal detoxification and free radical scavenging (Kelly *et al.*, 1996; Palmiter, 1998; Hathout *et al.*, 2001; Gold *et al.*, 2008; Zeitoun-Ghandour *et al.*, 2011).

It is postulated that *Synechococcus* sp. CC9311 might either have a greater need for metals, or a greater need to respond to excess metal levels, or that cells experience episodic metal concentrations (Palenik *et al.*, 2006b). In this project, this strain was cultured in a range of metal conditions (Zn, Cd) in comparison with two other strains, *Synechococcus* sp. WH8102 and WH7805. As observed (Chapter 5), *Synechococcus* sp. CC9311 demonstrated remarkable tolerance to cadmium (up to 10 μM; and it was also able to maintain surprisingly constant yields in a broad range of zinc concentrations (0.7 nM to 2500 nM) compared to

the other two strains. My studies provide evidence that this coastal strain *Synechococcus* sp. CC9311 has developed adaption to its coastal environment.

However, as yet, little work has been performed to elucidate the physiological role or structure of the four metallothioneins in *Synechococcus* sp. CC9311 or to identify any ecological advantages for this strain. In this project, the four metallothionein genes were first cloned into *E.coli* successfully and three of them were isolated and characterised in *vitro*. The possible metal binding configurations of the three new BmtAs were also generated. The expression analysis of the four metallothionein genes under different conditions provides evidences that the four genes are selectively participating in zinc scavenging, zinc homeostasis, and cadmium detoxification. Interestingly, the *sync_0853*, *sync_1081* and *sync_2379* were found to play a role in protection form oxidising conditions, which leads to a new research direction. My research verified the hypothesis raised in the beginning: the four cyanobacterial metallothioneins with distinct biophysical properties (protein folding and structure, metal release kinetics and metal binding affinity), are expressed in response to different environmental conditions (Zn, Cd and high ligh).

In this chapter I present a brief summary of MT expression profiles under stresses in *Synechococcus* sp. CC9311 as evidence for the biological function of the metallothioneins in this coastal cyanobacterium; this will be put in the context of biophysical structural information and metal release kinetics of three of the metallothioneins from *Synechococcus* sp. CC9311 described in previous chapters. Potential future work is also included.

7.2 Key findings

At the beginning of this investigation, the metallothioneins from *Synechococcus* sp. CC9311 were cloned into vector pET-26b(+) and expressed in *E. coli* (chapter 3). ESI-MS spectra and elemental analysis (by ICP-OES) demonstrated the different metal binding stoichiometry and metal release kinetics of three of these metallothioneins (chapter 4); NMR spectra also provided information on their solution structures (chapter 4).

7.2.1 BmtA 0853

One of these metallothioneins, BmtA0853, was shown to be able to bind up to three zinc ions at neutral pH 7.4; Zn_1 and the apo form were also observed but with negligibly small abundances. A three-metal cluster is in agreement with the expectation that site C is not present in BmtA0853, because two terminal ligands involved in this site are not conserved in this homologue of SmtA from *Synechococcus* sp. PCC7942. The 1D ^{111}Cd and 2D ^{1}H NMR spectra also confirmed the loss of site C. The homology model indicated that the 8 Cys and His 40 can form an unambiguous Zn_3Cys_8His cluster with site A, B and D formed by the equivalent residues in SmtA (section 4.4). Reactions with EDTA demonstrated that this cluster is extremely labile. After the addition of EDTA, the Zn_3 species diminished extremely quickly and was present in only 2.2% of all observed species after 150 minutes.

This extremely fast metal loss after addition of EDTA and the observation of the demetallated Zn_1 species and the absence of demetallated Zn_2 species suggests that the loss of site C (known to be the most reactive site in SmtA (ref) and predicted to be replaced by salt bridges) leads to a extremely labile cluster. One of site B' or D' is extremely labile and may be exposed in the structure that can be rapidly demetallated by EDTA; after loss of the first metal ion, the other site D' or B' becomes labile as well. The remaining zinc ion in the Zn_1 species is likely to bind to zinc finger site A, as previously observed for SmtA (Leszczyszyn *et al.*, 2007b). Whether access of the site B' and D' requires breakage of the salt bridge, or is accessible otherwise, is not clear at this stage. The zinc-binding constant for BmtA0853 (11.3, see section 4.5.2) also suggests that the zinc ions bound to this metallothionein may be more readily transferable to other molecules compared to either SmtA from *Synechococcus* sp. PCC7942 (>13, Blindauer, 2008) or BmtA1081 (13.5). Besides, the cadmium-edited 2D ^{1}H NMR spectra indicated a well-folded BmtA0853, which, in comparison with the discussed below, demonstrates that folding of these homologues MTs can be metal specific. This may bring advantages in terms of physiological needs, which have been observed in other metallothioneins (Zeitoun-Ghandour *et al.*, 2010; Leszczyszyn *et al.*, 2011). Gene expression analysis (chapter 6) suggests that *sync_0853* participates in zinc scavenging, protection against cadmium as well as protecting against oxidised metal ions.

7.2.2 BmtA1081

For BmtA1081, four metal binding sites were observed in the 1D ^{111}Cd spectra, also agreed for the protein expressed in the presence of Zn by ESI-MS spectra and ICP-OES. With the information provided by NMR spectra, sites A (Cys 8, 13, 31 and 35), B' (Cys 13, 45, 54 and 56) and D' (Cys 10, 35, 56 and His 39) were unambiguously assigned with metal binding ligands. For the site C' only Cys 15 was observed, which leaves Cys 52, His 28 and 46 unclear and leads to three possible configurations (Figure 4.24, section 4.4). The EDTA reaction indicates that although the fully-formed Zn_4 BmtA1081 cluster is highly resilient to metal removal, once the first zinc ion is lost, it becomes very unstable and releases all three other zinc ions. This very particular zinc binding site that is critical for metal occupation is predicted to be site C'. A possible explanation is that the altered geometry caused by the 'CH' motif (as distinguished from the CxH motif in SmtA) generates a more buried site C'. The zinc-binding constant for BmtA1081 (13.5) is much higher than those for BmtA0853 (11.3) and BmtA2426 (11.1), indicating the zinc ions bound to this metallothionein are more difficult to transfer to other molecules. Gene expression analysis suggests that this metallothionein plays a role in zinc scavenging and protection against oxidising metal ions but not cadmium detoxification.

7.2.3 BmtA2426

Another metallothionein in *Synechococcus* sp. CC9311, BmtA2426 is also capable of binding 4 zinc ions as shown both by ESI-MS spectra and ICP-OES. The ^{111}Cd and ^{1}H NMR spectra indicated a possible $Zn_4Cys_9His_2$ metal binding cluster of BmtA2426: site A demonstrates high similarity to site A in SmtA (Cys 8, 31, 35 and possibly Cys 13, equivalent to the same residues in SmtA); Cys 10, 13 and 55 are highly likely to coordinate to Zn in site B'; His 50, Cys 15 and 31 may be part of site C'; site D' involves His 39, Cys 10, 35 and 57; the remaining Cys 53 may bridge between site B' and C' (Figure 4.25, section 4.4). In competition reactions with EDTA, only demetallated Zn_3 and apo species of BmtA2426 were observed; the first zinc ion was attacked more slowly than that in BmtA0853, which suggests that this zinc ion is relatively more difficult to attack, but after loss of the first metal ion, predicted in site C', BmtA2426 still forms a moderately stable Zn_3 cluster. Once a second zinc ion is lost, BmtA2426 releases the remaining two zinc ions immediately; including the one in site A. Which of site B' or D' is the second metal to be released is not clear at this point. Further work is required in the future. BmtA2426 was the only metallothionein not to respond to high light exposure, but it may play a key role in zinc homeostasis in *Synechococcus* sp. CC9311.

7.2.4 *Sync_2379*

Sync_2379 was the only metallothionein sub-cloned into pET-26b(+) vector that was not biophysically characterised due its low expression level in *E. coli*. However, gene expression analysis in *Synechococcus* sp. CC9311 indicates this metallothionein plays a key role during high light stress, and also participates in cadmium detoxification.

To summarise, the four metallothioneins from *Synechococcus* sp. CC9311 exhibit distinct characters, not only in terms of their biophysical properties but also selectively participating in zinc scavenging, zinc homeostasis, cadmium detoxification, and protection from oxidising metal ions. This work reiterates the metal intensive physiology of *Synechococcus* sp. CC9311 consistent with its proposed adaption to a coastal environment (Palenik *et al.*, 2006b).

7.3 Future work

Full structural determination using distance restraints generated from the acquired ^{1}H and ^{111}Cd NMR data will provide more conclusive information on the solution structures of BmtA1081 and BmtA2426.

Site-specific mutagenesis may be employed to explore the role of individual metal ligands, and it could also be attempted to generate mutant proteins that can fold in a defined way in the presence of cadmium. For BmtA1081, Cys 52, 54 and 56 compose a CxCxC motif (as distinguished from the CxC motif in SmtA),

although there is a highly likely possibility that Cys 54 and 56 are functioning in an equivalent manner to residues Cys 52 and Cys 54 in SmtA. Hence, removal of Cys 52 (for example mutant to Ser) in BmtA1081 may help to confirm the suggested cluster arrangement (Figure 4.24). Multiple configurations were observed for both of BmtA1081 and BmtA2426 in the presence of cadmium, switching His to Cys residues could help in order to generate more homogeneous cadmium-loaded protein samples. Besides, removal of the individual His 28 or His 46 residues (for example, mutation to Arg or Ala) also could attempt to identify their role in the metal binding clusters of BmtA1081 more conclusively.

Expression analysis suggested that the four individual metallothionein genes fulfil distinct and different roles in *Synechococcus* sp. CC9311. To provide further evidence for these roles, gene knockout mutations, such as knocking out of *sync_2426* that may play a key role in zinc homeostasis in this organism, could be established. Growth experiments analogous to those described in Chapter 6 could be carried out to check if this mutant *Synechococcus* sp. CC9311 is more sensitive to zinc (both excess and depletion). The generation of multiple-genes knockout mutants is also a possibility, for example knocking out of the two metallothionein genes participating in zinc scavenging (*sync_0853* and *sync_1081*).

Gene expression analysis carried out in this thesis, particularly with regard to high light exposure, potentially leads to an interesting future research direction, namely, that bacterial metallothioneins participate in protection against oxidising conditions, a hypothesis that has so far been rarely studied. The generation of various knockout mutants, including a triple-KO of the three metallothioneins

that are likely involved in protection against high levels of photosynthetic activity (*sync_0853*, *sync_1081* and *sync_2379*) could be a first step to tackle this hypothesis.

The *E. coli* strain Rosetta (DE3 α) was used for production of the recombinant protein *sync_2379* in this work. Other strains, such as the *E. coli* Rosetta gami (DE3)pLysS host strain, could also be used in order to enhance the expression level of *sync_2379*. Alternatively, the low yields of *sync_2379* may be related to *E. coli* not being able to properly metallate this protein, and therefore, alternative routes to its production could be explored, including peptide synthesis.

References

Alfonso, M.; Perewoska, I.; Kirilovsky, D., (2001), Redox control of ntcA gene expression in Synechocystis sp. PCC 6803. Nitrogen availability and electron transport regulate the levels of the NtcA protein. *Plant Physiol 125* (2), 969-81.

Aparicio-Gonzáleza, A.; Duarte, C. M.; Tovar-Sánchez, A., (2012), Tracemetals in deepocean waters: A review. *Journal of Marine Systems 100–101*, 26-33.

Banci, L.; Bertini, I.; Ciofi-Baffoni, S.; Su, X. C.; Borrelly, G. P.; Robinson, N. J., (2004), Solution structures of a cyanobacterial metallochaperone: insight into an atypical copper-binding motif. *J Biol Chem 279* (26), 27502-10.

Barnett, J. P.; Millard, A.; Ksibe, A. Z.; Scanlan, D. J.; Schmid, R.; Blindauer, C. A., (2012), Mining genomes of marine cyanobacteria for elements of zinc homeostasis. *Front Microbiol 3*, 142.

Ben-Bassat, A.; Bauer, K.; Chang, S. Y.; Myambo, K.; Boosman, A.; Chang, S., (1987), Processing of the initiation methionine from proteins: properties of the Escherichia coli methionine aminopeptidase and its gene structure. *J Bacteriol 169* (2), 751-7.

Benters, J.; Flögel, U.; Schäfer, T.; Leibfritz, D.; Hechtenberg, S.; Beyersmann, D., (1997), Study of the interactions of cadmium and zinc ions with cellular calcium homoeostasis using 19F-NMR spectroscopy. *Biochem J 322 (Pt 3)*, 793-9.

Bettmer, J.; Montes Bayón, M.; Encinar, J. R.; Fernández Sánchez, M. L.; Fernández de la Campa, M. e. R.; Sanz Medel, A., (2009), The emerging role of ICP-MS in proteomic analysis. *J Proteomics 72* (6), 989-1005.

Blindauer, C. A., (2008a), Metallothioneins with unusual residues: Histidines as modulators of zinc affinity and reactivity. *Journal of Inorganic Biochemistry 102* (3), 507-521.

Blindauer, C. A., (2008b), Zinc-handling in Cyanobacteria : an update. *Chem. Biodivers. 5* (10), 1990-2013.

Blindauer, C. A., (2009); Metallothioneins and Related Chelators. Sciences, M. I. i. L., Ed. RSC Publisher: Vol. 5, pp 51-81.

Blindauer, C. A., (2011), Bacterial metallothioneins: past, present, and questions for the future. *J Biol Inorg Chem 16* (7), 1011-24.

Blindauer, C. A.; Harrison, M. D.; Parkinson, J. A.; Robinson, A. K.; Cavet, J. S.; Robinson, N. J.; Sadler, P. J., (2001), A metallothionein containing a zinc finger within a four-metal cluster protects a bacterium from zinc toxicity. *Proceedings of the National Academy of Sciences of the United States of America 98* (17), 9593-9598.

Blindauer, C. A.; Harrison, M. D.; Robinson, A. K.; Parkinson, J. A.; Bowness, P. W.; Sadler, P. J.; Robinson, N. J., (2002), Multiple bacteria encode metallothioneinsand SmtA-like zinc fingers. *Molecular Microbiology 45* (5), 1421-1432.

Blindauer, C. A.; Leszczyszyn, O. I., (2010), Metallothioneins: unparalleled diversity in structures and functions for metal ion homeostasis and more. *Nat. Prod. Rep. 27* (5), 720-741.

Blindauer, C. A.; Polfer, N. C.; Keiper, S. E.; Harrison, M. D.; Robinson, N. J.; Langridge-Smith, P. R.; Sadler, P. J., (2003), Inert site in a protein zinc cluster: isotope exchange by high resolution mass spectrometry. *J Am Chem Soc 125* (11), 3226-7.

Blindauer, C. A.; Razi, M. T.; Campopiano, D. J.; Sadler, P. J., (2007a), Histidine ligands in bacterial metallothionein enhance cluster stability. *J Biol Inorg Chem 12* (3), 393-405.

Blindauer, C. A.; Razi, M. T.; Campopiano, D. J.; Sadler, P. J., (2007b), Histidine ligands in bacterial metallothionein enhance cluster stability. *Journal of Biological Inorganic Chemistry 12* (3), 393-405.

Bofill, R.; Orihuela, R.; Romagosa, M.; Domènech, J.; Atrian, S.; Capdevila, M., (2009), Caenorhabditis elegans metallothionein isoform specificity--metal binding abilities and the role of histidine in CeMT1 and CeMT2. *FEBS J 276* (23), 7040-56.

Bonvin, A. M.; Boelens, R.; Kaptein, R., (2005), NMR analysis of protein interactions. *Curr Opin Chem Biol 9* (5), 501-8.

Brouwer, M.; Enghild, J.; Hoexum-Brouwer, T.; Thogersen, I.; Truncali, A., (1995), Primary structure and tissue-specific expression of blue crab (Callinectes sapidus) metallothionein isoforms. *Biochem J 311 (Pt 2)*, 617-22.

Bruland, K. W.; Lohan, M. C., (2006); Control of Trace Metals in Seawater. In *Controls of Trace Metals in Seawaters: Treatise on Geochemistry*, Elderfield, H., Ed. Pergamon: Vol. 6.

Cai, L.; Klein, J. B.; Kang, Y. J., (2000), Metallothionein inhibits peroxynitrite-induced DNA and lipoprotein damage. *J. Biol. Chem 275* (50), 38957-38960.

Cavet, J. S.; Borrelly, G. P.; Robinson, N. J., (2003), Zn, Cu and Co in cyanobacteria: selective control of metal availability. *FEMS Microbiol Rev 27* (2-3), 165-81.

Cerda, B. D. l.; Castielli, O.; Duran, R. V.; Navarro, J. A.; Hervas, M.; Rosa, M. A. D. l., (2008), A proteomic approach to iron and copper homeostasis in cyanobacteria *Brief. Funct. Genomic. Proteomic. 6* (4), 322-329.

Chatthai, M.; Kaukinen, K. H.; Tranbarger, T. J.; Gupta, P. K.; Misra, S., (1997), The isolation of a novel metallothionein-related cDNA expressed in somatic and zygotic embryos of Douglas-fir: regulation by ABA, osmoticum, and metal ions. *Plant Mol Biol 34* (2), 243-54.

Chen, X.; Chu, M.; Giedroc, D. P., (2000), Spectroscopic characterization of Co(II)-, Ni(II)-, and Cd(II)-substituted wild-type and non-native retroviral-type zinc finger peptides. *J Biol Inorg Chem 5* (1), 93-101.

Clokie, M. R.; Shan, J.; Bailey, S.; Jia, Y.; Krisch, H. M.; West, S.; Mann, N. H., (2006), Transcription of a 'photosynthetic' T4-type phage during infection of a marine cyanobacterium. *Environ Microbiol 8* (5), 827-35.

Cobbett, C.; Goldsbrough, P., (2002), Phytochelatins and metallothioneins: roles in heavy metal detoxification and homeostasis. *Annu Rev Plant Biol 53*, 159-82.

Colvin, R. A.; Holmes, W. R.; Fontaine, C. P.; Maret, W., (2010), Cytosolic zinc buffering and muffling: their role in intracellular zinc homeostasis. *Metallomics 2* (5), 306-317.

Cook, N. L.; Vink, R.; Donkin, J. J.; Heuvel, C. v. d., (2009), Validation of reference genes for normalization of real-time quantitative RT-PCR data in traumatic brain injury. *Journal of Neuroscience Research 87* (1), 34–41.

Da Silva, J. J. R. F.; Williams, R. J. P., (2001); *The Biological Chemistry of the Elements: The Inorganic Chemistry of Life.* Oxford University Press.: Oxford.

Dalton, T.; Fu, K.; Palmiter, R. D.; Andrews, G. K., (1996), Transgenic mice that overexpress metallothionein-I resist dietary zinc deficiency. *J Nutr 126* (4), 825-33.

Daniels, M. J.; Turner-Cavet, J. S.; Selkirk, R.; Sun, H.; Parkinson, J. A.; Sadler, P. J.; Robinson, N. J., (1998), Coordination of Zn2+ (and Cd2+) by prokaryotic metallothionein. Involvement of his-imidazole. *J Biol Chem 273* (36), 22957-61.

Das, K.; De Groof, A.; Jauniaux, T.; Bouquegneau, J.-M., (2006), Zn, Cu, Cd and Hg binding to metallothioneins in harbour porpoises Phocoena phocoena from the southern North Sea. *BMC Ecol 6*, 2.

Davis, S. R. (2011),Characterizing the role of the bacterial metallothionein, SmtA, in mammalian infection. University of Connecticut,

Davis, S. R.; Cousins, R. J., (2000), Metallothionein expression in animals: a physiological perspective on function. *J. Nutr. 130* (5), 1085-1088.

Digilio, G.; Bracco, C.; Vergani, L.; Botta, M.; Osella, D.; Viarengo, A., (2009), The cadmium binding domains in the metallothionein isoform Cd(7)-MT10 from Mytilus galloprovincialis revealed by NMR spectroscopy. *J Biol Inorg Chem 14* (2), 167-78.

Dufresne, A.; Ostrowski, M.; Scanlan, D.; Garczarek, L.; Mazard, S.; Palenik, B.; Paulsen, I.; de Marsac, N.; Wincker, P.; Dossat, C.; Ferriera, S.; Johnson, J.; Post, A.; Hess, W.; Partensky, F., (2008), Unraveling the genomic mosaic of a ubiquitous genus of marine cyanobacteria. *Genome Biology 9* (5), R90.

Dunn, A. K.; Wallace, V. P.; Coleno, M.; Berns, M. W.; Tromberg, B. J., (2000), Influence of optical properties on two-photon fluorescence imaging in turbid samples. *Appl Opt 39* (7), 1194-201.

ELLMAN, G. L., (1958), A colorimetric method for determining low concentrations of mercaptans. *Arch Biochem Biophys 74* (2), 443-50.

Fowler, B. A.; Hildebrand, C. E.; Kojima, Y.; Webb, M., (1987), Nomenclature of metallothionein. *Experientia Suppl 52*, 19-22.

Fuller, N. J.; Marie, D.; Partensky, F.; Vaulot, D.; Post, A. F.; Scanlan, D. J., (2003a), Clade-Specific 16S Ribosomal DNA Oligonucleotides Reveal the Predominance of a Single Marine Synechococcus Clade throughout a Stratified Water Column in the Red Sea. *APPLIED AND ENVIRONMENTAL MICROBIOLOGY 69* (5), 2430-2443.

Fuller, N. J.; Marie, D.; Partensky, F.; Vaulot, D.; Post, A. F.; Scanlan, D. J., (2003b), Clade-specific 16S ribosomal DNA oligonucleotides reveal the predominance of a single marine Synechococcus clade throughout a stratified water column in the Red Sea. *Appl Environ Microbiol 69* (5), 2430-43.

Gierga, G.; Voss, B.; Hess, W. R., (2009), The Yfr2 ncRNA family, a group of abundant RNA molecules widely conserved in cyanobacteria. *RNA Biol 6* (3), 222-7.

Gold, B.; Deng, H.; Bryk, R.; Vargas, D.; Eliezer, D.; Roberts, J.; Jiang, X.; Nathan, C., (2008), Identification of a copper-binding metallothionein in pathogenic mycobacteria. *Nat Chem Biol 4* (10), 609-16.

Goldberg, H. A.; Warner, K. J., (1997), The staining of acidic proteins on polyacrylamide gels: enhanced sensitivity and stability of "Stains-all" staining in combination with silver nitrate. *Anal Biochem 251* (2), 227-33.

Good, M.; Hollenstein, R.; Sadler, P. J.; Vasak, M., (1988), CD-113 NMR-STUDIES ON METAL THIOLATE CLUSTER FORMATION IN RABBIT CD(II)-METALLOTHIONEIN - EVIDENCE FOR A PH-DEPENDENCE. *Biochemistry 27* (18), 7163-7166.

Griffiths, M. J.; Garcin, C.; van Hille, R. P.; Harrison, S. T., (2011), Interference by pigment in the estimation of microalgal biomass concentration by optical density. *J Microbiol Methods 85* (2), 119-23.

Grossman, A. R.; Schaefer, M. R.; Chiang, G. G.; Collier, J. L., (1993), The phycobilisome, a light-harvesting complex responsive to environmental conditions. *Microbiol Rev 57* (3), 725-49.

Gupta, A.; Whitton, B. A.; Morby, A. P.; Huckle, J. W.; Robinson, N. J., (1992), Amplification and rearrangement of a prokaryotic metallothionein locus smt in Synechococcus PCC 6301 selected for tolerance to cadmium. *Proc Biol Sci 248* (1323), 273-81.

Hasler, D. W.; Jensen, L. T.; Zerbe, O.; Winge, D. R.; Vasak, M., (2000), Effect of the two conserved prolines of human growth inhibitory factor (metallothionein-3) on its biological activity and structure fluctuation: Comparison with a mutant protein. *Biochemistry 39* (47), 14567-14575.

Hathout, Y.; Fabris, D.; Fenselau, C., (2001), Stoichiometry in zinc ion transfer from metallothionein to zinc finger peptides. *International Journal of Mass Spectrometry 204*, 1-6.

Heid, C. A.; Stevens, J.; Livak, K. J.; Williams, P. M., (1996), Real time quantitative PCR. *Genome Res 6* (10), 986-94.

Hemmingsen, L.; Olsen, L.; Antony, J.; Sauer, S. P., (2004), First principle calculations of (113)Cd chemical shifts for proteins and model systems. *J Biol Inorg Chem 9* (5), 591-9.

Henehan, C. J.; Pountney, D. L.; Zerbe, O.; Vasák, M., (1993), Identification of cysteine ligands in metalloproteins using optical and NMR spectroscopy: cadmium-substituted rubredoxin as a model [Cd(CysS)4]2- center. *Protein Sci 2* (10), 1756-64.

Herdman, M.; Castenholz, R. W.; Iteman, I.; Waterbury, J.; Rippka, R., (2001); The Archaea and the deeply branching and phototrophic bacteria. In *Bergey's Manual of Systematic Bacteriology.*, 2nd ed.; Boone, D. R.; Castenholz, R. W., Eds. Springer-Verlag: pp 493–514.

Herrmann, B.; Pettersson, B.; Everett, K. D.; Mikkelsen, N. E.; Kirsebom, L. A., (2000), Characterization of the rnpB gene and RNase P RNA in the order Chlamydiales. *Int J Syst Evol Microbiol 50 Pt 1*, 149-58.

Heywood, J. L.; Zubkov, M. V.; Tarran, G. A.; Fuchs, B. M.; Holligan, P. M., (2006), Prokaryoplankton standing stocks in oligotrophic gyre and equatorial provinces of the Atlantic Ocean: evaluation of inter-annual variability. *<xhtml:em style="margin: 0px; padding: 0px; ">Deep Sea Research II 53*, 1530-1547.

Higuchi, R.; Dollinger, G.; Walsh, P. S.; Griffith, R., (1992), Simultaneous amplification and detection of specific DNA sequences. *Biotechonology 10*, 413-417.

Holtzendorff, J.; Partensky, F.; Jacquet, S.; Bruyant, F.; Marie, D.; Garczarek, L.; Mary, I.; Vaulot, D.; Hess, W. R., (2001), Diel expression of cell cycle-related genes in synchronized cultures of Prochlorococcus sp. strain PCC 9511. *J Bacteriol 183* (3), 915-20.

Howard, M. J., (1998), Protein NMR spectroscopy. *Curr Biol 8* (10), R331-3.

Huckle, J. W.; Morby, A. P.; Turner, J. S.; Robinson, N. J., (1993), Isolation of a prokaryotic metallothionein locus and analysis of transcriptional control by trace metal ions. *Mol Microbiol 7* (2), 177-87.

Jacob, C.; Maret, W.; Vallee, B. L., (1998), Control of zinc transfer between thionein, metallothionein, and zinc proteins. *Proc. Natl. Acad. Sci. 95* (7), 3489-3494.

Jardillier, L.; Zubkov, M. V.; Pearman, J.; Scanlan, D. J., (2010), Significant CO2 fixation by small prymnesiophytes in the subtropical and tropical northeast Atlantic Ocean. *ISME J 4* (9), 1180-92.

Kägi, K. H. R., (1993); Metallothionein. Suzuki, N.; Imura, N.; Kimura, M., Eds. Vol. 3, pp 29-56.

Karin, M.; Imbra, R. J.; Heguy, A.; Wong, G., (1985), Interleukin 1 regulates human metallothionein gene expression. *Mol Cell Biol 5* (10), 2866-9.

Karl, D. M.; Michaels, A.; Bergman, B.; Capone, D.; Carpenter, E.; Letelier, R.; Lipschultz, F.; Paerl, H.; Sigman, D.; Stal, L., (2002), Dinitrogen fixation in the world's oceans. *Biogeochemistry 57*, 47-98.

Katoh, H.; Hagino, N.; Grossman, A. R.; Ogawa, T., (2001), Genes essential to iron transport in the cyanobacterium Synechocystis sp. strain PCC 6803. *J Bacteriol 183* (9), 2779-84.

Kelly, E. J.; Quaife, C. J.; Froelick, G. J.; Palmiter, R. D., (1996), Metallothionein I and II protect against zinc deficiency and zinc toxicity in mice. *J Nutr 126* (7), 1782-90.

Klaassen, C. D.; Liu, J.; Diwan, B. A., (2009), Metallothionein protection of cadmium toxicity. *Toxicol. Appl. Pharmacol. 238* (3), 215-220.

Kreusch, S.; Schwedler, S.; Tautkus, B.; Cumme, G. A.; Horn, A., (2003), UV measurements in microplates suitable for high-throughput protein determination. *Anal Biochem 313* (2), 208-15.

Kubista, M.; Andrade, J. M.; Bengtsson, M.; Forootan, A.; Jonák, J.; Lind, K.; Sindelka, R.; Sjöback, R.; Sjögreen, B.; Strömbom, L.; Ståhlberg, A.; Zoric, N., (2006), The real-time polymerase chain reaction. *Mol Aspects Med 27* (2-3), 95-125.

Kunert, A.; Vinnemeier, J.; Erdmann, N.; Hagemann, M., (2003), Repression by Fur is not the main mechanism controlling the iron-inducible isiAB operon in the cyanobacterium Synechocystis sp. PCC 6803. *FEMS Microbiol Lett 227* (2), 255-62.

Lax, J. E.; Arteni, A. A.; Boekema, E. J.; Pistorius, E. K.; Michel, K. P.; Rögner, M., (2007), Structural response of Photosystem 2 to iron deficiency: characterization of a new photosystem 2-IdiA complex from the cyanobacterium Thermosynechococcus elongatus BP-1. *Biochim Biophys Acta 1767* (6), 528-34.

Leão, P. N.; Vasconcelos, M. T.; Vasconcelos, V. M., (2007), Role of marine cyanobacteria in trace metal bioavailability in seawater. *Microb Ecol 53* (1), 104-9.

Leszczyszyn, O. I.; Evans, C. D.; Keiper, S. E.; Warren, G. Z. L.; Blindauer, C. A., (2007a), Differential reactivity of individual zinc ions in clusters from bacterial metallothioneins. *Inorganica Chimica Acta 360* (1), 3-13.

Leszczyszyn, O. I.; Schmid, R.; Blindauer, C. A., (2007b), Toward a property/function relationship for metallothioneins: histidine coordination and unusual cluster composition in a zinc-metallothionein from plants. *Proteins 68* (4), 922-35.

Leszczyszyn, O. I.; Zeitoun-Ghandour, S.; Stürzenbaum, S. R.; Blindauer, C. A., (2011), Tools for metal ion sorting: in vitro evidence for partitioning of zinc and cadmium in C. elegans metallothionein isoforms. *Chem Commun (Camb) 47* (1), 448-50.

Li, B.; Sher, D.; Kelly, L.; Shi, Y.; Huang, K.; Knerr, P. J.; Joewono, I.; Rusch, D.; Chisholm, S. W.; van der Donk, W. A., (2010), Catalytic promiscuity in the biosynthesis of cyclic peptide secondary metabolites in planktonic marine cyanobacteria. *Proc Natl Acad Sci U S A 107* (23), 10430-5.

Li, T. Y.; Kraker, A. J.; Shaw, C. F.; Petering, D. H., (1980), Ligand substitution reactions of metallothioneins with EDTA and apo-carbonic anhydrase. *Proc Natl Acad Sci U S A 77* (11), 6334-8.

Livak, K. J.; Schmittgen, T. D., (2001), Analysis of relative gene expression data using real-time quantitative PCR and the 2(-Delta Delta C(T)) Method. *Methods 25* (4), 402-8.

Long, G. J.; Rosen, J. F.; Schanne, F. A., (1994), Lead activation of protein kinase C from rat brain. Determination of free calcium, lead, and zinc by 19F NMR. *J Biol Chem 269* (2), 834-7.

Los, D. A.; Suzuki, I.; Zinchenko, V. V.; Murata, N., (2008); Stress responses in Synechocystis: regulated genes and regulatory systems. In *The Cyanobacteria: Molecular Biology, Genomics and Evolution.*, Herrero, A.; Flores, E., Eds. Caister Academic Press: Norfolk, pp 117–157.

Maret, W., (2004), Exploring the zinc proteome. ***J. Anal. At. Spectrom*** *19*, 15-19.

Maret, W., (2009), Molecular aspects of human cellular zinc homeostasis: redox control of zinc potentials and zinc signals. *Biometals 22* (1), 149-157.

Mary, I.; Tu, C. J.; Grossman, A.; Vaulot, D., (2004), Effects of high light on transcripts of stress-associated genes for the cyanobacteria Synechocystis sp. PCC 6803 and Prochlorococcus MED4 and MIT9313. *Microbiology 150* (Pt 5), 1271-81.

Miao, A. J.; Wang, W. X.; Juneau, P., (2005), Comparison of Cd, Cu, and Zn toxic effects on four marine phytoplankton by pulse-amplitude-modulated fluorometry. *Environ Toxicol Chem 24* (10), 2603-11.

Morel, F. M.; Price, N. M., (2003), The biogeochemical cycles of trace metals in the oceans. *Science 300* (5621), 944-7.

Morel, F. M. M.; Reinfelder, J. R.; Roberts, S. B.; Chamberlain, C. P.; Lee, J. G.; Yee, D., (1994), Zinc and carbon co-limitation of marine phytoplankton. *Nature 3**69**,* 740 - 742.

Morel, F. M. M.; Rueter, J. G.; Anderson, D. M.; Guilard, R. R. L., (1979), Aquil: a chemically defined phytoplankton culture medium for trace metal studies. *Phycol 15*, 6.

Münger, K.; Germann, U. A.; Lerch, K., (1985), Isolation and structural organization of the Neurospora crassa copper metallothionein gene. *EMBO J 4* (10), 2665-8.

Nies, D. H., (2003), Efflux-mediated heavy metal resistance in prokaryotes. *FEMS Microbiol Rev 27* (2-3), 313-39.

Nordberg, G. F.; Nordberg, M.; Piscator, M.; Vesterberg, O., (1972), Separation of two forms of rabbit metallothionein by isoelectric focusing. *Biochem J 126* (3), 491-8.

Nordberg, M.; Kojima, (1979), *Experimentia. Suppl 34*, 48-55.

Nordberg, M.; Nordberg, G. F., (2009); Metallothioneins: Historical development and overview. In *Metallothioneins and related chelators.*, Sigel, A.; Sigel, H.; Sigel, R. K. O., Eds. RSC Publishing.

Okumura, F.; Li, Y.; Itoh, N.; Nakanishi, T.; Isobe, M.; Andrews, G. K.; Kimura, T., (2011), The zinc-sensing transcription factor MTF-1 mediates zinc-induced epigenetic changes in chromatin of the mouse metallothionein-I promoter. *Biochim Biophys Acta 1809* (1), 56-62.

Olafson, R. W.; Abel, K.; Sim, R. G., (1979a), Prokaryotic metallothionein: preliminary characterization of a blue-green alga heavy metal-binding protein. *Biochem Biophys Res Commun 89* (1), 36-43.

Olafson, R. W.; Abel, K.; Sim, R. G., (1979b), Prokaryotic metallothionein: preliminary characterization of a blue-green alga heavy metal-binding protein. *Biochem Biophys Res Commun 89* (1), 36-43.

Olafson, R. W.; Loya, S.; Sim, R. G., (1980), Physiological parameters of prokaryotic metallothionein induction. *Biochem Biophys Res Commun 95* (4), 1495-503.

Olafson, R. W.; McCubbin, W. D.; Kay, C. M., (1988), Primary- and secondary-structural analysis of a unique prokaryotic metallothionein from a Synechococcus sp. cyanobacterium. *Biochem J 251* (3), 691-9.

Ono, E.; Cuello, J., (2007), Carbon dioxide mitigation using thermophilic cyanobacteria. *Biosystems Engineering 96*, 129–134.

Palenik, B.; Ren, Q.; Dupont, C. L.; Myers, G. S.; Heidelberg, J. F.; Badger, J. H.; Madupu, R.; Nelson, W. C.; Brinkac, L. M.; Dodson, R. J.; Durkin, A. S.; Daugherty, S. C.; Sullivan, S. A.; Khouri, H.; Mohamoud, Y.; Halpin, R.; Paulsen, I. T., (2006a), Genome sequence of Synechococcus CC9311: Insights into adaptation to a coastal environment. *Proc Natl Acad Sci U S A 103* (36), 13555-9.

Palenik, B.; Ren, Q. H.; Dupont, C. L.; Myers, G. S.; Heidelberg, J. F.; Badger, J. H.; Madupu, R.; Nelson, W. C.; Brinkac, L. M.; Dodson, R. J.; Durkin, A. S.; Daugherty, S. C.; Sullivan, S. A.; Khouri, H.; Mohamoud, Y.; Halpin, R.; Paulsen, I. T., (2006b), Genome sequence of Synechococcus CC9311: Insights into adaptation to a coastal environment. *Proceedings of the National Academy of Sciences of the United States of America 103* (36), 13555-13559.

Palmiter, R. D., (1998), The elusive function of metallothioneins. *Proc Natl Acad Sci U S A 95* (15), 8428-30.

Palumaa, P.; Njunkova, O.; Pokras, L.; Eriste, E.; Jörnvall, H.; Sillard, R., (2002), Evidence for non-isostructural replacement of Zn(2+) with Cd(2+) in the beta-domain of brain-specific metallothionein-3. *FEBS Lett 527* (1-3), 76-80.

Partensky, F.; Hess, W. R.; Vaulot, D., (1999), Prochlorococcus, a marine photosynthetic prokaryote of global significance. *Microbiol Mol Biol Rev 63* (1), 106-27.

Patzer, S. I.; Hantke, K., (2000), The zinc-responsive regulator Zur and its control of the znu gene cluster encoding the ZnuABC zinc uptake system in *Escherichia* coli. *J. Biol. Chem. 275*, 24321–24332.

Payne, C. D.; Price, N. M., (1999), EFFECTS OF CADMIUM TOXICITY ON GROWTH AND ELEMENTAL COMPOSITION OF MARINE PHYTOPLANKTON1 *J. Phycol. 35*, 293-302.

Pedersen, K. L.; Pedersen, S. N.; Højrup, P.; Andersen, J. S.; Roepstorff, P.; Knudsen, J.; Depledge, M. H., (1994), Purification and characterization of a cadmium-induced metallothionein from the shore crab Carcinus maenas (L.). *Biochem J 297 (Pt 3)*, 609-14.

Peroza, E. A.; Kaabi, A. A.; Meyer-Klaucke, W.; Wellenreuther, G.; Freisinger, E., (2009), The two distinctive metal ion binding domains of the wheat metallothionein Ec-1. *J Inorg Biochem 103* (3), 342-53.

Pfaffl, M. W., (2001), A new mathematical model for relative quantification in real-time RT-PCR. *Nucleic Acids Res 29* (9), e45.

Pfaffl, M. W., (2006); Relative quantification. In *Real-time PCR*, Dorak, T., Ed. International University Line: pp 63-82.

Pfafflm, M. W.; Hageleit, M., (2001), Validities of mRNA quantification using recombinant RNA and recombinant DNA external calibration curves in real-time RT-PCR. *Biotechnology Letters 23*, 275-282.

Pohl, C.; Croot, P. L.; Hennings, U.; Daberkow, T.; Budeus, G.; Rutgers v.d. Loeff, M., (2011), Synoptic transects on the distribution of trace elements (Hg, Pb, Cd, Cu, Ni, Zn, Co, Mn, Fe, and Al) in surface waters of the Northern- and Southern East Atlantic *Journal of Marine Systems 84*, 28-41.

Pokrovsky, O. S.; Martinez, R. E.; Golubev, S. V.; Kompantseva, E. I.; Shirokova, L. S., (2008), Adsorption of metals and protons on Gloeocapsa sp. cyanobacteria: A surface speciation approach. *Applied Geochemistry 23*, 2574-2588.

Polevoda, B.; Arnesen, T.; Sherman, F., (2009), A synopsis of eukaryotic Nalpha-terminal acetyltransferases: nomenclature, subunits and substrates. *BMC Proc 3 Suppl 6*, S2.

Price, N. M.; Harrison, G. I.; Hering, J. G.; Hudson, R. J.; Nirel, P. M. V.; Palenik, B.; Moorel, F. M. M., (1989), Preparation and chemistry of the artificial algal culture medium Aquil. *Biol. Oceanogr 6*, 18.

Prudent, M.; Girault, H. H., (2009), The role of copper in cysteine oxidation: study of intra- and inter-molecular reactions in mass spectrometry. *Metallomics 1* (2), 157-65.

Rauser, W. E., (1990), PHYTOCHELATINS. *Annual Review of Biochemistry 59*, 61-86.

Raven, J.; Evans, M.; Korb, R., (1999), The role of trace metals in photosynthetic electron transport in O2-evolving organisms. *Photosynthesis Research. 60*, 111-149.

Robinson, N. J., (2008), A bacterial copper metallothionein. *Nature Chemical Biology 4* (10), 582-583.

Robinson, N. J.; Gupta, A.; Fordham-Skelton, A. P.; Croy, R. R.; Whitton, B. A.; Huckle, J. W., (1990), Prokaryotic metallothionein gene characterication and expression: chromosome crawling by ligation-mediated PCR. *Proc Biol Sci 242* (1305), 241-7.

Saito, M.; Sigman, D.; Morel, F., (2003), The bioinorganic chemistry of the ancient ocean: the co-evolution of cyanobacterial metal requirements and biogeochemical cycles at the Archean-Proerozoic boundary? *Inorganica. Chimica. Acta. 356*, 308-318.

Salem, K.; van Waasbergen, L. G., (2004a), Light control of hliA transcription and transcript stability in the cyanobacterium Synechococcus elongatus strain PCC 7942. *J Bacteriol 186* (6), 1729-36.

Salem, K.; van Waasbergen, L. G., (2004b), Photosynthetic electron transport controls expression of the high light inducible gene in the cyanobacterium Synechococcus elongatus strain PCC 7942. *Plant Cell Physiol 45* (5), 651-8.

Sandmann, G.; Reck, H.; Kessler, E.; Böger, P., (1983), Distribution of plastocyanin and soluble plastidic cytochrome c in various classes of algae. *Arch. Microbiol 134*, 23–27.

Scanlan, D. J.; Ostrowski, M.; Mazard, S.; Dufresne, A.; Garczarek, L.; Hess, W. R.; Post, A. F.; Hagemann, M.; Paulsen, I.; Partensky, F., (2009), Ecological genomics of marine picocyanobacteria. *Microbiol Mol Biol Rev 73* (2), 249-99.

Scopes, R. K., (2001a), Overview of protein purification and characterization. *Curr Protoc Protein Sci Chapter 1*, Unit 1.1.

Scopes, R. K., (2001b), Strategies for protein purification. *Curr Protoc Protein Sci Chapter 1*, Unit 1.2.

Sen, A.; Dwivedi, K.; Rice, K. A.; Bullerjahn, G. S., (2000), Growth phase and metal-dependent regulation of the dpsA gene in Synechococcus sp. strain PCC 7942. *Arch. Microbiol. 173* (5-6), 352-357.

Sherman, F.; Stewart, J. W.; Tsunasawa, S., (1985), Methionine or not methionine at the beginning of a protein. *Bioessays 3* (1), 27-31.

Shi, J.; Lindsay, W. P.; Huckle, J. W.; Morby, A. P.; Robinson, N. J., (1992a), Cyanobacterial metallothionein gene expressed in Escherichia coli. Metal-binding properties of the expressed protein. *FEBS Lett 303* (2-3), 159-63.

Shi, J.; Lindsay, W. P.; Huckle, J. W.; Morby, A. P.; Robinson, N. J., (1992b), Cyanobacterial metallothionein gene expressed in Escherichia coli. Metal-binding properties of the expressed protein. *FEBS Lett 303* (2-3), 159-63.

Silver, S.; Phung, l. T., (2005), A bacterial view of the periodic table: genes and proteins for toxic inorganic ions. *J Ind Microbiol Biotechnol 32* (11-12), 587-605.

Singh, A. K.; McIntyre, L. M.; Sherman, L. A., (2003), Microarray analysis of the genome-wide response to iron deficiency and iron reconstitution in the cyanobacterium Synechocystis sp. PCC 6803. *Plant. Physiol. 132* (4), 1825-1839.

Sousa, S. F.; Fernandes, P. A.; Ramos, M. J., (2007), The carboxylate shift in zinc enzymes: a computational study. *J. Am. Chem. Soc. 129* (5), 1378-1385.

Stuart, R. K.; Dupont, C. L.; Johnson, D. A.; Paulsen, I. T.; Palenik, B., (2009), Coastal strains of marine Synechococcus species exhibit increased tolerance to copper shock and a distinctive transcriptional response relative to those of open-ocean strains. *Appl Environ Microbiol 75* (15), 5047-57.

Sunda, W. G.; Price, N. M.; Morel, F. M. M., (2005); Trace metal ion buffers and their use in culture studies. In *Algal Culturing Techniques.*, Elsevier, A., Ed.

TANG, E. P. Y.; VINCENT, W. F., (1998), Strategies of thermal adaptation by highlatitude cyanobacteria. *New Phytologist 142*.

Thelwell, C.; Robinson, N. J.; Turner-Cavet, J. S., (1998), An SmtB-like repressor from Synechocystis PCC 6803 regulates a zinc exporter. *Proc Natl Acad Sci U S A 95* (18), 10728-33.

Thomas, D. N., (2005), Photosynthetic microbes in freezing deserts. *Trends Microbiol 13* (3), 87-8.

Vallee, M. M. a. B. L., (1957), A cadmium protein from equine kidney cortex. *J. Am. Chem. Soc. 79* (17), 4813-4814.

Vasak, M., (1998), Application of Cd-113 NMR to metallothioneins. *Biodegradation 9* (6), 501-512.

Vasak, M.; Kägi, J. H. R., (1994); Metallothioneins. In *Encyclopedia of Inorganic Chemisty*, King, R. B., Ed. John Wiley and Sons Ltd.: Vol. 4, pp 2229-2241.

Wagner, G.; Vasak, M.; Worgotter, E.; Braun, W.; Schultze, P.; Arseniev, A.; Wuthrich, K., (1988), SOLUTION STRUCTURE OF METALLOTHIONEIN FROM DIFFERENT SOURCES AS DETERMINED BY 2D NMR. *Faseb Journal 2* (6), A1738-A1738.

Wang, H.; Zhang, Q.; Cai, B.; Lia, H.; Szea, K.; Huang, Z.; Wu, H.; Sun, H., (2006), Solution structure and dynamics of human metallothionein-3 (MT-3). *FEBS 580*, 795–800.

Wang, M.; Wang, W. X., (2008), Cadmium toxicity in a marine diatom as predicted by the cellular metal sensitive fraction. *Environ Sci Technol 42* (3), 940-6.

Wang, Y.; Mackay, E. A.; Zerbe, O.; Hess, D.; Hunziker, P. E.; VasÏaÂk, M.; KaÈ gi, J. H. R., (1995), Characterization and sequential localization of the metal clusters in sea urchin metallothionein *Biochemistry 34*, 7460-7467.

Webb, R.; Sherman, L. A., (1994); The cyanobacterial heat-shock response and the molecular chaperones. In *The Molecular Biology of Cyanobacteria.* , Bryant, D., Ed. pp 751-767.

Wehofsky, M.; Hoffmann, R.; Hubert, M.; Spengler, B., (2001), Isotopic deconvolution of marix-assisted laser desorption/ionization mass spectra for substanceclass specific analysis of complex samples. *Eur J Mass Spectrom 7*, 39-46.

Wells, M.; Trick, C., (2004), Controlling iron availability to phytoplankton in iron-replete coastal waters. *Mar Chem 86*, 1–13.

Williams, R. J., (2011), Chemical advances in evolution by and changes in use of space during time. *J. Theor. Biol. 268* (1), 146-159.

Williams, R. J.; Silva, J. J. F. D., (2003), Evolution was chemically constrained. *J Theor Biol 220* (3), 323-43.

Wishart, D.; Sykes, B.; Richards, F., (1992), The chemical shift index: a fast and simple method for the assignment of protein secondary structure through NMR spectroscopy. *Biochemistry 31*, 1647-1651.

Wu, C. H.; Yeh, L. S.; Huang, H.; Arminski, L.; Castro-Alvear, J.; Chen, Y.; Hu, Z.; Kourtesis, P.; Ledley, R. S.; Suzek, B. E.; Vinayaka, C. R.; Zhang, J.;

Barker, W. C., (2003), The Protein Information Resource. *Nucleic Acids Res 31* (1), 345-7.

Yang, Z.; Wu, Y. R.; Li, Y.; Ling, H. Q.; Chu, C. C., (2009), OsMT1a, a type 1 metallothionein, plays the pivotal role in zinc homeostasis and drought tolerance in rice. *Plant Molecular Biology 70* (1-2), 219-229.

Ybarra, G. R.; Webb, R., (1999), Effects of Divalent Metal Cations and Resistance Mechanisms of the Cyanobacterium *Synechococcus* sp. Strain PCC 7942. *Journal of Hazardous Substance Research 2*, 1-9.

Zeitoun-Ghandour, S.; Charnock, J. M.; Hodson, M. E.; Leszczyszyn, O. I.; Blindauer, C. A.; Stürzenbaum, S. R., (2010), The two Caenorhabditis elegans metallothioneins (CeMT-1 and CeMT-2) discriminate between essential zinc and toxic cadmium. *FEBS J 277* (11), 2531-42.

Zeitoun-Ghandour, S.; Leszczyszyn, O. I.; Blindauer, C. A.; Geier, F. M.; Bundy, J. G.; Stürzenbaum, S. R., (2011), C. elegans metallothioneins: response to and defence against ROS toxicity. *Mol Biosyst 7* (8), 2397-406.

Zeng, J.; Wang, W. X., (2011), Temperature and irradiance influences on cadmium and zinc uptake and toxicity in a freshwater cyanobacterium, Microcystis aeruginosa. *J Hazard Mater 190* (1-3), 922-9.

Zhang, L.; McSpadden, B.; Pakrasi, H. B.; Whitmarsh, J., (1992), Copper-mediated regulation of cytochrome c553 and plastocyanin in the cyanobacterium Synechocystis 6803. *J. Biol. Chem. 267* (27), 19054-9.

Zhou, J.; Goldsbrough, P. B., (1994), Functional homologs of fungal metallothionein genes from Arabidopsis. *The Plant Cell 6* (6), 875-884.

Zhou, Z.; Sun, X.; James Kang, Y., (2002), Metallothionein protection against alcoholic liver injury through inhibition of oxidative stress. *Exp. Biol. Med (Maywood) 227* (3), 214-222.

Zwirglmaier, K.; Heywood, J. L.; Chamberlain, K.; Woodward, E. M. S.; Zubkov, M. V.; Scanlan, D. J., (2007), Basin-scale distribution patterns of picocyanobacterial lineages in the Atlantic Ocean. *Environmental Microbiology 9* (5), 1278–1290.

Zwirglmaier, K.; Jardillier, L.; Ostrowsk, M.; Mazard, S.; Garczarek, L.; Vaulot, D.; Not, F.; Massana, R.; Ulloa, O.; Scanlan, D. J., (2008), Global phylogeography of marine Synechococcus and Prochlorococcus reveals a distinct partitioning of lineages among oceanic biomes. *Environmental Microbiology 10* (1), 147–161.

Appendix

Appendix A

2D [^{1}H, ^{1}H] NOESY resonance assignments of Zn_3*sync_0853* at 298 K and pH 7.0 recorded at 700 MHz.

Residues	H_N	H(α)	H(β)	Others
Asn3	8.5	4.57	2.73;2.63	H(γ):6.78;7.52
Glu4	8.16	4.24	-	
Val5	8.44	3.88	1.92	H(γ):0.82
Leu6	8.11	4.38	1.53	H(δ):0.95
Leu7	8.71	4.32	1.25	H(γ):1.15; H(δ):0.36;0.26
Leu8	8.22	4.27	1.46	H(γ):1.33
Cys9	8.23	3.96	2.95	
Asp10	8.41	4.57	2.45;1.43	
Cys11	8.76	4.6	3.94;3.08	
Leu13	8.68	4.54	1.98	
Cys14	7.99	4.27	3.43;3.27	
Arg16	-	4.53	1.69	H(γ):1.45; H(δ):2.92
Ser17	8.22	5.23	3.45	
Val18	8.51	4.45	1.82	H(γ):0.72; 0.67
Glu19	9.02	4.27	2.2	H(γ):1.73
Glu20	7.92	4.34	2.08	
Ser21	8.77	4.14	3.91	
Arg22	7.6	4.46	1.97	
Ser23	7.43	4.23	3.65	
Ile24	8.72	4.18	1.62	H(γ):0.72
Arg25	8.68	5.04	1.68;1.57	H(δ):3.03
Ile26	7.73	4.23	-	H(γ):1.06
Gly28	-	3.871;3.78	-	
Gln29	7.86	4.32	1.98	H(γ):2.20; H(δ):6.83; 7.49
His30	9.19	5.05	2.70;2.63	
Phe31	9.28	5.83	3.08;2.70	H(δ):7.07; H(ε):6.98
Cys32	10.21	4.32	3.00;2.60	
Ser33	7.11	4.71	4.21;4.03	
Glu34	9.42	3.77	2.08;2.20	H(γ):1.91
Ser35	8.51	3.66	3.58;3.45	
Cys36	6.89	3.74	3.15;2.82	

Appendix A continued

Residues	H_N	H(α)	H(β)	Others
Ala37	7.47	1.49	0.91	
Lys38	7.46	3.93	1.66	
Gly39	7.24	3.907;3.823	-	
His40	8	3.89	3.41;2.89	H(δ):6.81; H(ε):7.33
Pro41	-	4.27	2.22	H(γ):1.96; 1.90; H(δ):3.61
Asn42	9.57	4.82	2.72;2.36	H(γ):6.86; 7.74
Met43	7.99	3.95	1.95;1.78	H(γ):2.46; H(ε):2.10
Glu49	7.92	-	-	
Arg50	8.66	4.08	1.8	H(γ):1.60
Asp51	7.62	4.66	2.82;2.43	
Gly52	7.81	4.133;3.694	-	
Cys53	-	4.22	-	
Asn54	8.59	4.95	2.83;2.64	H(γ):6.72; 7.45
Cys55	8.31	3.96	-	
Gly56	8.1	3.01;2.66	-	
Ile57	6.95	4.15	1.86	
Ala58	7.57	4.06	1.26	
Glu59	8.26	4.11	-	
Leu60	7.96	4.12	1.55	
Glu61	8.2	4.06	-	H(γ):1.90
Leu62	7.89	4.18	1.59	

Appendix B

2D [^{1}H, ^{1}H] NOESY resonance assignments of Zn_4*sync_1081* at 298 k and pH 7.0 recorded at 700 MHz.

Residues	H_N	H(α)	H(β)	Others
Val3	-	4.14	-	H(γ):0.93
Thr4	8.37	4.32	4.03	H(γ):1.06
Val5	8.11	4.37	1.79	H(γ):0.75;0.70
Val6	8.63	4.3	1.95	H(γ):0.66
Lys7	8.15	4.07	1.58;1.5	H(γ):1.35; H(δ):1.77; H(ε):2.98,2.92
Cys8	8.2	3.73	2.85;2.80	
Ala9	7.92	3.95	0.82	
Cys10	8.48	4.43	3.86;2.99	
Ser11	8.76	4.03	3.91	
Ser12	8.25	4.44	3.87;3.76	
Cys13	8.08	4.35	3.31;3.22	
Thr14	9.21	4.45	4.54	
Cys15	8.63	4.2	3.44;2.93	
Glu16	8.48	4.58	2.18;1.94	H(γ):1.76
Val17	8.7	4.27	1.81	H(γ):0.59
Ser18	8.37	4.7	3.94;3.77	
Ser20	-	4.33	3.86;3.78	
Ser21	7.61	4.57	3.86;3.77	
Ala22	7.4	4.12	1.18	
Ile23	8.33	4.11	1.54	H(γ):1.10,1.24; H(δ):0.66
Ser24	8.64	5.45	3.67;3.59	
Arg25	8.95	4.42	1.75;1.65	H(γ):1.52; H(δ):3.10
Asn26	-	4.32	3.07;2.90	H(δ):6.86,7.69
Gly27	8.68	3.83;3.41	-	
His28	7.87	4.74	2.96;2.41	H(δ):7.02; H(ε):8.01
Ser29	8.21	4.93	3.44;3.37	
Tyr30	9.14	5.62	2.89	H(δ):6.96
Cys31	9.88	4.26	2.77	
Ser32	6.91	4.4	3.88;3.58	
Asp33	9.88	4.1	2.57;2.43	
Ala34	9.01	3.44	1.13	
Cys35	6.58	3.58	3.11;2.62	

Appendix B continued

Residues	H_N	H(α)	H(β)	Others
Ala36	7.84	1.61	0.81	
Ser37	7.87	4.09	3.84;3.69	
Gly38	7.27	3.86	-	
His39	8	4.01	3.36;2.99	H(δ):6.77; H(ε):7.04
Arg40	8.13	3.89	1.77;1.71	H(γ):1.62; H(δ):3.14
Asn41	9.43	4.91	2.74;2.23	H(δ):7.57,6.76
Asn42	7.89	4.27	2.96;2.67	H(δ):6.70; H(ε):7.54
Glu43	10.22	4.15	-	
Pro44	8.68	4.21	2.16;1.82	H(γ):1.64,1.60; H(δ):3.75,3.40
Cys45	8.68	3.54	3.17;2.76	
His46	7.44	3.65	3.57;3.53	H(δ):7.18; H(ε):7.74
Asp47	7.92	4.08	3.01;2.75	
Ala48	7.44	4.38	1.31	
Ala49	8.68	4.12	1.3	
Gly50	9.15	4.01;3.75	-	
Ala51	7.86	4.03	1.47	
Cys52	8.19	4.63	2.85;2.29	
Gly53	8.33	3.58	-	
Cys54	8.96	4.3	3.36	
Asn55	8.49	4.89	2.88;2.68	H(δ):7.47,6.78
Cys56	9.2	4.05	3.07	
Gly57	8	3.18	-	
Ser58	7.28	4.04	3.79;3.72	

Appendix C

2D [^{1}H, ^{1}H] NOESY resonance assignments of Zn_4*sync_2426* at 298 K and pH 7.0 recorded at 700 MHz.

Residues	HN	H(α)	H(β)	Others
Thr3	-	4.38	4.11	
Asn4	8.77	4.67	2.7	H(γ):7.54,6.79
Leu5	8.14	4.53	-	
Val6	8.8	4.34	1.97	
Arg7	8.2	4.44	-	H(γ):7.07; H(ε):3.11
Cys8	8.02	3.88	2.98;2.76	
Asp9	8.44	4.57	-	
Cys10	8.29	5.05	3.75;3.13	
Pro11	-	4.44	2.26;2.14	
Pro12	-	4.56	2.06;1.89	H(γ):1.77,1.71
Cys13	8.21	4.37	3.56	
Thr14	9.14	4.46	4.595	
Cys15	8.42	4.05	-	
Ser16	8.46	5.05	-	
Ile17	8.94	4.4	1.72	
Glu18	8.35	4.34	1.98;1.84	H(γ):2.20,2.13
Glu19	8.66	3.69	-	
Ala20	8.47	4.14	-	
Thr21	7.48	4.35	4.13	
Ala22	7.44	4.19	-	
Ala23	8.12	4.41	-	
Met24	8.22	5	2.42;2.35	H(γ):1.97,1.83
Tyr25	8.43	4.58	-	
Gly26	8.76	3.80;3.59	-	
Asn27	8.5	4.55	-	H(γ):7.46,6.80
Lys28	7.81	4.34	-	H(γ):1.47,1.40; H(δ):1.65,1.26
Leu29	8.7	4.79	-	H(γ):1.39
Phe30	8.72	5.97	3.02;2.66	
Cys31	10.05	4.65	3.63;2.76	
Ser32	7.3	4.77	-	
Glu33	9.27	3.84	-	
Ala34	8.46	4.19	-	

Appendix C continued

Residues	H_N	H(α)	H(β)	Others
Cys35	7.01	3.57	3.25;2.82	
Ala36	7.46	1.31	-	
Thr37	7	3.94	4.34	
Ala38	7.43	4.06	-	
His39	8.16	3.72	3.25;3.15	H(δ):6.70; H(ε):7.10
Ile40	7.11	3.98	1.8	
Asn41	8.64	4.57	2.78;2.63	H(γ):7.48,6.84
Gln42	7.96	4.15	1.96;1.84	H(δ):6.98,7.47
Glu43	8.43	4.53	1.81;1.74	H(γ):2.23,2.01
Pro44	-	4.31	-	
Ser45	8.12	4.28	3.84;3.76	
Asn46	8.16	4.66	-	H(γ):7.52,6.84
Ser47	8.08	4.38	-	
Ala48	8.13	4.03	-	
Glu49	9.07	4.33	1.99;1.76	H(γ):2.22,2.11
His50	9.5	5.09	4.03;2.76	H(δ):6.90; H(ε):8.03
Thr51	7.57	3.87	4.24	
Glu52	8.78	4.17	2.08;1.89	H(γ):2.21,2.17
Cys53	8.13	4.57	3.12;3.04	
Ser54	8.7	4.71	3.92;3.84	
Cys55	10.27	4.27	3.18;2.58	
Gly56	8.35	4.20;3.41	-	
Cys57	7.6	4.19	3.51;3.02	

Appendix D

Constructing a Relative Standard Curve

The qPCR data generated form ABI system was exported to an Excel spreadsheet. The exported file contains information of the sample well number, sample description, standard deviation of the baseline, and Ct

Sample (ng)	Detector	Log ng	Ct
1.09	rnpB_IDT	0.03742	25.8537
1.09	rnpB_IDT	0.03742	24.589
1.09	rnpB_IDT	0.03742	25.6728
0.109	rnpB_IDT	-0.96257	29.8673
0.109	rnpB_IDT	-0.96257	30.4058
0.109	rnpB_IDT	-0.96257	30.3754
0.0109	rnpB_IDT	-1.96257	34.4295
0.0109	rnpB_IDT	-1.96257	34.8465
0.0109	rnpB_IDT	-1.96257	34.7636
0.00109	rnpB_IDT	-2.96257	37.4752
0.00109	rnpB_IDT	-2.96257	37.2901
0.00109	rnpB_IDT	-2.96257	37.6404
NGC	rnpB_IDT	Undetermined	
NGC	rnpB_IDT	Undetermined	
NGC	rnpB_IDT	Undetermined	

1. Select the log input (log ng) and Ct data as shown above.
2. Using the Excel chart to draw XY (marked scatter) plot with the log input as X values and Ct as Y values.
3. Click one of the data points and insert a Trendline, select Display equation on chart and Display R-squared value on chart. The generated equation (y = mx + b) will be used to calculate the input amount for unknown samples.

Appendix E

Constructing the Input amount using a Relative Standard Curve, the fold change and transcription abundance.

1. The input amount for a unknown sample are calculated using the following equation:

$$input\ amount\ (ng) = 10^{\frac{Ct\ value\ -b}{m}}$$

m = slope of standard curve line

b = y-intercept of standard curve line

2. Repeat the steps to all samples; because the four metallothionein (MT) genes and the reference gene rnpB are amplified in separated tubes, average the three technical replication of MT and rnpB values separately.

3. Divide the amount of MT by the amount of rnpB to determine the normalized values of the MT, and then average the values of the two biological replicates to determine the amount of the MT (MT_N),

4. Multiply the MT_N by 392000 (the number of *Synechococcus* sp. CC9311 genome equivalents per 1 ng genomic DNA) to determine the transcription abundance of MT in sample.

5. Divide the MT_N of the treated sample by the MT_N (MT_N') of the untreated sample to generate the fold change for each gene.